CRC Report No. A-91

PROJECTED OZONE TRENDS AND CHANGES IN THE OZONE-PRECURSOR RELATIONSHIP IN THE SOUTH COAST AIR BASIN IN RESPONSE TO VARYING REDUCTIONS OF PRECURSOR EMISSIONS

Final Report

March 2015

COORDINATING RESEARCH COUNCIL, INC.
5755 NORTH POINT PARKWAY·SUITE 265·ALPHARETTA, GA 30022

The Coordinating Research Council, Inc. (CRC) is a non-profit corporation supported by the petroleum and automotive equipment industries. CRC operates through the committees made up of technical experts from industry and government who voluntarily participate. The four main areas of research within CRC are: air pollution (atmospheric and engineering studies); aviation fuels, lubricants, and equipment performance, heavy-duty vehicle fuels, lubricants, and equipment performance (e.g., diesel trucks); and light-duty vehicle fuels, lubricants, and equipment performance (e.g., passenger cars). CRC's function is to provide the mechanism for joint research conducted by the two industries that will help in determining the optimum combination of petroleum products and automotive equipment. CRC's work is limited to research that is mutually beneficial to the two industries involved, and all information is available to the public.

CRC makes no warranty expressed or implied on the application of information contained in this report. In formulating and approving reports, the appropriate committee of the Coordinating Research Council, Inc. has not investigated or considered patents which may apply to the subject matter. Prospective users of the report are responsible for protecting themselves against liability for infringement of patents.

Projected Ozone Trends and Changes in the Ozone-Precursor Relationship in the South Coast Air Basin in Response to Varying Reductions of Precursor Emissions

CRC A-91

FINAL REPORT

Prepared for

Coordinating Research Council, Inc.
5755 North Point Parkway, Ste. 265
Alpharetta, GA 30022

Prepared by

Eric M. Fujita and David E. Campbell
Desert Research Institute
Division of Atmospheric Sciences
2215 Raggio Parkway
Reno, NV 89512

Rosa Fitzgerald and Roberto Perea
University of Texas El Paso
Physics Department

William R. Stockwell and Emily Saunders
Howard University
Department of Chemistry

March 31, 2015

DISCLAIMER AND ACKNOWLEDGMENTS

This report was prepared by Desert Research Institute (DRI) as an account of work sponsored by the Coordinating Research Council (CRC) and the Truck and Engine Manufacturers Association (EMA). Neither the EMA, CRC, members of the EMA or CRC, DRI nor any person acting on their behalf: (1) makes any warranty, express or implied, with respect to the use of any information, apparatus, method, or process disclosed in this report, or (2) assumes any liabilities with respect to use of, inability to use, or damages resulting from the use or inability to use, any information, apparatus, method, or process disclosed in this report. We gratefully acknowledge the South Coast Air Quality Management District for providing the CMAQ modeling input and output files.

TABLE OF CONTENTS

LIST OF TABLES

LIST OF FIGURES

1. PROJECT OVERVIEW AND SUMMARY

The Coordinating Research Council (CRC) Project A-91 was conducted to forecast the changes in ambient ground-level ozone (O_3) concentrations[1] in California's South Coast Air Basin (SoCAB) in response to changes in ambient concentrations of the ozone precursors, volatile organic compounds (VOC)[2] and oxides of nitrogen (NOx)[3]. This study focused on the effects of varying reductions of NOx and VOC emissions on the location and magnitude of peak ozone levels within the basin, and the persistence and magnitude of an interim period of elevated ozone levels that could result from a NOx-focused control strategy in some areas of the SoCAB prior to transition from VOC-sensitive to NOx-sensitive ozone formation. It also examined the implications of underestimating current (Fujita et al., 2012a; Fujita et al., 2013) or future inventories of ROG emissions by forecasting the response of ozone to varying reductions in NOx emissions with alternative base and future year ROG emissions. The A-91 Study was co-sponsored by the CRC and the Truck and Engine Manufacturers Association (EMA) and was conducted by the Desert Research Institute (DRI), Howard University (HU) and University of Texas El Paso (UTEP).

1.1 Introduction

The South Coast Air Basin has historically experienced the most severe ground-level ozone pollution in the United States. Prior to the implementation of emission reduction measures in the early 1950s, hourly averaged ozone mixing ratios approaching 700 ppb were reported in the SoCAB, and Stage III episodes (ozone exceeding 500 ppb) were relatively frequent events during the 1960s. Four decades of progressively more stringent controls of NOx and ROG

---

[1] Gas-phase species are usually measured as molar ratios (e.g., ppbv or ppmv), which are technically mixing ratios. The term concentration denotes units of mass per unit volume (e.g, $\mu g/m^3$). In common usage, these terms are used interchangeably.

[2] Volatile organic compounds are normally defined as all organic compounds that may be present in the ambient air irrespective of their photochemical reactivity or ability of measurement methods to quantify their concentrations. The following subsets of VOC are used throughout this report. These terms are operational definitions that reflect the sensitivity and selectivity of the analytical methods or photochemical reactivity.

- Non-methane hydrocarbons (NMHC): C_2 through C_{11} hydrocarbons collected in stainless steel canisters and measured by gas chromatography with flame ionization detection (GC-FID) by EPA method TO-14A (U.S. EPA, 1997). Known halocarbons and oxygenated compounds (e.g., aldehydes, ketones, ethers and alcohols) are excluded from NMHC.
- Carbonyl compounds: Aldehydes and ketones, the most common being formaldehyde, acetaldehyde, and acetone, that are operationally defined as C_1 through C_7 oxygenated compounds measured by collection on acidified 2,4-dinitrophenylhydrazine (DNPH)-impregnated C_{18} or silica gel cartridges and analyzed by high performance liquid chromatography with UV detection (HPLC/UV). Photochemical Assessment Monitoring Station (PAMS) carbonyl data normally include only formaldehyde, acetaldehyde, and acetone.
- Non-methane organic compounds (NMOC): Sum of quantifiable peak by EPA Method TO-14A, including unidentified but excluding halocarbons, or by continuous instruments with flame ionization detection. NMOC also refers to the sum of NMHC plus carbonyl compounds by EPA Method TO-11.
- Reactive organic gases (ROG): Organic gases with potential to react with the hydroxyl radical and other chemicals with half-life of <30 days that produce ozone and secondary organic aerosol. ROG is a specific subset of VOC that is typically used in reference to emission inventory estimates.

[3] Oxides of nitrogen (NOx) include nitric oxide (NO) and nitrogen dioxide (NO_2).

emissions have reduced the number of exceedances of the 2008 eight-hour ozone National Ambient Air Quality Standard (NAAQS)[4] of 75 ppb from 211 days in 1975 to 88 days in 2013 and the basin design value[5] from 275 ppb to 107 ppb (Figure 1-1). Despite these efforts, the current ozone NAAQS is exceeded in the basin on most summer days and attainment of the standard by the 2032 deadline remains a long-term challenge.

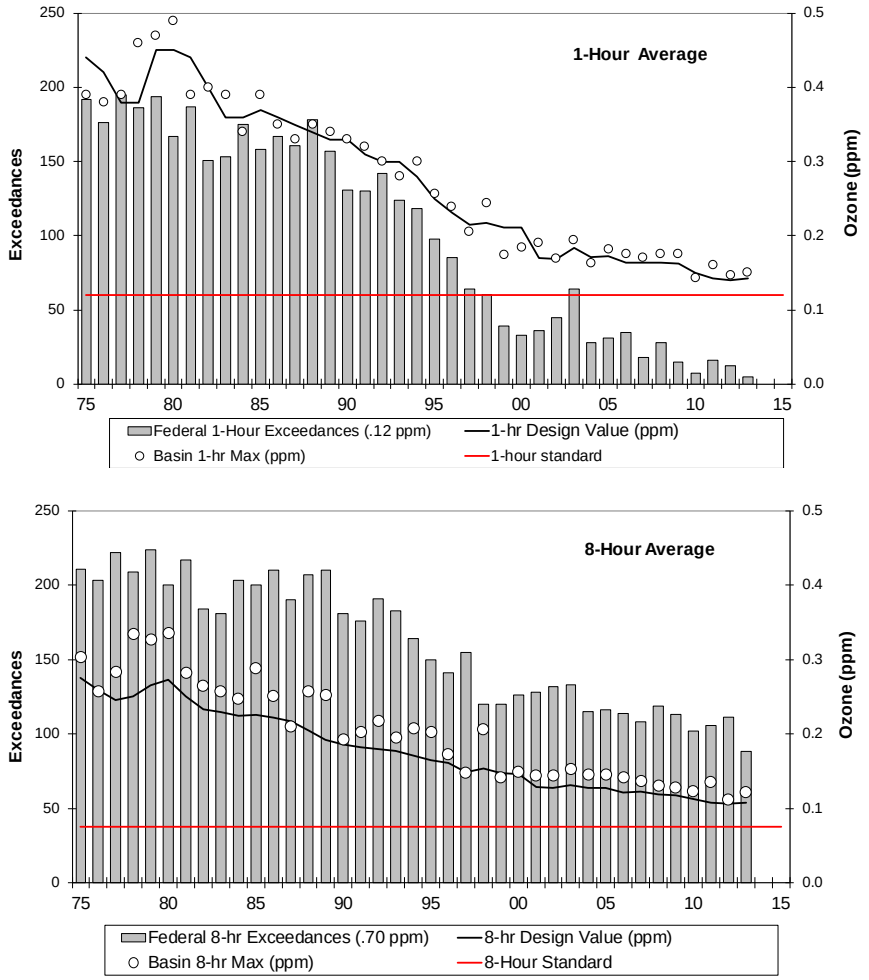

Figure 1-1. Trend (1975 to 2013) in basin-wide 1-hour and 8-hour average ozone maxima, design value, and standard exceedances in the SoCAB.

[4] EPA is currently considering a lower standard between 60 and 70 ppb based upon the recommendations from the latest 5-year review of the ozone standard by the Clean Air Scientific Advisory Committee (CASAC).

[5] Basin design value (DV) for the ozone NAAQS is the highest design value within an air basin. A design value is the three-year average of the annual fourth highest daily 8-hour average ozone concentration measured at a particular measurement station. Attainment is achieved when the DV meets the ozone NAAQS.

The South Coast Air Basin (Figure 1-2) encompasses 10,743 square miles and is home to over 17.8 million people (2010 U.S. Census). It is in the semi-permanent high-pressure zone of the eastern Pacific. Frequent and persistent temperature inversions are caused by subsidence of descending air that warms when it is compressed over cool, moist marine air. These inversions often occur during periods of maximum solar radiation which create daytime mixed layers of ~1,000 m thickness. Summertime flow patterns in the SOCAB are from the west and south during the morning, switching to predominantly westerly winds by the afternoon. On-shore breeze is strong during the day and winds are calm overnight with a weak land-sea breeze. The land/sea breeze circulation moves air back and forth between the SoCAB and the Pacific Ocean, as well as along the coast to other air basins. Heating of the San Gabriel and San Bernardino Mountains during the daytime causes upslope flows that can transport pollutants from the surface into the upper parts of, and sometimes above, the mixed layer. When the slopes cool after sunset, the denser air flows back into the SoCAB with pollutants entrained in it. High concentrations of ozone and fine suspended particles in the SoCAB result from the combination of high mountains that contain air pollutants, adverse meteorology that results in low mixing layers and conditions that limit atmospheric dispersion, and emissions from the second largest urban area in the U.S.

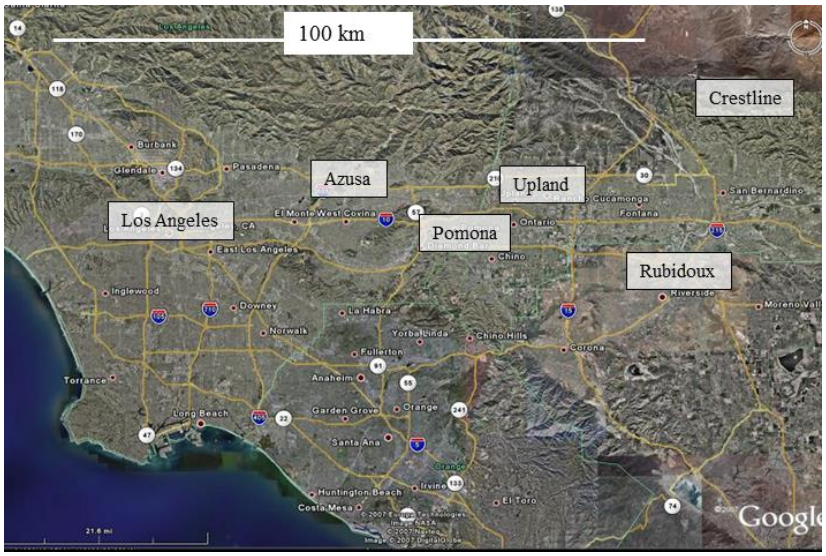

Figure 1-2. Map of the South Coast Air Basin with approximate locations of the air quality monitoring stations that are referenced in this report.

Whereas local topography, meteorology and pollutant emissions make attainment of the ozone standard more difficult in the **S**oCAB than other urban areas of the country, it is ozone's nonlinear chemistry that is the primary reason why closing the remaining gap between current ozone levels and the NAAQS will be a prolonged intractable problem. As described in more detail in Section 2.1, ozone formation is nonlinear with respect to VOC and NOx because they compete with one another for the hydroxyl (HO) radicals. HO initiates the oxidation of VOC that produce organic peroxy (RO_2) and hydroperoxy (HO_2) radicals that convert NO to NO_2, which leads to formation of new O_3. At a given level of VOC, there exists a NO_x mixing ratio at which a maximum amount of ozone is produced. This optimum VOC/NOx ratio, expressed as a molar

ratio of VOC in parts per billion carbon (ppbC) to NOx in ppb, is about 10 to 12, which corresponds to the ridgeline in an isopleth plot of maximum ozone produced relative to initial concentrations of VOC and NOx (see Figure 2-3). The HO radical chain length, which is the number of times a newly formed HO radical is regenerated through radical chain propagation before it is removed by forming hydrogen peroxide and organic peroxides, reaches a maximum at this VOC/NOx ratio. NOx also acts as a catalyst and is regenerated during the production of ozone from VOC. An approximation of the NOx chain-length is the ozone production divided by the NOx removed by conversion to NOy, which is the sum of nitric acid (HNO_3), peroxyacetylnitrate (PAN) and other organic nitrates. Reducing NOx increases ozone production efficiency by lowering the conversion rate of NOx to NOy.

Reductions of VOC and NOx have varying effect on the rate and efficiency of ozone formations depending upon the VOC/NOx ratio relative to the optimum ratio of 10 to 12. In the "NOx-limited" or "NOx-sensitive" region below the ridgeline in an ozone isopleth plot (VOC/NOx ratios > 12), lowering NOx effectively reduces O_3 while reductions in VOC have practically no effect. Ozone is reduced near the ridgeline by simultaneous reductions in VOC and NOx emissions. In the "VOC-limited" or "VOC-sensitive" region above the ridgeline (VOC/NOx ratios < 10), lowering VOC effectively reduces O_3. However, NOx reductions can increase O_3 under VOC-limited conditions by lowering the rate at which OH and NO_2 are removed by formation of HNO_3. "NO_x-disbenefit" refers to this situation. The ambient VOC/NOx ratio varies within the air basin depending upon the mix and type of local emission sources. The instantaneous VOC/NOx ratio increases during atmospheric transport of emissions because the HO radical reacts more rapidly with NO_2 than VOC. This varying rate of chemical processing of VOC and NOx causes ambient VOC/NOx ratios to increase during the day leading to varying VOC/NOx ratios within the basin depending upon time of day, pattern of transport and timing of additional fresh emission. Consequently, while reducing NOx may be counter-productive in and near source areas under VOC-limited conditions, such emission reductions can result in lower ozone levels in downwind receptor locations.

The ozone-precursor relationship has evolved in the SoCAB over the past four decades with varying relative reductions of VOC and NOx emissions. Ozone levels in the SoCAB dropped sharply during the 1980s and 90s when emission controls were more VOC-focused, but have subsequently leveled off even with further VOC emission reductions and a transition to greater control of NOx emissions. The measured 6-9 am ambient VOC/NOx ratios in the basin were near the optimum ratio of 10 in the 1980s when control of either NOx alone or simultaneous control of VOC and NOx would have been effective. However, emission control technology development allowed for earlier and more effective control of VOC and CO than NOx. The weekday 6-9 am ambient VOC/NOx ratio steadily decreased through the 1990s, reaching a minimum of about 4 in the early 2000s. At the same time, VOC/NOx ratios were about 40% and 20% higher on Sundays and Saturdays, respectively, due to lower vehicle emissions during the morning, especially from heavy-duty diesel trucks on Sundays. The higher weekend VOC/NOx ratios resulted in more efficient and rapid O_3 formation and 25% and 50% higher ambient O_3 levels on Saturdays and Sundays, respectively, despite substantially lower NOx emissions (i.e. "weekend ozone effect", see Section 2.3). VOC/NOx ratios have increased in recent years to about 5 to 6 and are projected to increase with greater future emphasis on NOx controls (Figure 1-3). Recent increasing VOC/NOx ratios resulted in more rapid formation of O_3. Over 90 and 80 percent of the cumulative reductions in ambient ozone levels during the past 30 years were achieved by the late 1990s on weekdays and Sundays, respectively (Figure 1-4).

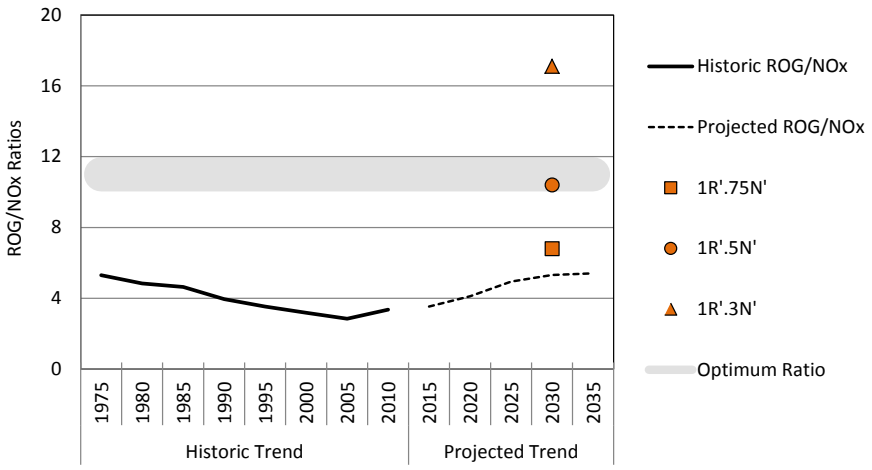

Figure 1-3. Historic and projected trends in the ratios of ROG to NOx emissions. Also shown are ROG/NOx ratios corresponding to further incremental NOx reductions from the 2030 baseline NOx emissions (N' = 284 tpd, -61% from 2008) of 0.75 x N' (213 tpd, -70%), 0.5 x N' (141 tpd, -81%) and 0.3 x N' (85 tpd, -88%) while holding ROG emissions at 2030 baseline levels (R' = 437 tpd, -32% from 2008 base ROG emissions).

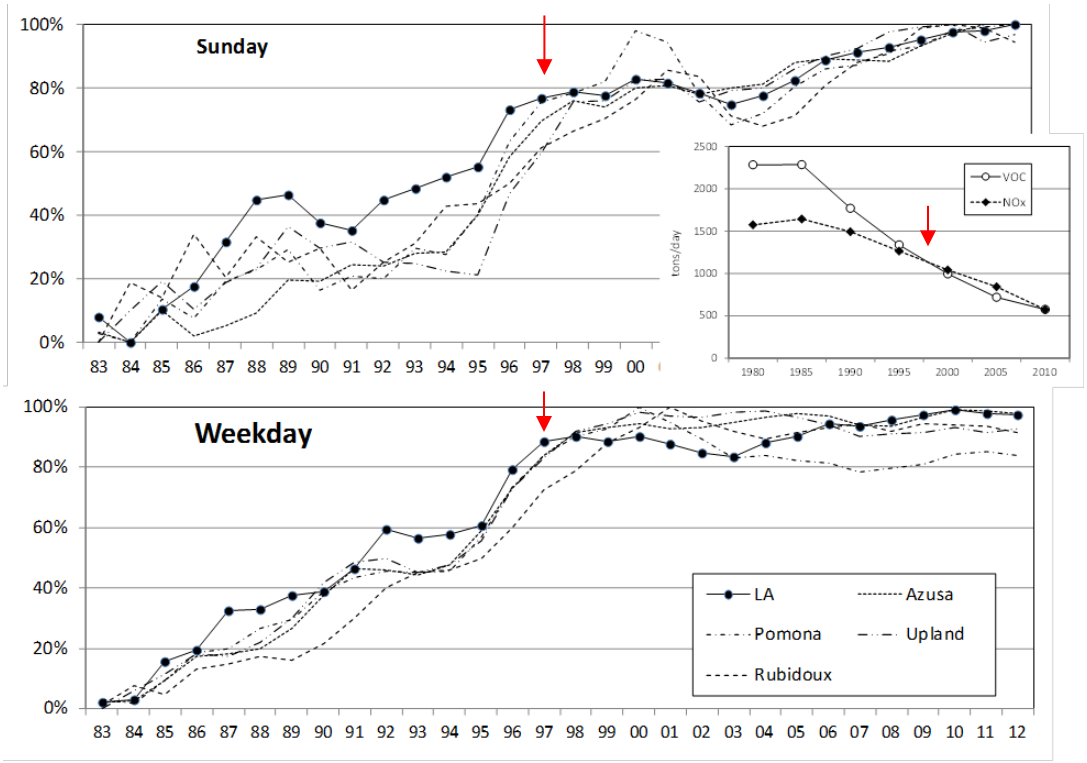

Figure 1-4. Cumulative ambient ozone reduction trends from 1982 to 2012 of (30 year max - annual max)/(30 year max – 30 year min) in percent. Ratios are based on three-year running averages of the annual means of the daily maximum 1-hour ozone mixing ratios. Insert shows trends in basin-wide average daily total emissions in tons/day and red arrows mark 1997.

Air quality statistics that are used to track progress toward attainment of the NAAQS, such as the basin-wide DV and standard exceedances have been driven by ozone values on weekends, especially Sundays. While O_3 levels declined slowly during the past decade at downwind locations (e.g., current basin design value site at Crestline in the San Bernardino Mountains), the weekday ozone trends in the central basin have flattened and even increased at some central basin locations (Figure 1-5). The historically low weekday average ozone levels at some central basin locations from about 2000-2004 coincided with the minima in the ambient VOC/NOx ratios and maxima in the magnitude of the observed weekend ozone effect. These observations illustrate that the basin DV can be a misleading indicator of basin-wide ozone trends and mask the relative lack of progress during the past 15 years in the central basin compared to Crestline, which currently determines the ozone attainment status for the basin.

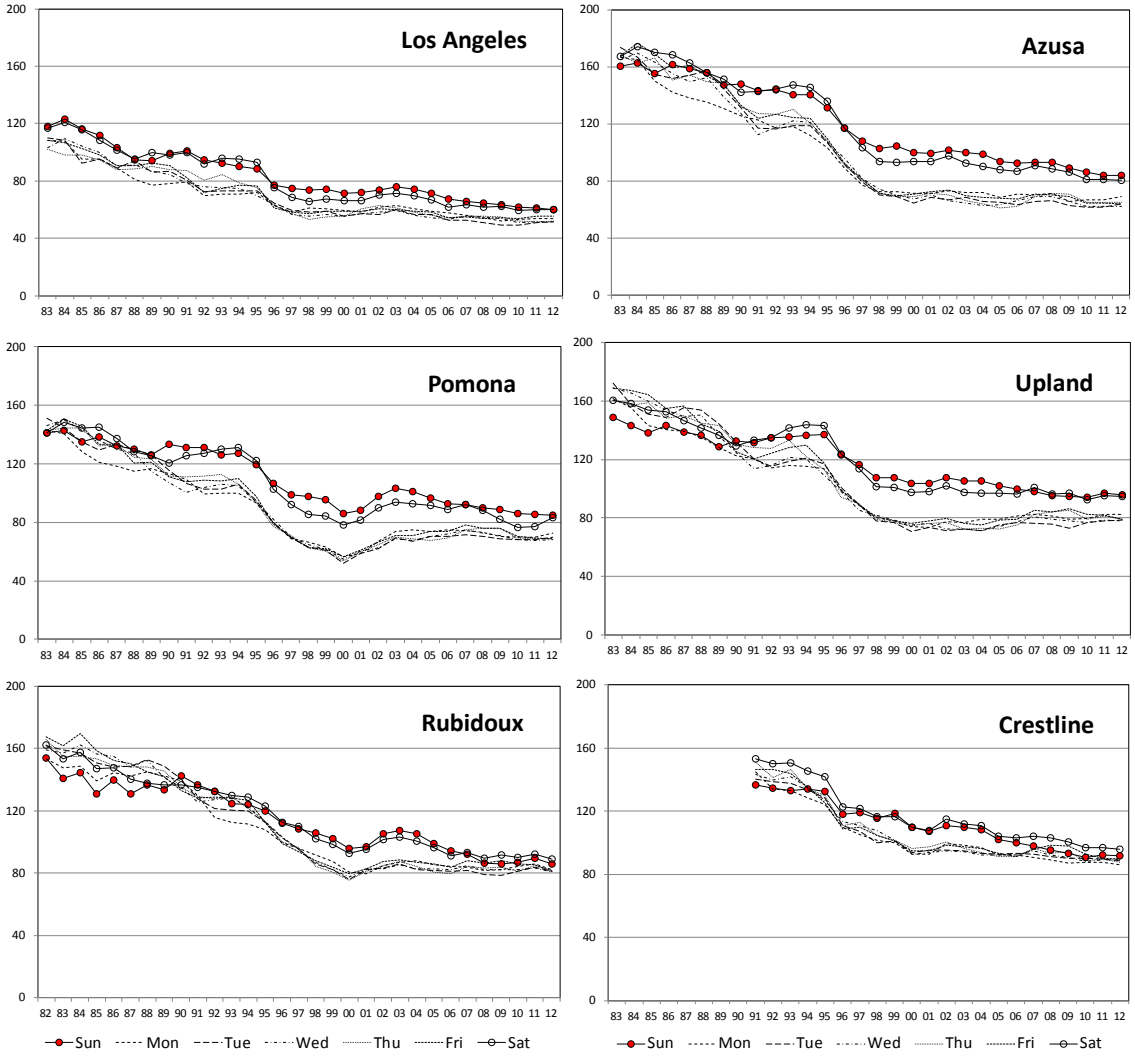

Figure 1-5. 30-year trend in 3-year running seasonal (6/1 to 9/30) mean daily maximum 1-hour ozone (ppb) by day of week for Los Angeles, Azusa, Pomona, Upland and Rubidoux and Crestline. Trend for Sundays and Saturdays are shown as solid lines with red filled circles and open circles, respectively, and weekdays are shown as broken lines. WE-WD differences peaked about 2000 when ambient VOC/NOx ratios were lowest (i.e. most VOC-limited).

1.2 Study Objectives and Approach

The Coordinating Research Council (CRC) Project A-91 was conducted to forecast the changes in the magnitude and spatial variations of peak ambient ozone levels within the SoCAB in response to varying relative reductions of VOC and NOx. The study involved a series of base and sensitivity air quality model simulations using the CMAQ-ready emissions and meteorological inputs for 2008 and 2030 used by the South Coast Air Quality Management District (SCAQMD) to develop their 2012 Air Quality Management Plan (SCAQMD, 2013). Adjustments were applied to the 2008 base ROG emissions to examine potential underestimation of ROG emissions and to the 2030 "baseline" emissions to simulate further incremental reductions of NOx emissions. CRC A-91 addressed the following objectives.

1. Update ozone and precursor trends.

The historic trends (1980 to 2013) in spatial and day-of-week variations of peak ozone levels in the SoCAB were related to corresponding changes in mean daily maximum NOx and VOC (or carbon monoxide as surrogate) concentrations. Future trends in NOx and VOC concentrations were estimated based on expected changes in emissions from 2010 to 2030. The analyses update our prior work, which are summarized in the following two publications.

- Fujita, E.M., W.R. Stockwell, D.E. Campbell, and R.E. Keislar (2003). Evolution of the magnitude and spatial extent of the weekend ozone effect in California's South Coast Air Basin 1981-2000, J. Air Waste Manage. Assoc. 53:802-815.
- Fujita, E.M.; Campbell, D.E.; Stockwell, W.R.; Lawson, D.R. (2013). Past and future ozone trends in California's South Coast Air Basin: reconciliation of ambient measurements with past and projected emission inventories, J. Air Waste Manage. Assoc. 63:54-69

2. Determine whether the current emission inventory underestimates ROG emissions.

The predicted ozone and VOC (by lumped species) concentrations for the 2008 base year simulations by the South Coast Air Quality Management District (SCAQMD) were compared to corresponding ambient data from the SoCAB Photochemical Assessment Monitoring Stations. This is an update of similar analysis that was conducted as part of the 2010 Van Nuys Tunnel Study (Fujita et al., 2012; Fujita et al., 2013). Additionally, model simulations were made as part of objective #3 to determine whether model performance is improved with upward adjustment to the 2008 base ROG emissions.

3. Simulate the changes in ambient ozone levels from 2008 to 2030 in response to varying changes in ROG and NOx emissions.

Researchers at the University of Texas at El Paso (UTEP) ran the Community Multiscale Air Quality (CMAQ) model simulations for summer 2008 using the meteorological and emissions inputs and model setup obtained from the SCAQMD. The simulations were made with the same spatial resolution with chemical mechanisms used by the SCAQMD. Following successful reproduction of the SCAQMD 2008 base year simulations, a series of simulations were made by adjusting the 2008 and 2030 emission inputs to forecast the effects of varying incremental NOx reductions and potential underestimations of ROG emissions to reproduce SCAQMD's preliminary estimate that a 90% reduction of NOx emissions will be necessary to attain the 8-hour ozone NAAQS of 75 ppb. The model sensitivity analysis also examined the potential magnitude and persistence of an interim period of increased ozone levels that could

result from a NOx-focused control strategy (i.e., NOx disbenefit). As previously mentioned in Objective #2, sensitivity simulations were made to determine whether model performance is improved with upward adjustment to the 2008 base ROG emissions by factors of 1.5 and 2.0. Effect of adjustments to the base ROG emissions on the relative response factors (RRF), projected design values (DV) and extent of emission reductions necessary to show attainment of the ozone NAAQS were examined.

4. Relate the ozone-precursor relationship in the SoCAB to historic and projected trends emissions of VOC and NOx.

Researchers at Howard University performed chemical box modeling simulations that were analyzed to examine the retrospective and prospective changes in the maximum ozone mixing ratios and rates of ozone formation that would be expected given the observed historic trends in the ambient VOC and NOx mixing ratios. The modeling procedure used examines changes in ozone photochemistry independently rather than the combined effects of chemistry and pollutant transport. These modeling results were used to examine the effects of historic changes in ozone precursor concentrations within the Basin on ozone chemistry. The response of ozone concentrations to changes in VOC and NOx were reconciled with past ambient ozone trends and used to project the effects of projected future changes in precursor emissions.

1.3 Summary of Findings

Objective 1 – Update ozone and precursor trends.

- Ozone trends show rapid and steady decline from 1982 to 2000, followed by a relatively flat trend during the last 12 years (Figure 3-3). Over 90 and 80 percent of the cumulative reductions in ambient ozone levels during the past 30 years were achieved by the late 1990s on weekdays and Sundays, respectively (Figure 3-4).
- While the ozone levels at Crestline shows slight decreasing trends in the past decade for both Sunday and weekdays, the weekday ozone levels at some central basin sites show a slightly increasing trend in the past decade (Figure 3-2). Statistics commonly used to track progress toward attainment (e.g., basin DV, exceedances) mask the increasing weekday ozone trends in the central basin that began about a decade ago.
- Minima in the weekday ozone trends at some central Basin sites coincided with minima in the trends in 6-9 am ambient VOC/NOx ratios and ratios of ROG to NOx emissions.
- Differences between weekend and weekday ozone levels were minimal in the early 1980s, increased in the late 1980s in the western half of the SoCAB, and gradually spread further east during the 1990s. Maxima in WE-WD differences occurred at about 2000 and coincided with the time when ozone trends began to flatten. Currently, the WE effect is strongest in the central basin and has weakened in western and eastern portions of the basin.
- The duration of ozone accumulation has increased in recent years due likely to greater reductions of NOx emissions resulting in less ozone inhibition in the morning. The trend in ozone accumulation rates have flattened in the past decade with narrowing of the weekday-weekend differences in recent years.

Objective 2 – Determine whether the current emission inventory underestimates ROG emissions.

- The 2008 base year simulation tends to under predict VOC species to varying degrees. In general, the underestimation of VOC is for species that are mostly associated with motor vehicle exhaust emissions.
- The 2008 simulation using the unadjusted base ROG emissions under predicts the observed ozone values by 21% in the central and eastern basin. A factor of 1.5 adjustment results in good agreement and a factor of 2.0 adjustment results in over prediction of 17% (Figure 1-6). These results combined with the findings of the 2010 Van Nuys Tunnel Study (Fujita et. al., 2012) and the most recent top-down emission inventory evaluation (Fujita et al., 2013) support the conclusion that the 2008 base ROG emissions are underestimated (see Section 2.6) and that these emissions should be increased by a factor of 1.5. Underestimations of current ROG emissions have important implications for air quality modeling used to demonstrate future attainment of the ozone NAAQS (see objective 3).

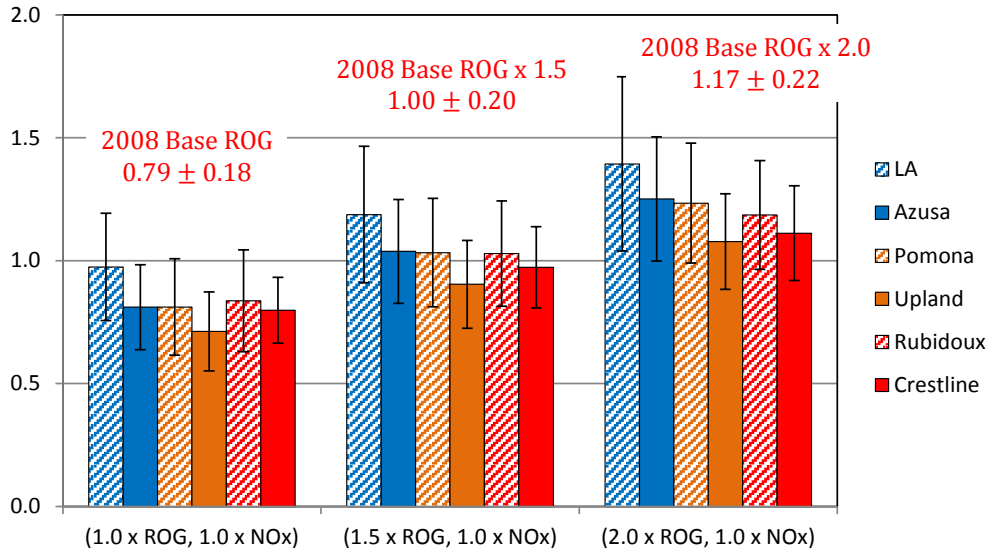

Figure 1-6. Ratios (mean ± standard deviations) of predicted/observed daily maximum 8-hour ozone for 6/15 - 6/20 and 7/2 - 7/8 with 1.0, 1.5, and 2.0 time 2008 base ROG. Values are for the nine cells (12 x 12 km) containing the SoCAB air quality monitoring station.

Objective 3 – Simulate the changes in ambient ozone levels from 2008 to 2030 in response to varying changes in ROG and NOx emissions.

- The model results obtained by UTEP for the 2008 base year simulation were virtually identical to those obtained by the SCAQMD.
- With 2030 baseline NOx emissions (-61% from 2008, 723 to 284 tpd) and 2030 baseline ROG emissions (-32% from 2008 base, 639 to 437 tpd) (left half of Figure 1-7), the average daily maximum 8-hour ozone concentrations are predicted to increase by 18, 14, 11 and 10 percent at Los Angeles, Azusa, Pomona and Upland, respectively, and decrease by 2 and 4 percent at Rubidoux and Crestline, respectively. Ozone levels are not significantly different with 70% reduction in NOx emissions (723 to 213 tpd) except for further marginal deceases

in the eastern basin. At 81% reduction in NOx (723 to 141 tpd), the average 8-hour ozone concentration at Los Angeles remains about 18% higher than 2008 levels and most of the central basin remains at 2008 levels. However, ozone levels at Rubidoux and Crestline are predicted to be 13 and 17 percent lower, respectively, relative to 2008 levels and the basin DV site shifts to the central basin. With 88% reduction in NOx, ozone levels at Azusa, Pomona, Upland, Rubidoux and Crestline are decreased by 8, 12, 13, 24 and 27 percent from 2008, respectively.

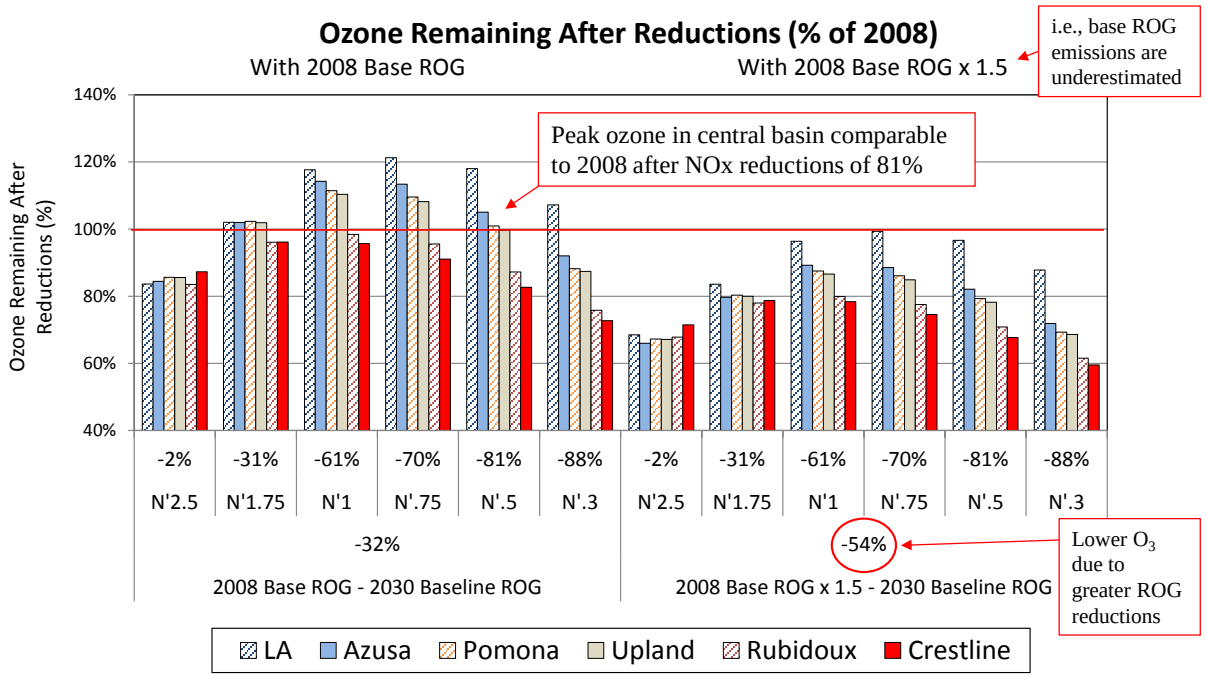

Year	Case	ROG				NOx				ROG/NOx
		Total ROG (tpd)	Adj Factor	Δ 2008 Base	Δ 2030 Baseline	Total NOx (tpd)	Adj Factor	Δ 2008 Base	Δ 2030 Baseline	
2008	2R1N	1277	2.0	100%	192%	723	1.0	0%	155%	5.9
	1.5R1N	958	1.5	50%	119%					4.4
	1R1N	639	1.0	0%	46%					2.9
2030	1R'2.5N'	437	1.0	-32% from 1R -54% from 1.5R	0%	710	2.5	-2%	150%	2.1
	1R'1.75N'					497	1.75	-31%	75%	2.9
	1R'1N'					284	1.0	-61%	0%	5.1
	1R'.75N'					213	0.75	-70%	-25%	6.8
	1R'.5N'					141	0.5	-81%	-50%	10.4
	1R'.3N'					85	0.3	-88%	-70%	17.1

Figure 1-7. Ozone remaining relative to the 2008 base simulation with base ROG emissions (left half) and base ROG x 1.5 (right half) in percent for future year simulations with 2030 baseline ROG and varying incremental reduction in NOx emissions. 2008 base and 2030 baseline ROG and NOx emissions (highlighted in the grey) are shown in the table along with sensitivity cases with varying adjustments to NOx emissions. R and N denote 2008 base ROG and NOx emission and R' and N' denote 2030 baseline ROG and NOx emissions.

- If 2008 base ROG emissions are underestimated by 50% (right half of Figure 1-7), ozone levels are reduced by about 30% at all sites in the basin with 2030 baseline ROG (-54% from 2008, 958 to 437 tpd) and NOx remaining at 2008 levels. NOx reductions are counterproductive or ineffective in the western and central basin even with 88% reduction. Only the eastern basin show marginal further reduction in ozone.
- Using the relative response factors (RRF)[6] referenced to the 2008 simulations with base ROG emissions (left half of Figure 1-8), all projected design values will exceed the ozone NAAQS even with 88% NOx reduction. DVs for the western and central basin are projected to be equal to or higher than 2008 levels with 50% reduction from 2030 baseline (-81% from 2008). If 2008 base ROG emissions are underestimated by 50% (i.e., ROG reductions from 2008 of -54% rather than -32%), all sites except Crestline show attainment with NOx emissions remaining at 2008 levels (right half of Figure 1-8) (Case 1). Close to 90% reduction in NOx would be required to show attainment at Crestline (Case 2). Failure to reach 90% NOx reduction would leave the central basin in nonattainment of the ozone NAAQS due to NOx disbenefit.

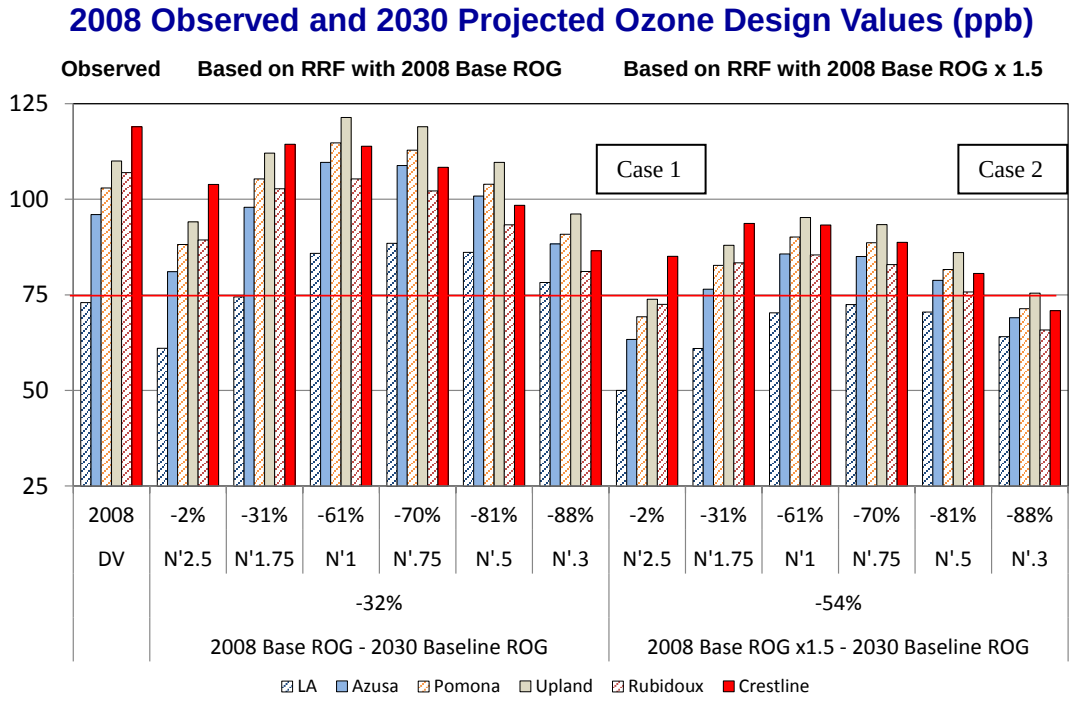

Figure 1-8. 2008 observed (baseline) design value and 2030 projected future design values (ppb) based on relative response factors reference to 2008 simulation with base ROG emissions (left half) and to the 2008 simulation with base ROG x 1.5 (right half). R and N denote 2008 base ROG and NOx emission and R' and N' denote 2030 baseline ROG and NOx emissions.

[6] Attainment is demonstrated using ratios of the model's future to current (baseline) predictions at monitoring locations. These ratios are called relative reduction factors (RRF). Future ozone concentrations are estimated by multiplying the modeled RRF at a location near the monitoring site by the baseline design value (DV) of the site as follows: DV(future year) = RRF x DV(baseline).

Objective 4 - Ozone response to changes in VOC/NOx ratios and efficiency of ozone formation.

- Changes in precursor emissions over the recent decade correspond to predicted maximum ozone concentrations that move essentially parallel to the ozone isobars in the isopleth diagram shown in (Figure 1-9 left) resulting in little net change in ozone concentrations. Note that all of the points lie above the ridgeline in the VOC limited area and that further incremental changes in VOC and NOx emission beyond the baseline 2030 emission occur very near the ridgeline. Ozone production and its daily maximum concentrations are highly nonlinear functions of the available NOx and VOC as shown in the ozone isopleth diagrams.
- The efficiency of NOx to produce ozone becomes more efficient as the concentration of NOx is decreased (Figure 1-9 right). This effect will change the spatial distribution of ozone, increasing it in the central air basin and lowering it towards the eastern basin.
- Reductions in VOC always lead to lower peak ozone concentrations. Reductions in NOx tend to increase the formation rate of ozone and may lead to higher or lower peak ozone concentrations when ozone formation is VOC-limited.

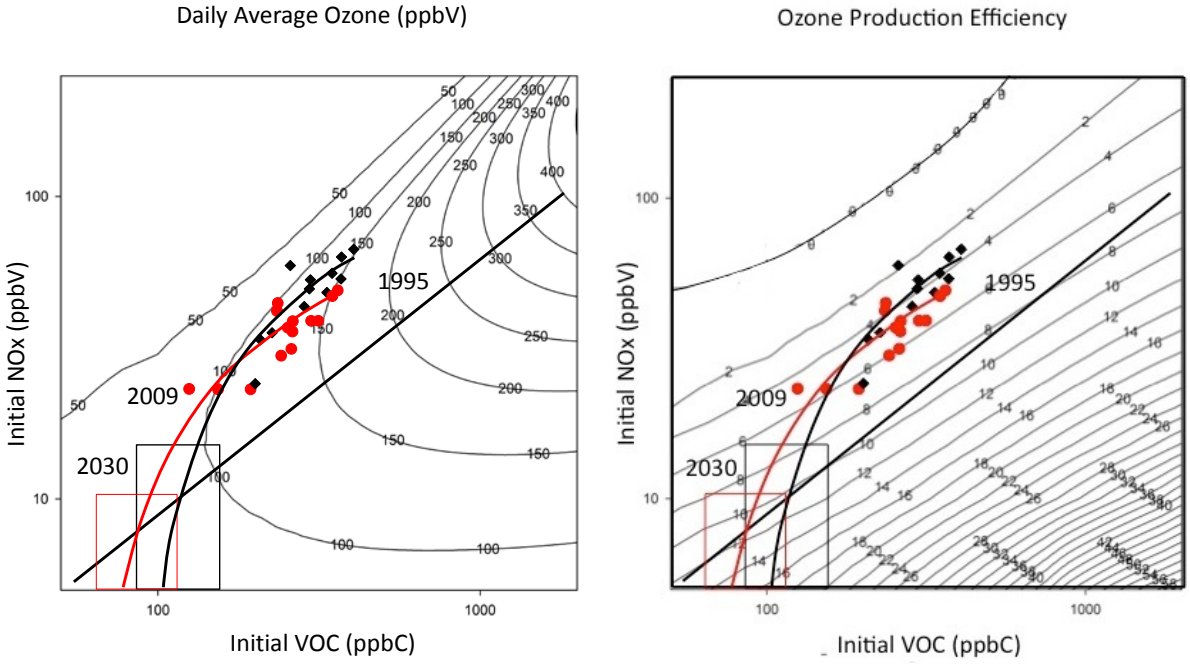

Figure 1-9. Isopleths for daily average ozone (left) and efficiency of ozone formation (right) for Upland-San Bernardino. Plotted on the ozone isopleths are average values of VOC and NOx for the years 1995-2011. The black diamonds are weekday averages and the red circles are weekends. Projections for 2030 are plotted as rectangles on the isopleths where the black rectangle represents weekdays and the red rectangle represents weekends. The trend lines for the VOC and NOx weekday (black line) and weekend (red line) concentrations are plotted. The ozone ridge-line is plotted in the ozone production efficiency isopleth for reference to the ozone isopleth.

1.4 Conclusions

The South Coast Air Quality Management District (SCAQMD) and the California Air Resources Board (CARB) are implementing a long-term multi-pollutant (ozone and $PM_{2.5}$) control strategy that is primarily NOx focused. Based on preliminary evaluations, the SCAQMD and CARB predict that reductions in NOx emissions from current levels of about 90% will be necessary to attain the ozone NAAQS (SCAQMD, 2013; CARB, 2014). These reductions equate to allowable emissions of NOx in the basin ("carrying capacity") of 80 tons per day (SCAQMD, 2013) compared to 2008 emissions of 723 tpd and projected 2030 "baseline" emissions of 284 tpd. The 2030 baseline takes into account the effects of only currently adopted control programs, which include the LEV (Low Emission Vehicle) -III standards. Thus, substantial additional NOx reductions (204 tpd) will be needed beyond currently adopted control measures. For perspective, on-road vehicles account for 95 tpd of NOx in the 2030 baseline inventory. Eliminating all remaining NOx emissions from on-road vehicles would leave a residual of 189 tpd, which more than doubles the projected carrying capacity. SCAQMD acknowledges that "it would be the greatest air quality challenge the region has ever faced relative to achieving the additional NOx emission reductions that would be necessary, and would further necessitate transformational technologies with zero or near-zero combustion emissions" (SCAQMD, 2013).

A NOx-focused control strategy for the SoCAB is based upon an implicit expectation that, with sufficient NOx reductions, ozone formation will transition from VOC to NOx limited ozone formation throughout the basin and further VOC reductions will not be effective at that point. As ozone formation is currently VOC limited in the basin, model simulations with the 2030 baseline emissions (-61% for NOx and -32% for ROG from 2008) predict 10-20 percent higher peak ozone levels in the western and central basin compared to 2008 levels. With further reductions of NOx emissions of 50% beyond the 2030 baseline (-81% from 2008), ozone levels in the western and central basin are predicted to remain comparable to 2008 levels and ozone will be reduced only in the eastern basin (~15% lower than 2008). Benefits of the projected reductions of ozone in the eastern basin will be offset by the likelihood that the basin maximum ozone site will have shifted by this time to the central basin. Falling short of the NOx reductions necessary to completely transition ozone formation in the SoCAB from VOC to NOx sensitivity (approaching -90% from 2008) would simply shift the basin DV site westward from the eastern basin to more populated areas of the western and central basin.

NOx disbenefit, though counterintuitive, is a well-established aspect of ozone photochemistry and the nonlinear nature of the ozone-precursor relationship. Past studies have also associated the root cause of the weekend ozone effect to a weekly inadvertent demonstration of NOx disbenefit (see Section 2.3). Despite its importance to understanding future ozone trends in the SoCAB, regulatory agencies have generally avoided public discussions of NOx disbenefit. For example, Figure 1-10 is a slide from the California Air Resources Board staff's presentation at the February 20, 2014 Board Meeting showing the ozone remaining (in percent) after independently reducing NOx or VOC by 75, 80 or 90 percent from 2012 with the other held at 2030 baseline level. Results are shown for Crestline only and for NOx reductions at which ozone chemistry begins to transition to NOx limitation, thus avoiding the interim period of NOx disbenefit. Figure 1-11 shows the A-91 results for Crestline (red bars) for emission reduction scenarios similar to Figure 1-10 as well as the monitoring sites in the western and central basin and for NOx reductions less than 75%. The red bars (Crestline) in Figure 1-11 indicated by arrows are roughly comparable to the blue bars in Figure 1-10 indicated by arrows.

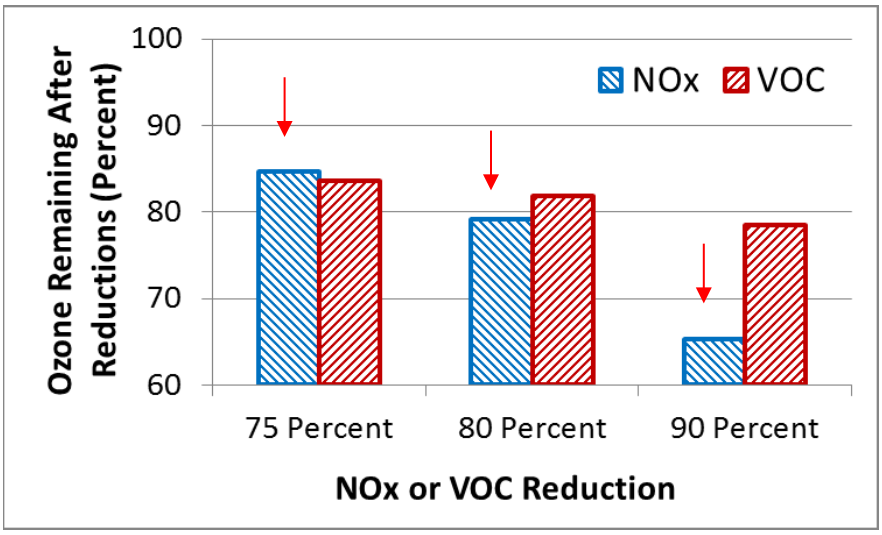

Figure 1-10. Slide 20 from California Air Resources Board staff presentation " Science of Ozone and PM2.5 Chemistry in the South Coast Air Basin and San Joaquin Valley" at the February 20, 2014 Board meeting in Sacramento, CA. These results are for Crestline only (personal communication with CARB Staff, 2014).

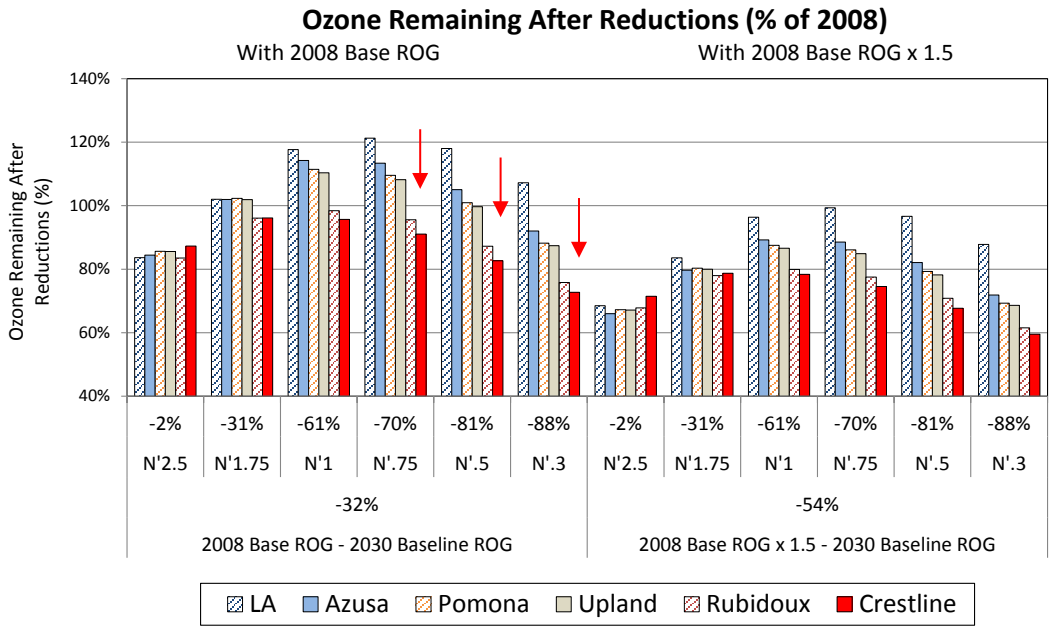

Figure 1-11. Response of ozone to incremental NOx reductions holding ROG emissions constant at 2008 base emissions. CRC A-91 results plotted in the same manner as slide 20 in CARB staff's presentation at the February 20, 2014 Board meeting in Sacramento, CA. The bars indicated by red arrows correspond roughly to the blue bars indicated by red arrow in Figure 1-10.

An important finding of the A-91 Study, which is supported by other recent work (Fujita et al., 2012; Fujita et al., 2013), is that current estimates of ROG emissions are underestimated by about 50%. As a result, the ROG emission reductions that are achievable by currently adopted controls (e.g., LEV-III vehicle standards) could be larger (-54% rather than -32% from 2008) than presently estimated. The 2008 simulation with base ROG x 1.5 predicts higher ozone levels at all sites than with the base ROG emissions. The upward adjustment of the base ROG inventory leads to lower relative response factors (RRF) and lower projected design values (DV).[7] Implications of the base ROG underestimation are apparent by comparing the 2008 observed site-specific DVs in Figure 1-8 with the two alternative sets of 2030 projected DVs. The projected DVs are much closer to the NAAQS using RRFs referenced to the 2008 simulations with base ROG x 1.5 (right half) than with the base ROG (left half). The projected DVs for Case 1 show attainment for all sites except Crestline with ROG at 2030 baseline (-54% from 2008 with base ROG x1.5) and zero reduction in NOx from 2008. VOC reductions effectively lower ozone when ozone formation is VOC limited. Once committed to a NOx-focus control strategy, NOx reductions approaching 90% from 2008 will be required to demonstrate attainment at all sites (Case 2). The effects of increasing incremental reductions of NOx emissions between Case 1 and Case 2 illustrate the consequences of NOx disbenefit on the spatial variations in peak ozone levels within the basin. While ROG reductions can reduce the effects of NOx disbenefit, simultaneous NOx reductions negate the benefits of ROG only reductions when ozone formation is VOC limited. VOC reductions become less effective relative to NOx reductions after ozone formations transitions to NOx limitation as shown Figure 1-10.

The effects of changes in VOC and NOx emissions on the formation of secondary organic aerosol was beyond the scope of the A-91 Study and should be examined relative to the changes in ozone and particulate nitrate. As a final note, the demonstrations of future attainment of the ozone NAAQS assumes that the projected emission reductions are actually achieved. Given the evidence that motor vehicle ROG emissions were underestimated in past emission inventories, steps should be taken to verify and ensure that the projected reductions of on-road vehicle ROG emissions from the LEV-III emission standards, especially for evaporative emissions, are fully achieved and the disproportionate contributions of the remaining high emitting vehicles are minimized.

1.5 References

California Air Resources Board. 2012. Ozone trend summary for the South Coast Air Basin, http://www.arb.ca.gov/adam/trends/trends2.php (accessed May 29, 2012).

California Air Resources Board staff presentation " Science of Ozone and PM2.5 Chemistry in the South Coast Air Basin and San Joaquin Valley" at the February 20, 2014 Board meeting in Sacramento, CA.

[7] As described in Section 2.6, the projected DV is estimated by multiplying the current observed DV by the RRF, which is the ratio of the model's future to current (baseline) prediction at monitoring locations. Attainment is deemed to be demonstrated if the projected future year DV is less than the NAAQS.

Fujita, E.M., W.R. Stockwell, D.E. Campbell, and R.E. Keislar (2003). Evolution of the Magnitude and Spatial Extent of the Weekend Ozone Effect in California's South Coast Air Basin from 1981 to 2000. *J. Air & Waste Manage. Assoc.* 53:802-815

Fujita E.M., D.E. Campbell, B. Zielinska, J.C. Chow, C.E. Lindhjem, A. DenBleyker, G.A. Bishop, B.G. Schuchmann, D.H. Stedman, and D.R. Lawson. 2012. Comparison of the MOVES2010a, MOBILE6.2 and EMFAC2007 mobile source emissions models with on-road traffic tunnel and remote sensing measurements. *J. Air Waste Manage. Assoc.* 62:1134–1149. doi:10.1080/10962247.2012.699016

Fujita, E.M.; Campbell, D.E.; Stockwell, W.R.; Lawson, D.R. (2013). Past and future ozone trends in California's South Coast Air Basin: Reconciliation of amibnet measurements with past and projected emission inventories. *J. Air & Waste Manage. Assoc.* 63:1, 54-69. DOI: 0:1080/10962247.2012.735211

South Coast Air Quality Management District (2013). Final 2012 Air Quality Management Plan. SCAQMD, diamong Bar, CA, Feburary 2013.

2. BACKGROUND AND PERSPECTIVE

This background chapter explains the impetus for the CRC A-91 study and provides the information necessary to understand the study objectives and technical approach. Sections 2.2 and 2.3 compare the historic trends in emissions and ambient concentrations of VOC and NOx with corresponding changes in the spatial and temporal (diurnal and day of week) variations of peak ground-level ozone concentrations in the SoCAB. Section 2.1 describes the underlying photochemical processes in the atmosphere that explain the nonlinear relationship of the formation of ozone and other products of photochemical reactions to changes in VOC and NOx, and Section 2.4 relates the historic changes in VOC and NOx concentrations and VOC/NOx ratios to the 30-year evolution of the ozone-precursor relationship in the SoCAB. With these subsections for context, Section 2.5 describes the preliminary assessments by the South Coast Air Quality Management District (SCAQMD) and California Air Resources Board (CARB) of the precursor emission reductions that would be necessary to attain the National Ambient Air Quality Standard (NAAQS) for 8-hour average ozone of 75 ppb[8] by the attainment date of 2032. CRC A-91 was conducted to reproduce the results of these initial evaluations and to determine the relative response of peak ozone levels to varying relative reductions of NOx and VOC emissions. Section 2.6 summarizes the results of past evaluations of emission inventory uncertainties and explains their implications for modeled projections of attainment of the ozone standard.

2.1 Fundamentals of Ozone Formation

Much of the difficulty in addressing the ozone problem is due to its complex chemistry in which ozone formation is a nonlinear function of the amount and relative mix of VOC and NOx. Decreases in NOx or VOC do not always lead to lower ozone levels. Depending upon the relative concentrations of VOC and NOx and the specific mix of VOC, the rate of ozone formation can be more sensitive to changes in VOC alone or to changes in NOx alone or to simultaneous changes in both VOC and NOx. Under certain conditions NOx reductions may result in higher peak ambient ozone levels in some areas of the basin. However, NOx reductions reduce nitric acid (HNO_3), the precursor to ammonium nitrate, which is a major component of airborne fine particulate matter ($PM_{2.5}$) in the basin. This ozone/$PM_{2.5}$ control conundrum, ozone NOx disbenefit, and day-of-week variations in ozone levels are manifestations of the nonlinear nature of the ozone-precursor relationship. The effect of varying magnitudes and relative amounts of VOC and NOx on the rate and efficiency of ozone formation is fundamental to understanding this nonlinear relationship.

The photochemical processes in the atmosphere that lead to the formation of ozone and products of photochemical reactions are well known (Seinfeld, 1986; Finlayson-Pitts and Pitts, 1986; Stockwell et al. 2012). The only significant chemical reaction producing ozone in the atmosphere is the reaction of atomic and molecular oxygen. At lower altitudes, where only UV radiation with wavelengths greater than 280 nm is present, the only significant oxygen atom production is from photodissociation of nitrogen dioxide (NO_2) into nitric oxide (NO) and oxygen atoms, O, Reaction (1). The oxygen atoms react with molecular oxygen to produce O_3, Reaction (2).

[8] EPA is currently considering a lower standard between 60 and 70 ppb based upon the recommendations from the latest 5-year review of the ozone standard by the Clean Air Scientific Advisory Committee (CASAC).

$$NO_2 + h\nu \rightarrow NO + O \qquad (1)$$

$$O(^3P) + O_2 + M \rightarrow O_3 \qquad (2)$$

When nitrogen oxides are present, O_3 reacts rapidly with NO to regenerate NO_2, Reaction (3).

$$O_3 + NO \rightarrow NO_2 + O_2 \qquad (3)$$

The first and third reactions occur rapidly, establishing a steady-state equilibrium ozone concentration $[O_3]$ that is determined by the "O_3-NO-NO_2-photostationary state equation," Equation (4)

$$[O_3] = \frac{J_1[NO_2]}{k_3[NO]} \qquad (4)$$

where J_1 is the photolysis frequency of Reaction (1), k_3 is the rate constant for Reaction (3), $[NO_2]$ and [NO] are the concentrations of nitrogen dioxide and nitric oxide. Because these reactions only recycle O_3 and NO_x, they are insufficient, by themselves, to produce new ozone. When carbon monoxide or volatile organic compounds are present, however, their oxidation produces the hydroperoxy radical (HO_2) and organic peroxy radicals (RO_2), which react with NO to form NO_2. The resulting higher concentrations of NO_2 produce O_3 while the resulting lower NO concentration reduce the rate of O_3 loss; together these processes allow ozone to be increased.

The hydroxyl radical (HO) is the key reactive species in the formation of O_3 in that it initiates the oxidation of VOCs that form the peroxy radicals. A fraction of O_3 photolyzes to produce an excited oxygen atom, $O(^1D)$, Reaction (5), which reacts with water to produce HO radicals, Reaction (6).

$$O_3 + h\nu \rightarrow O(^1D) + O_2 \qquad (5)$$

$$O(^1D) + H_2O \rightarrow 2\ HO \qquad (6)$$

Other sources of HOx radicals include the photolysis of carbonyl compounds and smaller contributions due to nitrous acid (HONO) and other radical precursors. The HO radicals react with CO or organic compounds (RH) to produce peroxy radicals (HO_2 or RO_2). The peroxy radicals react with NO to produce NO_2 which photolyzes to produce additional O_3:

$$CO + HO\ (+O_2) \rightarrow CO_2 + HO_2 \qquad (7)$$

$$RH + HO \rightarrow R + H_2O \qquad (8)$$

$$R + O_2 + M \rightarrow RO_2 + M \qquad (9)$$

$$RO_2 + NO \rightarrow RO + NO_2 \qquad (10)$$

$$RO + O_2 \rightarrow HO_2 + CARB \qquad (11)$$

$$HO_2 + NO \rightarrow HO + NO_2 \qquad (12)$$

The net reaction is the sum of Reactions (8) through (12) plus twice Reactions (1) and (2):

$$RH + 4\ O_2 + 2\ h\nu \rightarrow CARB + H_2O + 2\ O_3 \qquad (13)$$

where CARB is a carbonyl species, either an aldehyde (R'CHO) or a ketone (R'CR"O). The carbonyl compounds may further react with HO or they may photolyze to produce additional

peroxy radicals that react with NO to produce NO_2 (Seinfeld, 1986; Finlayson-Pitts and Pitts, 1986). The degradation reactions for all classes of VOCs, in addition to the conversion of NO to NO_2 and the formation of O_3, lead to the formation of carbonyl compounds (aldehydes, ketones, hydroxycarbonyls, and dicarbonyls), organic acids, organic nitrates (including peroxyacyl nitrates, the simplest member of which is peroxyacetyl nitrate [PAN]). PAN thermally decomposes back to its reactants, NO_2 and acetylperoxy radical but the decomposition rate is strongly temperature dependent slowing at lower temperatures. Thus, PAN can serve as a nighttime reservoir for NOx and a means of transport of NOx to downwind areas. Carbonyl compounds that are produced from hydrocarbon oxidation (Reaction 11) can be important reactive VOCs themselves, and thus important sources of peroxy radicals responsible for O_3 production.

Ozone Production Efficiency

As shown above, NOx can be considered as a catalyst for the production of ozone from VOC. The O_3 production mechanism is a chain reaction mechanism involving the initial production of HO radicals, the propagation of the radicals and their termination reactions.

Production $\rightarrow$ HO
HO + VOC $\rightarrow$ … HO_2 and RO_2

$HO_2 + NO \rightarrow NO_2 + HO$	Propagation
$RO_2 + NO \rightarrow NO_2$ + Organic Products + HO_2	Propagation

The free radical chain reactions are terminated when NOx is converted to nitric acid, organic nitrates and peroxides.

$HO + NO_2 \rightarrow HNO_3$	Termination	(14)
$RO_2 + NO \rightarrow RNO_3$	Termination	(15)
$RCO_3 + NO_2 \rightarrow$ PAN	Termination	(16)
$HO_2 + HO_2 \rightarrow H_2O_2$	Termination	(17)
$HO_2 + RO_2 \rightarrow HO_2R$	Termination	(18)
$RO_2 + RO_2 \rightarrow RO_2R$ + CARB + Alcohols	Termination	(19)

NOx chain-length is a measure of ozone production efficiency. Chain-length is the rate of propagation divided by the rate of termination. An approximation to the NOx chain-length is the ozone production divided by the NOx converted to HNO_3, PAN and organic nitrates (NOy). As the atmospheric concentration of NOx decreases the ozone production efficiency should increase due to lower rates of termination.

2.1.1 Dependence of Ozone Production Efficiency on VOC/NOx Ratios

Ozone formation is nonlinear with respect to concentrations of VOCs and NOx because they compete with one another for the HO radicals. Figure 2-1 shows the linkages among the reactions that propagate radicals and those that remove them. VOCs are consumed in the sequence of O_3 formation, while both HO/HO_2 and NOx act as catalysts. Termination occurs

when HO_2 combines to form hydrogen peroxide (H_2O_2) or by reaction of HO with NO_2 to form HNO_3. The production efficiency of O_3 per molecule of NOx varies with total concentration of NOx and the ratio of VOC to NOx. At low VOC-to-NO_2 ratios, HO reacts predominantly with NO_2 to form nitric acid, which removes radicals and retards O_3 formation. This reaction is a major sink of NOx because HNO_3 reacts slowly, and it is rapidly removed due to dry and wet deposition. Under these conditions, a decrease in NOx concentration favors O_3 formation (i.e., "NOx disbenefit"). High ratios of VOC to NOx concentration favor HO reaction with VOCs that generate new radicals that accelerate O_3 production. At a sufficiently low concentration of NOx, or a sufficiently high VOC-to NO_2 ratio, a further decrease in NOx favors peroxy-peroxy reactions, which retard O_3 formation by removing free radicals from the system. The diagrams in Figure 2-2 illustrate that ozone formation is suppressed at both high and low VOC/NOx ratios.

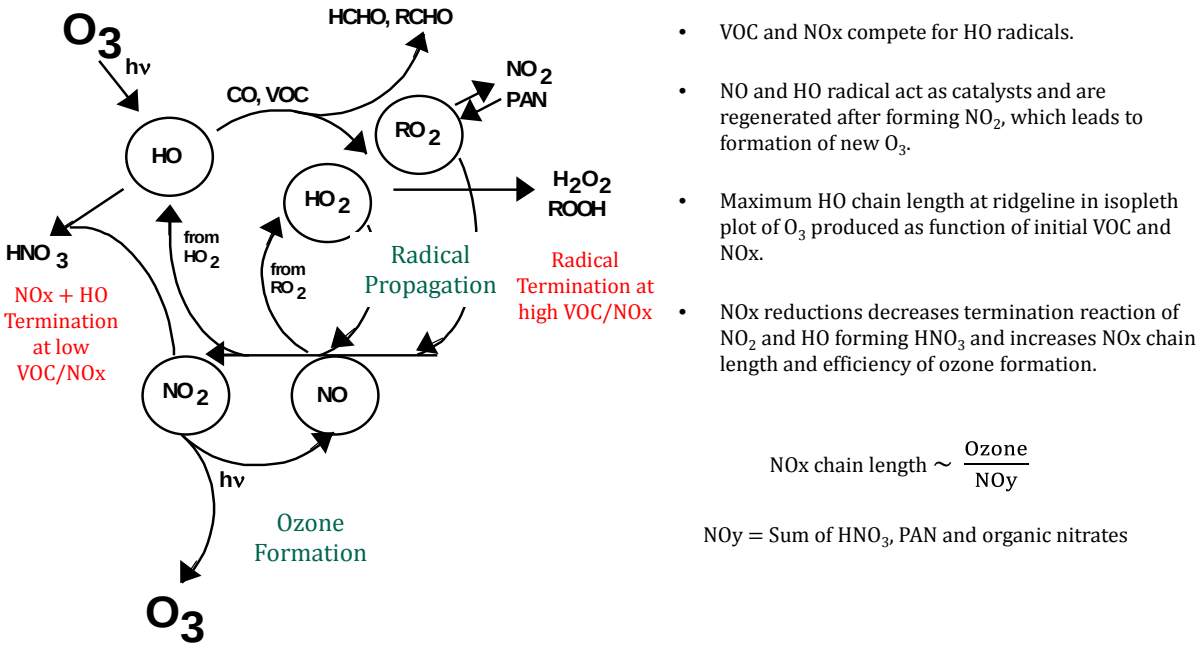

Figure 2-1. Schematic representation of ozone photochemistry showing the linkages among the reactions that propagate radicals and those that remove them.

O_3 isopleth diagrams, such as the example in Figure 2-3 (Stockwell et al. 1990), are used to represent the dependence of O_3 production on the initial amounts of VOC and NOx. To generate this plot, O_3 formation is simulated in a hypothetical well-mixed box of air from ground to the mixing height that is transported from an urban center to a downwind location of maximum ozone concentrations. Multiple simulations are performed with varying initial concentrations of NOx and anthropogenic VOC. At a given level of VOC, there exists a NO_x mixing ratio at which a maximum amount of ozone is produced. The optimum VOC/NOx ratio, expressed as a molar ratio of VOC in ppbC to NOx in ppbN, is about 10-12 and corresponds to the ridgeline in the isopleth plot. The HO radical chain length, which is the number of times a

newly formed HO radical is regenerated through radical chain propagation before it is destroyed, reaches a maximum at this VOC/NOx ratio. Thus, the ridgeline corresponds to the VOC/NOx ratio at which O_3 is most efficiently formed.

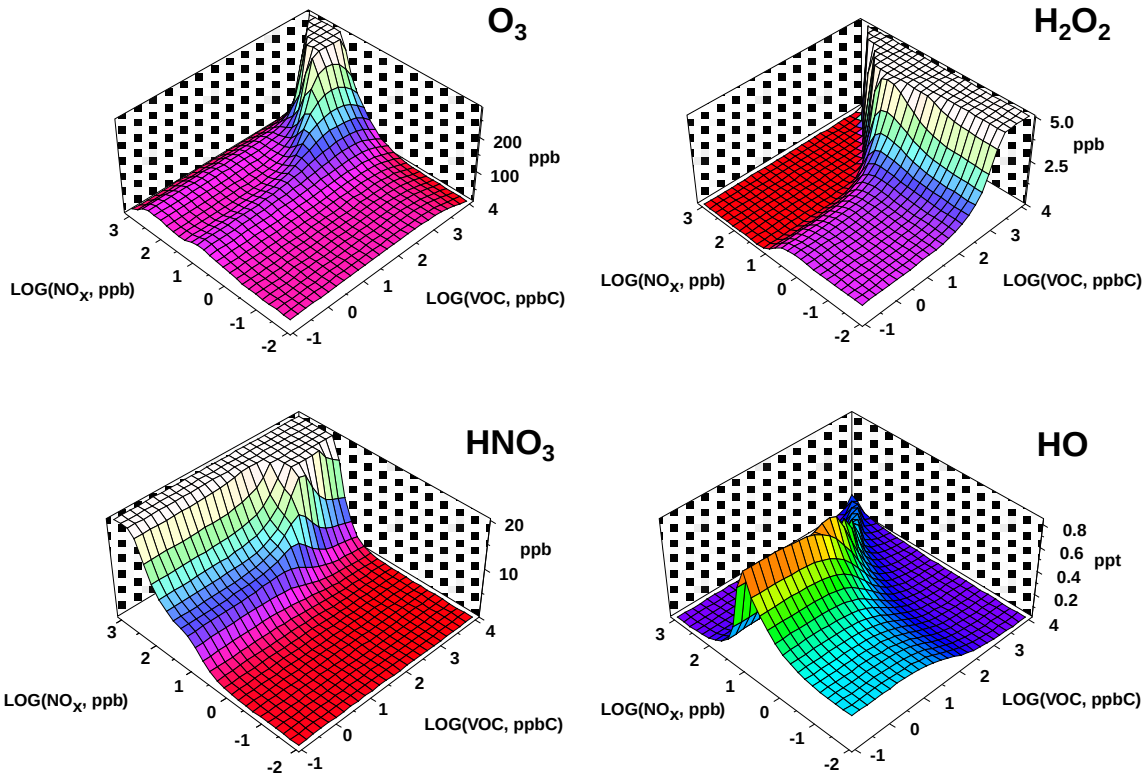

Figure 2-2. Isopleth diagrams representing the dependence of O_3, H_2O_2, HNO_3 and HO production on the initial amounts of VOC and NOx. Source: Stockwell et al., 1990).

Reductions of VOC and NOx emissions have varying effects on the rate and efficiency of ozone formations depending on the ratio of VOC and NOx relative to this ridgeline. The region below the ridgeline at low NOx concentrations is commonly described as "NOx-limited" where lowering NOx effectively reduces O_3 (case #3) and reductions in VOC have practically no effect on maximum O_3 (case #1). Ozone is effectively reduced near the ridgeline by simultaneous reductions in VOC and NOx emissions. The region above the ridgeline is described as "radical-limited" or "VOC-limited" (i.e., lowering VOC, as shown in case #2 effectively reduces O_3). A reduction in NO_x under VOC-limited conditions (case #4) lowers the rate at which OH and NO_2 are removed by formation of HNO_3 and leads to an increase in maximum O_3. "NO_x-disbenefit" refers to this situation. The well documented "weekend ozone effect" (i.e., higher or near equal weekend ozone values with substantially reduced NO_x emissions relative to weekdays) is indicative of VOC-limitation with respect to ozone formation.

Aging of the pollutant mix alters the initial VOC/NOx ratio and rate of ozone formation as pollutant emissions are transported across the SoCAB by the prevailing onshore winds. The

instantaneous VOC/NOx ratios tend to increase during transport because HO reacts more rapidly with NO_2 than with VOCs. Thus NOx is removed more rapidly from the system than VOCs and accounts for the tendency for O_3 formation to be NOx-limited in far downwind areas. Thus, VOC/NOx ratios vary within the air basin, resulting in either NOx-limited or VOC-limited areas depending upon the time of day, the mix and type of emission sources, timing of additional fresh emissions, and pattern of pollutant transport. These factors lead to differing diurnal variations and locations of peak ozone levels within the basin. While reductions in VOC emissions are effective in reducing peak ozone level in and near source regions with low VOC/NOx ratios, NOx emission reductions are more effective in reducing peak ozone levels in areas with high VOC/NOx ratios or in downwind receptor regions with few local emission sources.

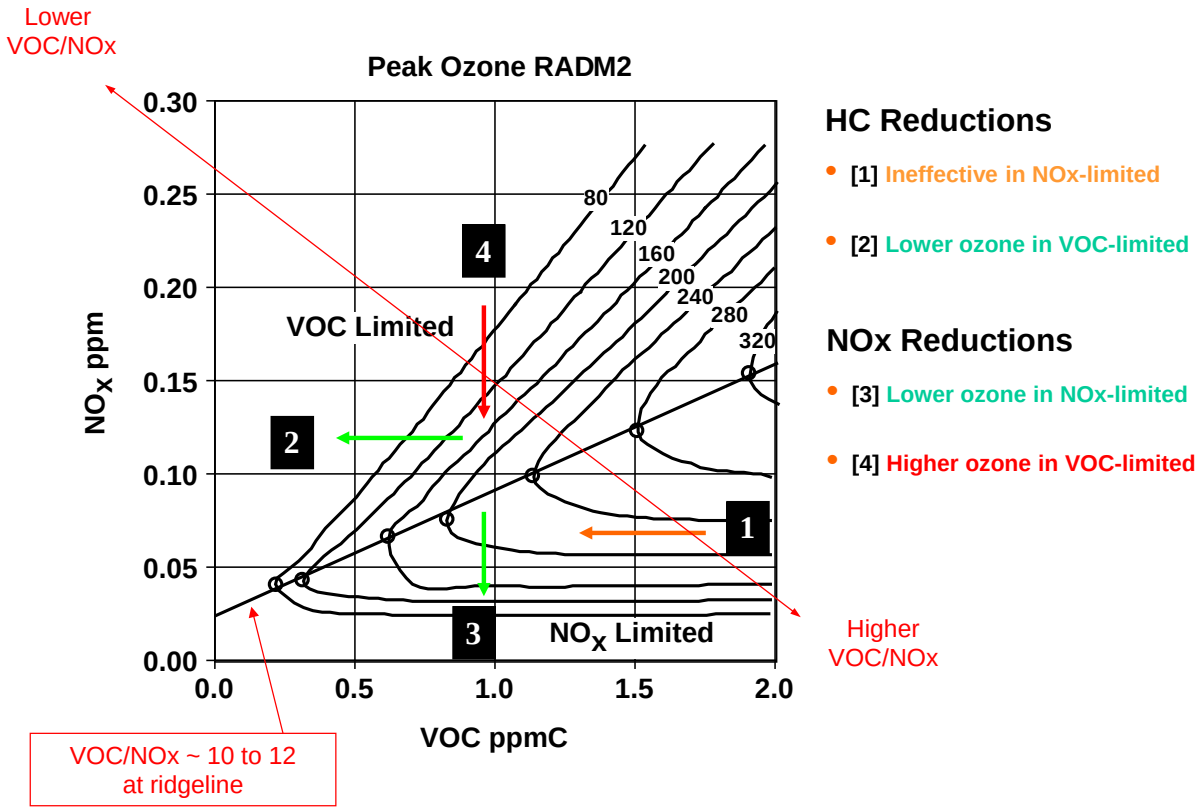

Figure 2-3. Isopleth diagram representing the dependence of O_3 (ppb) on the initial VOC (ppmC) and NOx (ppm) and effects of HC or NOx reductions. Source: Stockwell et al., 1990).

2.1.2 Indications of VOC- or NOx-Limited Ozone Formation

Observational methods that have been applied in past studies to infer VOC- or NOx-limited O_3 chemistry include VOC/NOx ratios, correlations of peak O_3 levels with oxidized nitrogen species, ratios of peak to potential O_3 or extent of reaction, day-of-week variations in

peak ozone, extent of ozone inhibition and ozone accumulation rates, upwind versus downwind pollutant levels and relative contribution of biogenic emissions to ambient VOC. Table 2-1 lists some important indicators of NOx limitation. If the region is not NOx limited then it is VOC limited. NOx is defined as the sum of NO and NO_2 while NOy is defined as the sum of the atmospheric concentrations of NOx, HNO_3, organic nitrates and inorganic nitrates. The sum of HNO_3, organic nitrates and inorganic nitrate is known as NOz. NOy represents the nitrogen budget of the atmosphere excluding NH_3. There is a good correlation between O_3 and NOy if the region is NOx limited, and the correlation is poor if it is not. Under typical atmospheric concentrations a low level of reactive nitrogen will indicate that the region is NOx limited. Milford et al. (1994) found that the threshold is between 10 and 26 ppb of NOy. Alternatively, the atmosphere is NOx limited if the O_3/NOy ratio is greater than 5 to 10 (Sillman, 1995; Jacob et al., 1995). Finally the ratio (O_3 - 40 ppb)/NOy is identical in concept to the O_3/NOy ratio except that O_3 values less than background levels of 40 ppb are excluded.

Table 2-1. Indicators of NOx limitation and references.
(http://www.epa.gov/oar/oaqps/pams/analysis/noy/noxtxt.html#indicator_methods)

Indicator	**Threshold for NOx-Limitation**	**Reference**
NOy	< 10 to 25 ppb	Milford et al., 1994
NOz	< 5 to 20 ppb	Milford et al., 1994
O_3/NOy	> 5 to 10	Sillman, 1995; Jacob et al., 1995
O_3/NOz	> 6 to 11	Sillman, 1995; Jacob et al., 1995
(O_3 - 40 ppb)/NOy	> 4	Sillman, 1995; Jacob et al., 1995
HCHO/NOy	> 0.2 to 0.4	Sillman, 1995; Jacob et al., 1995
H_2O_2/HNO_3	>0.3 to 0.5	Sillman, 1995; Jacob et al., 1995
H_2O_2/NOy	> 0.2 to 0.4	Sillman, 1995; Jacob et al., 1995
H_2O_2/NOz	> 0.2	Sillman, 1995; Jacob et al., 1995
Morning NMOC/NOx	> 10 to 15	National Research Council (1991)
Afternoon NMOC/NOx	> 15 to 20	National Research Council (1991)

As discussed above the peroxy radicals that produce O_3 either terminate in the formation of HNO_3 or other nitrates or the peroxy radicals terminate to produce H_2O_2, CH_3O_2H or other peroxides. Under conditions where NOx is relatively more abundant than VOC, the fraction of radicals that terminate to produce nitrates is also greater while the opposite is true if VOC is relatively more abundant than NOx. The atmosphere is considered NOx limited if the slope of the plot of the maximum O_3 concentration as a function of NOx is greater than about 8. The atmosphere is VOC limited if the slope of the plot is less than about 5 (Milford et al., 1994). The ratio O_3/NOz is an indicator of the O_3 production efficiency of nitrogen oxides; it represents the number of O_3 molecules produced per molecules of NOx converted to NOz. If O_3/NOz is relatively high, then the O_3 production is efficient and that occurs when NOx concentrations are low relative to VOC; if the ratio is greater than 6 to 11, the atmosphere is NOx limited (Sillman, 1995; Jacob et al., 1995).

The reactions that produce peroxy radicals that convert NO to NO_2 also lead to the production of HCHO and other carbonyl containing compounds. If VOC concentrations are relatively high, then more HCHO is produced relative to the NOx converted to NOy. The ratio HCHO/NOy will be high if the atmosphere is NOx limited and the threshold is a value of HCHO/NOy greater than 0.2 to 0.4. Similar reasoning applies to the ratios: H_2O_2/HNO_3, H_2O_2/NOy, H_2O_2/NOz. For H_2O_2/HNO_3 either the peroxy radical chains are terminating by the reaction, $HO_2 + HO_2 (+M + H_2O) \rightarrow H_2O_2$ under conditions of higher VOC or the reaction, $HO + NO_2 (+M) \rightarrow HNO_3 (+M)$. If the peroxy radical chains tend to terminate to produce H_2O_2, then the atmosphere will be NOx limited. It will be VOC limited if they terminate to form HNO_3. H_2O_2/HNO_3 greater than 0.3 to 0.5 indicated that the atmosphere is NOx limited (Sillman, 1995; Jacob et al., 1995). H_2O_2/NOy represents the fraction of HO_2 radicals reacting to produce H_2O_2 to the total nitrogen and it will be high, greater than 0.2 to 0.4 if the atmosphere is NOx limited. H_2O_2/NOz is the ratio of H_2O_2 to the total amount of NOx converted to NOz; if this ratio is high, greater than 0.2, then the atmosphere is NO_x limited.

2.1.3 Formation of Nitric Acid and Particulate Ammonium Nitrate

In additional to ozone, the SoCAB also exceeds the NAAQS for $PM_{2.5}$ (12 $\mu g/m^3$ annual average and 35 $\mu g/m^3$ 24-hour average). Particulate nitrate is a major component of $PM_{2.5}$ in the SoCAB and has been a major focus of control programs to reduce the concentrations $PM_{2.5}$ in the basin. As described previously, nitric acid (HNO_3) plays a key role in ozone formation as a terminal reaction product that inhibits ozone formation. The main daytime source of nitric acid is the reaction of nitrogen dioxide with hydroxyl radical:

$$NO_2 + HO \rightarrow HNO_3. \qquad (14)$$

While the formation of ozone and particulate nitrate in the atmosphere are chemically related, there are differences that lead to varying diurnal and seasonal patterns in their ambient levels. Formation of HNO_3 by reaction (14) occurs mostly during the daytime because sufficiently high concentrations of HO radicals are present only during the day. Reaction of HNO_3 with ammonia (NH_3) yields particulate ammonium nitrate (NH_4NO_3). NH_3 is a primary pollutant directly emitted by motor vehicles and livestock operations in the eastern Basin (Cass et al., 1982). Ammonium nitrate is in equilibrium with NH_3 and HNO_3 at typical summertime temperatures in southern California, but particulate nitrate is favored overnight when temperatures are lower and relative humidy is greater. Nitric acid can also form during the night in a series of reactions involving NO_2, H_2O, and O_3. First ozone reacts with nitrogen dioxide to form NO_3:

$$NO_2 + O_3 \rightarrow NO_3 + O_2, \qquad (15)$$

During the daytime the NO_3 is rapidly photolyzed. NO_3 quickly photodissociates soon after it is formed so it does not accumulate (Stockwell et al., 1997):

$$NO_3 + h\upsilon \rightarrow NO + O_2. \qquad (16)$$

The net effect is that the production of HNO_3 by the heterogeneous gas phase reaction of N_2O_5 and H_2O is minimal during the day. However, during the nighttime, NO_3 accumulates as NO_2 reacts with O_3 (Calvert and Stockwell, 1983) in the absence of NO.

The newly formed NO_3 may react with NO_2 to produce N_2O_5:

$$NO_3 + NO_2 \leftrightarrow N_2O_5. \quad (17)$$

N_2O_5 exists in equilibrium with NO_2 and nitrate radical (NO_3) and exists primarily aloft in urban areas. N_2O_5 then reacts with liquid water on aerosol particles such as fog or cloud water droplets to form nitric acid:

$$N_2O_5 + H_2O \rightarrow 2HNO_3. \quad (18)$$

The isopleth diagram in Figure 2-4 shows the trend in nitric acid with historic changes in ambient VOC and NOx concentrations. The NOx emission reductions during the past decade have resulted in sharp reductions in nitric acid and associated particulate nitrate.

The ambient levels of ammonium nitrate have declined significantly with reductions in NOx emissions, and have contributed to the recent declining trend in ambient $PM_{2.5}$ (Figure 2-5). Although a NOx-focus control strategy will pose additional challenges for attainment of the ozone NAAQS, these reductions in ambient levels of nitrate and $PM_{2.5}$ are cited as additional rationale for the current multi-pollutant attainment strategy. With these recent reductions, the SCAQMD projected attainment of the $PM_{2.5}$ NAAQS by 2014 (2012 AQMP, SCAQMD 2013). However the future trend in ammonium nitrate and $PM_{2.5}$ may depend upon the relative contributions of the two pathways to ambient HNO_3 and nitrate, which depend on a number of factors, whose importance varies diurnally and seasonally. Unlike ozone, the highest $PM_{2.5}$ and particle nitrate levels in the SoCAB historically occurred during the fall stagnation period (Kim et al. 2000). However, the reductions in NOx emissions during the past decade have lowered nitrate concentrations during fall to levels that are now comparable to summer. Under these conditions SOA may become more important for $PM_{2.5}$ exceedances and the NOx disbenefit for ozone may apply to the formation of SOA as well and complicate projections of future $PM_{2.5}$ levels in the SoCAB.

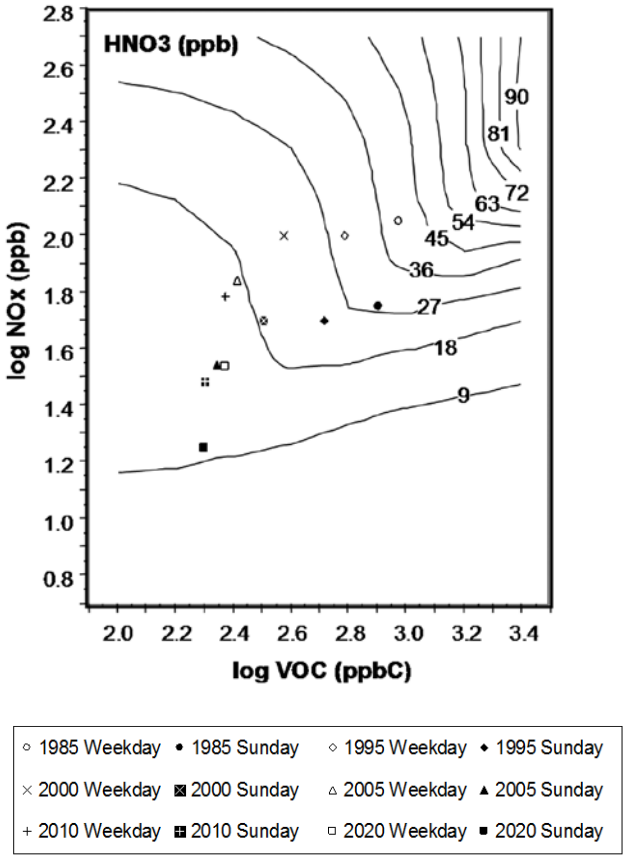

Figure 2-4. Isopleth diagrams of nitric acid for summer conditions in Los Angeles

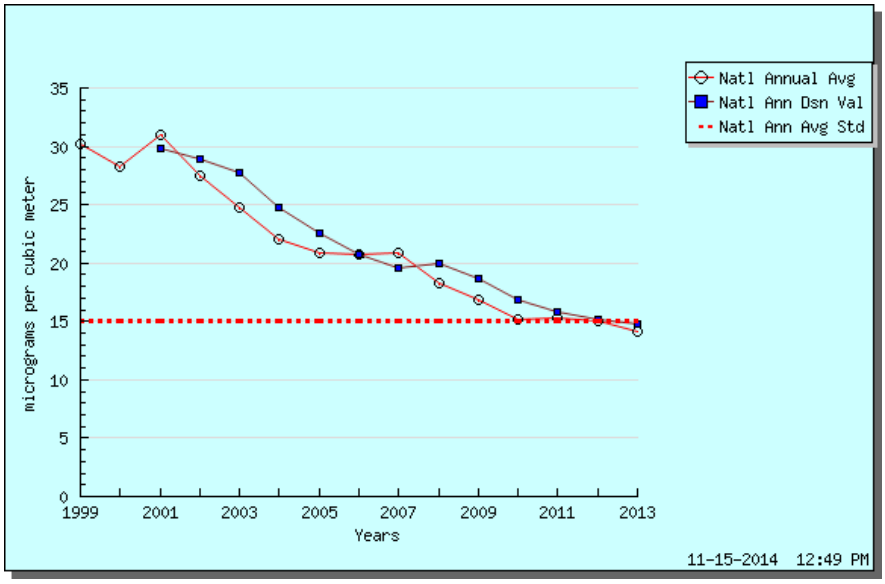

Figure 2-5. $PM_{2.5}$ trends in the South Coast Air Basin. Source: CARB Aerometric Data Analysis and Management (ADAM) air quality database, accessed November 15, 2014). http://www.arb.ca.gov/adam/trends/graphs/graphtrendpm25area.php.

2.2 Trends in VOC and NOx Emissions

The California Air Resources Board (CARB) is responsible for emission controls on motor vehicles in the state and stationary sources in the SoCAB are regulated by the South Coast Air Quality Management District (SCAQMD). Emissions of CO and VOC (and to a lesser extent NO_X) from new passenger vehicles were reduced by a factor of a hundred in comparison to pre-control vehicles in 1963. Major controls include passive crankcase exhaust gas recirculation adopted for the 1971 model year, oxidation reduction ("three way") catalytic converters first introduced in 1977, and the Low Emission Vehicles and Clean Fuels (LEV/CF) and Zero-Emission Vehicle (ZEV) regulations currently in effect. Reformulated gasoline and diesel fuels have resulted in further reductions. Stationary source NOx emissions have been reduced by a factor of two since 1980 using low-NOx burners, selective catalytic reduction, cleaner fuels (i.e., natural gas), vapor recovery, and low-VOC coatings and solvents. From 1980 to 2010, basinwide emissions from mobile sources are estimated to have decreased from 1517 to 328 tons/day for ROG and from 1250 to 495 tons/day for NOx. Emission from stationary and other area sources decreased from 767 to 247 tons/day for ROG and from 324 to 77 tons/day for NOx.

The most current emission data available are for 2012. The base year of 2012 was used for the emission estimates from 2005 to 2035. Data prior to 2012 are derived from historical emissions data and backcast emissions based on historical socioeconomic growth and emission control information. The future projections take into account projected growth rates and the effects of currently adopted emission control programs including the LEV III emission standards. The trends in emissions of NOx, ROG and CO in the SoCAB are shown in Table 2-2, Table 2-3, and Table 2-4, respectively (CARB, 2014). In the SoCAB, on-road mobile sources are the single largest source category for ozone precursor pollutants, accounting in 2010 for about 62, 32, and 63 percent of average daily NOx, ROG, and CO, respectively. Most of the on-road emissions are due to gasoline vehicles, but diesel vehicles contribute substantially to NOx emissions. Second to on-road mobile sources, stationary and area-wide sources are significant sources of VOC, while other mobile sources are currently a less important source of VOC. In contrast, other mobile sources generate relatively large emissions of NOx, while stationary and area-wide sources are less important NOx contributors. The vast majority of CO emissions are associated with on-road and other mobile sources.

Table 2-2. Trends in emissions of oxides of nitrogen in the South Coast Air Basin (2005 base year for 1975-2000 and 2012 base year for 2005-2035)[a]. Source: http://www.arb.ca.gov/ei/ei.htm (accessed on 08/28/14).

NOx Emissions (ton/day)	1975	1980	1985	1990	1995	2000	2005	2010	2015	2020	2025	2030	2035
STATIONARY													
Fuel Combustion	281	275	209	156	104	117	58	47	50	50	51	51	52
Waste Disposal	2	1	1	2	1	2	2	2	3	3	3	3	3
Cleaning and Surface Coatings	0	0	0	1	0	0	0	0	0	0	0	0	0
Petroleum Production and Marketing	16	11	10	5	9	7	5	12	2	2	2	2	2
Industrial Processes	10	11	25	8	7	10	2	0	1	1	1	1	1
AREAWIDE													
Solvent Evaporation													
Consumer Products	0	0	0	0	0	0	0	0	0	0	0	0	0
Architectural Coatings	0	0	0	0	0	0	0	0	0	0	0	0	0
Others	0	0	0	0	0	0	0	0	0	0	0	0	0
Misc. Processes	24	26	26	20	20	24	21	15	13	13	12	12	11
MOBILE SOURCES													
On-Road Vehicles													
LD Auto & Trucks	818	660	660	549	443	283	147	95	53	31	21	15	10
MD-HD Trucks Gasoine	39	49	65	94	100	66	67	55	42	31	23	19	15
LH-MH Trucks Diesel	2	9	27	48	50	75	96	66	42	26	17	13	11
HHD Trucks Diesel	87	155	247	218	194	183	194	109	70	52	33	35	42
Others	17	21	27	29	30	39	32	27	23	19	16	14	12
Off-Road Vehicles	357	357	345	364	307	236	218	143	132	116	102	96	94
TOTAL Stationary and Areawide	334	324	271	192	140	160	88	77	68	68	68	68	69
TOTAL Mobile Sources	1320	1250	1372	1301	1124	882	754	495	363	276	212	191	184
TOTAL All Sources	1654	1574	1643	1493	1264	1041	842	572	431	343	280	260	253
% Change from 1975		-5%	-1%	-10%	-24%	-37%	-49%	-65%	-74%	-79%	-83%	-84%	-85%
% Change from 2010									-25%	-40%	-51%	-55%	-56%

[a] Mobile source estimates from EMFAC2011.

Table 2-3. Trends in emissions of reactive organic gases in the South Coast Air Basin (2005 base year for 1975-2000 and 2012 base year for 2005-2035) [a]. Source: http://www.arb.ca.gov/ei/ei.htm (accessed on 08/28/14).

ROG Emissions (tons/day)	1975	1980	1985	1990	1995	2000	2005	2010	2015	2020	2025	2030	2035
STATIONARY													
Fuel Combustion	12	18	16	15	13	15	8	8	9	10	10	11	11
Waste Disposal	3	3	4	4	3	6	9	8	8	8	9	9	9
Cleaning and Surface Coatings	334	348	378	250	157	92	44	36	43	49	53	57	60
Petroleum Production and Marketing	252	130	105	155	106	78	39	56	38	37	38	39	40
Industrial Processes	25	46	76	32	15	30	24	14	12	14	15	15	16
AREAWIDE													
Solvent Evaporation													
Consumer Products	112	121	134	152	129	106	98	91	85	88	91	93	96
Architectural Coatings	72	77	79	54	54	54	44	23	18	19	20	21	21
Others	9	9	9	12	5	4	3	2	2	3	3	3	3
Misc. Processes	14	15	15	16	15	19	14	9	8	8	8	8	8
MOBILE SOURCES													
On-Road Vehicles													
LD Auto & Trucks	1462	1159	1068	690	484	313	180	126	68	43	32	25	16
MD-HD Trucks Gasoine	93	102	120	101	84	42	40	35	27	22	20	18	15
LH-MH Trucks Diesel	0	0	1	1	1	3	3	2	1	1	1	1	1
HHD Trucks Diesel	5	9	14	11	9	10	11	6	3	3	3	4	4
Others	34	33	36	27	19	13	14	12	10	9	9	9	9
Off-Road Vehicles	202	213	230	251	242	207	188	147	123	110	103	101	101
TOTAL Stationary and Areawide	834	767	817	689	497	405	282	247	224	236	247	257	265
TOTAL Mobile Sources	1795	1517	1468	1081	840	589	437	328	232	188	168	157	146
TOTAL All Sources	2629	2283	2285	1770	1337	994	718	575	457	424	415	414	411
% Change from 1975		-13%	-13%	-33%	-49%	-62%	-73%	-78%	-83%	-84%	-84%	-84%	-84%
% Change from 2010									-21%	-26%	-28%	-28%	-29%
On-Road Vehicle Evap	575	488	486	338	241	154	108	87	60	46	40	34	26
On-Road Vehicle Total	1593	1304	1239	830	598	382	249	181	109	79	65	56	45
On-Road Evap/Exhaust (%)	36%	37%	39%	41%	40%	40%	44%	48%	55%	59%	61%	60%	57%
ROG/NOx Ratios *	**5.3**	**4.8**	**4.6**	**4.0**	**3.5**	**3.2**	**2.8**	**3.4**	**3.5**	**4.1**	**4.9**	**5.3**	**5.4**

[a] Mobile source estimates from EMFAC2011. * Molar ratios of ROG in ppbC (13.8 g/mole) to NOx in ppb (46 g/mole).

Table 2-4. Trends in emissions of carbon monoxide in the South Coast Air Basin (2005 base year for 1975-2000 and 2012 base year for 2005-2035)[a]. Source: http://www.arb.ca.gov/ei/ei.htm (accessed on 08/28/14).

CO Emissions (tons/day)	1975	1980	1985	1990	1995	2000	2005	2010	2015	2020	2025	2030	2035
STATIONARY													
Fuel Combustion	152	113	62	86	54	61	54	48	50	52	53	55	56
Waste Disposal	2	0	1	2	1	1	1	1	1	1	2	2	2
Cleaning and Surface Coatings	0	0	0	0	0	0	0	0	1	1	1	1	1
Petroleum Production and Marketing	2	18	4	3	5	5	9	36	5	5	5	5	5
Industrial Processes	130	217	10	4	3	5	3	1	1	1	2	2	2
AREAWIDE													
Solvent Evaporation													
Consumer Products	0	0	0	0	0	0	0	0	0	0	0	0	0
Architectural Coatings	0	0	0	0	0	0	0	0	0	0	0	0	0
Others	0	0	0	0	0	0	0	0	0	0	0	0	0
Misc. Processes	15	17	18	20	21	49	45	43	43	43	43	43	43
MOBILE SOURCES													
On-Road Vehicles													
LD Auto & Trucks	12588	9705	9367	6968	5110	3035	1682	1120	657	402	293	230	173
MD-HD Trucks Gasoine	1086	1314	1547	1259	973	547	503	395	282	201	151	126	104
LH-MH Trucks Diesel	0	1	4	7	9	9	13	10	7	7	7	8	9
HHD Trucks Diesel	21	40	65	52	44	44	48	27	16	19	19	20	25
Others	275	279	318	232	190	105	97	100	76	65	60	56	51
Off-Road Vehicles	1379	1451	1545	1682	1498	966	886	840	849	883	926	974	1027
Total Stationary and Areawide	302	365	96	116	83	120	112	129	102	103	105	107	108
Total Mobile Sources	15349	12790	12846	10200	7824	4705	3229	2493	1888	1576	1455	1414	1390
TOTAL	15651	13155	12942	10316	7907	4825	3341	2622	1990	1680	1560	1521	1498
% Change from 1975		-16%	-17%	-34%	-49%	-69%	-79%	-83%	-87%	-89%	-90%	-90%	-90%
% Change from 2010									-24%	-36%	-41%	-42%	-43%
CO/NOx *	**15.5**	**13.7**	**12.9**	**11.4**	**10.3**	**7.6**	**6.5**	**7.5**	**7.6**	**8.0**	**9.2**	**9.6**	**9.7**

[a] Mobile source estimates from EMFAC2011.

* Molar ratios of CO in ppb (28 g/mole) to NOx in ppb (46 g/mole).

2.3 Historic Trends in the Spatial and Temporal Variations in Ozone Levels

Since the mid-1970's many research studies have observed that ozone levels were higher on weekends than on weekdays in California's South Coast Air Basin (SoCAB) and other urban areas (San Francisco, Washington, D.C., Philadelphia, New York, and Chicago) even though the emissions of NOx, and to a lesser extent VOC, were lower on weekends (Elkus and Wilson, 1977; Horie et al., 1979; Levitt and Chock, 1976; Blier et al., 1998; Austin and Tran, 1999; Altshuler et al., 1995; Pun et al., 2001; Fujita et al., 2003a; Chinkin et al., 2003; Fujita et al., 2003b; Yarwood et al., 2003; Blanchard and Tannebaum, 2004). While peak ozone levels dropped sharply in the SoCAB during the 1990s, an increasing number of monitoring locations throughout the basin began to show higher levels of ozone on weekends. We previously documented the increase in the magnitude and spatial extent of the weekend effect during the 1990s (Fujita et al, 2003). Figure 2-6 shows that in the period 1981-84, peak ozone levels were higher on weekdays in most of the central and eastern portions of the Basin. Most monitoring sites in the western Basin showed slightly higher weekend ozone concentrations. By 1990-94, ozone concentrations were higher on weekends throughout the Basin and the weekend effect continued to strengthen after 1995. Figure 2-7 shows that mean peak daily ozone levels in the central SoCAB were 30% and 50% higher on Saturdays and Sundays, respectively, in summer 2000 despite substantially lower levels of NOx and to a lesser extent CO (Fujita et al., 2003). The larger reductions in peak ozone concentrations on weekdays were accompanied by a shift in the location of peak ozone levels from the central portion of the Basin to the eastern Basin and mountain locations.

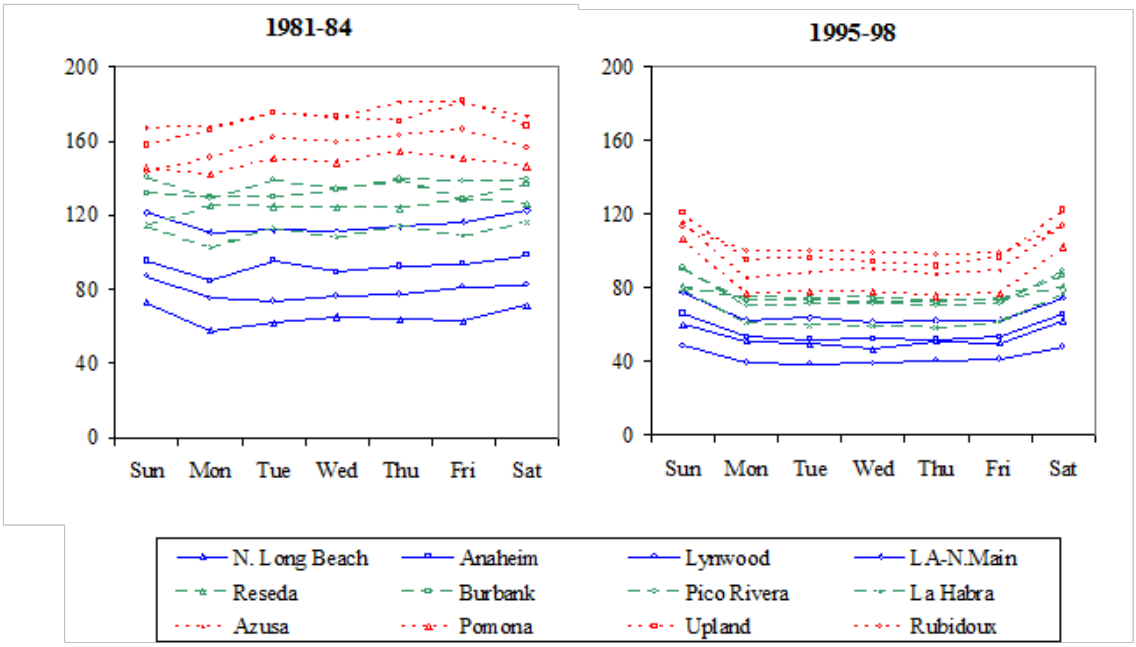

Figure 2-6. Mean maximum 1-hour ozone (ppb) during summers (June 1 to September 30) of 1981-84 and 1995-98 in the SoCAB. Sites in the western, northern and central, and central to eastern basin are denoted by solid, dash, and dotted lines, respectively. Source: Fujita et al. 2003.

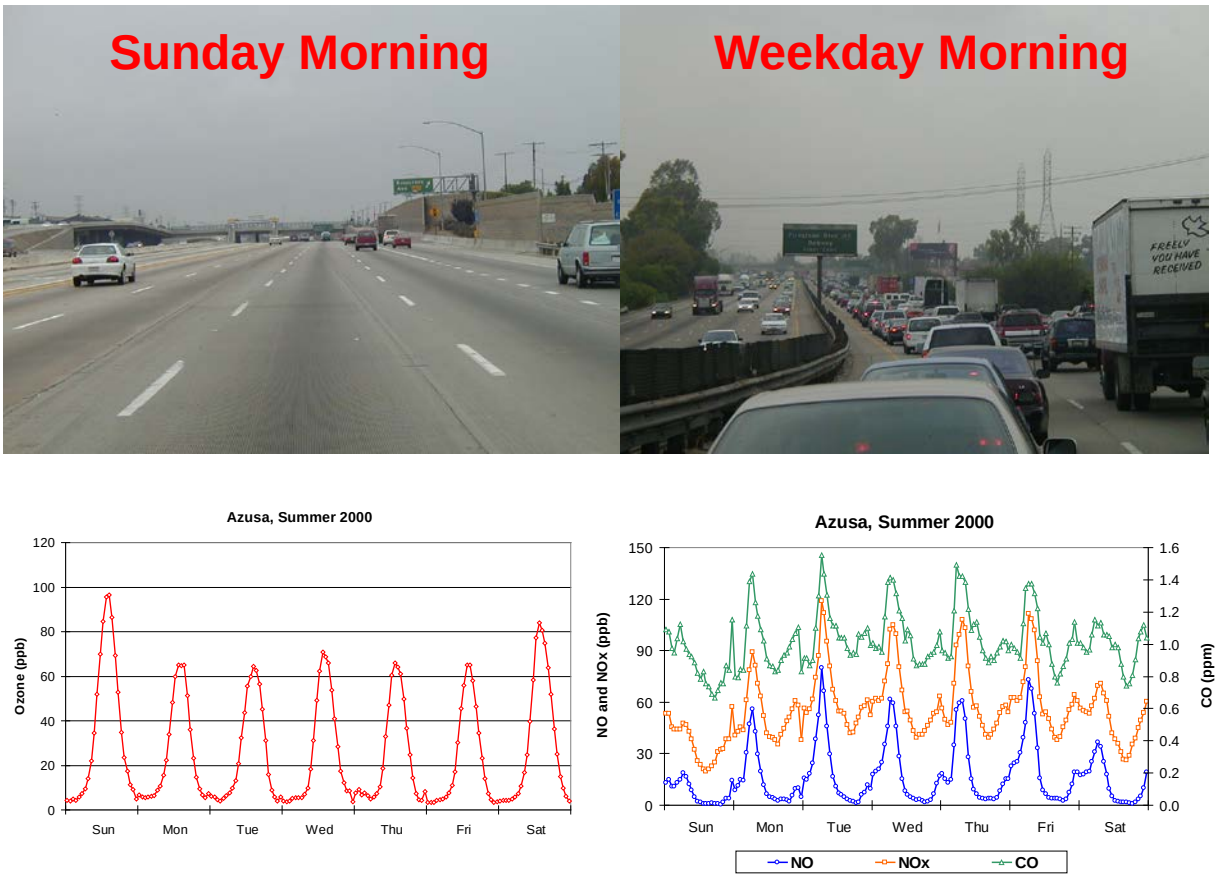

Figure 2-7. Mean concentrations of O_3, NO, NOx and CO at Azusa during summer 2000 by day of week.

Many of the prior studies have concluded that the weekend ozone effect is associated with the nonlinearity of ozone formation and increases in VOC/NOx ratios on weekends relative to weekdays under VOC-limited conditions. The nonlinearity of O_3 photochemistry imposes two necessary conditions for a reduction in NOx on the weekend to result in higher production of O_3. First is that ozone formation is VOC-limited. Removing NOx from a VOC-limited system reduces the removal of HO radical by reaction with NO_2 to form nitric acid, thereby increasing the efficiency and rate of O_3 formation. The weekend effect is greatest where the O_3 formation is more VOC-limited during the weekday and less VOC-limited during the weekends. The second condition is that the peak O_3 level on weekdays does not reach its maximum potential so that time is a limiting factor in O_3 production and accumulation. Our previous analysis of the ambient air quality data shows that this is the case in the SoCAB (Fujita et al., 2003). Consequently, peak O_3 levels are determined by the duration of O_3 accumulation, which is a function of the extent of O_3 inhibition caused by NO emission, and the rate of O_3 accumulation, which depends on the VOC/NOx ratio. Although the amount of O_3 that can potentially form on weekdays is greater, peak O_3 levels are higher on weekends because the duration of O_3 accumulation is longer and the rate of O_3 formation is greater on weekends.

Figure 2-8 illustrates the typical diurnal variations of ozone and nitric oxide at Azusa during the weekday and weekend in summer 1995. NO typically exists in excess of O_3 in the

urban center overnight, and suppresses the mixing ratio of O_3 to zero or near zero in the surface layer. Fresh NO emissions during the morning commute prolong the inhibition of O_3 accumulation after sunrise. During this inhibition period, the photolysis of carbonyl compounds and smaller contributions of HONO and other radical precursors are the primary source of HO radicals until a sufficient amount of NO has been converted to NO_2. Ozone carried over aloft from the previous day can mix down in the morning and contribute O_3 and radicals to the developing surface O_3 chemistry. The length of the morning O_3 inhibition period is largely determined by the mixing ratio of NO and NO_2/NOx ratios. Lower NOx emissions on weekends decrease NO titration of the O_3 newly formed at the surface and the O_3 transported from aloft. Lower NO mixing ratios and higher NO_2/NOx ratios during weekend mornings decrease the removal of O_3 by titration with NO, thereby allowing O_3 to accumulate about an hour earlier on weekends compared to weekdays. The morning crossover of NO and O_3, shown in

Figure 2-8, indicates the end of the inhibition period and beginning of O_3 accumulation via conversion of NO to NO_2 by peroxy radical.

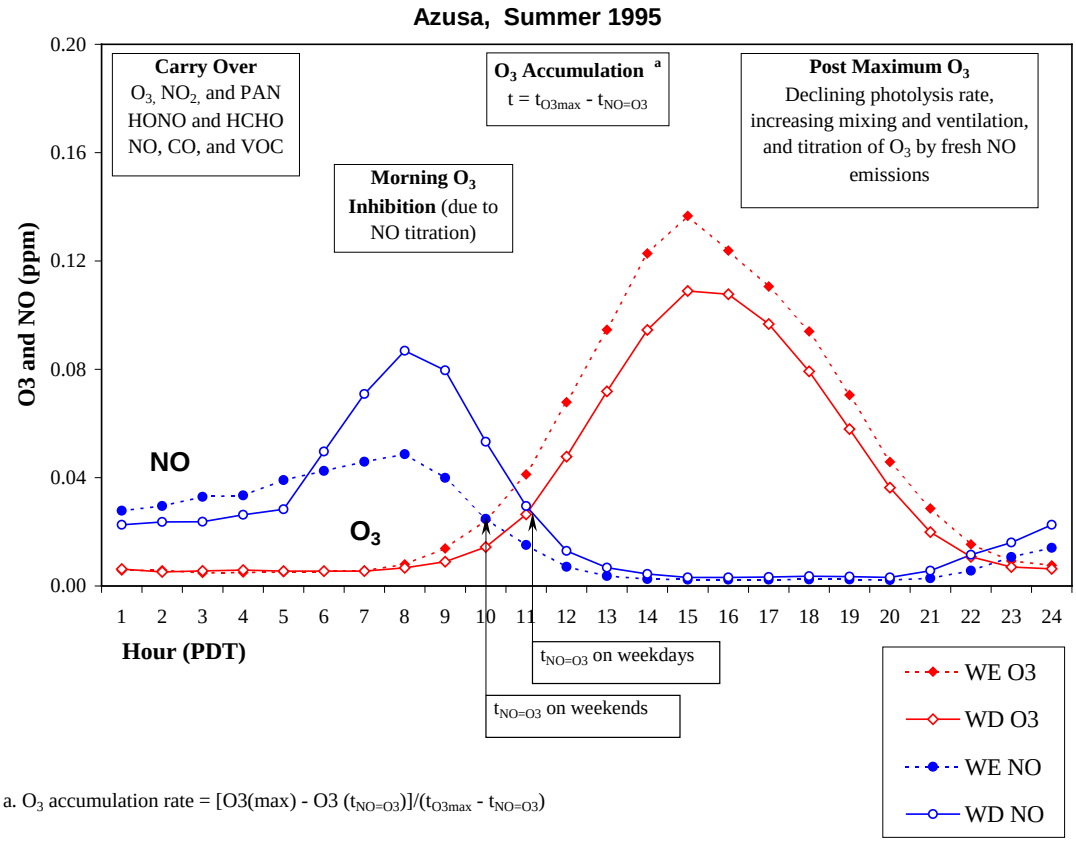

Figure 2-8. Average summer 1995 diurnal variations of ozone and nitric oxide at Azusa during the weekday and weekend. The shorter morning ozone inhibition period and higher rate of ozone accumulation are the main factors that result in higher ozone on weekends.

We estimated in our prior study (Fujita et al., 2003) that the O_3 inhibition period ends 0.5 to 0.7 hours earlier on Saturdays and about 1.1 to 1.3 hours earlier on Sundays. The delay in the start of O_3 accumulation caused by inhibition on weekdays relative to weekends had changed very little in during the 1980s and 90s, as shown in Figure 2-9. In contrast to the duration of O_3 accumulation, which has remained relatively constant, the O_3 accumulation rates were cut in half and a third on weekdays and Sundays, respectively, during the 18-year period. The largest reductions occurred in the central Basin. Figure 2-9 shows that O_3 accumulation rates were lower on weekends than on weekdays through most of the 1980s but became higher on weekends during the 1990s. The transition from lower to higher O_3 accumulation rates on weekends relative to weekdays coincides with increases in the magnitude and spatial extent of the weekend effect in the SoCAB. This also coincides with a steeper decline in O_3 during the 1990s, especially in the western and central parts of the Basin.

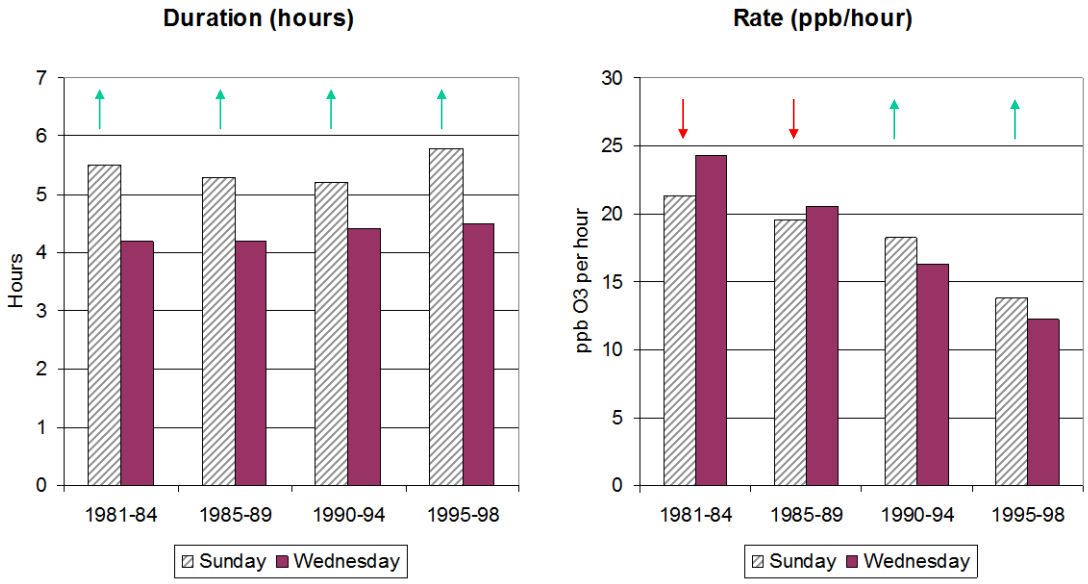

Figure 2-9. Mean duration and rate of ozone accumulation at 12 sites in the South Coast Air Basin from 1981 to 1999. Duration and rate of are opposed on Sundays during the 1980s and are additive during the 1990s.

Figure 2-10 shows the trends in the differences between Sunday and Wednesday O_3 accumulation rates as three-year running means for western, central, and eastern SoCAB sites. Changes in emissions from weekdays to weekends in the early 1980s resulted in little change in the O_3 accumulation rate at western sites and generally lower weekend rates at central and eastern sites. The lower weekend O_3 accumulation rate offsets the shorter O_3 inhibition period on weekends at central and eastern locations resulting in either no change or slightly lower O_3 mixing ratios on weekends (i.e., a small weekend effect). The weekend O_3 effect in the western Basin during the early 1980s was largely due to decreased O_3 inhibition. The transition to higher weekend O_3 accumulation rates occurred in the mid-1980s in the western Basin and in late 1980s in the central Basin. Ozone accumulation rates have been about equal on weekdays and weekends since the early 1990s in the eastern Basin. Coupled with the shorter inhibition period, O_3 mixing ratios were consistently higher on weekends during the 1990s with the strongest

weekend effect occurring in the central Basin on an absolute and relative basis. The spatial evolution in the weekend effect parallels the shift in peak ozone levels from the western to eastern portion of the basin.

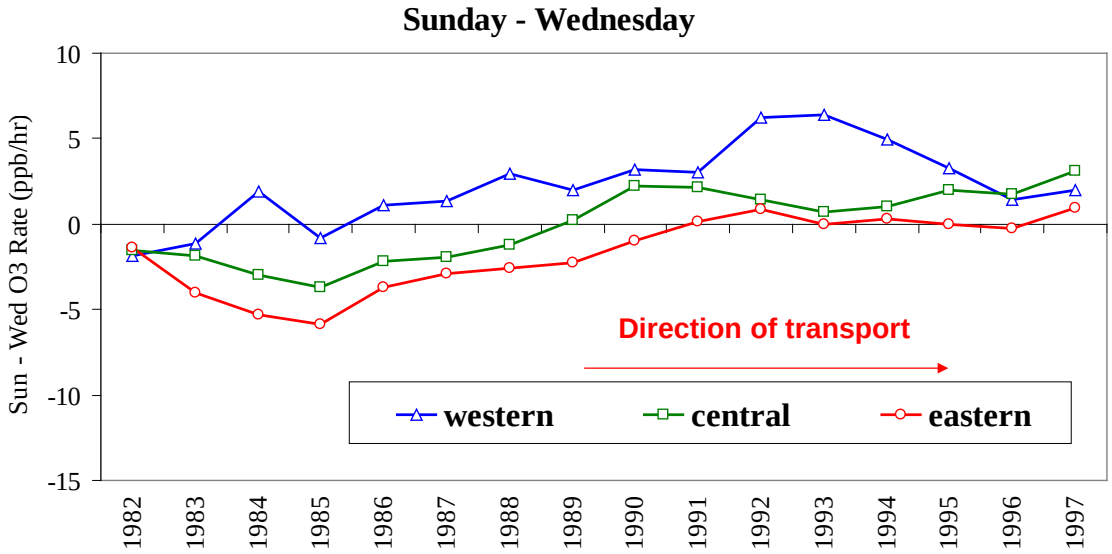

Figure 2-10. WE/WD Differences in Ozone Accumulation Rates in the SoCAB 3-Year Running Averages from 1982 to 1997.

During the summers of 1999 and 2000, the NMHC/NOx ratios at the four SoCAB Photochemical Assessment Monitoring Stations (PAMS) were 4-8 from sunrise to the time of peak O_3 so that O_3 formation was VOC-limited throughout this period. Blanchard and Tanenbaum (2000; 2003) concluded (based on their estimates of the extent of reaction) that most monitoring sites in the SoCAB were VOC-limited. Trends in mixing ratios of ozone precursors show a transition in the Basin to lower volatile organic compound (VOC)/NOx ratios caused by greater reductions in VOC emissions. Reductions in VOC/NOx ratios were greater on weekdays resulting in higher VOC/NOx ratios on weekends relative to weekdays (Figure 2-11). Trends in VOC/NOx ratios parallel the downward trend in peak ozone levels, a shift in the location of peak ozone from the central to eastern portion of the Basin, and an increase in the magnitude and spatial extent of the weekend ozone effect in the Basin.

In summary, the weekend ozone effect is rooted in the nonlinearity of ozone formation in that higher VOC/NOx ratios on weekends relative to weekdays under VOC-limited conditions results in more rapid and efficient formation of ozone on weekends relative to weekdays. The result is higher peak ozone levels in the central basin although total ozone production within the entire basin may be less. These observations are weekly inadvertent demonstrations of NOx disbenefit. The historically low average ozone levels in the central basin coincide with the minima in the trends of NMOC/NOx ratios (shown in Figure 2-12) that occurred in 2000-2004 (Fujita et al, 2013). The magnitude of the weekend ozone effect was at its historic high during this period and has eased following a reversal in the declining trend of VOC/NOx ratios of the previous two decades.

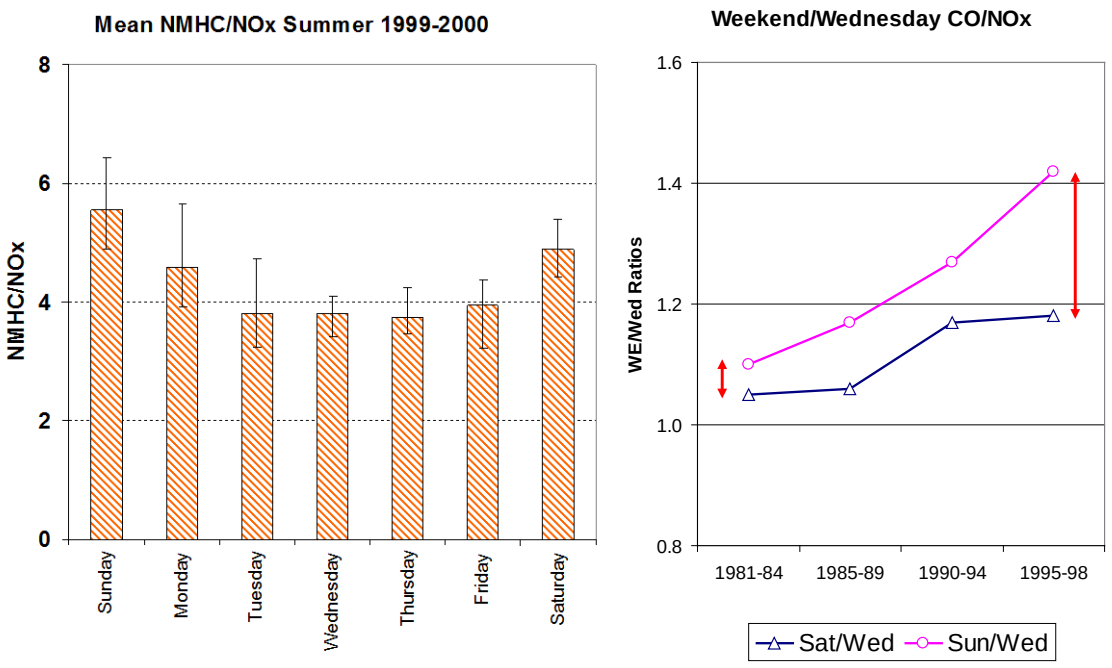

Figure 2-11. Weekday variations in 6-9 a.m. NMHC/NOx ratios and 1981-1998 trend in WE/WD ratios of CO/NOx. Whiskers are one standard deviation of mean ratios at four sites.

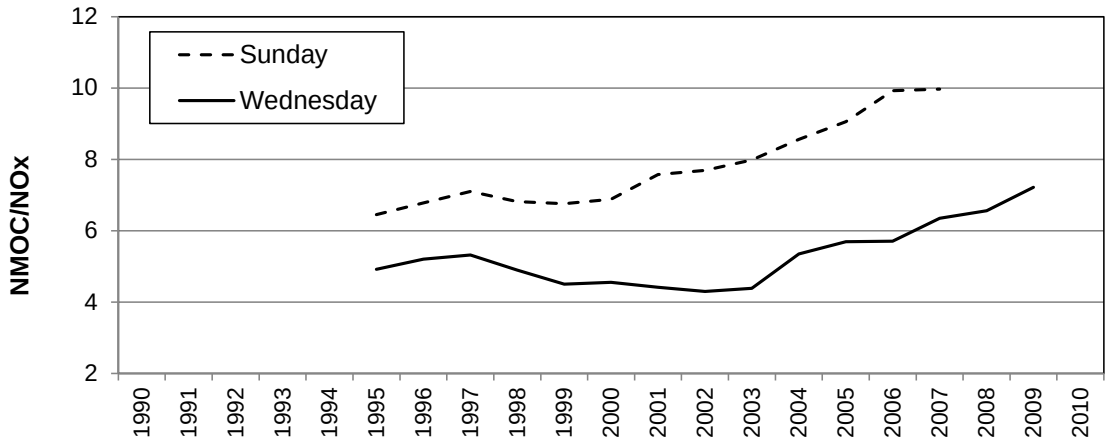

Figure 2-12. Trends in four-site (Los Angeles N. Main, Azusa, Pomona and Rubidoux) average summer Wednesday and Sunday 6-9 am ambient NMOC/NOx ratios in the South Coast Air Basin. Source: Figure 4 in Fujita et al. *J. Air Waste Manage. Assoc.* 63 (2013):1, 54-69.

2.4 Evolution of the Ozone-Precursor Relationship in the SoCAB

The ozone-precursor relationship in the SoCAB has evolved with varying relative reductions of VOC and NOx emissions over the past four decades. The VOC/NOx in the basin was near the optimum ratio of 10 in the 1980s and was likely higher prior to introduction of the catalytic converter in 1975. Thus, simultaneous control of VOC and NOx was an appropriate control strategy. However, control emission control technology allowed for implementation of the 1970 Clean Air Act vehicle emission standards for only VOC and carbon monoxide (CO) by the 1975 deadline and the emission standard for NOx was postponed to 1981. The VOC/NOx ratio steadily decreased through the 1990s due to VOC-focused emission controls, reaching a minimum of about 4 in the early 2000s. The historically low average ozone levels in the central basin coincided with the minima in the trends of VOC/NOx ratios that occurred in 2000-2004 (Fujita et al, 2013). However, the ambient VOC/NOx ratio has been increasing in recent years with greater emphasis on NOx controls, especially for heavy-duty diesel vehicles.

The historic trends in ozone levels within the SoCAB and long-term changes in the magnitude and relative amounts of VOC and NOx emissions are consistent with the ozone-precursor relationships depicted in Figure 2-13. The ozone isopleth diagram also explains the long-term evolution in the magnitude of the weekend ozone effect as well as the recent increasing ozone trend in the central SoCAB. The estimated 1985, 1995 and 2005 and projected 2020 initial weekday and weekend VOC and NOx concentrations are plotted on the ozone isopleth diagram to illustrate the long-term evolution of the ozone-precursor relationships in the SoCAB (Fujita et al., 2013). Reduction in VOC emissions during the period from 1985 to 2005 led to sharp reductions in ozone for both weekends and weekdays. Reductions in both NOx and VOC emissions between 2005 and 2010 caused the system to move more parallel to the isopleths and therefore ozone decreases were much less than in previous years. The historic ozone trends indicated by these simulations are consistent with monitoring observations. Figure 2-14 forecasts a period of stronger NOx disbenefit for the SoCAB between 2010 and 2020 with emission reductions of 50 percent for NOx and 10 percent for VOC emissions. With NOx emission reduction of 75 percent from 2010 levels, results of the box model simulations shown in Figure 2-14 predict that ozone formation would become precursor limited, but with higher initial ozone formation rates. While this would likely result in lower ozone levels in downwind areas where transport is more important than local production of ozone, the location of peak ozone levels will shift westward toward the central basin. The recent increasing ozone trends in the central SoCAB shown in Figure 3-2 (middle panel) are early indications of these projected trends. Although ozone levels at far downwind locations (e.g., Crestline and Riverside) continue to show a slow decline during the past decade, ozone levels appear to be increasing at central basin locations during weekdays (Fujita et al. 2013). At the same time, ozone levels in the central basin have been flat or decreased slightly on Sundays resulting in a reduction of the enhancement of ozone on weekends relative to weekdays.

The initial VOC and NOx concentrations are similarly plotted on isopleths of VOC/NOx ratios, ozone production efficiency, rates of ozone formation and maximum nitric acid concentrations (Figure 2-15) that were previously presented in Fujita et al (2013). These plots illustrate that further reduction in NOx emissions (i.e., loer VOC/NOx ratios) results in lower production of nitric acid (the termination product of NOx at low VOC/NOx ratio), and higher ozone production efficiency, which is the molecules of ozone produced per molecule of NOx consumed in the termination reaction to produced nitric acid.

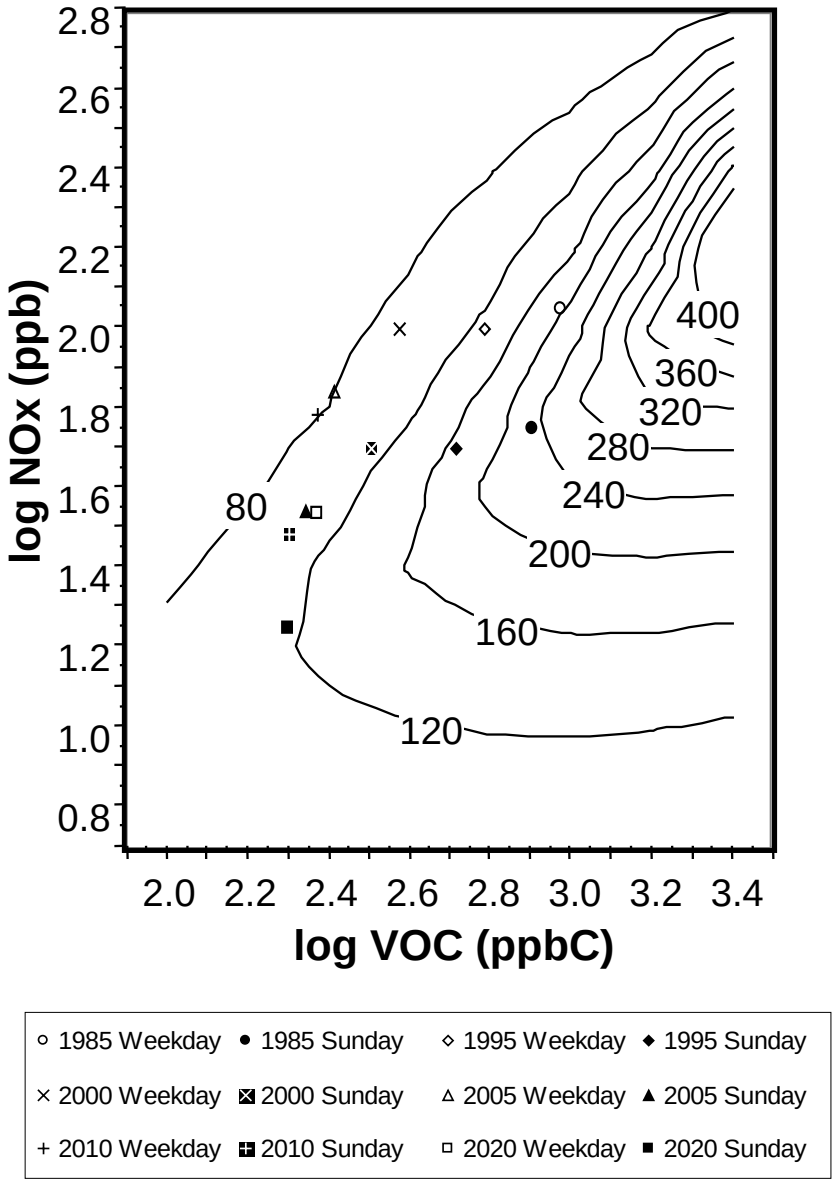

Figure 2-13. Ozone isopleth diagram for summer conditions in Los Angeles with initial weekday and Sunday NMHC and NOx mixing ratios (from Fujita et al., 2013). The two pairs of lines represent 2010 to 2020 changes of -10% VOC and – 50% NOx (indicated by box) and -75% NOx (indicated by end of arrow) NOx. The left pair of lines represents an underestimation of VOC emission of a factor of two relative to the right pair of lines. Source: Figure 9 in Fujita et al. *J. Air Waste Manage. Assoc.* 63 (2013):1, 54-69

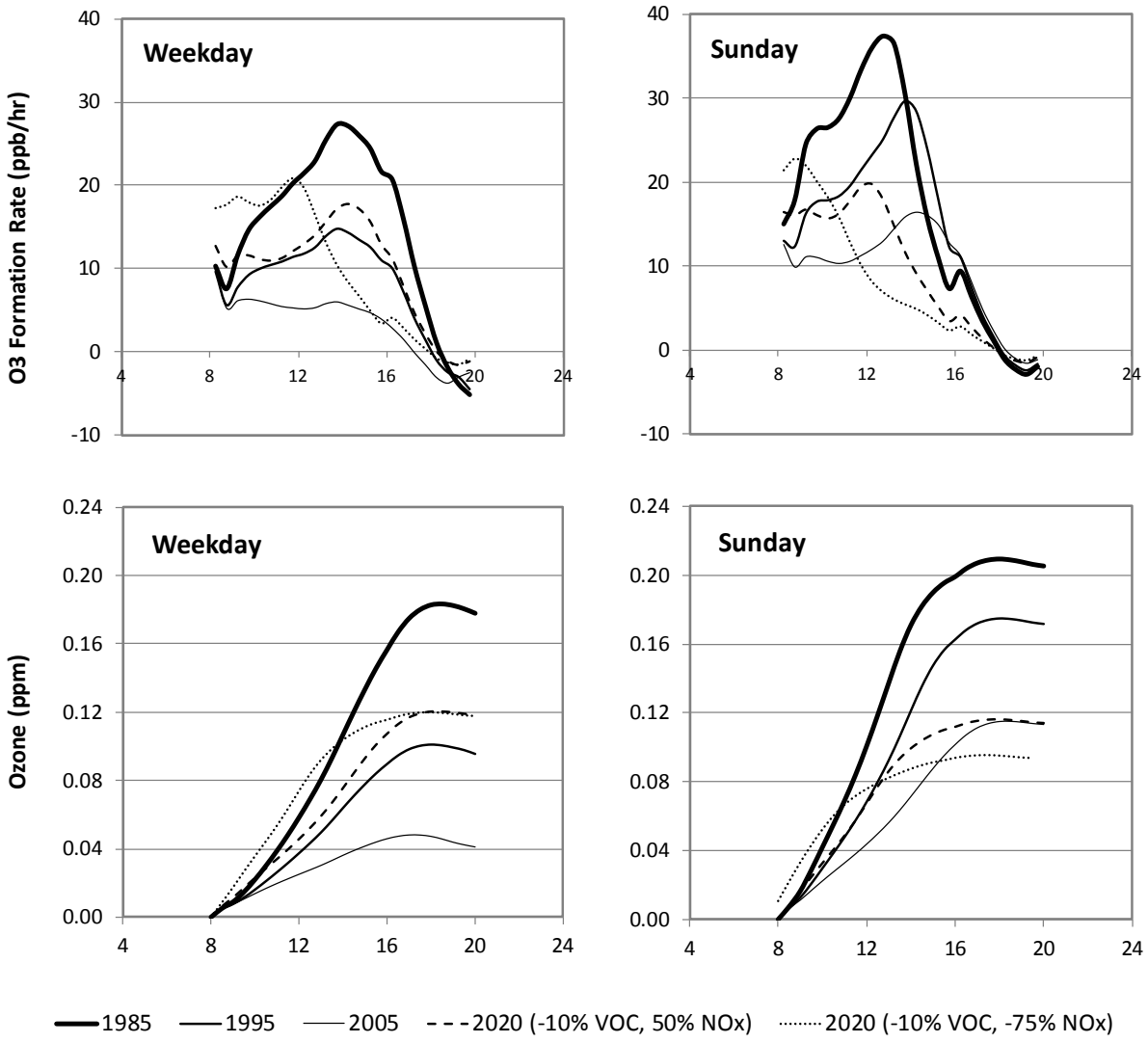

Figure 2-14. Predicted ozone mixing ratios (ppm) and formation rates (ppb/hr) from box model ozone simulations. Source: Figure 8 in Fujita et al. *J. Air Waste Manage. Assoc.* 63 (2013):1, 54-69

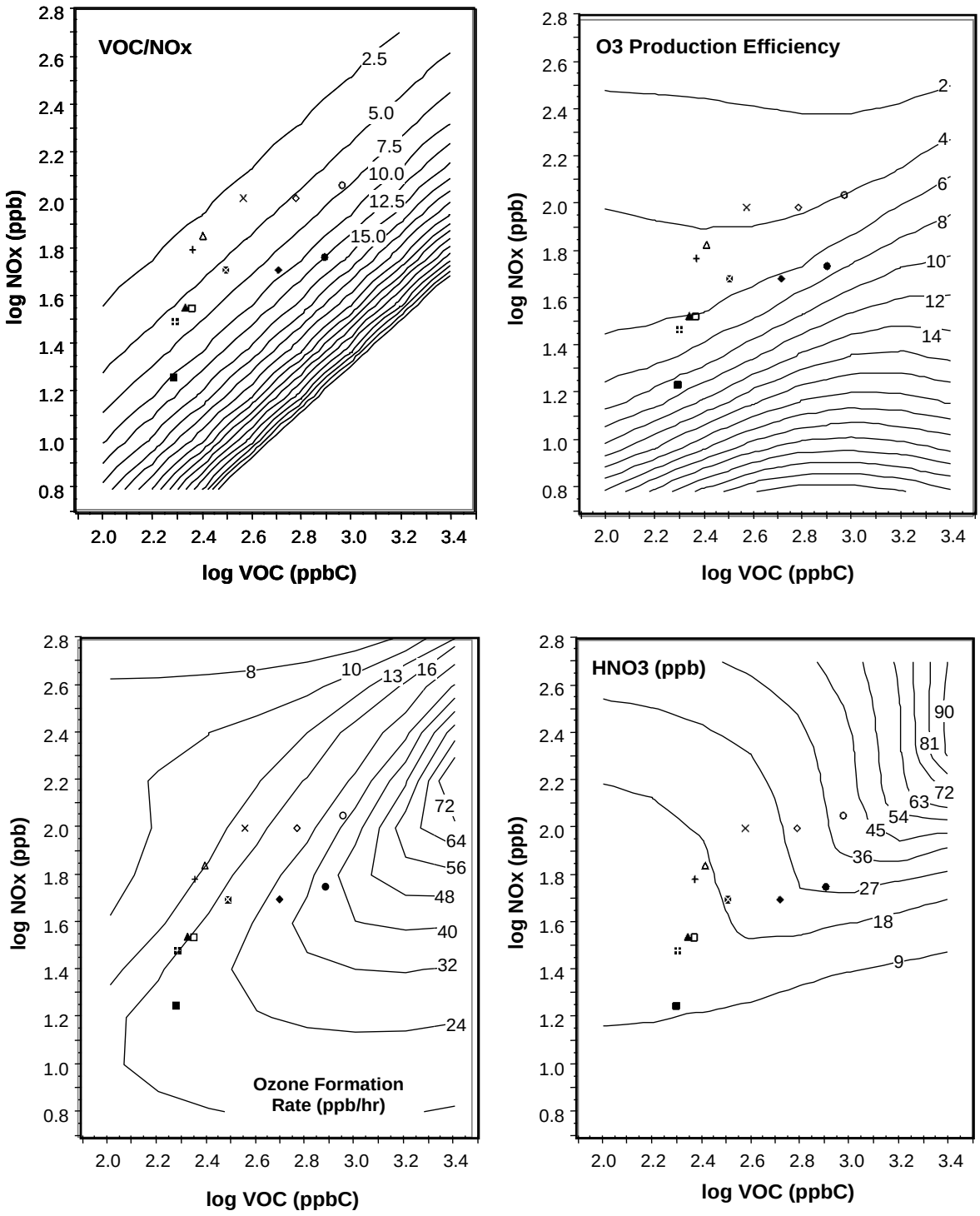

Figure 2-15. Ozone isopleth diagrams of VOC/NO_x ratios, ozone production efficiency, ozone formation rate and nitric acid for summer conditions in Los Angeles

2.5 Air Quality Management Plan for the South Coast Air Basin

On March 12, 2008, the U.S. Environmental Protection Agency (EPA) revised the 8-hour national ambient air quality standard (NAAQS) for ground-level ozone from the previous standard, set in 1997, of 0.08 ppm to 0.075 ppm. The metric for attainment is the design value (DV), which for ozone is the annual fourth-highest daily maximum 8-hour concentration averaged over three years. The South Coast Air Basin of California was classified in 2012 as extreme nonattainment (DV equal to or exceeding 0.175 ppm) for the 2008 8-hour ozone NAAQS. The attainment deadline for extreme nonattainment areas is December 31, 2032. The 2016 Air Quality Management Plan (AQMP) that the South Coast Air Quality Management District will prepare next year will specify the set of emission control programs that will be required to attain the 2008 8-hour ozone NAAQS. Future attainment will be demonstrated using an air quality simulation model by projecting future ozone levels in response to planned emission reductions.

The 2012 AQMP (SCAQMD, 2013) specified the emission control program for attainment of the federal 24-hour $PM_{2.5}$ standard by 2014, but also included a preliminary modeling analysis for attainment of the ozone standard. The ROG and NOx emission inventories used in SCAQMDs modeling for the 2012 AQMP are shown in Table 2-5. The SCAQMD projects a carrying capacity for NOx emissions of 80 tons per day (tpd) in order to attain the 2008 8-hour ozone NAAQS of 75 ppb by 2032 (equivalent to a 90 percent reduction from 2010 levels). SCAQMD estimates total NOx emissions in 2030 of 284 tpd. This "baseline" projection takes into account only currently adopted control programs, which includes the LEV (Low Emission Vehicle) III standards. Thus, substantial additional NOx reductions will be required beyond currently adopted control measures. The prior 2007 State Implementation Plan (SIP) for the 1997 8-hour ozone NAAQS of 80 ppb contained commitments for emission reductions that rely on advancement of technologies, as authorized under Section 182(e)(5) of the federal Clean Air Act. These measures are known as the "black box" or to be adopted measures account for a substantial portion of the additional 200 tons/day of NOx emission reductions needed to attain the federal ozone standards. Mobile sources emit over 80 percent of NOx in the basin and, therefore, are anticipated to be the largest part of these additional reductions.

2.6 Implications of Emission Inventory Uncertainties

As motor vehicles are the largest category of both VOC and NOx emissions in an urban area, changes in ozone photochemistry, historic trends in ambient ozone levels, and the magnitude and spatial extent of the weekend ozone effect in the SoCAB have been closely linked to changes in vehicle emissions (Fujita et al., 2003a; Chinkin et al., 2003). It is now generally acknowledged that hydrocarbon emissions from automobiles were underestimated in past inventories (Ingalls, 1989; Seinfeld, 1989; Pierson et al., 1990; Fujita et al., 1992; Calvert et al., 1993; Harley et al., 1993). Ingalls (1989) showed that on-road emissions measured in the Sherman Way (Van Nuys) tunnel during the 1987 Southern California Air Quality Study (SCAQS) were significantly larger than those calculated by the California Air Resource Board (ARB) mobile source emission model (EMFAC7E at that time) for hydrocarbons (3.5x with 7D and 2.2x with 7E) and CO (3.0x with 7D and 2.1x with 7E). Pierson et al. (1990) demonstrated that the SCAQS tunnel results were consistent with observations from other on-road studies, and that the SCAQS tunnel experiment could not be dismissed as an indicator that the emission factors might be wrong. Additionally, Fujita et al. (1992) found that the ambient CO/NOx and

NMOG/NOx ratios during SCAQS were about 1.5 and 2 to 2.5 times higher, respectively, than the corresponding emission inventory ratios.

Table 2-5. Summer planning emissions inventory for the SoCAB from the 2012 AQMP.

Summer Planning Emissions

	VOC (tpd)			NOx (tpd)			
SOURCE CATEGORY	2008	2023	2030	2008	2023	2030	2032*
Stationary Sources							
Fuel Combustion	14	14	15	41	27	29	
Waste Disposal	12	14	15	2	2	2	
Cleaning and Surface Coatings	43	56	62	0	0	0	
Petroleum Production and Marketing	41	37	38	0	0	0	
Industrial Processes	19	18	19	0	0	0	
Solvent Evaporation							
Consumer Products	100	91	95	0	0	0	
Architectural Coatings	25	20	21	0	0	0	
Others	2	3	3	0	0	0	
Misc. Processes	9	9	9	19	13	12	
RECLAIM SOURCES	0	0	0	24	27	27	
Total Stationary Sources	264	261	277	87	70	70	
Mobile Sources							
On-Road Vehicles							
LD Auto & Trucks	153	38	26	118	24	15	
MD-HD Trucks Gasoline	36	21	18	59	26	19	
LH-MH Trucks Diesel	3	1	1	71	18	13	
HHD Trucks Diesel	9	3	4	152	31	35	
Others	12	8	8	28	17	14	
Off-Road Vehicles	162	108	104	208	133	119	
Total Mobile Sources	375	177	160	636	249	214	
TOTAL	639	438	437	723	319	284	80
Projected Reductions (% from 2008)		**-31%**	**-32%**		**-56%**	**-61%**	**-89%**
Projected Reductions (% from 2023 baseline)			**0%**			**-12%**	**-75%**
Evap/Exhaust for on-road (%)	47%	62%	63%				
Exhaust all on-road vehicles	112	30	25				
Evaporative all on-road vehicles	99	49	44				
% Evap	47%	62%	63%				

* Carrying capacity projected by the SCAQMD to attain the 8-hr ozone NAAQS of 75 ppb by 2032.

Since ozone formation is most efficient at a VOC/NOx ratio near 10, the actual rate of ozone formation was substantially faster than what was indicated by the emission inventory data or by air quality modeling using the “official emissions inventory”. The California Air Resources Board (Wagner and Wheeler, 1993), South Coast Air Quality Management District (Chico et al., 1993) and Carnegie Mellon/California Institute of Technology (Harley et al., 1993) used the SCAQS database for model verification studies, and all obtained predicted ozone values which

were substantially lower than observed. Model performance was greatly improved when the assumed on-road motor vehicle reactive organic gas (ROG) emissions were increased over the official ones by substantial margins (ARB and SCAQMD increased total on-road motor vehicle emissions by a factor of 2.5 (Figure 2-16), and CMU/CIT increased hot exhaust emissions by a factor of 3).

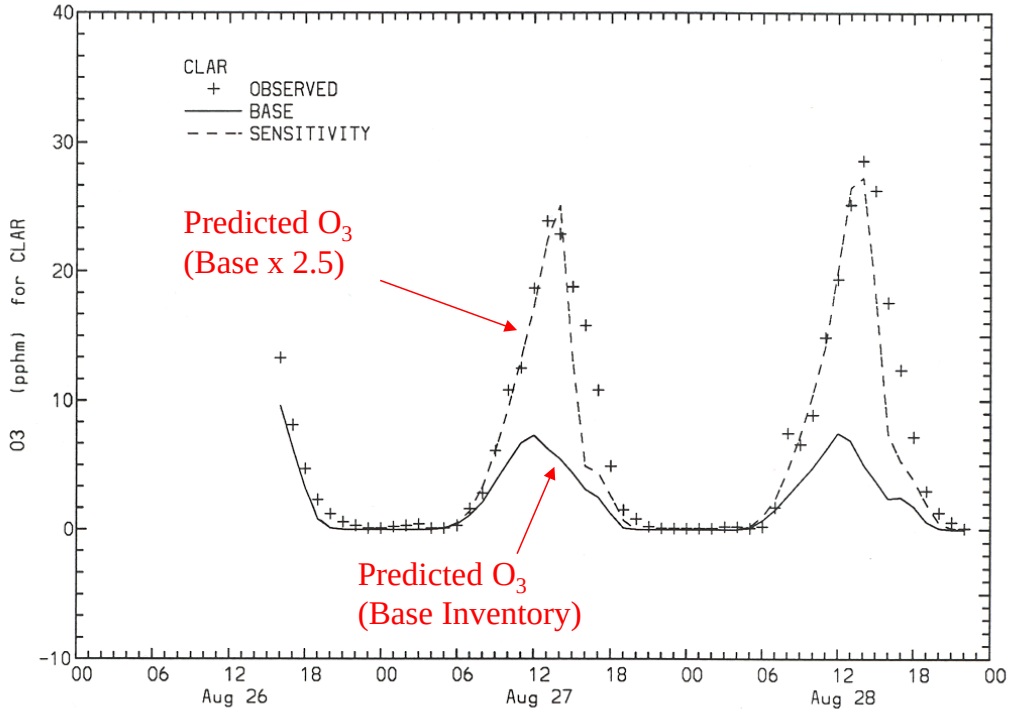

Figure 2-16. 1987 SCAQS air quality model ozone predictions using base inventory versus on-road motor vehicle reactive organic gas emission increased by factor of 2.5. Source California Air Resources Board, Technical Support Division, 1993.

Since the 1987 SCAQS results were published, modifications that were incorporated into successive versions of the mobile source emission factor models, MOBILE and EMFAC, have substantially increased all emissions (for a common base year). During the same time, ambient CO, VOC, and ratios of VOC to nitrogen oxides (NOx) declined significantly. Figure 2-17 shows the relationships between the published inventories using then current emission models to revisions of the inventory for the same year using updated models. Estimates of CO emissions (tons/day) for the South Coast Air Basin that were published by the California Air Resources Board in the past twenty years (marked by x) are compared in to the trend in number of exceedances of the NAAQS for CO and backcast inventories based on emissions for the year 2000. While the ambient data and backcast inventories show substantial decreasing trends, successive estimates of CO emissions in the "official" (i.e., current) inventories have remained relatively constant. For the mid-1980s, the backcast estimates are about a factor of three higher than the published estimates at that time, which is consistent with results of SCAQS emission

inventory evaluations. While not shown, published and revised HC emissions inventories showed similar differences.

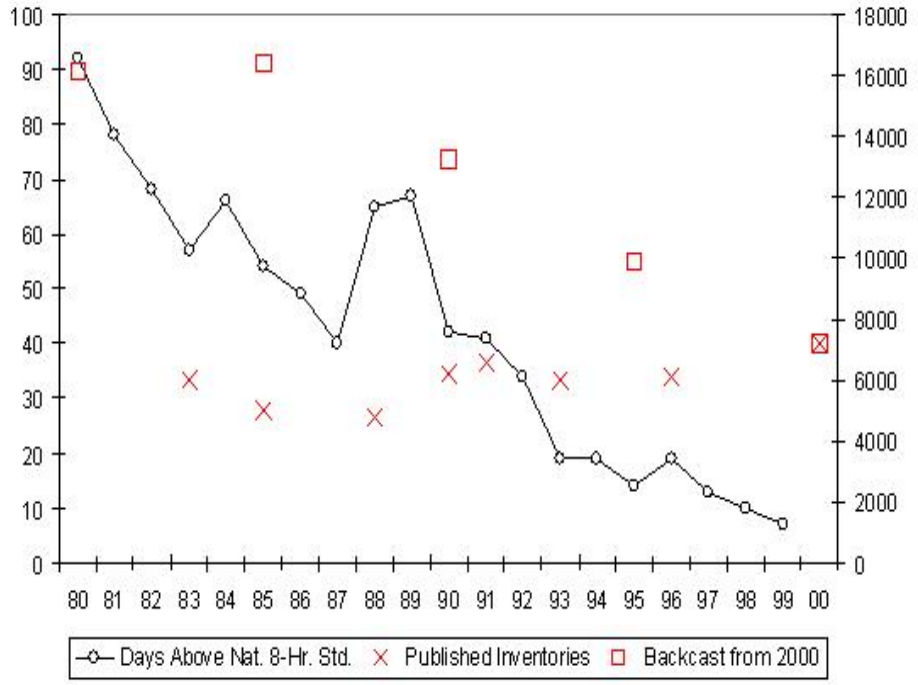

Figure 2-17. Published CO emission inventories (right axis in tons/day) in the South Coast Air Basin (marked by x) versus updated inventories using 2000 base-year emissions and methodologies to backcast the inventories for prior years (marked by box). Line shows trends in number of exceedances (left axis) of the NAAQS for CO.

The implications of Figure 2-17 are profoundly relevant to the intense debate that occurred around 1990 to explain the lack of significant progress toward attainment of the ozone NAAQS during the 1980s. Large underestimation of VOC emissions during the late 1980s meant that the actual ambient VOC/NOx ratios were substantially greater (~8 to 10 in ppbC VOC to ppb NOx) than were indicated by corresponding emission inventory data (~4). However, current and future projections of emission inventory estimates are the accounting basis for developing appropriate ozone reduction strategies so these emissions could not be arbitrarily adjusted as was done to test the air quality model's response to various adjustments to the emissions inventory.

Prior to the 1987 SCAQS, the nation's ozone reduction strategy was based on the premise that VOC/NOx ratios in most urban areas were less than 10. VOC controls are more effective at VOC/NOx less than 10 (hydrocarbon sensitive) and NOx controls are more effective at VOC/NOx greater than 20 (NOx sensitive). NOx controls at low VOC/NOx ratios are ineffective or may cause an increase in ozone (NOx disbenefit), especially within urban core areas. VOC/NOx ratios were 8 to 10 in 1987 and were likely higher during the preceding two decades due to increasingly stringent HC controls that were implemented. As shown in Figure 2-18, there was no significant reduction during the decades of the 1970s and 80s in the number of annual exceedances of the 1-hour ozone NAAQS of 120 ppb. As a result of the lack of significant

progress toward attainment of the ozone standard in many urban areas during the 1980s, the National Research Council (NRC) Committee on Tropospheric Ozone Formation and Measurement concluded that the 20-year effort to attain the ozone NAAQS had largely failed (NRC, 1991). Based partly on the SCAQS emission evaluations previously mentioned, the NRC Committee found that emission inventories significantly underestimated anthropogenic emissions of VOC. The Committee suggested that past ozone control strategies might have been misdirected due to this significant underestimation of VOC emissions. The consequence of this recommendation was control of both VOC and NOx with greater emphasis on developing emission controls to reduce motor vehicle NOx emissions. However, the historic trend in the basin 8-hour ozone Design Value (3-year running average of the annual fourth highest mixing ratio) shows that steady and continued progress was made during the past three decades. In retrospect, it appears that the reductions in VOC emissions and ozone that were anticipated by 1990 were not fully realized until about a decade later.

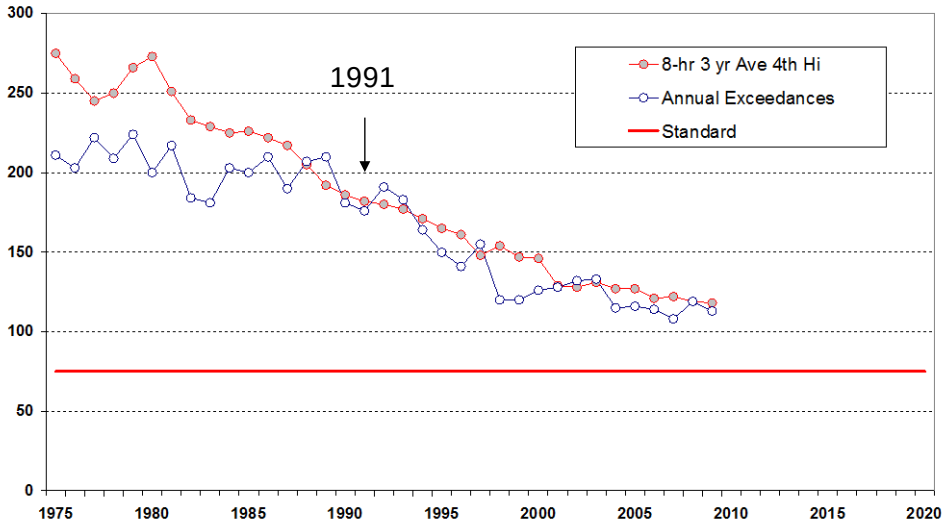

Figure 2-18. Trend in number of annual exceedances of the current 8-hour ozone NAAQS in the South Coast Air Basin from 1973 to 2009 and basinwide 8-hour ozone design value in ppb.

Ten years after the 1987 SCAQS, the ambient versus emissions inventory reconciliation for the SoCAB was updated during the 1997 Southern California Ozone Study (SCOS97-NARSTO). In a study by ENVIRON and the Desert Research Institute (Yarwood et al., 2003), ambient NMHC and NMOC mixing ratios and NMHC/NOx and NMOC/NOx ratios were compared to corresponding values from CAMx simulations of the August 3-7, 1997 SCOS97-NARSTO episode. Results are summarized in Table 2-6. In contrast to the 1987 SCAQS "top-down" evaluation, which indicated that hydrocarbon emissions were underestimated by a factor of two to three relative to NOx, this analysis showed no significant differences in NMHC/NOx or NMOC/NOx ratios derived from ambient and emission inventory data. The most significant change between the ambient/inventory reconciliation for SCAQS and SCOS97 is that the ambient VOC/NOx ratio had dropped by about a factor of two between 1987 and 1997 from 8.8 to about 4 due to greater reductions over this time of VOC emissions relative to NOx. The

changes in on-road motor vehicle emissions predicted by EMFAC versions show that while both HC and NOx emissions increased substantially for a common base year, the HC/NOx ratio remained nearly constant. Therefore, the ambient ratios came into line with the emissions model ratios, which remained essentially the same. We can conclude from these results that the benefits of new vehicle emission standards were overly optimistic in the late 1980s and that the expected benefits were not fully realized until almost a decade later. This was most likely due to extreme skewness of the distribution of real-world emissions within the vehicle population and underestimation in the emission models of the disproportionate impact of a small number of high emitters.

Table 2-6. Observed VOC/NOx ratios in 1987 and 1999-2000 and predicted weekday VOC/NOx ratios for the August 4-7, 1997 SCOS97 ozone episode. Source: CRC A-38, Yarwood et al. 2003).

	1987	August 4-7 1997			1999-2000
Locations	SCAQS 07-08 Observed NMOG*/NOx	PAMS 06-09 Observed NMHC*/NOx	CAMx/MM5 06-09 CB4/E2K1 NMHC/NOx	06-09 Observed/ Predicted	PAMS 06-09 Observed NMHC*/NOx
Anaheim	9.3				
Azusa	8.1	4.6	4.0	1.2	4.4
Burbank	9.2				
Los Angeles	8.6	4.3	3.7	1.2	3.8
Claremont	8.7				
Hawthorne	9.5				
Long Beach	8.7				
Rubidoux	8.6				
Pico Rivera		2.9	4.1	0.7	3.7
Upland		3.9	3.0	1.3	4.0
Mean	**8.8**	**3.9**	**3.7**	**1.1**	**4.0**
Std Dev	**0.4**	**0.7**	**0.5**	**0.3**	**0.3**
EI MV ROG/NOx	**4.0**				
Amb/EI Ratio	**2.2**				

The top-down emission inventory evaluation was recently updated by reconciling the ambient VOC/NOx ratios with the corresponding ratios derived from the 2005 and 2009 emission data (Fujita et al., 2013). The results for 2009 included in Table 2-7 show that the average ambient NMOC/NOx ratios are again about a factor of two higher than the emission inventory ratios. As part of the evaluation of the emission inventory and update of the 1987 and 1997 ambient versus inventory reconciliation analyses for the SoCAB, the Desert Research Institute conducted an on-road mobile source emissions study in August 2010 at the same traffic tunnel used in 1987 SCAS Tunnel Study (Fujita et al., 2012). The measured fleet-averaged, fuel-based emission factors were compared to the corresponding modeled factors using the EPA MOVES2010a and MOBILE6.2 models, and CARB's EMFAC2007 emission model. A

significant finding of the 2010 Van Nuys Tunnel Study was that measured NMHC fuel-based emission factors were about 3.5 times higher during hot temperature periods (38.5 ^{o}C) than cool periods (22 ^{o}C). The increased emissions during hot periods were attributed to light hydrocarbons that are associated with headspace evaporative emissions. These results are generally consistent with an ambient source apportionment study that estimated a 6.5 ± 2.5% increase in the contributions of evaporative emissions from motor vehicles per degree Celsius increase in maximum temperature (Rubin et al., 2006). While the NMHC emission rates predicted by all three models were in good agreement with measurements during cool periods, the running evaporative emissions for all models exhibited insufficient sensitivity to temperature during hot periods, especially MOVES. The measured NMHC/NOx ratios were 3.1, 1.7 and 1.4 times higher than predicted by MOVES, MOBILE and EMFAC, respectively, during hot periods. These results suggest there is an overall increase in motor vehicle NMHC emissions on hot days that is not fully accounted for by the emissions models. Hot temperatures and concomitant higher ratios of NMHC emissions relative to NOx both contribute to more rapid and efficient formation of ozone.

Table 2-7. Comparisons of ambient NMOC/NOx ratios measured at the SoCAB Photochemical Assessment Monitoring Stations with corresponding ratios of the average emissions for the nine 5x5 km grid cells surrounding the monitoring site for the month of July in 2009. Similar comparisons from the 1987 SCAQS and SCOS97-NARSTO are also shown (Fujita et al. 2013).

	1987 (SCAQS) [1]			1997 (SCOS97-NARSTO) [2]			2009 Weekdays		
Location	Ambient	EI	Amb/EI	Ambient	Modeled [3]	Amb/Mod	Ambient	EI	Amb/EI
Anaheim	9.3	3.7	2.5						
Azusa	8.1	4.0	2.0	4.6	4.0	1.2	6.4	3.2	2.0
Burbank	9.2	3.5	2.6						
Los Angeles	8.6	4.2	2.0	4.3	3.7	1.2	5.1	2.8	1.8
Claremont	8.7	4.3	2.0						
Hawthorne	9.5	5.2	1.8						
Long Beach	8.7	3.8	2.3						
Rubidoux	8.6	2.9	3.0				5.6	2.6	2.2
Pico Rivera				2.9	4.1	0.7	4.5	2.5	1.8
Upland				3.9	3.0	1.3			
Mean	8.8	4.0	**2.3**	3.9	3.7	**1.1**	5.4	2.8	**2.0**

[1] 1987 SCAQS ambient data are for ten weekdays and one Saturday in summer 1987.
[2] SCOS97-NARSTO ambient data are for the August 4-7, 1997 ozone episode (Monday – Thursday).
[3] CAMx photochemical model predictions for 9-cell average surrounding the monitoring site locations.

The indications that current estimates of VOC emissions may be underestimated relative to NOx emissions have important implications for modeled demonstrations that the selected emission reductions will result in ambient concentrations that meet the NAAQS. For this modeled attainment test, model estimates are used in a "relative" rather than "absolute" sense. Attainment is demonstrated using ratios of the model's future to current (baseline) predictions at monitoring locations. These ratios are called relative reduction factors (RRF). Future ozone

concentrations are estimated by multiplying the modeled RRF at a location near the monitoring site by the baseline design value (DV) of the site as follows:

DV(future year) = RRF x DV(baseline)

Where DV is the 3 year average of the fourth highest monitored daily 8-hour maximum value at each monitoring site. Attainment is deemed to be demonstrated if the projected future year DV is less than the NAAQS. In region that are VOC limited with respect to ozone formation, such as the SoCAB, an underestimation of VOC emissions in the base year will result in lower predicted ozone and higher RRF ratio. Correcting the underestimation will yield a lower RRF and decrease the emission reduction necessary to demonstrate attainment. In other word, underestimation of base year emission will result in overestimation of required emission reductions.

2.7 References

Altshuler, S.L.; Arcado, T.D.; Lawson, D.R. Weekend vs. Weekday Ambient Ozone Concentrations: Discussion and Hypotheses with Focus on Northern California; *J. Air & Waste Manage. Assoc.* 1995, 45, 967-972.

Austin, J.; Tran, H. A Characterization of the Weekend-Weekday Behavior of Ambient Ozone Concentrations in California; Technical Support and Planning Division, California Air Resources Board: Sacramento, CA, 1999.

Blanchard, C.L., S. Tanenbaum, VOC and NOx limitation of ozone formation at monitoring sties in Illinois, Indiana, Michigan, Missouri, Ohio, and Wisconsin, 1998-2002. Final report submitted by Envair to the Lake Michigan Air Directors Consortium, February 24, 2004.

Blanchard, C.L.; Tanenbaum, S. Data Analysis Complementing Proximate Modeling of the Weekday/Weekend Ozone Differences in Southern California. Final report prepared by Envair for the Coordinating Research Council, Alpharetta, GA (CRC Contract No. A-36A-2), and the National Renewable Energy Laboratory: Golden, CO, 2000.

Blier, W.; Winer, A.M.; Hansen, D.; Chavira, R. Analysis of Weekday/Weekend Differences in Ambient Air Quality and Meteorology in the South Coast Air Basin; Contract No. 95–334p; Final report prepared by the Department of Atmospheric Sciences and Environmental Science and Engineering, University of California, Los Angeles for the California Air Resources Board: Sacramento, CA, 1999.

Blier, W.; Winer, A.M.; Hansen, D.; Verma, N. Characterization of Ozone Episodes in the South Coast Air Basin: Effects of Air Parcel Residence Time and Weekend/Weekday Differences; Contract No. 93–316; Final report prepared by the Department of Atmospheric Sciences and Environmental Science and Engineering, University of California, Los Angeles, for the California Air Resources Board: Sacramento, CA, 1996.

California Air Resources Board. 2012. Ozone trend summary for the South Coast Air Basin, http://www.arb.ca.gov/adam/trends/trends2.php (accessed May 29, 2012).

Calvert, J.G., Stockwell, W.R., 1983. Acid generation in the troposphere by gas-phase chemistry. *Environ. Sci. and Technol.* 17, 428A-443A.

Chico, T., M. Bassett, J. Cassmassi, S. Mitsutomi, X. Zhang and H. Hogo (1993). "Application of the Urban Airshed Model for a SCAQS Episode in the South Coast Air Basin." In Proceedings, Southern California Air Quality Study - Data Analysis A&WMA Specialty Conference, VIP-26. Air & Waste Management Association, Pittsburgh, PA, pp. 257-263.

Chinkin, L.R., D.L. Coe, T.H. Funk, H.R. Hafner, P.T. Roberts, P.A. Ryan, and D.R. Lawson. 2003. Weekday versus weekday activity pattern for ozone precursor emission in California's South Coast Air Basin. *J. Air Waste Manage. Assoc*. 53:829–843. doi:10.1080/10473289.2003.10466223Elkus, B.; Wilson, K.R. Photochemical Air Pollution: Weekend-Weekday Differences; Atmos. Environ. 1977, 11, 509-515.

Elkus, B. and K.R. Wilson (1977). Photochemical Air Pollution: Weekend-Weekday Differences. *Atmospheric Environment*, 11, 509-515.

Finlayson-Pitts, B.J., and J.N. Pitts, Jr., *Atmospheric Chemistry: Fundamentals and Experimental Techniques*, John Wiley and Sons, New York, 1986.

Fujita, E.M., B.E. Croes, C.L. Bennett, D.R. Lawson, F.W. Lurmann, H.H. Main (1992). Comparison of Emission Inventory and Ambient Concentration Ratios of CO, NMOG, and NOx in California's South Coast Air Basin. *J. Air Waste Manage. Assoc*. 42:264-276.

Fujita, E.M., D.E. Campbell, B. Zielinska, J.C. Sagebiel, J.L. Bowen, W. Goliff, W.R. Stockwell, and D.R. Lawson (2003). Diurnal and Weekday Variations in Source Contributions of Ozone Precursors in California's South Coast Air Basin. *J. Air & Waste Manage. Assoc.* 53: 844-863.

Fujita, E.M., W.R. Stockwell, D.E. Campbell, and R.E. Keislar (2003). Evolution of the Magnitude and Spatial Extent of the Weekend Ozone Effect in California's South Coast Air Basin from 1981 to 2000. *J. Air & Waste Manage. Assoc.* 53:802-815

Fujita, E.M.; Campbell, D.E.; Zielinska, B.; Chow, J.C.; Lindhjem, C.E.; DenBleyker, A; Bishop, G.A; Schuchmann B.G.; Stedman, D.H.; Lawson, D.L. (2012). Comparison of the MOVES2010a, MOBILE6.2 and EMFAC2007 Mobile Source Emissions Models with On-Road Traffic Tunnel and Remote Sensing Measurements. *J. Air & Waste Manage. Assoc*. 62:1134-1149. DOI:10.1080/10962247.2012.699016

Fujita, E.M.; Campbell, D.E.; Stockwell, W.R.; Lawson, D.R. (2013). Past and future ozone trends in California's South Coast Air Basin: Reconciliation of amibnet measurements with past and projected emission inventories. *J. Air & Waste Manage. Assoc.* 63:1, 54-69. DOI: 0:1080/10962247.2012.735211

Harley, R.A., M.P. Hannigan, and G.R. Cass (1992). Respeciation of organic gas emissions and the detection of excess unburned gasoline in the atmosphere. *Environ. Sci. Technol*. 26:2395-408.

Harley, R.A., A.G. Russell, G.J. McRae, G.R. Cass, J.H. Seinfeld (1993). Photochemical Modeling of the Southern California Air Quality Study. *Environ. Sci. Technol*., 27:378 388.

Horie, Y.; Cassmassi, J.; Lai, L.; Gurtowski, L. Weekend/Weekday Differences in Oxidants and Their Precursors; Report prepared by Technology Services Corp. for the U.S. Environmental Protection Agency under Contract No. 68–02-2595; 1979.

Ingalls, M.N., L.R. Smith and R.E. Kirksey (1989). "Measurement of On-Road Vehicle Emission Factors in the California South Coast Air Basin - Volume I: Regulated Emissions." Report No. SwRI-1604 prepared for Coordinating Research Council, Atlanta, GA, by the Southwest Research Institute, June 1989.

Levitt, S.B.; Chock, D.P. Weekend-Weekday Pollutant Studies of the Los Angeles Basin; *J. Air Poll. Control Assoc.* 1976, 26, 1091-1092.

Milford, J.B, D. Gao, S. Sillman, P. Blossey, and A.G. Russell. (1994). Total Reactive Nitrogen (NO_y) as an Indicator of the Sensitivity of Ozone to Reductions in Hydrocarbon and NO_x Emissions. *J. Geophys. Res.*, 99, 3533-3542.

Pierson, W.R., A.W. Gertler, and R.L. Bradow (1990). Comparison of the SCAQS Tunnel Study with Other On-Road Vehicle Emission Data. *J. Air Waste Manage. Assoc*. 40:1495-1504.

Pun, B.K.; Seigneur, C.; White, W. Data Analysis for a Better Understanding of the Weekday/Weekend Ozone and PM Differences; Final report prepared by Atmospheric and Environmental Research, Inc., San Ramon, CA, under CRC contract Number A-36B for the Coordinating Research Council: Alpharetta, GA, June 2001.

Rubin, J.I., A.J. Keen, R.A. Harley, D.B. Millet, and A.H. Goldstein. 2006. Temperature dependence of volatile organic compound evaporative emissions from motor vehicles. *J. Geophys. Res*. 111:D03305. doi:10.1029/2005JD006458.

Seinfeld, J. H., *Atmospheric Chemistry and Physics of Air Pollution*, John Wiley, New York, 1986.

Sillman, S. 1995. The use of NOy, H2O2, and HNO3 as indicators for ozone-NOx-hydrocaron sensitivity in urban locations. *J Geophys. Res.* 100: 14,175-14,188.

South Coast Air Quality Management District (2013). Final 2012 Air Quality Management Plan. SCAQMD, diamong Bar, CA, Feburary 2013.

Stockwell, W.R., P. Middleton, J.S. Chang and X. Tang, (1990). The Second Generation Regional Acid Deposition Model Chemical Mechanism for Regional Air Quality Modeling, *J. Geophys. Res.*, 95, 16343-16367.

Stockwell, W.R., Kirchner, F., Kuhn, M., Seefeld, S., 1997. A new mechanism for regional atmospheric chemistry modeling. *Journal of Geophysical Research* 102, 25847-25879.

Stockwell, W.R., C.V. Lawson, E. Saunders, and W.S. Goliff. 2012. A review of tropospheric atmospheric chemistry and gas-phase chemical mechanisms for air quality modeling. *Atmosphere* 3:1–32. doi:10.3390/atmos3010001

Wagner, K.K., N.J.M. Wheeler (1993). Multi-Species Evaluation of the Urban Airshed Model with the SCAQS Database. In Proceedings of the International Specialty Conference on the Southern California Air Quality Study Data Analysis, Los Angeles, CA, July 21 23, 1992, E.M. Fujita, Ed. VIP-26. Air & Waste Management Assoc., Pittsburgh, PA, pp. 264-269.

Yarwood, G., C. Tran, S. Lau, E. Fujita. 2003. Impact of updates to on-road mobile source emission factor models (EMFAC) for the Los Angeles region: ozone model sensitivity and ambient/inventory reconciliation. Final report prepared for the Coordinating Research Council, Alpharetta GA, September 29, 2003.

3. LONG-TERM CHANGES IN THE SPATIAL AND TEMPORAL VARIATIONS OF PEAK OZONE LEVELS IN THE SOUTH COAST AIR BASIN

This section summarizes the historic trends in the daily maximum ozone concentrations in the SoCAB from 1982 to 2013 by location and day of week and examines the evolution of the magnitude and spatial extent of the weekend ozone effect over this period. The analyses update our prior work, which are summarized in the following two publications.

- Fujita, E.M., W.R. Stockwell, D.E. Campbell, and R.E. Keislar (2003). Evolution of the magnitude and spatial extent of the weekend ozone effect in California's South Coast Air Basin 1981-2000, JAWMA 53:802-815.
- Fujita, E.M.; Campbell, D.E.; Stockwell, W.R.; Lawson, D.R. (2013). Past and future ozone trends in California's South Coast Air Basin: reconciliation of ambient measurements with past and projected emission inventories, J. Air Waste Manage. Assoc. 63:54-69

3.1 Approach and Methods

The trends in daily maximum 8-hour average ozone mixing ratios from 1980 to 2013 were examined by day-of-week. Ambient ozone trends not only reflect changes in the temporal and spatial patterns of precursor emissions, but also the complex non-linear relationship of the varying mixtures of VOC and NOx in the atmosphere with rates of ozone production and accumulation. We examined these historic changes by comparing the ozone trends for 1980-2013 by day of the week for six SCAQMD monitoring stations in the SoCAB with the corresponding trends in ambient CO and NOx, and CO/NOx ratios. Sampling locations include downtown Los Angeles in the upwind western basin, three central basin sites in Azusa, Pomona and Upland, a downwind eastern basin site in Riverside-Rubidoux, and a far downwind site at Crestline/Lake Gregory (1,300 m elevation) in a forested area in the San Bernardino Mountains. Figure 3-1 shows the location of the relevant monitoring sites. The basin design value for ozone is mostly driven by measurements at Crestline. These ambient trends in ozone precursors are also compared to historic trends in emission inventory data and future projections.

The analysis focuses on day-of-the-week differences in the extent of inhibition of ozone formation during the morning due to titration with NO and the rate of ozone accumulation from the end of the inhibition period to time of peak ozone. Hourly criteria pollutant data for the summers (May 1–October 31) of 1990–2013 were obtained from CARB and the key daily parameters of interest shown in Table 3-1 were calculated. Refer to Figure 2-8 in Section 1.4 for definition of the key parameters. This new data set was combined with data that were compiled from our prior analysis for 1980-1998. Values of pollutants from 2:00 to 3:00 a.m. PST (4-5 PDT) are surrogates for carryover from the previous day. Values of pollutants from 6:00 to 7:00 a.m. (7-8 PDT) represent the morning commute. The end of the O_3 inhibition period, *t_xover*, was determined by subtracting the mixing ratio of O_3 from NO and finding the hour between 7:00 a.m. and 2:00 p.m. at which this difference transitions from greater than to less than zero. The interpolation involves the intersection of the two line segments represented by the decreasing NO and the increasing O_3.

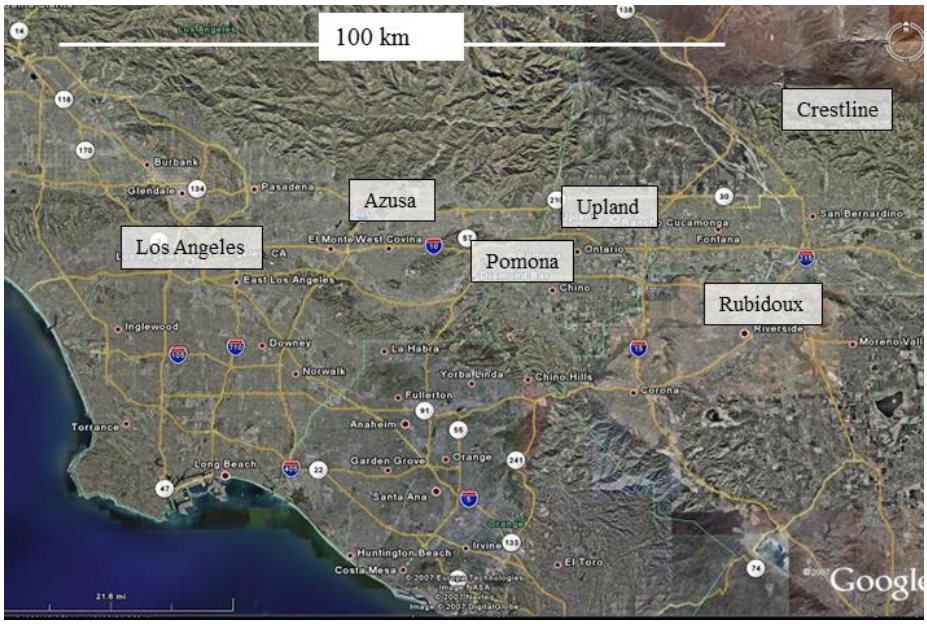

Figure 3-1. Map of the South Coast Air Basin with approximate locations of relevant air quality monitoring stations.

Table 3-1. Air quality parameters for the conceptual explanation of the weekend O_3 effect.

No.	Parameter	Purpose
1	$[O_3]$max (ppb)	WE/WD effect indicator
2	4-5 PDT [NO] (ppb)	Carryover
3	4-5 PDT [NO2] (ppb)	Carryover
4	4-5 PDT [NO2]/[NOx] (ppb)	Carryover
5	4-5 PDT [NMHC] (ppbC)	Carryover (via Bendix or regression with CO)
6	7-8 PDT [NO] (ppb)	Ozone titration potential (morning rush hour)
7	7-8 PDT [NO2] (ppb)	For NO_2-NO comparison
8	7-8 PDT [CO] (ppm)	Surrogate for gas-powered morning emissions
9	7-8 PDT [NMHC] (ppbC)	Fresh emissions (morning rush hour)
10	6-9 PDT NMHC/NOx	Reaction efficiency/rate for morning commute
11	tNO=O3 (PST)	Interpolated time of morning crossover of O_3 and NO. Marks ends of O_3 inhibition period and the beginning of the ozone accumulation period.
12	tO3max (PST)	Interpolated time of daily maximum O_3
13	tO3max-tNO=O3	Duration of O_3 accumulation
14	O_3rate (ppb/hour)	Rate of O_3 accumulation (see definition below)
15	NMHC/NOx(t_{O3max})	Reaction efficiency/rate at t_{O3max}

Rate of O3 accumulation: ([O3]max-[O3(tNO=O3)])/(tO3max-tNO=O3)

3.2 Results

This task updates the historic trends in the daily maximum ozone concentrations in the SoCAB from 1982 to 2013 by location and day of week and examines the evolution of the magnitude and spatial extent of the weekend ozone effect over this period. Figure 3-2 shows the 1980-2013 trends in summer mean daily maximum 8-hour ozone in the SoCAB on Sunday and weekdays. The trend for the most upwind site located in downtown Los Angeles is shown with open circles and data for the monitoring sites in the central basin are shown as broken lines. Ozone values are typically highest at the extreme downwind site at Crestline (shown with filled circles). While the ozone at Crestline for both Sunday and weekdays shows slight decreasing trends in the past decade, the weekday ozone levels at the central basin sites show a slightly increasing trend in the past decade. The minima in the ozone trends at the central Basin sites coincided with minima in the ambient VOC/NOx ratio trends shown in Figure 2-12. The magnitude of the weekend ozone effect (Sunday-Weekday in Figure 3-2) was at historic highs during this period and has eased in recent years with increases in the ambient VOC/NOx ratios.

The varying ozone trends throughout the SoCAB and evolution of the weekend ozone effect are evident in the day-of-week and site-specific ozone trends shown in Figure 3-3. After steep reductions in the 1990s, ozone trends have leveled off since 2000. While ozone levels continued to decline slowly on weekends, the decline was slower on weekdays with some part of the central basin ozone showing increasing ozone trends since 2000. The net effect is a reduction in the weekend ozone effect in recent years compared to 2000 (see Sunday-Weekday plot in Figure 3-2).

The 30-year ozone trends shown in Figure 3-4 are characterized by different trends for weekdays and weekends. The weekday trends show rapid and steady decline in ozone levels from 1982 to 2000, but a relatively flat trend during the last 12 years. Weekends show a relatively slow decline during the first 12 years, followed by six years of rapid decrease from mid-1990s to 2000, and back to a slow declining trend during the last 12 years. WE-WD differences were minimal in the early 1980s, increase in the late 1980s in the western half of the SoCAB and gradually spread further east during the 1990s. The maxima in WE-WD differences occurred at about 2000 throughout the basin and coincided with the beginning of the flattening ozone trends. Currently, the WE effect is strongest in the central basin and has weakened in the western and eastern portions of the basin.

The ozone trends are alternatively displayed in Figure 3-10 as (trend max - annual max)/(trend max – trend min), which is the incremental progress toward the total reduction in ozone over the 30-year trend period. Over 80 percent of the total reduction in ozone was achieved on weekdays by the late 1990s. Very little further progress was made during the past 12 years. Most of the marginal improvement made during the past 12 years occurred on the weekends.

The historic trends in CO mixing ratios in Figure 3-5 are consistent with more rapid decline of ozone levels on weekday than weekends from 1983 to the mid-1990s. While both ozone and CO levels decline steadily during this period on weekdays, the corresponding trends were flatter on weekends until the mid-1990s. The Long term trends in NO mixing ratios in Figure 3-6 show relatively flat trend until about 2000 and steady declining trend thereafter. Compared to weekdays, NO mixing ratios were 30-40% and 55-70% lower on Saturdays and Sundays, respectively. However, the weekday differences have narrowed in the recent years.

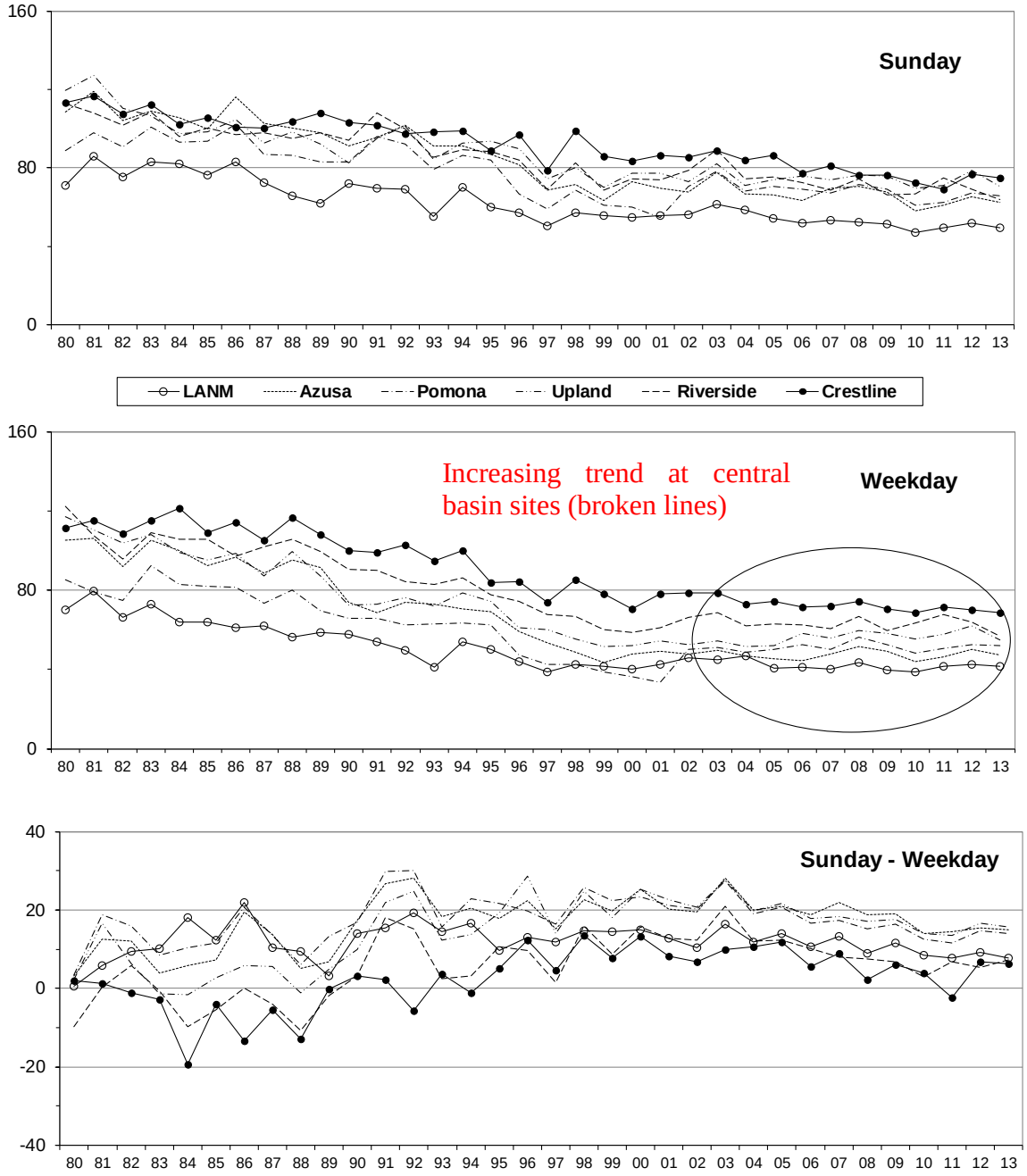

Figure 3-2. Trends in Sunday, weekdays and Sunday minus weekday mean maximum 8-hour ozone (ppb) during May-Oct 1980-2013 at Los Angeles N. Main, Azusa, Pomona, Upland, Riverside and Crestline. The trends for the most upwind site located in downtown Los Angeles are shown with open circles and data for the monitoring sites in the central basin are shown as broken lines. Ozone values are typically highest at the extreme downwind site at Crestline (shown with filled circles). Note the increasing and decreasing magnitude of the WE effect (lower panel), which peaked about 2000 to 2005. Source: update of Figure 5 in Fujita et al. *J. Air Waste Manage. Assoc.* 63 (2013):1, 54-69.

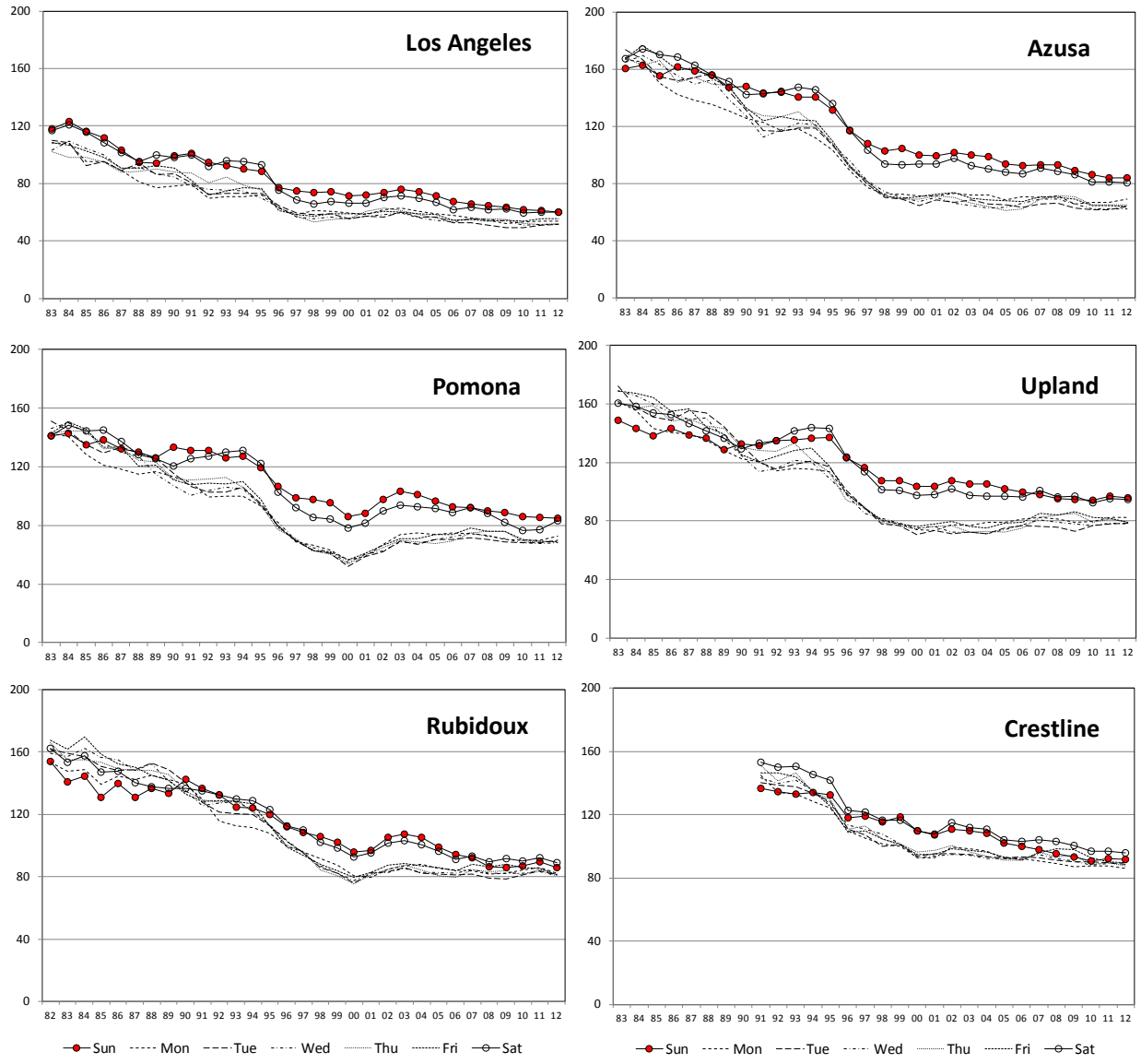

Figure 3-3. Seasonal (6/1 to 9/30) 3-year running mean daily maximum 1-hour ozone by day of week.

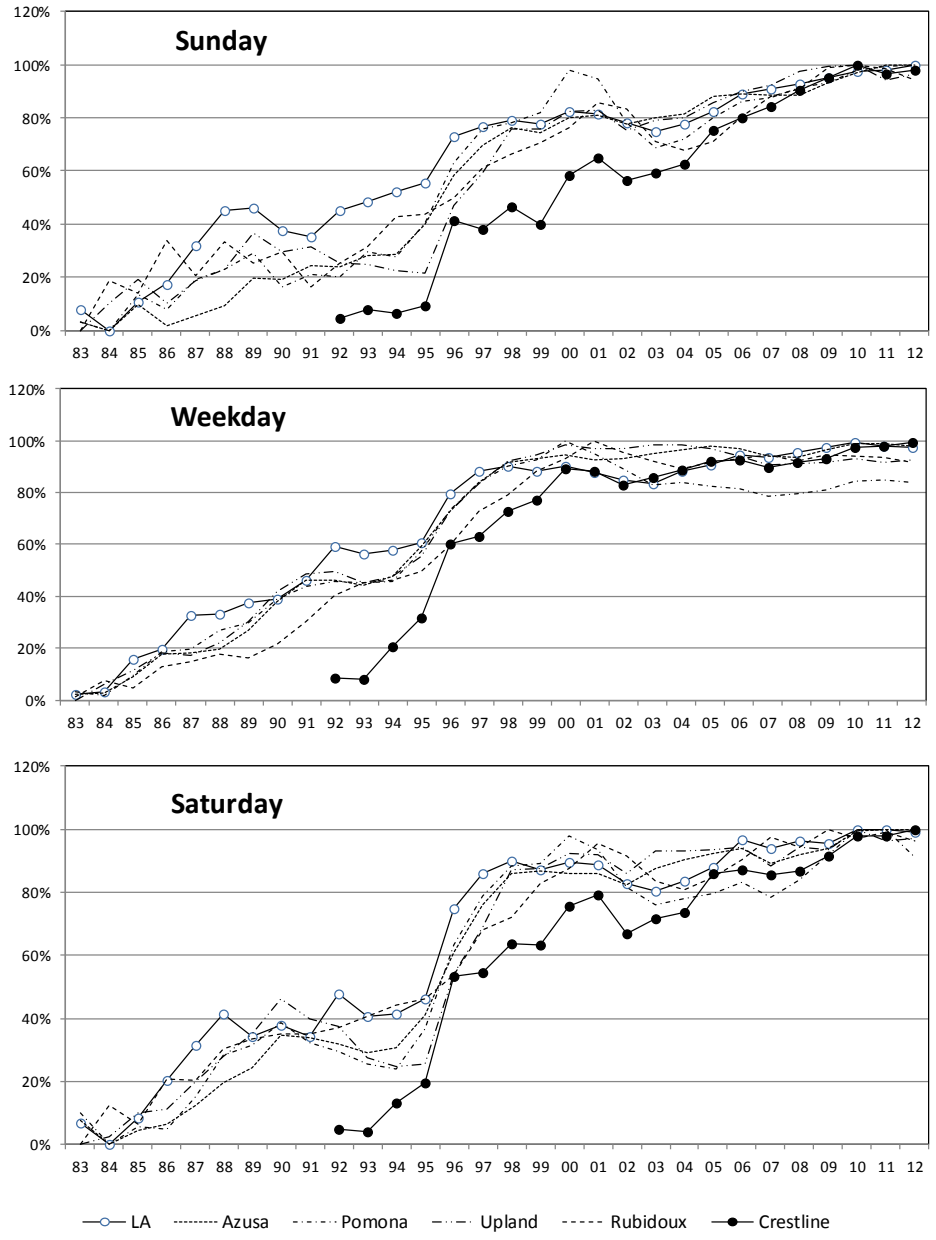

Figure 3-4. Trends from 1982 to 2012 of (30-year max - annual max)/(30-year max – 30-year min) in percent. Ratios are based on three-year running averages of the annual means of the daily maximum 1-hour ozone mixing ratios (see Figure 3-9). Trend line for Crestline is not directly comparable to other sites since data are not available for this site before 1992.

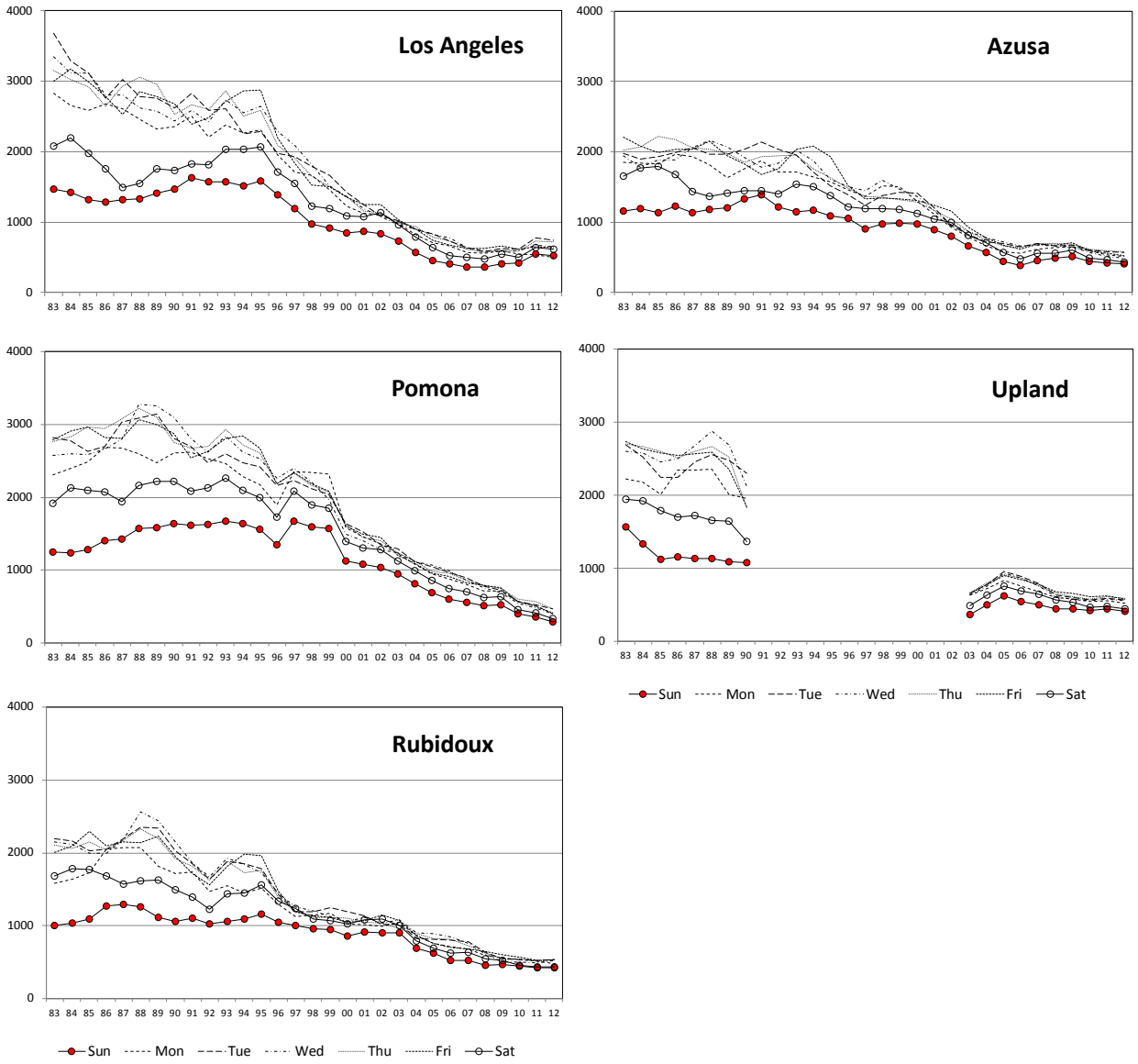

Figure 3-5. Seasonal (6/1 to 9/30) 3-year running mean 6-7 am CO (ppb) by day of week.

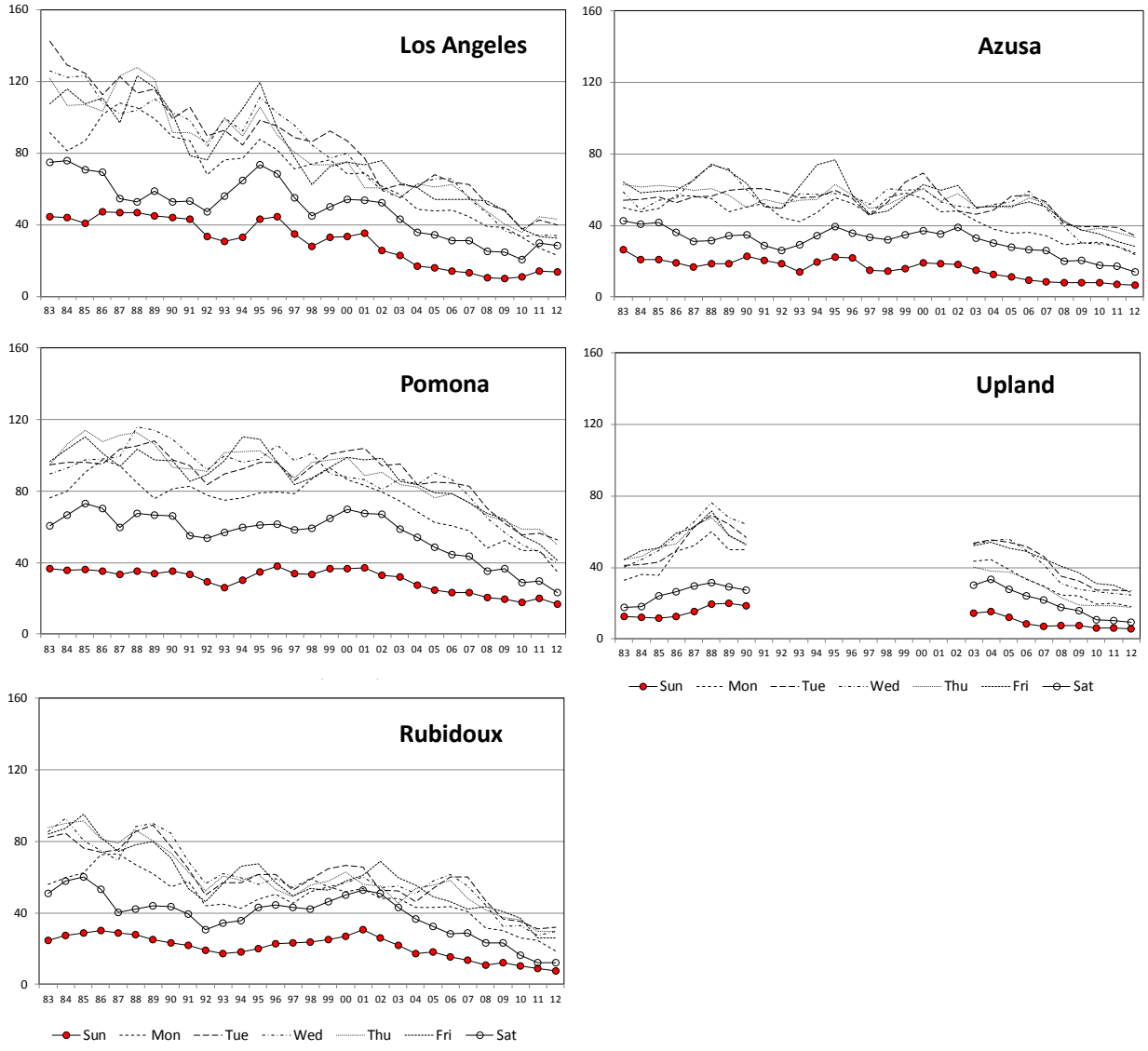

Figure 3-6. Seasonal (6/1 to 9/30) 3-year running mean 6-7 am NO (ppb) by day of week.

The intensity and spatial extent of the weekend ozone effect are associated with weekday-weekend differences in the degree of ozone inhibition and rate of ozone accumulation. Lower NO concentrations and higher NO_2/NOx ratios during weekend mornings decrease the removal of ozone by titration with NO, thereby allowing ozone to accumulate about an hour earlier on weekends compared to weekdays (Fujita et al., 2003). This advance in timing of ozone accumulation on weekends is similar throughout the Basin, and it remained relatively constant from 1981 to 1999. In contrast, the rate of ozone accumulation from the end of ozone inhibition to the time of ozone maximum decreased by one-half over the same time period with largest reductions occurring in the central Basin. Rates of ozone accumulation were consistently lower on weekends than weekdays through most of the 1980s but became consistently higher on weekends during the 1990s. A switch to higher weekend ozone accumulation rates in the 1990s, coupled with a shorter inhibition period, resulted in higher weekend ozone concentrations during the 1990s and a strengthening of the weekend ozone effect within the Basin.

Updated trends in the duration of ozone accumulation and ozone accumulation rates are summarized in Table 3-2. Incremental four-year averages were derived Los Angeles, Azusa, Pomona, Upland and Rubidoux for the years from 1982 to 2013. The same data are plotted as 3-year running mean for duration of ozone accumulation in Figure 3-7 and for ozone accumulation rate in Figure 3-8. The duration of ozone accumulation has increased in recent years due likely to greater reductions of NO emissions resulting in less ozone inhibition in the morning. The trend in ozone accumulation rates have flattened in the past decade with narrowing of the weekday-weekend differences in recent years.

Table 3-2. Changes in duration and rate of ozone accumulation within the South Coast Air Basin.

	Duration of Ozone Accumulation (hours)							Rate of Ozone Accumulation (ppb/hour)						
	Sun	Mon	Tue	Wed	Thu	Fri	Sat	Sun	Mon	Tue	Wed	Thu	Fri	Sat
Los Angeles														
1982-85	4.4	3.2	3.4	2.9	2.9	3.3	3.7	25.5	27.3	26.3	28.1	27.2	27.2	29.2
1986-89	3.6	3.1	2.3	3.0	3.0	2.9	3.9	26.3	21.1	21.9	24.9	22.9	28.1	22.9
1990-93	3.7	3.2	3.2	3.2	3.4	3.1	3.9	18.6	13.7	14.4	14.4	15.4	16.8	17.3
1994-97	3.9	3.9	3.4	3.1	3.1	3.5	3.8	14.1	9.9	9.3	12.1	11.5	9.6	14.5
1998-01	4.2	3.7	3.4	3.4	3.5	3.8	4.6	10.6	7.4	7.4	7.2	7.5	7.6	8.0
2002-05	4.8	3.7	3.9	3.2	3.7	3.5	4.2	10.0	7.7	6.7	7.2	7.9	8.3	9.0
2006-09	4.9	3.9	4.1	3.5	3.9	3.8	4.4	9.0	7.1	6.3	6.8	7.3	7.0	8.2
2010-13	4.6	4.3	3.3	3.6	4.0	4.3	4.6	8.2	6.2	5.9	6.3	4.9	5.9	7.5
Azusa														
1982-85	5.8	5.1	5.1	4.3	4.7	4.8	5.5	24.7	27.2	28.3	29.2	31.6	30.3	29.4
1986-89	6.3	5.0	4.5	4.9	4.5	4.9	5.5	24.1	23.6	30.2	27.9	26.6	28.2	26.4
1990-93	6.0	4.9	4.5	4.4	4.9	4.5	5.4	18.7	18.7	19.8	20.0	20.3	21.7	22.0
1994-97	6.1	5.0	4.5	3.9	3.9	4.3	5.1	13.2	13.2	15.2	17.2	17.6	15.5	18.5
1998-01	5.5	4.0	3.9	4.0	3.3	4.0	4.8	10.6	10.6	9.8	10.0	11.3	10.1	14.4
2002-05	5.7	3.6	3.8	4.3	3.5	3.6	4.9	11.3	11.3	9.6	7.9	9.6	10.9	12.6
2006-09	6.4	4.7	4.6	4.6	4.4	4.3	4.9	9.1	9.1	8.1	8.6	8.7	9.8	13.1
2010-13	6.6	5.1	4.4	4.2	4.4	4.3	5.7	8.3	8.3	8.4	7.8	8.9	8.6	10.4
Pomona														
1982-85	6.2	4.8	4.6	4.8	4.9	4.7	5.3	21.7	22.7	25.8	26.1	26.2	25.4	24.4
1986-89	5.9	4.6	4.4	4.4	4.6	4.6	5.2	19.6	20.2	25.6	21.5	22.2	21.7	20.6
1990-93	5.4	4.3	4.7	4.9	4.6	4.7	4.8	19.3	18.3	16.9	15.0	18.4	18.6	20.4
1994-97	5.4	4.4	4.1	4.0	3.6	4.0	4.6	15.9	12.9	13.6	14.1	15.8	14.9	17.5
1998-01	5.0	3.9	3.4	3.7	3.2	3.4	4.4	13.8	9.5	9.6	9.0	11.0	10.5	13.1
2002-05	5.6	4.3	3.9	4.0	3.5	4.1	5.1	13.0	9.8	8.4	8.9	9.8	9.1	12.0
2006-09	5.9	5.0	4.6	4.7	4.4	5.0	5.4	11.1	8.8	8.3	9.1	9.0	9.5	11.2
2010-13	5.9	5.4	5.1	5.3	4.9	5.3	5.1	10.1	7.9	8.0	7.7	8.1	7.8	10.7
Upland														
1982-85	7.5	6.7	6.5	6.2	6.3	6.6	7.0	18.1	19.4	22.3	20.7	22.8	22.2	20.9
1986-89	7.3	6.1	5.4	6.0	5.8	6.2	6.4	15.9	20.2	21.6	21.1	19.8	19.3	18.7
1990-93	7.4	6.2	6.0	6.2	5.6	5.9	6.9	15.4	15.1	15.9	14.3	18.2	16.6	16.3
1994-97	7.1	5.3	5.5	5.4	5.1	6.1	6.5	15.0	14.2	13.6	13.1	15.2	13.3	15.6
1998-01	6.3	4.7	4.2	4.7	4.3	5.0	5.7	13.0	9.9	10.0	9.7	10.8	9.6	12.5
2002-05	6.6	5.0	4.2	4.6	4.4	4.9	6.2	12.6	9.9	8.8	8.5	9.3	9.2	11.1
2006-09	7.5	6.0	5.3	5.7	5.5	5.3	6.4	10.9	9.0	9.2	8.7	9.3	10.4	11.5
2010-13	8.1	6.5	5.6	5.6	5.8	5.7	7.1	10.2	8.7	8.5	8.4	8.9	9.1	10.7
Rubidoux														
1982-85	6.9	6.3	6.3	5.8	5.8	6.3	6.0	19.1	20.2	21.3	23.7	23.0	21.5	22.6
1986-89	6.4	6.2	5.9	6.0	5.6	5.6	6.0	19.7	20.1	22.6	21.7	22.8	22.5	21.0
1990-93	6.4	5.8	5.8	5.2	5.2	5.4	6.3	17.2	17.2	16.7	17.6	19.2	18.2	17.4
1994-97	6.5	5.8	5.6	5.5	5.0	5.3	5.7	13.9	13.3	14.3	14.5	15.5	14.5	15.7
1998-01	6.2	5.3	5.0	5.0	5.1	5.3	5.6	12.2	11.1	10.4	10.8	10.6	10.5	12.6
2002-05	6.4	5.4	4.8	4.9	4.9	5.1	6.0	12.2	10.5	11.1	10.2	10.8	11.3	11.7
2006-09	6.4	5.9	4.9	5.4	5.5	5.5	6.1	10.3	9.5	10.3	10.2	9.6	10.0	10.9
2010-13	6.7	6.1	5.9	6.2	5.9	5.7	6.4	9.7	9.4	9.8	9.3	9.3	9.9	10.2

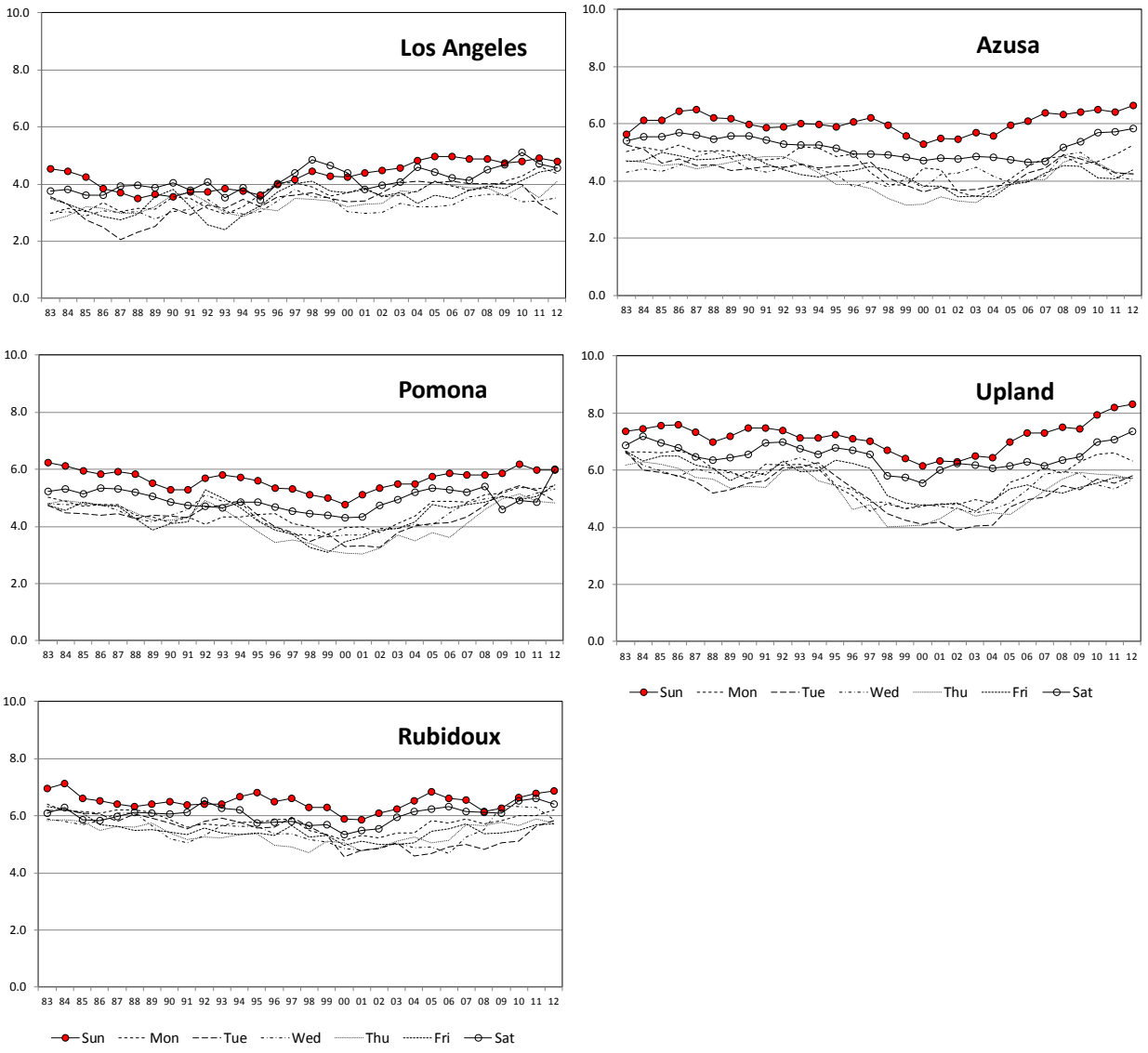

Figure 3-7. Seasonal (6/1 to 9/30) 3-year running mean duration of ozone accumulation (hrs) by day of week. Duration is define here as the difference in time between when ambient ozone begin to exceed NO in the morning marking the end ozone inhibition period and the time of daily maximum ozone.

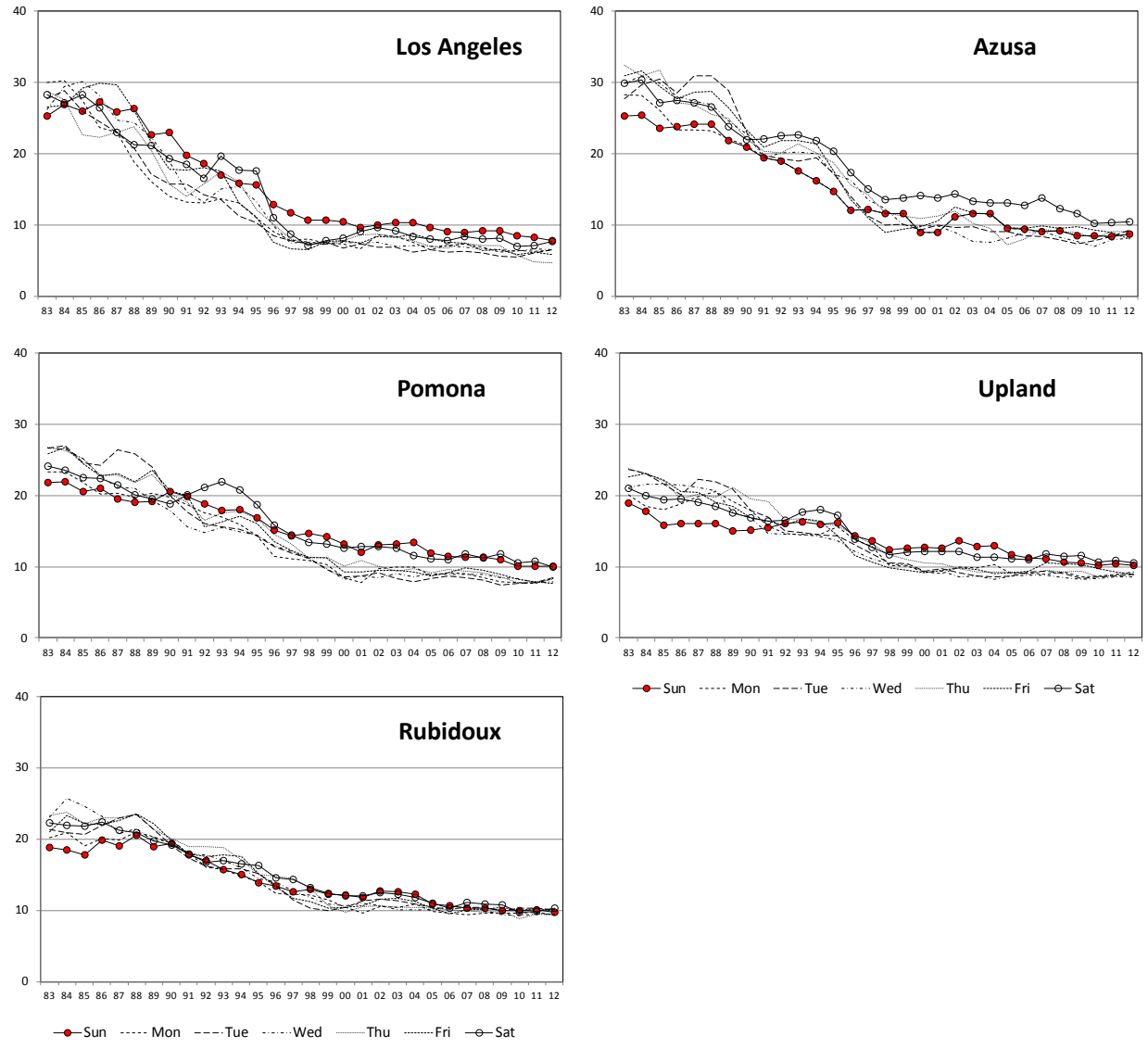

Figure 3-8. Seasonal (6/1 to 9/30) 3-year running mean rate of ozone accumulation (ppb/hr) by day of week.

3.3 Discussion and Conclusions

The trends in ambient ozone levels in the SoCAB over the past 30 years are characterized by different trends for weekdays and weekends. On weekdays, over 90 percent of the total reduction of ozone during the past 30 years was achieved by the late 1990s or at the mid-point of the trend period. Very little further progress was made on weekdays during the past 12 years and progress even reversed at some central basin locations. The flattening of the ozone trend occurred despite continued steady reductions in VOC emissions and more aggressive reductions of NOx emissions during the past decade. The marginal reductions in ozone levels during the past 12 years occurred mostly on weekends leading to a narrowing of the WE-WD differences in ozone. Differences between weekend and weekday ozone levels were minimal in the early

1980s, increased in the late 1980s in the western half of the SoCAB, and gradually spread further east during the 1990s. The maxima in WE-WD differences occurred at about 2000 and coincided with the time when ozone trends began to flatten. Currently, the WE effect is strongest in the central basin and has weakened in the both western and eastern portions of the basin. While ozone levels at the far downwind site at Crestline show slight decreasing trends in the past decade for both weekends and weekdays, the weekday ozone levels at central basin sites show a slightly increasing trend in the past decade. The minima in the ozone trends at the central Basin sites coincided with minima in the ambient VOC/NOx ratio trends. The magnitude of the weekend ozone effect was at historic highs during this period and has eased in recent years with increases in the ambient VOC/NOx ratios.

3.4 References

Blanchard, C.L. and S. Tanenbaum (2000). Data Analysis Complementing Proximate Modeling of the Weekday/Weekend Ozone Differences in Southern California. Final report prepared by Envair for the Coordinating Research Council, Alpharetta, GA (CRC Contract No. A-36A-2), and the National Renewable Energy Laboratory, Golden, CO.

Blanchard, C.L. and S.J. Tanenbaum (2003). Differences Between Weekday and Weekend Air Pollutant Levels in Southern California. Submitted to J. Air & Waste Manage. Assoc.

California Air Resources Board, 2014. Emission inventory data from 1975 to 2035 downloaded from http://www.arb.ca.gov/ei/ei.htm (accessed on 08/28/14).

Fujita, E.M., W.R. Stockwell, D.E. Campbell, and R.E. Keislar (2003). Evolution of the Magnitude and Spatial Extent of the Weekend Ozone Effect in California's South Coast Air Basin from 1981 to 2000. *J. Air & Waste Manage. Assoc.* 53:802-815

Fujita E.M., D.E. Campbell, B. Zielinska, J.C. Chow, C.E. Lindhjem, A. DenBleyker, G.A. Bishop, B.G. Schuchmann, D.H. Stedman, and D.R. Lawson. 2012. Comparison of the MOVES2010a, MOBILE6.2 and EMFAC2007 mobile source emissions models with on-road traffic tunnel and remote sensing measurements. *J. Air Waste Manage. Assoc.* 62:1134–1149. doi:10.1080/10962247.2012.699016

Fujita, E.M.; Campbell, D.E.; Stockwell, W.R.; Lawson, D.R. (2013). Past and future ozone trends in California's South Coast Air Basin: Reconciliation of amibnet measurements with past and projected emission inventories. *J. Air & Waste Manage. Assoc.* 63:1, 54-69. DOI: 0:1080/10962247.2012.735211

South Coast Air Quality Management District (2013). Final 2012 Air Quality Management Plan. SCAQMD, Diamond Bar, CA, Feburary 2013.

4. EVALUATION OF THE EMISSION INVENTORY

As part of the evaluation of the emission inventory and update of the 1987 and 1997 ambient versus inventory reconciliation analyses for the SoCAB, the Desert Research Institute conducted an on-road mobile source emissions study in August 2010 at the same traffic tunnel used in 1987 SCAS Tunnel Study (Fujita et al., 2012). The measured fleet-averaged, fuel-based emission factors were compared to the corresponding modeled factors using the EPA MOVES2010a and MOBILE6.2 models, and CARB's EMFAC2007 emission model. A significant finding of the 2010 Van Nuys Tunnel Study was that measured NMHC fuel-based emission factors were about 3.5 times higher during hot temperature periods (101-102 ^{o}F) than cool periods (71-72 ^{o}F). The increased emissions during hot periods were attributed to light hydrocarbons that are associated with headspace evaporative emissions. These results are generally consistent with an ambient source apportionment study that estimated a 6.5 ± 2.5% increase in the contributions of evaporative emissions from motor vehicles per degree Celsius increase in maximum temperature (Rubin et al., 2006). While the NMHC emission rates predicted by all three models were in good agreement with measurements during cool periods, the running evaporative emissions for all models exhibited insufficient sensitivity to temperature during hot periods, especially MOVES. The measured NMHC/NOx ratios were 3.1, 1.7 and 1.4 times higher than predicted by MOVES, MOBILE and EMFAC, respectively, during hot periods. These results suggest there is an overall increase in motor vehicle NMHC emissions on hot days that is not fully accounted for by the emissions models.

During the 2010 Van Nuys tunnel study, researchers from the University of Denver measured on-road fuel-specific light-duty vehicle emissions from nearly 13,000 vehicles on Sherman Way (0.4 miles west of the tunnel) with its multispecies Fuel Efficiency Automobile Test (FEAT) remote sensor a week prior to the tunnel measurements by DRI (Bishop et al., 2012). Comparisons with the 1987 Van Nuys Tunnel Study measurements show large reductions in CO, HC, and NOx, but little change in the HC/NOx mass ratio since 1995. The fleet CO and HC emissions are increasingly dominated by a few gross emitters, with more than a third of the total emissions being contributed by less than 1% of the fleet. An example of this is a 1995 vehicle measured three times with an average HC emission of 419 g/kg fuel. These three measurements account for 4% of the total HC emissions from the 13,000 measurements. The authors conclude that finding and repairing and/or scrapping as little as 2% of the dirtiest vehicles from the fleet would reduce on-road tailpipe emissions by as much as 50%.

4.1 Approach and Methods

To evaluate the emissions inventory a top-down approach was taken by comparing the measured concentrations of ozone and ozone precursors at several ambient monitoring stations to the model predicted concentrations for the grid cells corresponding to the location of those monitoring locations. The comparisons of predicted and measured ozone concentrations are described in the Section 4 including the effects of upward adjustments in ROG emissions on model performance. This section compares the predicted and measured NO, NOx, CO, CO/NOx ratio, NMOC/NOx, and VOC by lumped species groups.

Ambient concentrations of NO, NOx, CO and speciated hydrocarbons at three Photochemical Assessment Monitoring Stations (PAMS) in the South Coast Air Basin were obtained from the EPA AQS data system for the summer of 2008. The three sites are located in Azusa, Pico Rivera, and Upland and reported hourly concentrations of ozone as well as 3-hour

average concentrations of total NMOC and 54 individual VOC species. VOC data were collected daily at Pico Rivera and every third day at Azusa and Upland from July 2 to Sept 30, 2014. PAMS located in Westchester (near LAX), Banning, Santa Clarita, and Burbank also reported speciated VOC data during the same period but were not included in the analysis because the analysis was focused on the central and eastern portion of the basin where higher ozone levels occur.

CMAQ model output files for the period from June 1 to Sept. 2, 2008 were provided by SCAQMD. These files contained the modeled mean hourly concentrations of NO, NOx, CO and individual and lumped VOC species (using SAPRC99 methodology) for each 2 km x 2 km grid cell in the basin. The mean concentrations of the criteria pollutants and individual and lumped VOC which encompassed the 54 PAMS species in the grid cells where the 3 PAMS are located were extracted from the CMAQ output files for the morning commute (5 to 8 PST) and late morning (8 to 11 PST) PAMS sampling periods. To investigate the impact of spatial scale on the evaluation, the CMAQ modeled mean concentrations for 9-cell (6 km x 6 km) areas surrounding the three PAMS sites were also extracted.

To allow direct comparison of the ozone precursor concentrations measured by the PAMS network to the CMAQ model output, we combined individual VOC species concentrations into categories corresponding to the lumped species in SAPRC99 (Carter, W. 2000. Implementation of the Saprc-99 Chemical Mechanism into the Models-3 Framework, Report to USEPA) as shown in Table 4-1. Although total NMOC was not included in the CMAQ output, we estimated that parameter by summing the categories listed in the table and multiplying the result by the ratio (measured NMOC)/(sum of measured species) for the corresponding PAMS samples. This allowed us to also compare VOC/NOx ratios from the PAMS network and CMAQ model. The results were tabulated for the two time periods and ratios of measured to modeled concentrations were calculated for each site, day, and species category. Descriptive statistics (mean, median, standard deviation) and the correlation to local daily mean and daily maximum temperature were calculated for the ratios in each species category.

4.2 Results and Discussion

The ambient NMOC (by SAPRC lumped species) from the Azusa, Upland and Pico Rivera Photochemical Assessment Monitoring Stations (PAMS) were compared to corresponding day-specific averages of the nine grid cell (12 x 12 km) CMAQ simulation outputs for the 2008 base year. Comparisons of ambient pollutant concentrations to the corresponding CMAQ model predictions for the 6-9 am and 9-noon sampling periods (weekdays in July and August 2008) are summarized in Table 1. Table 4-2 lists the ratios of measured ambient concentrations to CMAQ model predictions for weekdays in July and August 2008. Ratios are presented for major categories of the SAPRC99 lumped and individual species that correspond to the PAMS speciated hydrocarbon data plus criteria pollutants. The relative magnitude of measured to modeled mean values for two ratios important to ozone formation, NMOC/NOx and its surrogate CO/NOx are also included in the table. The model tends to under predict the ozone precursors (NMOC and NOx) to varying degrees. In general, the underestimation of VOC is for species that are mostly associated with tailpipe emissions (OLE1, ARO1, ARO2, BENZE and ETHENE) but the light alkanes (ALK3) that could be related to evaporative emissions are significantly overestimated.

Table 4-1. Mapping of PAMS VOC species to CMAQ output.

Name	CAS	C_no	SAPRC99	Description
Ethylene	74-85-1	2	ETHENE	Ethene
Ethane	74-84-0	2	ALK1	Alkanes (Primarily ethane)
Acetylene	74-86-2	2	ALK2	Alkanes (Primarily propane and acetylene)
Propane	74-98-6	3	ALK2	Alkanes (Primarily propane and acetylene)
N-Butane	106-97-8	4	ALK3	Alkanes
2,2,4-Trimethylpentane	540-84-1	8	ALK3	Alkanes
Isobutane	75-28-5	4	ALK3	Alkanes
2,2-Dimethylbutane	75-83-2	6	ALK3	Alkanes
2-Methylpentane	107-83-5	6	ALK4	Alkanes
2,4-Dimethylpentane	108-08-7	7	ALK4	Alkanes
N-Pentane	109-66-0	5	ALK4	Alkanes
N-Hexane	110-54-3	6	ALK4	Alkanes
N-Heptane	142-82-5	7	ALK4	Alkanes
Cyclopentane	287-92-3	5	ALK4	Alkanes
2,3,4-Trimethylpentane	565-75-3	8	ALK4	Alkanes
Isopentane	78-78-4	5	ALK4	Alkanes
2,3-Dimethylbutane	79-29-8	6	ALK4	Alkanes
3-Methylpentane	96-14-0	6	ALK4	Alkanes
Methylcyclopentane	96-37-7	6	ALK4	Alkanes
Methylcyclohexane	108-87-2	7	ALK5	Alkanes
Cyclohexane	110-82-7	6	ALK5	Alkanes
N-Octane	111-65-9	8	ALK5	Alkanes
N-Nonane	111-84-2	9	ALK5	Alkanes
N-Undecane	1120-21-4	11	ALK5	Alkanes
N-Decane	124-18-5	10	ALK5	Alkanes
2,3-Dimethylpentane	565-59-3	7	ALK5	Alkanes
3-Methylhexane	589-34-4	7	ALK5	Alkanes
3-Methylheptane	589-81-1	8	ALK5	Alkanes
2-Methylhexane	591-76-4	7	ALK5	Alkanes
2-Methylheptane	592-27-8	8	ALK5	Alkanes
Isoprene	78-79-5	5	ISOPRENE	Isoprene
Benzene	71-43-2	6	BENZENE	Benzene
Ethylbenzene	100-41-4	8	ARO1	Aromatics
N-Propylbenzene	103-65-1	9	ARO1	Aromatics
Toluene	108-88-3	7	ARO1	Aromatics
Isopropylbenzene	98-82-8	9	ARO1	Aromatics
P-Diethylbenzene	105-05-5	10	ARO2	Aromatics
M/P Xylene	106-42-3	8	ARO2	Aromatics
1,3,5-Trimethylbenzene	108-67-8	9	ARO2	Aromatics
M-Diethylbenzene	141-93-5	10	ARO2	Aromatics
1,2,3-Trimethylbenzene	526-73-8	9	ARO2	Aromatics
O-Ethyltoluene	611-14-3	9	ARO2	Aromatics
M-Ethyltoluene	620-14-4	9	ARO2	Aromatics
P-Ethyltoluene	622-96-8	9	ARO2	Aromatics
O-Xylene	95-47-6	8	ARO2	Aromatics
1,2,4-Trimethylbenzene	95-63-6	9	ARO2	Aromatics
1-Butene	106-98-9	4	OLE1	Olefins
1-Pentene	109-67-1	5	OLE1	Olefins
Propylene	115-07-1	3	OLE1	Olefins
Styrene	100-42-5	8	OLE2	Olefins
Cis-2-Butene	590-18-1	4	OLE2	Olefins
Trans-2-Butene	624-64-6	4	OLE2	Olefins
Cis-2-Pentene	627-20-3	5	OLE2	Olefins
Trans-2-Pentene	646-04-8	5	OLE2	Olefins

Table 4-2. Ratios (average ± standard deviation) of ambient concentrations to the nine-cell CMAQ model predictions for weekdays in July and August 2008.

	Azusa		Pico Rivera		Upland	
	06-09	09-12	06-09	09-12	06-09	09-12
n samples	12	12	28	35/23*	12	12
ALK1	1.33 ± 0.49	1.18 ± 0.38	1.25 ± 0.67	1.12 ± 0.35	1.82 ± 0.65	1.15 ± 0.24
ALK2	3.03 ± 1.49	3.60 ± 1.18	2.26 ± 1.38	2.96 ± 1.14	3.42 ± 1.30	2.94 ± 0.83
ALK3	0.51 ± 0.22	0.74 ± 0.29	0.47 ± 0.19	0.52 ± 0.17	0.78 ± 0.28	0.69 ± 0.17
ALK4	1.22 ± 0.55	1.25 ± 0.30	0.68 ± 0.28	0.75 ± 0.22	1.79 ± 0.67	1.37 ± 0.27
ALK5	0.62 ± 0.32	0.64 ± 0.15	0.32 ± 0.15	0.37 ± 0.11	0.90 ± 0.34	0.67 ± 0.13
OLE1	1.71 ± 0.80	1.70 ± 0.58	2.49 ± 0.82	3.78 ± 1.20	2.32 ± 0.85	1.65 ± 0.49
OLE2	0.86 ± 0.52	1.10 ± 0.46	0.63 ± 0.43	0.97 ± 0.52	1.09 ± 0.54	0.85 ± 0.38
ARO1	1.78 ± 0.76	2.00 ± 0.78	0.85 ± 0.39	0.86 ± 0.24	2.63 ± 1.14	1.82 ± 0.47
ARO2	1.42 ± 0.54	1.82 ± 0.90	1.32 ± 0.60	1.48 ± 0.49	2.05 ± 0.88	1.45 ± 0.51
BENZENE	2.53 ± 0.83	2.24 ± 0.54	1.09 ± 0.45	1.15 ± 0.33	3.79 ± 1.42	2.55 ± 0.62
ETHENE	2.25 ± 0.86	2.26 ± 0.63	1.45 ± 0.71	1.95 ± 0.68	2.86 ± 1.22	2.15 ± 0.61
SUM	1.30 ± 0.56	1.44 ± 0.39	0.99 ± 0.44	1.13 ± 0.25	1.80 ± 0.66	1.39 ± 0.28
NMOC **	1.85 ± 0.77	2.16 ± 0.51	1.03 ± 0.45	1.20 ± 0.31	2.44 ± 0.88	2.11 ± 0.49
O3max	1.02 ± 0.20	1.02 ± 0.20	0.84 ± 0.24	0.84 ± 0.24	1.09 ± 0.33	1.09 ± 0.33
NO	8.87 ± 15.90	1.97 ± 1.04	1.70 ± 2.61	1.08 ± 0.59	8.37 ± 7.33	1.98 ± 0.74
NOX	1.81 ± 1.12	1.56 ± 0.49	0.65 ± 0.58	1.04 ± 0.36	2.00 ± 0.76	1.65 ± 0.45
CO	1.70 ± 0.36	1.62 ± 0.29	0.78 ± 0.39	0.91 ± 0.29	1.64 ± 0.43	1.24 ± 0.28
CO/NOX	1.25 ± 0.70	1.13 ± 0.33	0.80 ± 0.65	1.02 ± 0.29	0.88 ± 0.15	0.79 ± 0.13
NMOC/NOx	1.16 ± 0.40	1.45 ± 0.39	0.86 ± 0.63	1.22 ± 0.25	1.28 ± 0.31	1.34 ± 0.38

* Samples including values for NO, NOx, CO/NOx and NMOC/NOx.
** NMOC values for CMAQ outputs were estimated using PAMS ppbC/ppbv ratios.

The result for evaporative emissions is contrary to our expectations and hypothesis that these emissions are currently underestimated. We also examined the variations in the measured/CMAQ ratios with ambient temperature and daily maximum ozone but did not find any consistent relationships. However, tailpipe emissions from local vehicle traffic can have disproportionate impacts on ambient pollutant concentrations near air monitoring locations compared to other area and stationary sources. Furthermore, the spatial incompatibility of comparing point ambient measurements to grid averaged model predictions could make such reconciliation analysis unreliable, especially as the fractional contribution of vehicle emissions to total emissions has become smaller over time. Nevertheless, evidence of errors in past emissions inventories underscores the continued need to evaluate the consequence of emission inventory uncertainties on projected trends in ambient air quality.

4.3 References

Fujita, E.M., B.E. Croes, C.L. Bennett, D.R. Lawson, F.W. Lurmann, H.H. Main (1992). Comparison of Emission Inventory and Ambient Concentration Ratios of CO, NMOG, and NOx in California's South Coast Air Basin. *J. Air Waste Manage. Assoc*. 42:264-276.

Fujita, E.M., W.R. Stockwell, D.E. Campbell, and R.E. Keislar (2003). Evolution of the Magnitude and Spatial Extent of the Weekend Ozone Effect in California's South Coast Air Basin from 1981 to 2000. *J. Air & Waste Manage. Assoc.* 53:802-815

Fujita, E.M.; Campbell, D.E.; Zielinska, B.; Chow, J.C.; Lindhjem, C.E.; DenBleyker, A; Bishop, G.A; Schuchmann B.G.; Stedman, D.H.; Lawson, D.L. (2012). Comparison of the MOVES2010a, MOBILE6.2 and EMFAC2007 Mobile Source Emissions Models with On-Road Traffic Tunnel and Remote Sensing Measurements. *J. Air & Waste Manage. Assoc*. 62:1134-1149. DOI:10.1080/10962247.2012.699016

Fujita, E.M.; Campbell, D.E.; Stockwell, W.R.; Lawson, D.R. (2013). Past and future ozone trends in California's South Coast Air Basin: Reconciliation of amibnet measurements with past and projected emission inventories. *J. Air & Waste Manage. Assoc.* 63:1, 54-69. DOI: 0:1080/10962247.2012.735211

5. PROJECTED CHANGES IN THE MAGNITUDE AND SPATIAL VARIATIONS OF PEAK OZONE LEVELS IN THE SOCAB IN RESPONSE TO VARYING REDUCTIONS IN PRECURSOR EMISSIONS

The Coordinating Research Council (CRC) Project A-91 was conducted to forecast the changes in the magnitude and spatial variations of peak ambient ozone levels within the SoCAB in response to varying relative reductions of VOC and NOx. The study involved a series of base and sensitivity air quality model simulations using the CMAQ-ready emissions and meteorological inputs for 2008 and 2030 used by the South Coast Air Quality Management District (SCAQMD) to develop their 2012 Air Quality Management Plan (SCAQMD, 2013). Adjustments were applied to the 2008 base ROG emissions to examine potential underestimation of ROG emissions and to the 2030 "baseline" emissions to simulate further incremental reductions of NOx emissions.

5.1 Approach and Methods

The model simulations were conducted by researchers at the University of Texas El Paso (UTEP) with CMAQ 4.7 using the WRF meteorological, emission inventory and other input files provided by the SCAQMD. Much of the needed supporting information is given in Appendix V (Modeling and Attainment Demonstrations) of the 2012 AQMP (SCAQMD, 2013). The simulations were made with the same spatial grid resolution (4x4 km) and chemical mechanisms (SAPRC99 photochemical, 5 aerosol module and saprc99_ae5_aq aqueous chemistry) as those used by the SCAQMD. In this project the existing script codes from SCAQMD were enhanced to run CMAQ in parallel; ninety-six processors were used for the new simulations. For the multi-day simulations SCAQMD Profile files were used to initialize the model and subsequently daily CMAQ generated output files were used as input for the initial conditions of the following day.

The first modeling objective was to reproduce the SCAQMD 2008 base year simulations. The simulations made by UTEP were compared to the CMAQ output files provided by the SCAQMD for 91 days in summer 2008 (June 1 to August 30). Following the successful reproduction of the SCAQMD simulations, a series of simulations were made by adjusting the 2008 and 2030 emission inputs by the factors shown in Table 5-1 to forecast the effects of varying incremental NOx reductions and potential underestimation of VOC emissions. The model sensitivity analysis examined the spatial and diurnal variations of peak ozone levels within the SoCAB resulting from current and future underestimation of ROG emissions coupled with varying incremental NOx emission reductions beyond the projected 2030 baseline inventory. Additional sensitivity simulations were included to allow more detailed examination the response of ozone to incremental reductions in either NOx or VOC while leaving the other precursor constant. Site-specific projected future design values were estimated using alternative sets of RRFs derived from ratios of the future model predictions to the 2008 base year model predictions with and without upward adjustment of the base ROG emissions.

5.2 Results and Discussion

5.2.1 2008 Base Year Simulations

The base year simulations included 91 days in June through August 2008. The predicted and measured values are compared in the time series plots in Figure 5-1 for the daily maximum 1-hour ozone mixing ratios and in Figure 5-2 for daily maximum 8-hour mixing ratios. There

were seven well defined multiday ozone episodes during summer 2008 with 75 total days having daily Basin-wide maximum concentrations of 80 ppb or higher. The SCAQMD assessed the seven episodes for normalized meteorological ozone episode potential using a regression based weighting covering 30-years of data (1998-2010) (SCAQMD, 2013). Eight days during the 2008 period were ranked above the 95th percentile in the long term distribution of potentials, and another 19 were ranked between the 90th and 94th percentile. The measured and predicted daily 1-hour and 8-hour maximum ozone at Central Los Angeles, Azusa, Pomona, Upland, Rubidoux and Crestline are compared for the six main ozone episodes in Table 5-2 and Table 5-3, respectively. Hourly diurnal time series of measured and predicted ozone during the six episodes are shown in Figure 5-3 for Upland and in Figure 5-4 for Crestline.

Table 5-1. 2008 and 2030 model simulations with baseline total ROG and NOx emissions (highlighted in grey) and sensitivity cases with varying adjustments to baseline emissions.

		ROG				NOx				
Year	Case	Total ROG (tpd)	Adj Factor	Δ 2008	Δ 2030	Total NOx (tpd)	Adj Factor	Δ 2008	Δ 2030	ROG/NOx
2008	2R1N	1277	2.00	100%	192%	723	1.00	0.00	1.55	5.9
	1.5R1N	958	1.50	50%	119%	723	1.00	0%	155%	4.4
	1R1N	639	1.00	0%	46%	723	1.00	0%	155%	2.9
2030	1.5R'2.5N'	655	1.50	3%	50%	710	2.50	-2%	150%	3.1
	1.5R'1.75N'	655	1.50	3%	50%	497	1.75	-31%	75%	4.4
	1.5R'1N'	655	1.50	3%	50%	284	1.00	-61%	0%	7.7
	1.5R'.75N'	655	1.50	3%	50%	213	0.75	-70%	-25%	10.2
	1.5R'.5N'	655	1.50	3%	50%	141	0.50	-81%	-50%	15.5
	1.5R'.3N'	655	1.50	3%	50%	85	0.30	-88%	-70%	25.7
	1R'2.5N'	437	1.00	-32%	0%	710	2.50	-2%	150%	2.1
	1R'1.75N'	437	1.00	-32%	0%	497	1.75	-31%	75%	2.9
	1R'1N'	437	1.00	-32%	0%	284	1.00	-61%	0%	5.1
	1R'.75N'	437	1.00	-32%	0%	213	0.75	-70%	-25%	6.8
	1R'.5N'	437	1.00	-32%	0%	141	0.50	-81%	-50%	10.4
	1R'.3N'	437	1.00	-32%	0%	85	0.30	-88%	-70%	17.1
	.5R'2.5N'	218	0.50	-66%	-50%	710	2.50	-2%	150%	1.0
	.5R'1N'	218	0.50	-66%	-50%	284	1.00	-61%	0%	2.6

The model results obtained by UTEP were virtually identical to those obtained by the SCAQMD. Therefore we summarize and reference the following performance evaluations reported by the SCAQMD in Appendix V of the 2012 AQMP (SCAQMD, 2013). Model performance was evaluated by SCAQMD using the unpaired peak ratio (equation 5-1), paired mean normalized gross error (equation 3-2) and paired mean normalized bias (equation 5-3).

	Statistic	Criteria (%)
(5-1)	$UPPR = \frac{Model_{max}}{Obs_{max}}$	$\leq \pm 15$

(5-2) $$PMNGE = \frac{1}{N}\sum_{1}^{N}\left(\frac{|Model - Obs|}{Obd}\right) \bullet 100\% \qquad \leq 35$$

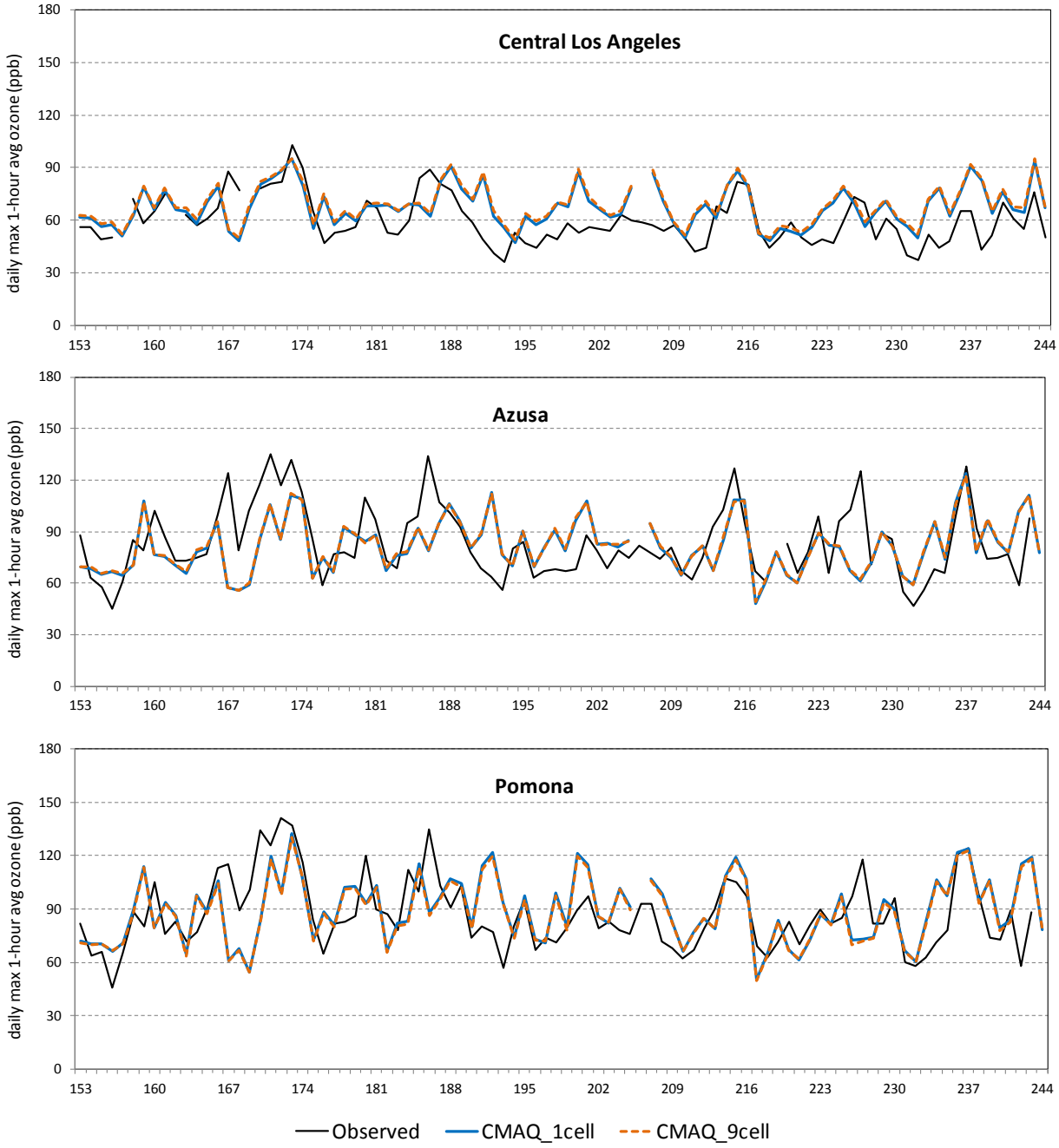

Figure 5-1. Time series of measured and CMAQ predicted daily max 1-hour ozone for all 91 summer days in 2008 (June 1 to August 31).

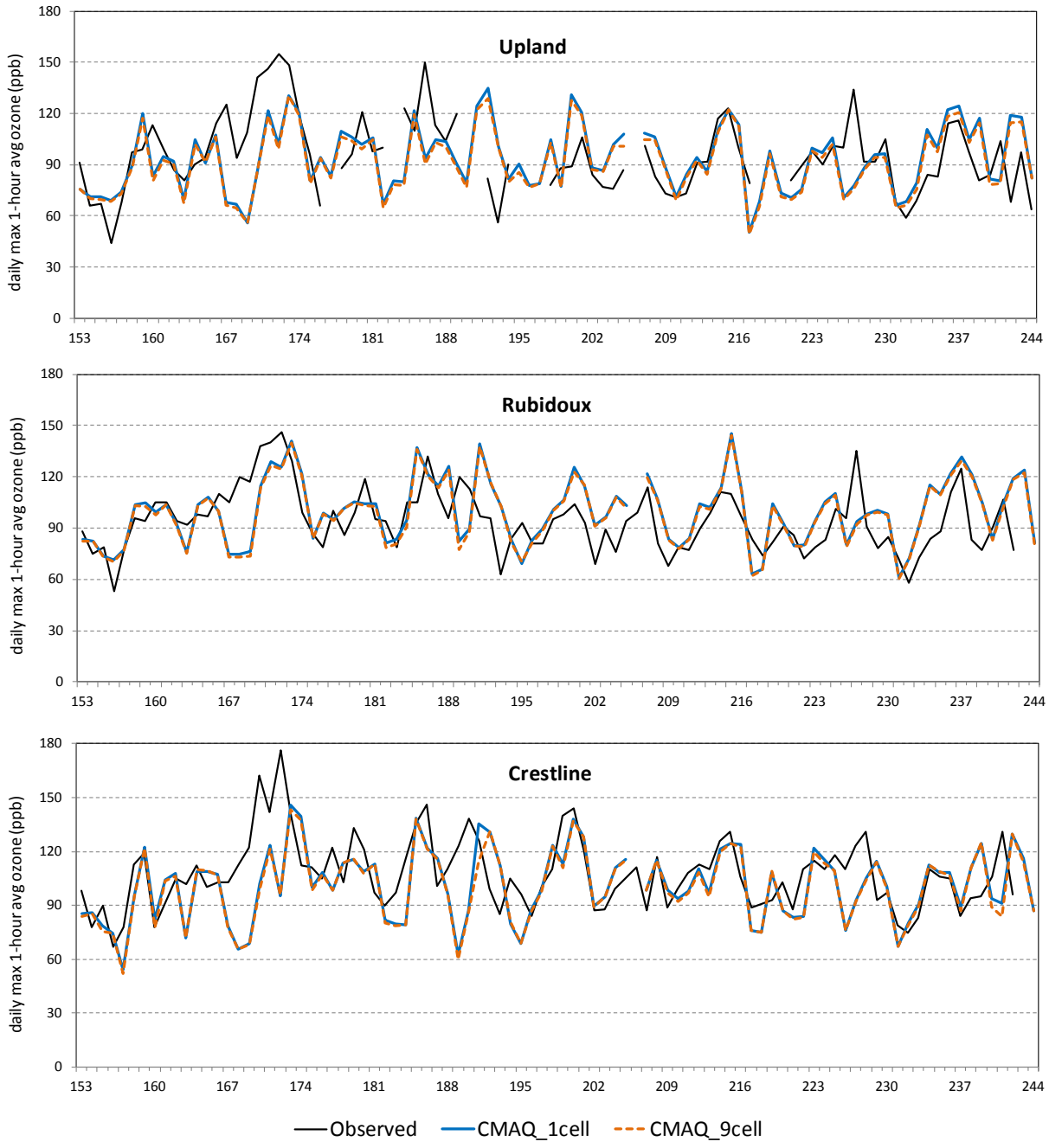

Figure 4-1 (continued). Time series of measured and CMAQ predicted daily max 1-hour ozone for all 91 summer days in 2008 (June 1 to August 31).

(5-3) $$PMNB = \frac{1}{N}\sum_{1}^{N}\left(\frac{(Model - Obs)}{Obs}\right) \bullet 100\% \qquad \leq \pm 20$$

For the model performance evaluation, the Basin was represented by three zones: Zone 3 – the San Fernando Valley, Zone 4 – the Eastern San Gabriel, Riverside and San Bernardino Valleys, and Zone 5 – the Los Angeles and Orange County emissions source areas. Of the three areas, Zone 4 has the maximum ozone concentrations and is the primary downwind impact zone. The CMAQ ozone simulations generally meet the 1-hour average unpaired peak and normalized error model performance goal in all three zones on most days. Normalized bias tended to be negative, particularly in June (see the diurnal time series plots in Figure 5-3 and Figure 5-4). Zone-5 however showed a tendency for over prediction in all three months. Zone 4 displayed the best unpaired peak performance with 54 out of 58 days meeting the 20 percent criteria. Unpaired peak performance in Zones 3 and 5 lagged, with only 76 and 79 percent of the days meeting the criteria.

Table 5-2. Measured and predicted daily one-hour maximum ozone for six episodes in 2008 for Central Los Angeles, Azusa, Pomona, Upland, Rubidoux and Crestline.

		Measured 1-hour max ozone (ppb)						Predicted 1-hour max ozone (ppb)					
DOW	date	LA	Azusa	Pomona	Upland	Rubidoux	Crestline	LA	Azusa	Pomona	Upland	Rubidoux	Crestline
Sun	6/15	88	124	115	125	105	103	54	57	61	68	75	79
Mon	6/16	77	79	89	94	120	113	48	56	68	67	75	66
Tue	6/17		102	101	109	117	122	67	59	54	56	76	69
Wed	6/18	78	117	134	141	138	162	81	85	84	88	114	102
Thu	6/19	81	135	126	146	140	142	84	106	120	122	129	123
Fri	6/20	82	117	141	155	146	176	88	86	99	102	125	95
Sat	6/21	103	132	137	148	129	140	95	111	132	130	141	146
Wed	7/2	60	95	112	123	105	117	69	77	83	80	94	79
Thu	7/3	84	99	100	110	105	136	69	92	115	122	137	139
Fri	7/4	89	134	135	150	132	146	62	79	88	93	121	122
Sat	7/5	81	107	103	113	110	101	82	95	97	105	115	116
Sun	7/6	77	101	91	104	96	110	91	106	107	104	126	96
Mon	7/7	65	93	103	120	120	123	78	96	104	91	82	62
Tue	7/8	59	78	74		113	138	71	80	80	79	90	87
Wed	7/16	49	68	71	78	95	110	70	91	99	105	101	123
Thu	7/17	58	67	79	88	98	140	67	79	80	77	106	113
Fri	7/18	53	68	89	89	104	144	88	97	121	131	125	138
Sat	7/19	56	88	97	106	93	120	71	108	115	121	115	128
Thu	7/31	68	93	90	92	99	110	61	67	79	86	102	97
Fri	8/1	64	103	107	117	111	126	80	85	108	111	113	121
Sat	8/2	82	127	105	123	110	131	88	109	119	122	145	125
Sun	8/3	80	95	97	100	97	106	79	109	107	113	111	124
Tue	8/12	60	96	85	101	101	118	79	81	99	106	110	109
Wed	8/13	73	103	97	100	96	110	69	67	73	71	80	76
Thu	8/14	70	125	118	134	135	123	56	61	73	78	94	93
Fri	8/15	49	71	82	92	91	131	65	72	74	88	98	105
Thu	8/21	44	68	71	84	84	110	78	96	106	111	115	112
Fri	8/22	48	66	78	83	88	106	62	74	98	100	110	108
Sat	8/23	65	100	121	114	111	105	76	107	122	122	122	108
Sun	8/24	65	128	124	116	125	84	90	124	124	124	132	89

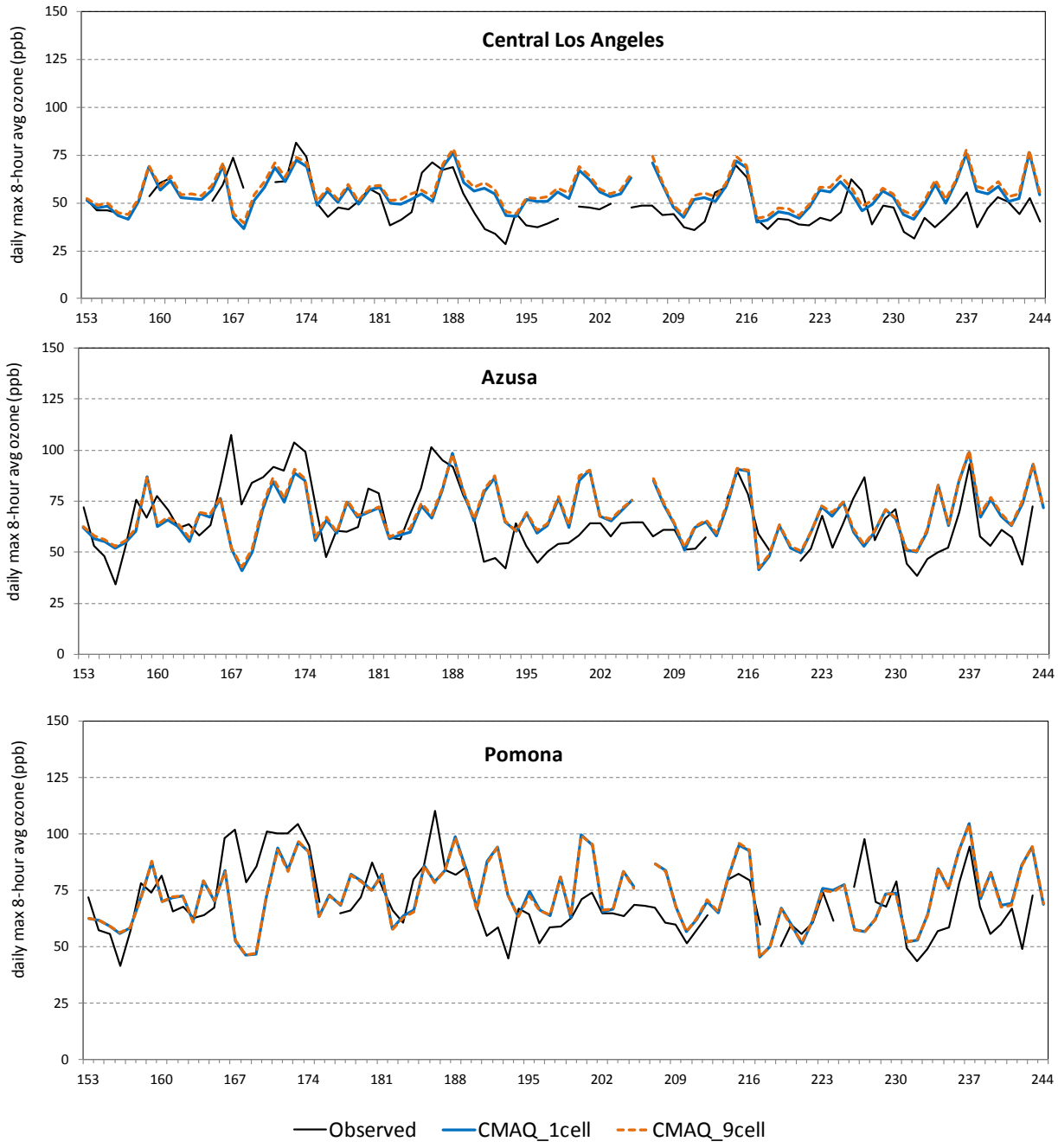

Figure 5-2. Time series of measured and CMAQ predicted daily max 8-hour ozone for all 91 summer days in 2008 (June 1 to August 31; Julian date 153 to 244).

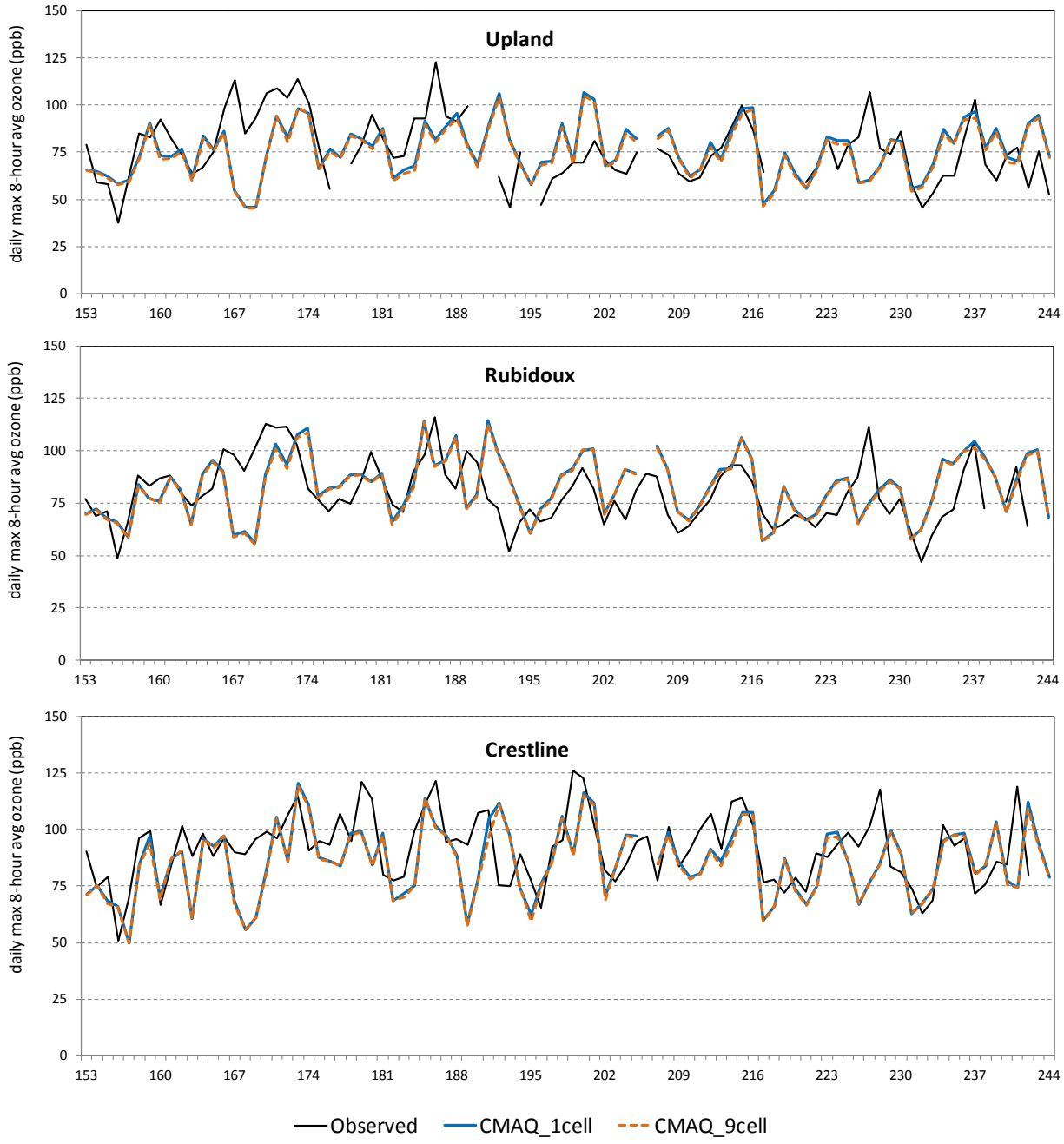

Figure 5-2 (continued). Time series of measured and CMAQ predicted daily max 8-hour ozone for all 91 summer days in 2008 (June 1 to August 31; Julian date 153 to 244).

Table 5-3. Measured and predicted daily eight-hour maximum ozone for six episodes in 2008 for Central Los Angeles, Azusa, Pomona, Upland, Rubidoux and Crestline.

		Measured 8-hour max ozone (ppb)						Predicted 8-hour max ozone (ppb)					
DOW	date	LA	Azusa	Pomona	Upland	Rubidoux	Crestline	LA	Azusa	Pomona	Upland	Rubidoux	Crestline
Sun	6/15	74	108	102	113	98	90	42	51	53	55	60	69
Mon	6/16	58	73	78	85	91	89	37	41	46	46	62	56
Tue	6/17		84	86	93	101	96	51	50	47	46	56	61
Wed	6/18		87	101	106	113	99	58	71	72	73	89	82
Thu	6/19	61	92	100	109	111	96	68	85	94	94	103	106
Fri	6/20	61	90	100	104	112	106	61	75	84	82	93	86
Sat	6/21	81	104	104	114	103	115	72	89	96	98	108	120
Wed	7/2	45	69	80	93	90	99	52	60	66	68	84	75
Thu	7/3	66	81	86	93	98	111	55	72	86	91	114	114
Fri	7/4	71	101	110	123	116	122	51	67	79	82	93	102
Sat	7/5	67	95	84	94	88	95	69	80	84	89	95	97
Sun	7/6	69	92	82	91	82	96	76	98	99	96	107	88
Mon	7/7	55	78	85	100	100	93	60	80	84	79	73	58
Tue	7/8	45	68	68		95	107	56	65	67	69	79	77
Wed	7/16	42	54	59	64	77	95	56	76	81	90	88	106
Thu	7/17		55	63	69	83	126	52	62	63	70	92	89
Fri	7/18	48	58	71	70	92	123	67	85	99	107	100	116
Sat	7/19	48	64	74	81	82	101	62	90	95	103	101	112
Thu	7/31	55			78	88	92	51	58	65	71	91	86
Fri	8/1	58	76	80	89	93	112	58	72	81	87	92	97
Sat	8/2	70	90	82	100	93	114	72	91	95	98	106	107
Sun	8/3	64	78	79	86	85	102	68	90	92	98	96	107
Tue	8/12	45	64		79	80	99	61	74	78	81	87	85
Wed	8/13	63	76	77	83	87	92	55	60	57	59	65	67
Thu	8/14	57	87	98	107	112	102	46	53	57	60	75	76
Fri	8/15	39	56	70	77	77	118	49	60	62	67	81	85
Thu	8/21	37	50	57	62	69	102	60	83	85	87	96	95
Fri	8/22	42	52	59	63	72	93	50	63	76	80	94	98
Sat	8/23	48	70	78	84	91	96	61	85	92	93	100	98
Sun	8/24	55	93	95	103	104	72	76	99	104	97	104	81

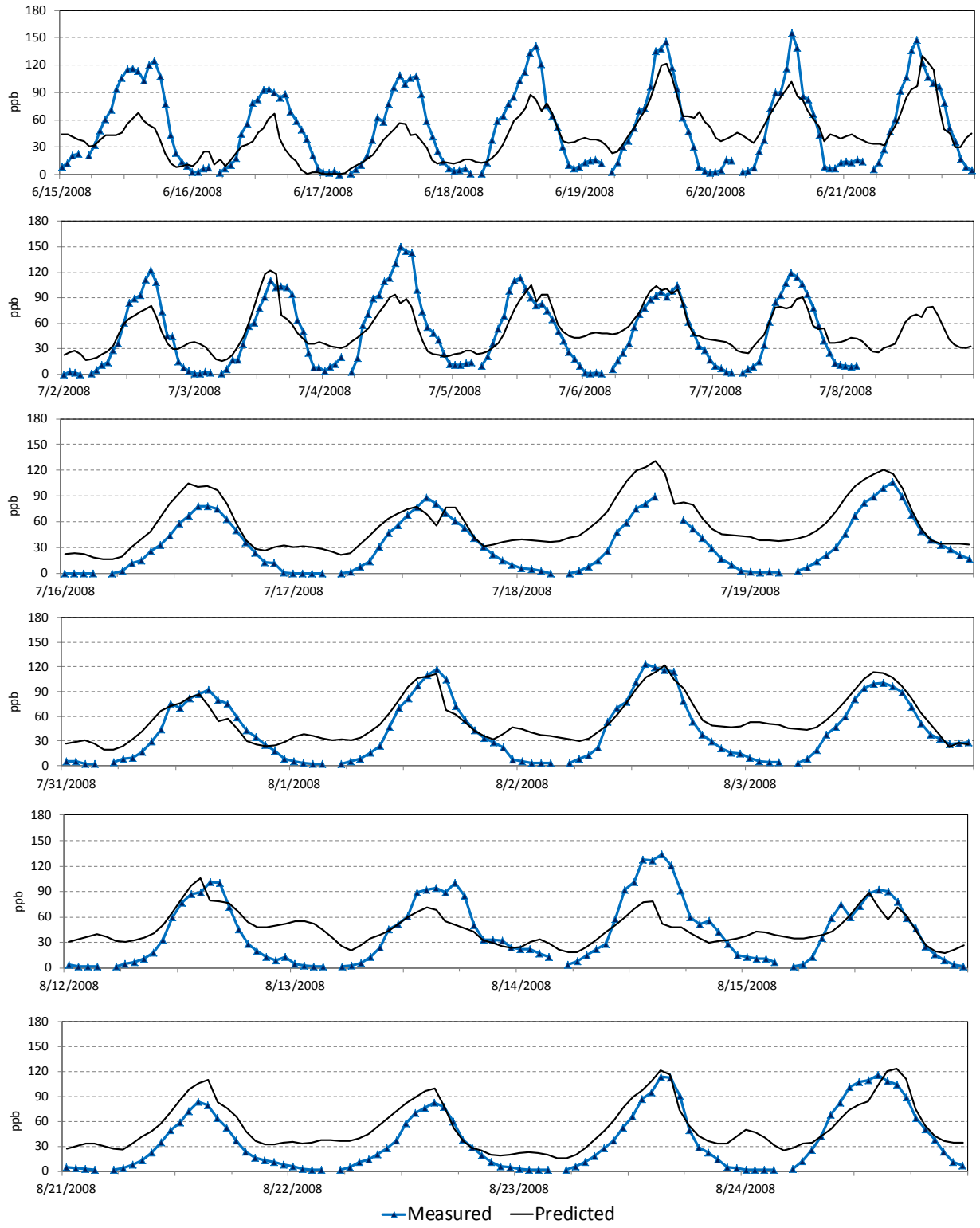

Figure 5-3. Hourly diurnal time series of measured and CMAQ predicted ozone for six episodes in 2008 for Upland.

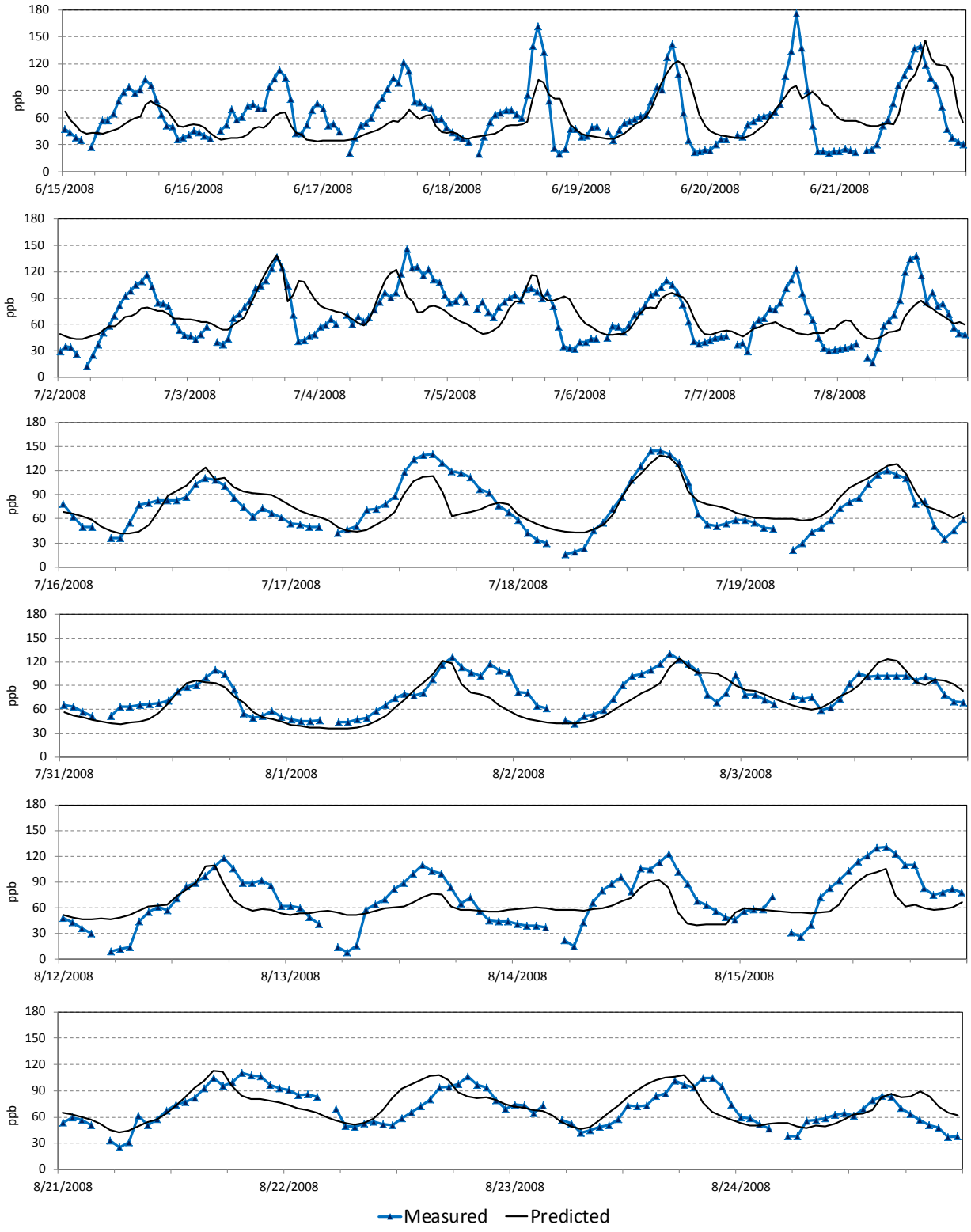

Figure 5-4. Hourly diurnal time series of measured and CMAQ predicted ozone for six episodes in 2008 for Crestline.

5.2.2 2008 Simulations with Upward Adjustments to the Base ROG Emissions

The diurnal plots in Figure 5-3 and Figure 5-4 comparing the modeled ozone values to the measurements for the 2008 base case show a tendency for the model simulations to under predict ozone value for these episodes in the central and eastern portions of the basin. In addition to the base case simulations, two additional sets of simulations were run for the 2008 base year to simulate the effect of increasing the 2008 base ROG emissions by factors of 1.5 and 2.0. Table 5-4 summarize the CMAQ model predicted daily maximum 1-hour and 8-hour ozone for 6/15/08 to 6/20/08 with 1.0, 1.5, and 2.0 time base ROG. Values are for the nine cells (12 x 12 km) surrounding the SoCAB air quality monitoring stations. Exceedances of the 1-hour and 8-hour ozone standards are highlighted in the Table. Ratios of the observed and predicted daily maximum 1-hour and 8-hour ozone values are given in Table 5-5 for the three alternative 2008 base year simulations. Figure 5-5 shows the observed and predicted values as comparative time series plots and Figure 5-6 gives an example of the differences as contour plots for June 19, 2008.

The objective of these series of model simulations was to determine whether upward adjustments to the 2008 base year ROG inventory (factors of 1.5 or 2.0) yield better agreement between observed and predicted ozone values. Figure 5-7 shows the predicted daily maximum 1-hour and 8-hour ozone with the 2008 base ROG emissions multiplied by factors of 1.0, 1.5, and 2.0 as ratios to observations. The base ROG inventory with no adjustment yielded predicted ozone values in good agreement with observations near the western edge of the basin at Los Angeles (average observed/predicted ratios of 0.95 ± 0.21 for 1-hour ozone and 0.97 ± 0.22 for 8-hour ozone), but under-predicts the observed ozone values at all other sites from the central basin to the far downwind eastern edge of the basin (average observed/predicted ratios of 0.77 ± 0.19 for 1-hour ozone and 0.79 ± 0.18 for 8-hour ozone). Upward adjustments by factors of 1.5 and 2.0 results in predicted 8-hour ozone values that are 1.19 ± .28 and 1.39 ± .35 times higher, respectively, than the observed values at Los Angles. A factor of 1.5 adjustment results in good agreement for the other five sites with average observed/predicted ratios of 0.98 ± 0.2 for 1-hour ozone and 1.00 ± 0.2 for the 8-hour ozone, and a factor of 2.0 result in over-prediction with ratios of 1.18 ± 0.22 and 1.17 ± 0.22 for 1-hour and 8-hour ozone, respectively. These results combined with the findings of the 2010 Van Nuys Tunnel Study (Fujita et. al., 2012) and the most recent top-down emission inventory evaluation (Fujita et al., 2013) support the conclusion that ROG emissions in the 2008 base inventory are underestimated (see Section 1.7) and that the 2008 total ROG emissions should be increased by a factor of 1.5 or on-road mobile ROG emissions only by a factor of 2.

Table 5-4. CMAQ model predicted daily maximum 1-hour and 8-hour ozone for 6/15 - 6/20 and 7/2 - 7/8 with 1.0, 1.5, and 2.0 time base ROG. Values are for the nine cells (12 x 12 km) containing the SoCAB air quality monitoring station. Values below the table are the mean daily maxima.

		1-hour max ozone (ppb)						Max Ozone 8-hour					
DOW	date	LA	Azusa	Pomona	Upland	Rubidoux	Crestline	LA	Azusa	Pomona	Upland	Rubidoux	Crestline
2008 (Observations)													
Sun	6/15	88	124	115	125	105	103	74	108	102	113	98	90
Mon	6/16	77	79	89	94	120	113	58	73	78	85	91	89
Tue	6/17	74	102	101	109	117	122	58	84	86	93	101	96
Wed	6/18	78	117	134	141	138	162	53	87	101	106	113	99
Thu	6/19	81	135	126	146	140	142	61	92	100	109	111	96
Fri	6/20	82	117	141	155	146	176	61	90	100	104	112	106
Sat	6/21	103	132	137	148	129	140	81	104	104	114	103	115
Wed	7/2	60	95	112	123	105	117	45	69	80	93	90	99
Thu	7/3	84	99	100	110	105	136	66	81	86	93	98	111
Fri	7/4	89	134	135	150	132	146	71	101	110	123	116	122
Sat	7/5	81	107	103	113	110	101	67	95	84	94	88	95
Sun	7/6	77	101	91	104	96	110	69	92	82	91	82	96
Mon	7/7	65	93	103	120	120	123	55	78	85	100	100	93
Tue	7/8	59	78	74		113	138	45	68	68		95	107
2008 (1.0 x ROG, 1.0 x NOx)													
Sun	6/15	51	53	54	60	65	67	41	47	48	48	52	59
Mon	6/16	51	57	65	63	74	69	40	45	48	49	62	61
Tue	6/17	66	58	57	57	74	71	53	51	47	46	56	64
Wed	6/18	79	84	80	82	104	93	59	70	68	67	81	77
Thu	6/19	80	104	110	112	114	114	69	83	88	88	94	98
Fri	6/20	85	84	92	94	120	94	62	74	80	76	86	82
Sat	6/21	91	109	123	120	130	129	69	87	92	93	102	112
Wed	7/2	68	77	76	72	87	79	54	61	63	63	79	73
Thu	7/3	68	91	111	112	131	126	56	75	85	86	111	107
Fri	7/4	62	77	82	87	111	109	52	66	74	75	89	94
Sat	7/5	83	93	93	99	106	110	69	79	81	82	91	93
Sun	7/6	90	102	101	94	114	89	77	94	93	85	102	81
Mon	7/7	79	90	91	81	76	61	62	78	77	74	70	59
Tue	7/8	72	81	82	78	89	85	60	68	70	69	81	76
2008 (1.5 x ROG, 1.0 x NOx)													
Sun	6/15	57	68	74	83	89	90	46	60	62	64	68	76
Mon	6/16	59	72	85	84	90	84	48	56	61	60	78	72
Tue	6/17	81	85	83	85	100	96	67	71	68	65	77	82
Wed	6/18	105	124	118	120	147	126	77	98	97	97	111	100
Thu	6/19	116	126	133	138	138	135	94	110	109	110	114	111
Fri	6/20	109	110	130	123	163	129	83	96	102	98	107	110
Sat	6/21	126	162	160	164	149	178	89	111	114	117	121	140
Wed	7/2	78	101	106	106	115	102	60	78	82	83	100	91
Thu	7/3	84	116	134	135	152	142	68	97	108	107	130	125
Fri	7/4	68	97	104	112	130	131	58	83	93	96	109	113
Sat	7/5	97	122	118	121	128	130	79	99	103	105	111	116
Sun	7/6	107	124	116	114	131	107	90	111	109	99	116	90
Mon	7/7	95	115	110	99	102	65	76	97	94	85	80	62
Tue	7/8	83	103	103	105	113	112	67	85	90	91	105	96
2008 (2.0 x ROG, 1.0 x NOx)													
Sun	6/15	61	83	89	99	103	105	50	70	72	75	80	86
Mon	6/16	68	87	101	100	109	96	57	68	74	73	91	82
Tue	6/17	98	115	113	118	126	121	81	93	92	88	98	100
Wed	6/18	135	168	159	161	183	160	96	125	123	123	133	118
Thu	6/19	146	144	147	154	153	149	117	132	125	126	128	120
Fri	6/20	133	144	162	157	190	164	102	116	120	119	122	134
Sat	6/21	163	199	194	196	168	208	106	127	129	133	133	157
Wed	7/2	91	134	139	143	147	128	68	101	107	110	124	110
Thu	7/3	102	136	151	151	166	159	82	119	128	126	143	140
Fri	7/4	77	118	127	136	149	150	63	100	110	114	128	129
Sat	7/5	109	145	140	147	150	150	90	116	122	123	126	132
Sun	7/6	121	139	134	130	142	120	102	123	120	108	125	96
Mon	7/7	110	139	137	124	129	68	89	113	108	95	89	64
Tue	7/8	93	123	126	133	136	138	74	102	109	113	124	112
Observations													
June 15-21		83	115	120	131	128	137	64	91	96	103	104	99
July 2-8		74	101	103	120	112	124	60	83	85	99	96	103
All 14 days		78	108	112	126	120	131	62	87	90	101	100	101
2008 Design Value		108	141	141	150	140	164	73	96	103	110	107	119
2008 1.0xROG		73	83	87	87	100	92	59	70	72	72	83	81
2008 1.5xROG		90	109	112	113	125	116	72	89	92	91	102	99
2008 2.0xROG		108	134	137	139	146	137	84	108	110	109	117	113

Table 5-5. Ratio of observed and predicted daily maximum 1-hour and 8-hour ozone for 6/15/08 - 6/20/08 and 7/2/08 - 7/8/08 with 1.0, 1.5 and 2.0 time base ROG. Values are for the nine cells (12x12 km) containing the SoCAB air quality monitoring station.

			1-hour max ozone (ppb)						Max Ozone 8-hour				
DOW	date	LA	Azusa	Pomona	Upland	Rubidoux	Crestline	LA	Azusa	Pomona	Upland	Rubidoux	Crestline
2008 (1.0 x ROG, 1.0 x NOx)													
Sun	6/15	0.58	0.43	0.47	0.48	0.62	0.65	0.56	0.44	0.47	0.43	0.54	0.66
Mon	6/16	0.67	0.72	0.73	0.67	0.62	0.61	0.69	0.62	0.61	0.58	0.68	0.68
Tue	6/17	0.89	0.57	0.56	0.53	0.63	0.58	0.92	0.61	0.55	0.49	0.55	0.67
Wed	6/18	1.01	0.72	0.59	0.58	0.75	0.57	1.11	0.81	0.68	0.63	0.72	0.78
Thu	6/19	0.99	0.77	0.87	0.77	0.82	0.80	1.13	0.90	0.88	0.81	0.85	1.01
Fri	6/20	1.04	0.72	0.65	0.60	0.82	0.54	1.02	0.83	0.79	0.73	0.78	0.77
Sat	6/21	0.88	0.82	0.89	0.81	1.01	0.92	0.85	0.84	0.88	0.82	0.99	0.97
Wed	7/2	1.13	0.81	0.68	0.59	0.82	0.67	1.19	0.88	0.80	0.68	0.88	0.74
Thu	7/3	0.81	0.92	1.11	1.02	1.25	0.93	0.84	0.92	0.99	0.92	1.13	0.96
Fri	7/4	0.70	0.57	0.61	0.58	0.84	0.74	0.73	0.65	0.68	0.61	0.76	0.77
Sat	7/5	1.02	0.87	0.90	0.88	0.96	1.09	1.02	0.83	0.97	0.88	1.03	0.99
Sun	7/6	1.16	1.01	1.11	0.90	1.19	0.81	1.12	1.02	1.14	0.93	1.25	0.84
Mon	7/7	1.21	0.97	0.88	0.68	0.63	0.49	1.14	1.00	0.90	0.74	0.70	0.63
Tue	7/8	1.22	1.04	1.10		0.79	0.61	1.33	1.01	1.04		0.86	0.71
2008 (1.5 x ROG, 1.0 x NOx)													
Sun	6/15	0.64	0.55	0.64	0.66	0.85	0.88	0.63	0.56	0.60	0.56	0.70	0.85
Mon	6/16	0.77	0.91	0.95	0.89	0.75	0.75	0.83	0.76	0.78	0.71	0.86	0.80
Tue	6/17	1.09	0.84	0.82	0.78	0.86	0.79	1.16	0.84	0.79	0.70	0.76	0.86
Wed	6/18	1.35	1.06	0.88	0.85	1.07	0.78	1.46	1.13	0.96	0.91	0.99	1.01
Thu	6/19	1.43	0.93	1.05	0.94	0.99	0.95	1.54	1.19	1.09	1.01	1.02	1.16
Fri	6/20	1.33	0.94	0.92	0.79	1.12	0.74	1.35	1.07	1.02	0.95	0.96	1.03
Sat	6/21	1.23	1.23	1.17	1.11	1.16	1.27	1.10	1.07	1.09	1.03	1.17	1.22
Wed	7/2	1.30	1.06	0.94	0.86	1.09	0.87	1.33	1.13	1.03	0.89	1.11	0.91
Thu	7/3	1.01	1.17	1.34	1.23	1.45	1.04	1.03	1.20	1.25	1.15	1.32	1.13
Fri	7/4	0.77	0.72	0.77	0.74	0.99	0.89	0.81	0.82	0.84	0.78	0.94	0.93
Sat	7/5	1.19	1.14	1.14	1.07	1.16	1.29	1.18	1.04	1.23	1.12	1.26	1.23
Sun	7/6	1.40	1.22	1.28	1.09	1.37	0.97	1.31	1.21	1.33	1.08	1.41	0.94
Mon	7/7	1.46	1.24	1.07	0.83	0.85	0.53	1.39	1.25	1.10	0.86	0.80	0.66
Tue	7/8	1.41	1.32	1.39		1.00	0.81	1.49	1.26	1.34		1.11	0.89
2008 (2.0 x ROG, 1.0 x NOx)													
Sun	6/15	0.69	0.67	0.77	0.79	0.99	1.02	0.68	0.65	0.71	0.66	0.81	0.96
Mon	6/16	0.88	1.10	1.14	1.07	0.90	0.85	0.99	0.93	0.94	0.86	1.00	0.92
Tue	6/17	1.32	1.13	1.11	1.09	1.07	0.99	1.40	1.11	1.08	0.95	0.98	1.04
Wed	6/18	1.73	1.43	1.18	1.14	1.33	0.99	1.80	1.44	1.22	1.16	1.18	1.19
Thu	6/19	1.80	1.07	1.17	1.05	1.10	1.05	1.93	1.44	1.25	1.15	1.15	1.25
Fri	6/20	1.62	1.23	1.15	1.01	1.30	0.93	1.67	1.29	1.20	1.15	1.09	1.26
Sat	6/21	1.58	1.51	1.42	1.32	1.30	1.49	1.31	1.22	1.24	1.17	1.29	1.37
Wed	7/2	1.51	1.41	1.24	1.17	1.40	1.09	1.51	1.46	1.34	1.18	1.38	1.11
Thu	7/3	1.22	1.37	1.51	1.37	1.58	1.17	1.24	1.46	1.49	1.36	1.46	1.26
Fri	7/4	0.87	0.88	0.94	0.91	1.13	1.03	0.89	0.99	0.99	0.92	1.10	1.06
Sat	7/5	1.35	1.35	1.36	1.30	1.37	1.49	1.34	1.22	1.45	1.31	1.43	1.40
Sun	7/6	1.57	1.37	1.47	1.25	1.48	1.09	1.48	1.34	1.47	1.19	1.52	1.01
Mon	7/7	1.70	1.49	1.33	1.03	1.07	0.55	1.63	1.45	1.27	0.95	0.90	0.69
Tue	7/8	1.57	1.58	1.70		1.20	1.00	1.65	1.51	1.62		1.31	1.05
Ratio to observations													
2008 (1.0 x ROG, 1.0 x NOx)													
Mean		0.95	0.78	0.80	0.70	0.84	0.72	0.97	0.81	0.81	0.71	0.84	0.80
Stdev		0.21	0.18	0.21	0.16	0.20	0.17	0.22	0.17	0.20	0.16	0.21	0.13
2008 (1.5 x ROG, 1.0 x NOx)													
Mean		1.17	1.02	1.03	0.91	1.05	0.90	1.19	1.04	1.03	0.90	1.03	0.97
Stdev		0.27	0.22	0.22	0.17	0.20	0.20	0.28	0.21	0.22	0.18	0.21	0.17
2008 (2.0 x ROG, 1.0 x NOx)													
Mean		1.39	1.26	1.25	1.12	1.23	1.05	1.39	1.25	1.23	1.08	1.19	1.11
Stdev		0.35	0.26	0.24	0.17	0.20	0.23	0.35	0.25	0.24	0.19	0.22	0.19

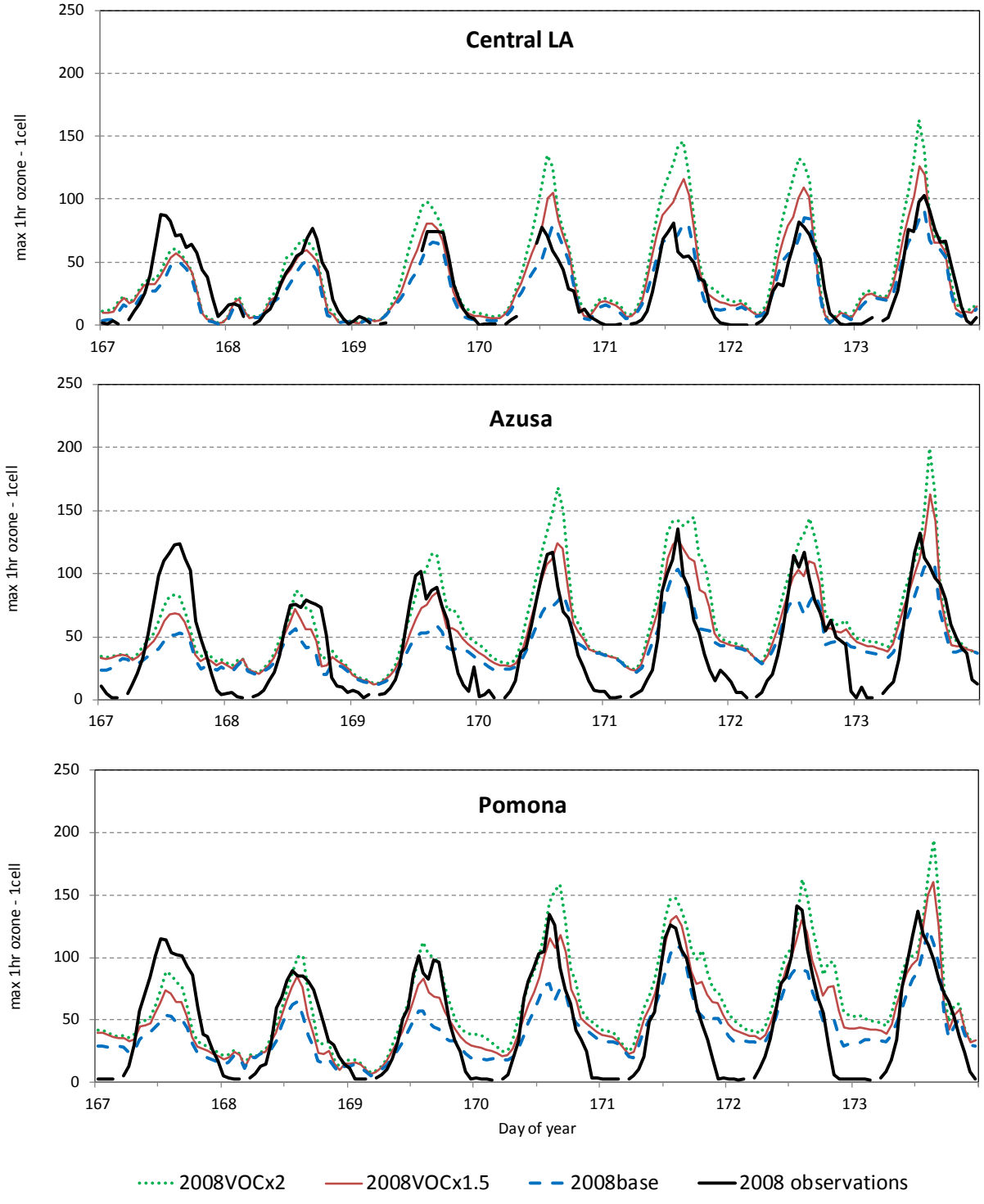

Figure 5-5. Diurnal time series of measured and CMAQ model predicted ozone (nine-cell averages, ppb) for 6/15/08 to 6/20/08 with 1.0, 1.5, and 2.0 time base ROG.

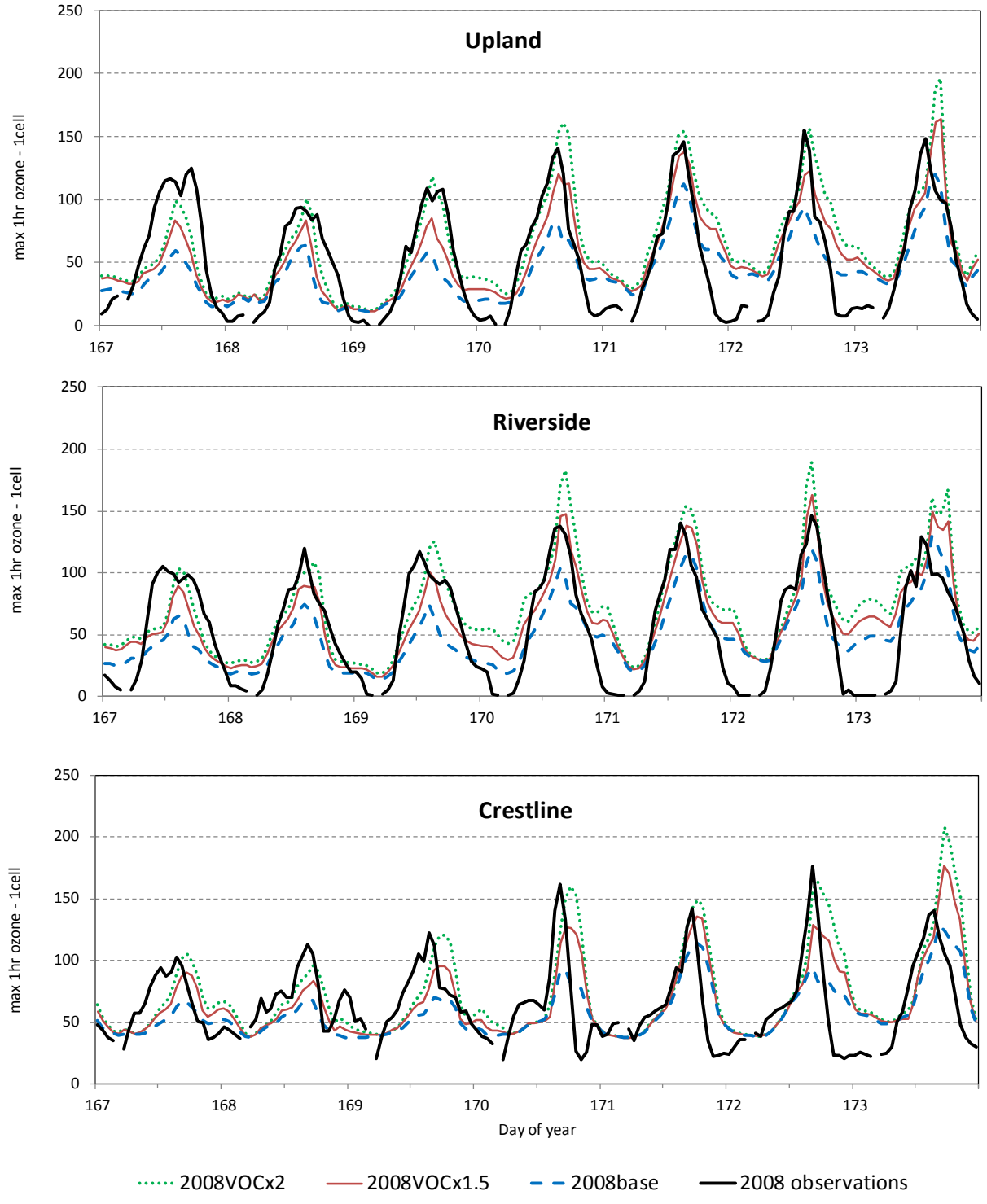

Figure 5-5 (continued). Diurnal time series of measured and CMAQ model predicted ozone (nine-cell averages, ppb) for 6/15/08 to 6/20/08 with 1.0, 1.5, and 2.0 time base ROG.

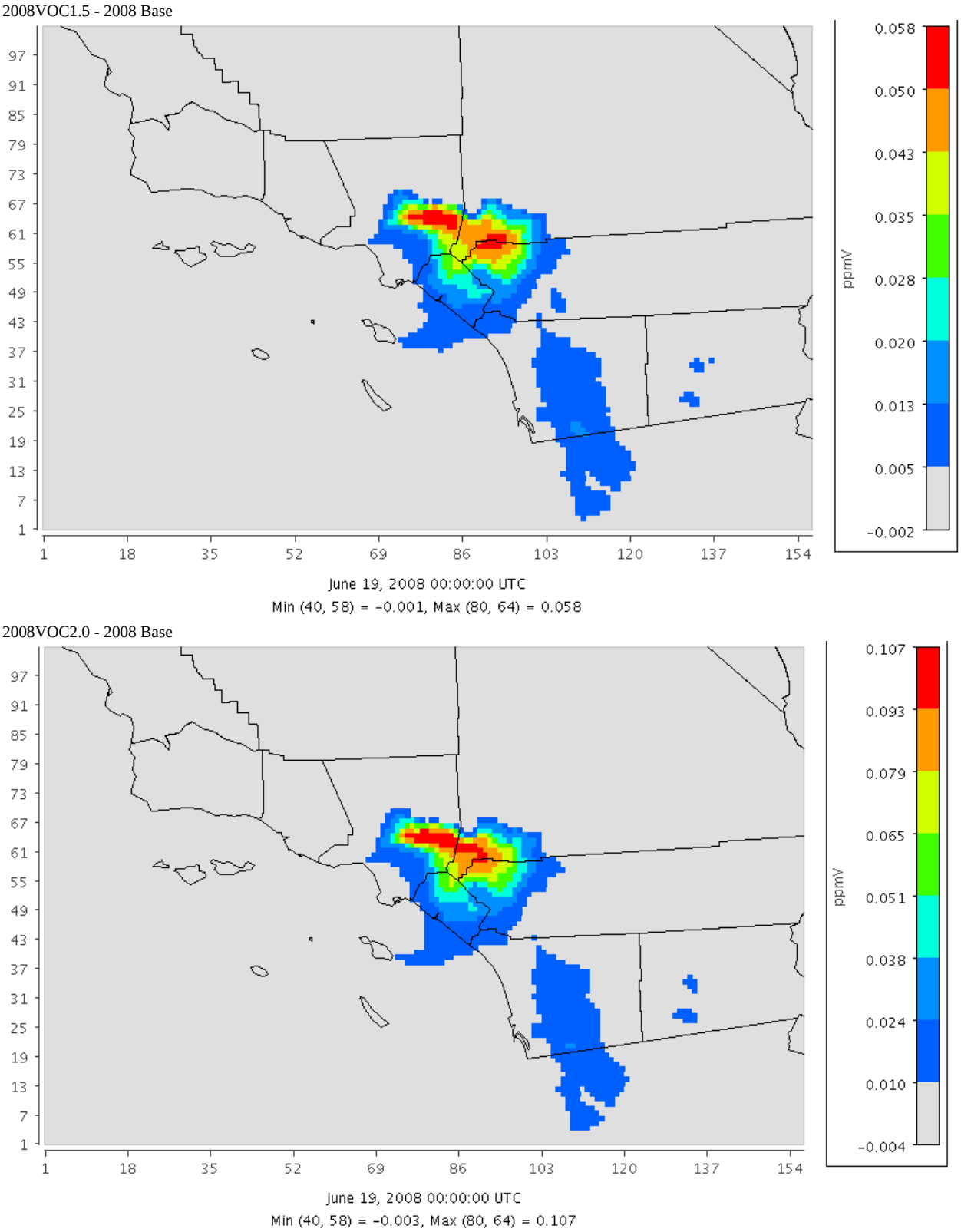

Figure 5-6. Contour plots of differences in ozone (ppm), 2008 VOC*1.5 minus 2008 Base (upper) and 2008 VOC*2.0 minus 2008 Base (lower) for June 19, 2008 at 5:00 pm (PST).

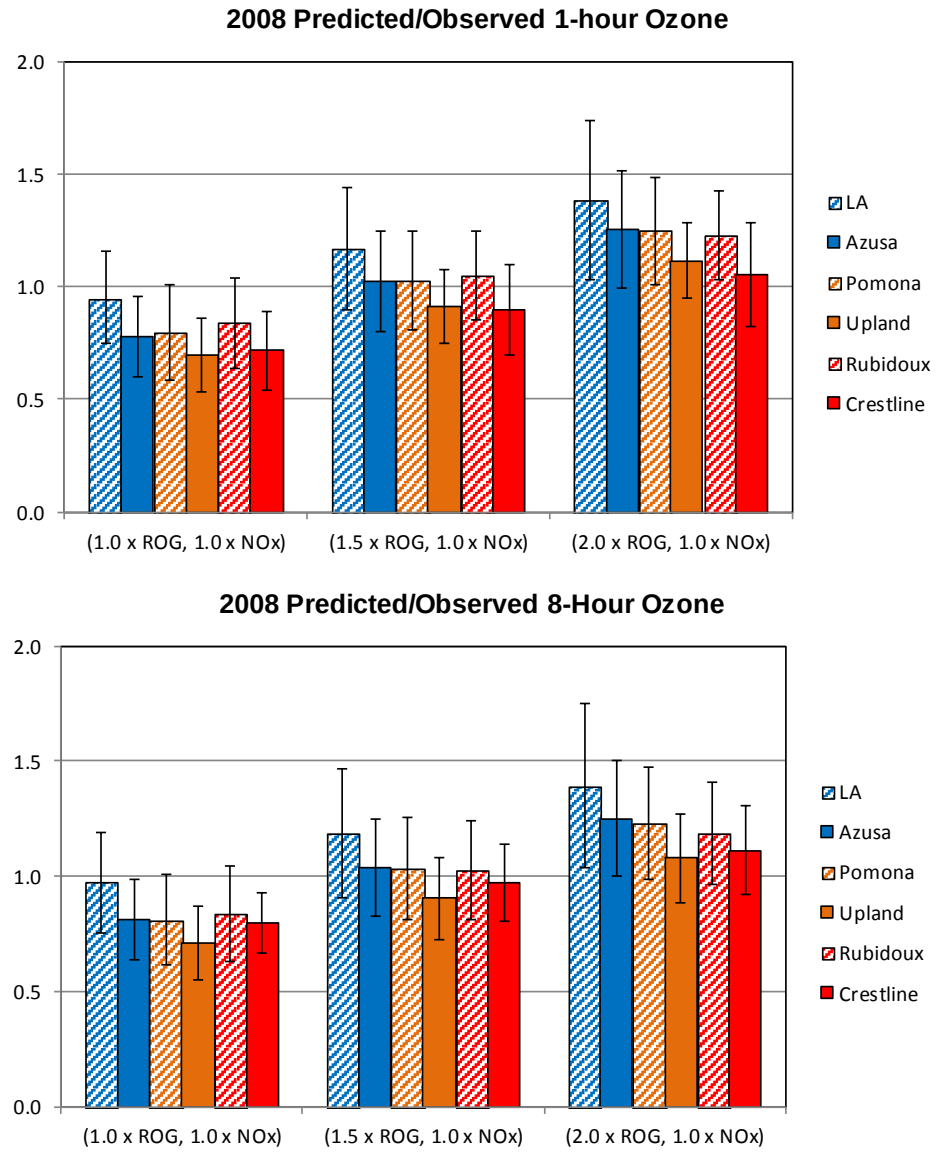

Figure 5-7. Ratios (mean ± standard deviations) of predicted/observed daily maximum 1-hour and 8-hour ozone for 6/15 - 6/20 and 7/2 - 7/8 with 1.0, 1.5, and 2.0 time 2008 base ROG. Values are for the nine cells (12 x 12 km) containing the SoCAB air quality monitoring station.

5.2.3 2030 Simulations, Relative Response Factors and 2030 Projected Design Values

The preliminary ozone modeling analysis by the SCAMD for the 2012 AQMP (SCAQMD, 2013) projected that reductions in NOx emissions from 2010 levels of 90% would be required to attain the 2008 8-hour ozone NAAQS of 75 ppb by 2032. This level of reduction is equivalent to a basin NOx carrying capacity of roughly 80 tpd. For the 2030 model simulations, we examine the effects of incremental reductions from the 2030 total baseline NOx emissions of 284 tpd to the estimated basin carrying capacity of 80 tpd. Table 5-6 shows the

predicted daily maximum 1-hour and 8-hour ozone for the 6/15 - 6/20 and 7/2-7/8 episodes with 2030 baseline ROG emissions (437 tpd, -32% from 2008) and 2030 baseline NOx emissions multiplied by factors of 1.0, 0.75, 0.5 and 0.3 resulting in the following total daily NOx emissions in tons per day (tpd) and percentage reductions from 2008 emission levels.

Factor	1	0.75	0.5	0.3
NOx emissions (tpd)	284	213	141	85
% reduction from 2008	-61%	-70%	-81%	-88%

Results for the same series of simulations but with the 2030 baseline total ROG emissions multiplied by a factor of 1.5 (655 tpd, +3% from 2008) are shown in Table 5-7. Exceedances of the 1-hour and 8-hour ozone standards are highlighted in the two tables. The summary of these results in Figure 5-8 show the mean maximum 8-hour ozone concentrations for varying reductions of NOx. NOx and ROG emissions (tons per day) are shown above the adjustment factors applied to the 2008 base year ROG (R) and NOx (N) emissions and 2030 baseline ROG (R') and NOx (N') emissions. The plot also includes the corresponding means of the observed ozone daily maximum 8-hour mixing ratios for the June 15-21 and July 2-8 episodes in 2008.

The indications that current estimates of VOC emissions may be underestimated relative to NOx emissions have important implications for modeled demonstrations that the selected emission reductions will result in ambient concentrations that meet the NAAQS. For this modeled attainment test, model estimates are used in a "relative" rather than "absolute" sense. Attainment is demonstrated using ratios of the model's future to current (baseline) predictions at monitoring locations. These ratios are called relative reduction factors (RRF). Future ozone concentrations are estimated by multiplying the modeled RRF at a location near the monitoring site by the baseline design value (DV) of the site as follows:

DV(future year) = RRF x DV(baseline)

where DV is the 3 year average of the fourth highest monitored daily 8-hour maximum value at each monitoring site. Attainment is deemed to be demonstrated if the projected future year DV is less than the NAAQS. In region that are VOC limited with respect to ozone formation, such as the SoCAB, an underestimation of VOC emissions in the base year will result in lower predicted ozone and higher RRF ratio. Correcting the underestimation will yield a lower RRF and decrease the emission reduction necessary to demonstrate attainment. In other word, underestimation of base year emission will result in overestimation of required emission reductions.

Table 5-6. CMAQ model predicted daily maximum 1-hour and 8-hour ozone for 6/15 - 6/20 and 7/2-7/8 episodes in 2030 with baseline ROG and 1.0, 0.75, 0.5 and 0.3 times 2030 baseline NOx. Values are for the nine grid cell (12x12 km) centered on the SoCAB air quality monitoring station.

		1-hour max ozone (ppb)						Max Ozone 8-hour					
DOW	date	LA	Azusa	Pomona	Upland	Rubidoux	Crestline	LA	Azusa	Pomona	Upland	Rubidoux	Crestline
2030 (1.0 x ROG, 1.0 x NOx)													
Sun	6/15	44	54	55	60	60	64	38	48	49	51	51	59
Mon	6/16	63	69	76	73	75	68	56	61	63	62	67	62
Tue	6/17	80	97	95	94	92	81	72	80	81	77	79	72
Wed	6/18	97	114	111	114	116	103	78	88	88	87	89	80
Thu	6/19	107	108	92	94	95	90	91	94	88	84	85	80
Fri	6/20	95	103	105	105	115	108	80	84	87	85	85	90
Sat	6/21	102	121	120	121	106	125	76	83	85	87	87	99
Wed	7/2	72	97	100	102	98	83	61	82	84	84	85	75
Thu	7/3	84	101	101	99	102	96	71	88	90	88	92	90
Fri	7/4	66	89	91	93	101	97	59	80	82	82	89	87
Sat	7/5	80	99	100	102	102	98	71	83	86	85	88	88
Sun	7/6	87	97	95	91	95	82	76	84	83	77	86	68
Mon	7/7	85	95	96	90	94	56	74	80	78	70	69	53
Tue	7/8	74	95	96	99	94	96	63	83	86	87	88	81
2030 (1.0 x ROG, 0.75 x NOx)													
Sun	6/15	54	69	70	72	71	68	48	59	60	61	62	60
Mon	6/16	70	82	84	84	78	71	62	67	68	67	67	63
Tue	6/17	87	102	101	97	95	77	76	82	83	78	81	69
Wed	6/18	99	113	114	115	111	99	80	86	86	85	86	76
Thu	6/19	112	109	89	87	88	83	93	91	83	80	80	74
Fri	6/20	103	105	99	101	107	105	82	82	84	83	81	87
Sat	6/21	104	117	116	115	102	118	74	79	80	82	82	92
Wed	7/2	72	96	97	99	93	78	63	82	82	82	81	71
Thu	7/3	89	100	102	96	95	91	74	85	86	84	86	83
Fri	7/4	67	88	88	89	99	92	60	79	78	78	85	82
Sat	7/5	81	96	99	99	99	94	71	80	82	82	84	83
Sun	7/6	86	92	92	88	89	77	76	80	79	73	80	64
Mon	7/7	85	92	93	87	91	53	75	77	75	67	68	51
Tue	7/8	72	94	94	96	90	92	63	81	83	84	83	77
2030 (1.0 x ROG, 0.5 x NOx)													
Sun	6/15	54	67	69	70	70	62	49	57	58	59	60	56
Mon	6/16	73	84	84	81	73	68	64	66	66	65	63	59
Tue	6/17	88	95	96	91	90	69	75	77	78	74	77	63
Wed	6/18	95	102	106	106	100	89	76	79	79	78	78	69
Thu	6/19	106	102	84	77	78	73	88	83	76	72	71	66
Fri	6/20	99	98	90	92	95	95	79	76	78	76	74	80
Sat	6/21	96	105	104	103	92	106	69	71	72	74	73	82
Wed	7/2	76	88	89	90	84	71	63	77	76	75	74	65
Thu	7/3	86	92	95	89	84	81	73	78	78	76	77	74
Fri	7/4	68	81	80	81	90	82	60	73	71	71	77	73
Sat	7/5	77	87	91	90	90	85	68	72	75	75	76	75
Sun	7/6	82	84	84	81	80	71	72	73	72	66	72	59
Mon	7/7	81	85	84	80	83	49	72	70	68	61	63	47
Tue	7/8	69	87	87	88	81	83	61	75	76	77	75	70
2030 (1.0 x ROG, 0.3 x NOx)													
Sun	6/15	47	56	58	58	58	53	43	48	50	50	51	52
Mon	6/16	69	75	74	72	63	61	61	61	60	59	56	53
Tue	6/17	80	82	84	80	79	60	69	68	69	66	68	56
Wed	6/18	84	87	91	91	87	76	68	69	69	68	68	61
Thu	6/19	92	88	74	66	66	62	77	72	66	63	62	57
Fri	6/20	87	85	77	79	79	81	71	67	68	67	64	69
Sat	6/21	82	88	88	87	78	88	61	61	62	64	62	70
Wed	7/2	71	76	76	77	73	61	59	68	66	66	65	57
Thu	7/3	77	80	82	78	72	70	67	68	68	66	66	63
Fri	7/4	66	71	70	70	77	70	56	64	62	63	67	63
Sat	7/5	69	75	79	78	78	73	61	63	65	65	66	65
Sun	7/6	72	72	73	70	69	62	65	63	63	59	62	52
Mon	7/7	71	73	73	70	72	45	66	61	60	55	57	44
Tue	7/8	65	75	75	76	70	71	56	66	66	66	65	61
2030													
1.0xROG, 1.0 NOx		81	96	95	95	96	89	69	80	81	79	81	77
1.0xROG, 0.75 NOx		84	97	96	95	93	85	71	79	79	77	79	74
1.0xROG, 0.5 NOx		82	90	89	87	85	77	69	73	73	71	72	67
1.0xROG, 0.3 NOx		74	77	77	75	73	67	63	64	64	63	63	59

Table 5-7. CMAQ model predicted daily maximum 1-hour and 8-hour ozone for 6/15 - 6/20 episode in 2030 with 1.5 x baseline ROG and 1.0, 0.75, 0.5 and 0.3 times 2030 baseline NOx. Values are for the nine grid cell (12x12 km) centered on the SoCAB air quality monitoring station.

		1-hour max ozone (ppb)						Max Ozone 8-hour					
DOW	date	LA	Azusa	Pomona	Upland	Rubidoux	Crestline	LA	Azusa	Pomona	Upland	Rubidoux	Crestline
2030 (1.5 x ROG, 1.0 x NOx)													
Sun	6/15	45	61	61	66	66	69	40	52	54	56	56	63
Mon	6/16	71	83	89	89	84	75	63	69	71	70	72	67
Tue	6/17	95	116	115	111	109	87	82	91	94	87	90	77
Wed	6/18	113	131	132	134	130	115	89	98	98	97	99	86
Thu	6/19	129	126	101	100	101	95	105	104	95	90	91	83
Fri	6/20	117	121	115	117	125	122	92	93	96	94	92	100
Sat	6/21	121	138	136	136	120	140	84	90	91	94	94	107
Wed	7/2	79	111	113	115	108	90	68	93	93	93	93	80
Thu	7/3	99	115	116	111	109	105	80	96	98	95	98	96
Fri	7/4	73	99	100	102	114	105	64	88	88	88	97	93
Sat	7/5	88	110	113	113	113	108	78	89	93	92	95	95
Sun	7/6	96	105	104	100	102	88	84	90	89	82	91	71
Mon	7/7	95	106	107	100	104	57	82	87	84	75	75	54
Tue	7/8	79	107	108	111	103	106	68	92	94	96	95	87
2030 (1.5 x ROG, 0.75 x NOx)													
Sun	6/15	45	58	59	62	61	63	40	50	52	54	53	58
Mon	6/16	68	78	80	80	75	69	60	65	66	65	66	62
Tue	6/17	86	101	101	97	95	76	75	81	83	77	80	68
Wed	6/18	98	112	113	114	111	99	80	86	86	84	86	76
Thu	6/19	112	109	89	87	88	83	92	91	83	80	80	74
Fri	6/20	102	105	99	101	107	104	82	82	84	82	80	87
Sat	6/21	104	117	116	115	102	118	74	79	80	82	81	92
Wed	7/2	72	96	97	99	93	78	63	82	82	82	81	71
Thu	7/3	89	100	102	96	95	91	74	85	86	84	86	83
Fri	7/4	67	88	88	89	99	92	60	79	78	78	85	82
Sat	7/5	81	96	99	99	99	94	71	80	82	82	84	83
Sun	7/6	86	92	92	88	89	77	76	80	79	73	80	64
Mon	7/7	85	92	93	87	91	53	75	77	75	67	68	51
Tue	7/8	72	94	94	96	90	92	63	81	83	84	83	77
2030 (1.5 x ROG, 0.5 x NOx)													
Sun	6/15	47	59	62	62	62	59	42	51	52	53	54	55
Mon	6/16	71	82	81	79	71	67	63	65	65	64	62	58
Tue	6/17	87	95	96	91	89	69	75	77	78	73	76	63
Wed	6/18	95	102	106	106	100	89	76	79	79	78	78	69
Thu	6/19	106	102	84	77	78	73	88	83	76	72	71	66
Fri	6/20	99	98	90	92	95	95	79	76	78	76	74	80
Sat	6/21	96	105	104	103	92	106	69	71	72	74	73	82
Wed	7/2	76	88	89	90	84	71	63	77	76	75	74	65
Thu	7/3	86	92	95	89	84	81	73	78	78	76	77	74
Fri	7/4	68	81	80	81	90	82	60	73	71	71	77	73
Sat	7/5	77	87	91	90	90	85	68	72	75	75	76	75
Sun	7/6	82	84	84	81	80	71	72	73	72	66	72	59
Mon	7/7	81	85	84	80	83	49	72	70	68	61	63	47
Tue	7/8	69	87	87	88	81	83	61	75	76	77	75	70
2030 (1.5 x ROG, 0.3 x NOx)													
Sun	6/15	55	63	67	66	68	56	50	55	56	56	57	52
Mon	6/16	76	82	81	79	67	64	65	64	63	61	58	54
Tue	6/17	86	87	89	85	85	61	74	71	72	69	71	57
Wed	6/18	89	91	97	97	92	79	71	71	71	70	70	62
Thu	6/19	97	94	78	66	67	62	81	74	67	63	62	56
Fri	6/20	92	90	80	83	81	85	75	69	70	69	65	71
Sat	6/21	85	91	91	89	81	92	63	62	63	65	63	71
Wed	7/2	76	79	80	81	75	62	62	71	68	68	66	58
Thu	7/3	81	84	87	82	75	72	71	70	70	68	67	63
Fri	7/4	71	73	72	72	81	72	59	66	63	64	68	64
Sat	7/5	72	78	83	81	81	76	63	65	67	67	67	66
Sun	7/6	75	75	76	73	71	64	67	65	64	60	63	53
Mon	7/7	76	77	77	73	75	45	69	63	62	56	58	44
Tue	7/8	69	78	78	79	72	74	58	68	68	68	66	62
2030													
1.5xROG, 1.0 NOx		93	109	108	107	106	97	77	88	88	86	88	83
1.5xROG, 0.75 NOx		83	96	94	94	92	85	70	78	79	77	78	73
1.5xROG, 0.5 NOx		81	89	88	86	84	77	69	73	73	71	72	67
1.5xROG, 0.3 NOx		79	82	81	79	77	69	66	67	66	65	65	60

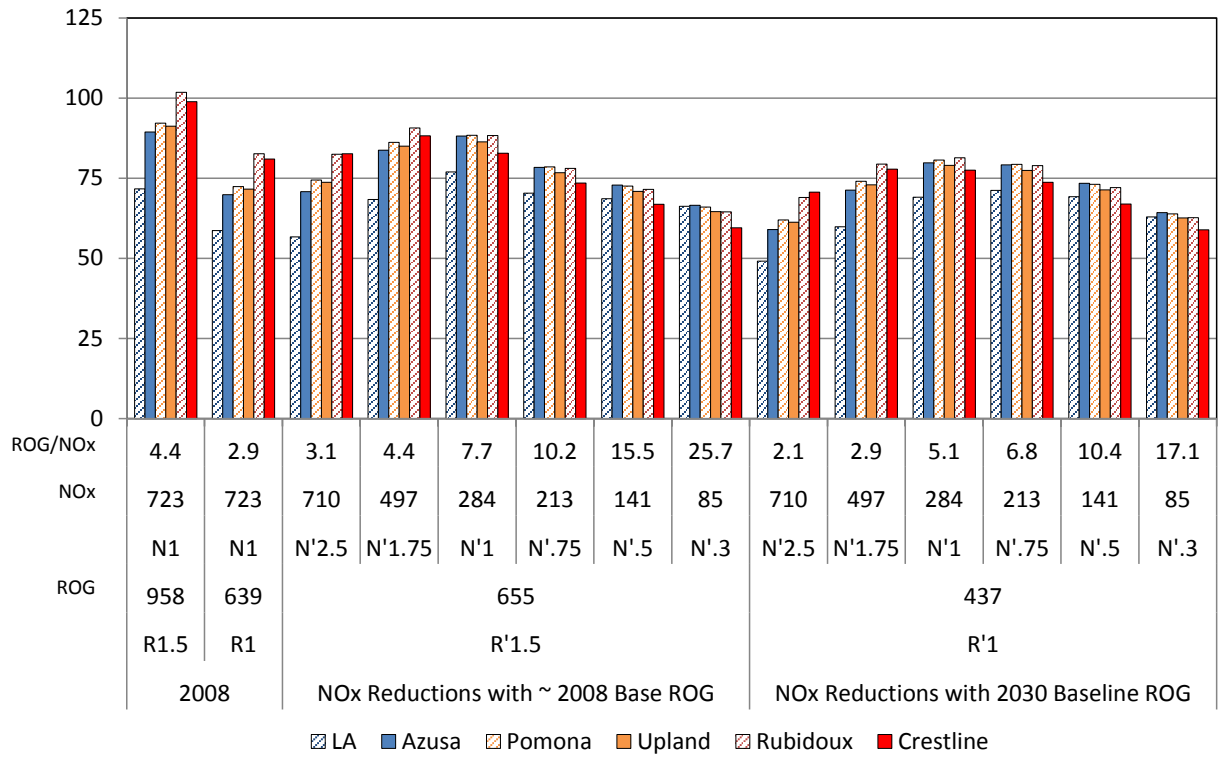

Figure 5-8. Mean observed and predicted 2008 base year and 2030 daily max 8-hour ozone concentrations (ppb) for the June 15-21 and July 2-8 episodes. Basinwide NOx and ROG emissions (tons per day) are shown above the adjustment factors applied to the 2008 base year ROG (R) and NOx (N) emissions and 2030 baseline ROG (R') and NOx (N') emissions.

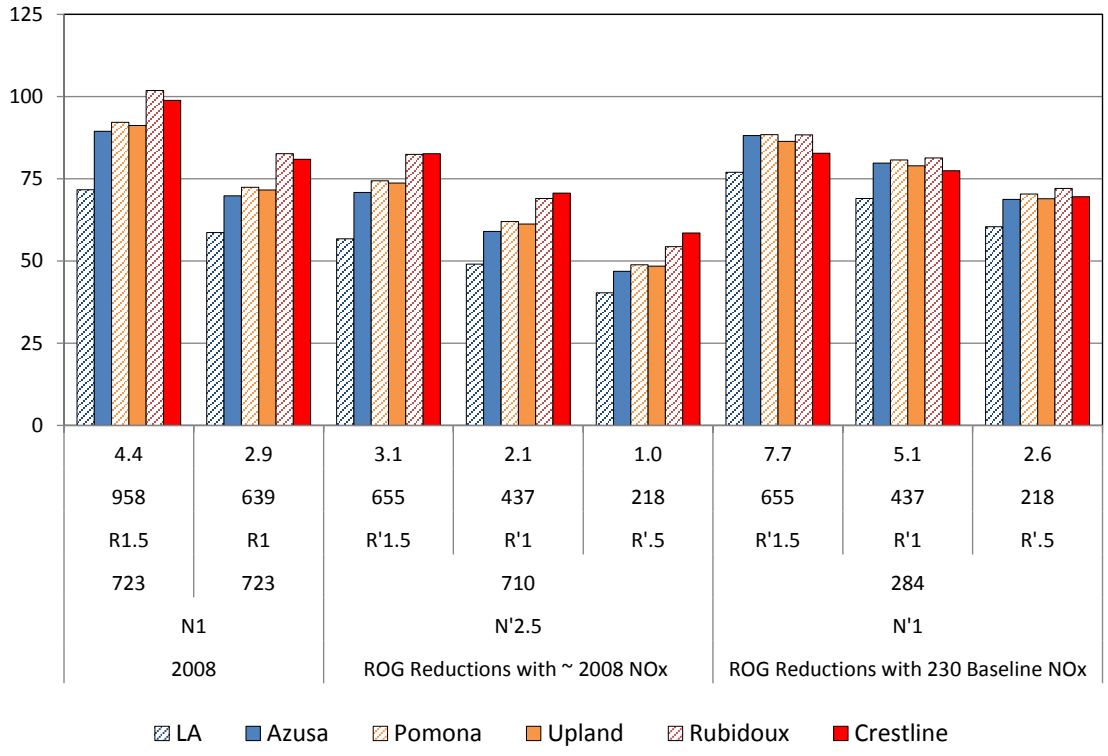

Figure 5-9. Mean predicted daily max 8-hour ozone concentrations (ppb) for the June 15-21 and July 2-8 episodes for varying reduction of ROG emissions with NO_X emissions held constant at 2008 base year emissions and 2030 baseline emissions. Basinwide NOx and ROG emissions (tons per day) are shown above the adjustment factors applied to the 2008 base year ROG (R) and NOx (N) emissions and 2030 baseline ROG (R') and NOx (N') emissions.

The indications from the results shown in Figure 5-7 and past evaluations of the emission inventory that current estimates of ROG emissions may be underestimated relative to NOx emissions have important implications for the attainment test. In a region that is VOC limited with respect to ozone formation, an underestimation of ROG emissions in the base year results in lower predicted ozone than the observed values. The inaccurate low predictions result in higher RRFs (i.e., future/current ratios) and higher projected DVs. Increasing the base ROG emissions lowers the RRFs and projected DVs and decreases the emission reductions necessary to show attainment. Three sets of RRFs and 2030 projected DVs were derived based upon: 1) 2008 base year simulations without adjustment to the base ROG emissions (Table 5-8); 2) 1.5 x base ROG (Table 5-9); and 3) 2.0 x base ROG (Table 5-10). The corresponding projected 2030 design values are shown in Table 5-11 through Table 5-13. Exceedances of the 1-hour and 8-hour ozone standards are highlighted in the Tables. Figure 5-10 show the differences in the projected 2030 DVs using the three alternative 2008 base year ROG emissions. The projected 2030 DVs are shown in groups of four cases that represent the incremental reductions of 1.0, 0.75, 0.5 and 0.3 times from the 2030 baseline NOx emissions. These cases are equivalent to 61, 71, 80 and 88 percent reductions from the 2008 emissions. The two groups of four cases further represent 2030

baseline ROG emissions multiplied by factors of 1.0 or 1.5 to simulate the potential underestimation in the 2030 ROG emissions.

Table 5-8. Relative response factors (RRF) referenced to 2008 base case without adjustments to 2008 base ROG emissions.

		1-hour max ozone (ppb)						Max Ozone 8-hour					
DOW	date	LA	Azusa	Pomona	Upland	Rubidoux	Crestline	LA	Azusa	Pomona	Upland	Rubidoux	Crestline
2030 (1.0 x ROG, 1.0 x NOx)													
Sun	6/15	0.86	1.02	1.03	1.00	0.91	0.96	0.93	1.01	1.02	1.05	0.97	1.00
Mon	6/16	1.23	1.22	1.17	1.15	1.01	0.99	1.40	1.35	1.33	1.26	1.08	1.03
Tue	6/17	1.22	1.66	1.67	1.64	1.24	1.14	1.36	1.57	1.74	1.68	1.41	1.13
Wed	6/18	1.23	1.36	1.40	1.40	1.11	1.11	1.33	1.26	1.29	1.29	1.10	1.04
Thu	6/19	1.34	1.04	0.83	0.84	0.83	0.79	1.32	1.13	1.00	0.96	0.91	0.82
Fri	6/20	1.12	1.23	1.14	1.12	0.96	1.15	1.28	1.13	1.09	1.12	0.98	1.10
Sat	6/21	1.12	1.12	0.98	1.00	0.82	0.97	1.09	0.96	0.92	0.93	0.86	0.89
Wed	7/2	1.06	1.27	1.31	1.41	1.13	1.05	1.15	1.35	1.33	1.33	1.08	1.03
Thu	7/3	1.23	1.11	0.92	0.88	0.78	0.76	1.27	1.17	1.06	1.02	0.83	0.84
Fri	7/4	1.07	1.16	1.11	1.07	0.92	0.89	1.14	1.21	1.10	1.09	1.00	0.93
Sat	7/5	0.96	1.07	1.08	1.02	0.96	0.89	1.04	1.05	1.06	1.03	0.96	0.95
Sun	7/6	0.97	0.95	0.95	0.97	0.83	0.91	0.99	0.90	0.89	0.90	0.84	0.84
Mon	7/7	1.08	1.05	1.06	1.10	1.24	0.92	1.19	1.03	1.02	0.96	0.99	0.91
Tue	7/8	1.03	1.16	1.18	1.26	1.06	1.14	1.06	1.21	1.23	1.26	1.08	1.07
2030 (1.0 x ROG, 0.75 x NOx)													
Sun	6/15	1.07	1.31	1.30	1.20	1.09	1.01	1.18	1.25	1.26	1.26	1.19	1.02
Mon	6/16	1.36	1.45	1.29	1.33	1.06	1.03	1.56	1.48	1.43	1.36	1.09	1.03
Tue	6/17	1.33	1.74	1.78	1.70	1.29	1.09	1.43	1.60	1.78	1.71	1.45	1.08
Wed	6/18	1.25	1.34	1.43	1.41	1.07	1.07	1.35	1.23	1.26	1.26	1.06	0.99
Thu	6/19	1.40	1.05	0.81	0.78	0.77	0.73	1.35	1.09	0.95	0.90	0.85	0.75
Fri	6/20	1.20	1.25	1.08	1.08	0.90	1.11	1.31	1.11	1.06	1.09	0.93	1.06
Sat	6/21	1.14	1.07	0.94	0.96	0.78	0.92	1.07	0.91	0.87	0.88	0.80	0.83
Wed	7/2	1.06	1.25	1.28	1.37	1.08	0.99	1.18	1.36	1.30	1.30	1.03	0.97
Thu	7/3	1.31	1.10	0.92	0.86	0.72	0.72	1.33	1.14	1.02	0.98	0.77	0.78
Fri	7/4	1.09	1.14	1.07	1.02	0.89	0.84	1.15	1.19	1.05	1.04	0.96	0.87
Sat	7/5	0.98	1.03	1.07	0.99	0.93	0.85	1.04	1.00	1.01	0.99	0.92	0.89
Sun	7/6	0.96	0.90	0.91	0.94	0.78	0.87	0.99	0.85	0.85	0.85	0.78	0.80
Mon	7/7	1.08	1.02	1.02	1.07	1.19	0.87	1.20	0.99	0.97	0.91	0.97	0.87
Tue	7/8	1.00	1.16	1.16	1.23	1.01	1.08	1.06	1.20	1.18	1.22	1.03	1.01
2030 (1.0 x ROG, 0.5 x NOx)													
Sun	6/15	1.07	1.27	1.29	1.17	1.07	0.92	1.19	1.21	1.22	1.21	1.15	0.95
Mon	6/16	1.42	1.49	1.29	1.29	0.99	0.99	1.61	1.46	1.39	1.32	1.02	0.97
Tue	6/17	1.34	1.62	1.68	1.59	1.21	0.98	1.43	1.51	1.67	1.61	1.37	0.99
Wed	6/18	1.20	1.22	1.33	1.30	0.97	0.96	1.29	1.12	1.15	1.16	0.96	0.90
Thu	6/19	1.32	0.98	0.76	0.69	0.68	0.64	1.28	1.00	0.86	0.82	0.76	0.67
Fri	6/20	1.16	1.17	0.98	0.98	0.79	1.01	1.26	1.02	0.98	1.00	0.85	0.97
Sat	6/21	1.06	0.96	0.85	0.86	0.71	0.82	1.00	0.82	0.79	0.79	0.72	0.74
Wed	7/2	1.13	1.15	1.16	1.24	0.97	0.90	1.17	1.27	1.20	1.20	0.94	0.89
Thu	7/3	1.26	1.01	0.86	0.80	0.64	0.65	1.31	1.04	0.93	0.89	0.69	0.69
Fri	7/4	1.09	1.06	0.98	0.93	0.81	0.76	1.14	1.11	0.96	0.95	0.87	0.78
Sat	7/5	0.94	0.93	0.98	0.90	0.85	0.77	0.99	0.91	0.92	0.90	0.83	0.80
Sun	7/6	0.92	0.82	0.83	0.86	0.70	0.79	0.94	0.77	0.77	0.78	0.70	0.73
Mon	7/7	1.02	0.94	0.93	0.98	1.09	0.80	1.16	0.90	0.89	0.83	0.90	0.81
Tue	7/8	0.96	1.07	1.06	1.12	0.91	0.97	1.02	1.11	1.08	1.11	0.93	0.92
2030 (1.0 x ROG, 0.3 x NOx)													
Sun	6/15	0.92	1.05	1.09	0.97	0.88	0.79	1.04	1.03	1.04	1.04	0.97	0.87
Mon	6/16	1.34	1.33	1.14	1.14	0.85	0.89	1.53	1.34	1.26	1.20	0.91	0.88
Tue	6/17	1.23	1.41	1.47	1.39	1.07	0.86	1.31	1.33	1.47	1.44	1.21	0.88
Wed	6/18	1.06	1.04	1.15	1.12	0.84	0.82	1.16	0.98	1.01	1.01	0.84	0.79
Thu	6/19	1.15	0.85	0.67	0.59	0.58	0.55	1.12	0.86	0.75	0.71	0.66	0.59
Fri	6/20	1.02	1.01	0.84	0.84	0.66	0.86	1.13	0.90	0.85	0.88	0.74	0.84
Sat	6/21	0.90	0.81	0.72	0.72	0.60	0.69	0.89	0.71	0.68	0.68	0.61	0.63
Wed	7/2	1.05	0.99	1.00	1.07	0.84	0.78	1.10	1.13	1.05	1.05	0.82	0.78
Thu	7/3	1.12	0.88	0.75	0.70	0.55	0.55	1.20	0.91	0.81	0.77	0.59	0.59
Fri	7/4	1.07	0.92	0.85	0.80	0.70	0.65	1.08	0.98	0.84	0.83	0.75	0.68
Sat	7/5	0.83	0.80	0.85	0.78	0.74	0.66	0.90	0.80	0.80	0.79	0.72	0.69
Sun	7/6	0.81	0.71	0.72	0.75	0.60	0.69	0.85	0.68	0.67	0.69	0.60	0.65
Mon	7/7	0.90	0.81	0.81	0.86	0.94	0.74	1.05	0.79	0.78	0.74	0.81	0.75
Tue	7/8	0.90	0.92	0.92	0.97	0.79	0.84	0.95	0.97	0.94	0.96	0.80	0.80

Table 5-9. Relative response factors (RRF) referenced to 2008 base case with 1.5 times 2008 base ROG emissions.

		1-hour max ozone (ppb)						Max Ozone 8-hour					
DOW	date	LA	Azusa	Pomona	Upland	Rubidoux	Crestline	LA	Azusa	Pomona	Upland	Rubidoux	Crestline
2030 (1.0 x ROG, 1.0 x NOx)													
Sun	6/15	0.77	0.79	0.75	0.72	0.67	0.71	0.82	0.79	0.79	0.80	0.74	0.78
Mon	6/16	1.07	0.96	0.90	0.87	0.84	0.81	1.15	1.09	1.04	1.02	0.86	0.87
Tue	6/17	0.99	1.14	1.15	1.10	0.92	0.84	1.08	1.13	1.20	1.18	1.03	0.87
Wed	6/18	0.93	0.92	0.94	0.95	0.79	0.81	1.01	0.90	0.91	0.90	0.80	0.80
Thu	6/19	0.93	0.86	0.69	0.68	0.69	0.67	0.97	0.86	0.81	0.77	0.75	0.71
Fri	6/20	0.88	0.94	0.81	0.86	0.71	0.84	0.97	0.88	0.85	0.87	0.79	0.83
Sat	6/21	0.81	0.75	0.75	0.74	0.71	0.70	0.85	0.75	0.74	0.74	0.72	0.70
Wed	7/2	0.92	0.97	0.95	0.96	0.85	0.81	1.02	1.05	1.02	1.01	0.85	0.83
Thu	7/3	1.00	0.87	0.75	0.73	0.67	0.68	1.04	0.90	0.84	0.82	0.71	0.71
Fri	7/4	0.97	0.91	0.87	0.83	0.78	0.74	1.03	0.96	0.88	0.86	0.81	0.77
Sat	7/5	0.82	0.82	0.85	0.84	0.80	0.75	0.90	0.84	0.83	0.81	0.79	0.76
Sun	7/6	0.81	0.78	0.82	0.80	0.72	0.76	0.85	0.76	0.76	0.78	0.74	0.76
Mon	7/7	0.90	0.82	0.88	0.90	0.92	0.86	0.97	0.83	0.83	0.83	0.87	0.87
Tue	7/8	0.89	0.92	0.94	0.94	0.84	0.86	0.95	0.97	0.96	0.96	0.84	0.85
2030 (1.0 x ROG, 0.75 x NOx)													
Sun	6/15	0.95	1.02	0.94	0.87	0.80	0.75	1.04	0.98	0.97	0.96	0.91	0.80
Mon	6/16	1.18	1.14	0.99	1.00	0.87	0.84	1.28	1.19	1.12	1.10	0.87	0.87
Tue	6/17	1.08	1.19	1.23	1.14	0.95	0.80	1.13	1.15	1.23	1.20	1.06	0.84
Wed	6/18	0.94	0.91	0.96	0.96	0.75	0.78	1.03	0.87	0.88	0.87	0.77	0.76
Thu	6/19	0.97	0.86	0.67	0.63	0.63	0.61	0.99	0.83	0.77	0.73	0.70	0.66
Fri	6/20	0.94	0.95	0.77	0.82	0.66	0.81	0.99	0.86	0.83	0.84	0.76	0.79
Sat	6/21	0.82	0.72	0.72	0.70	0.68	0.67	0.83	0.71	0.70	0.70	0.67	0.66
Wed	7/2	0.92	0.96	0.92	0.94	0.81	0.77	1.05	1.05	1.00	0.99	0.81	0.79
Thu	7/3	1.06	0.86	0.76	0.72	0.63	0.64	1.08	0.87	0.80	0.78	0.66	0.67
Fri	7/4	0.98	0.90	0.84	0.80	0.76	0.70	1.04	0.95	0.84	0.82	0.78	0.72
Sat	7/5	0.84	0.79	0.84	0.82	0.77	0.72	0.90	0.80	0.79	0.77	0.75	0.72
Sun	7/6	0.80	0.75	0.79	0.77	0.68	0.72	0.85	0.72	0.72	0.74	0.69	0.71
Mon	7/7	0.89	0.80	0.85	0.88	0.89	0.81	0.98	0.79	0.80	0.79	0.85	0.82
Tue	7/8	0.86	0.91	0.92	0.92	0.80	0.81	0.94	0.96	0.92	0.92	0.80	0.80
2030 (1.0 x ROG, 0.5 x NOx)													
Sun	6/15	0.95	0.99	0.94	0.84	0.78	0.69	1.05	0.95	0.94	0.92	0.88	0.74
Mon	6/16	1.23	1.17	0.99	0.97	0.81	0.81	1.33	1.18	1.08	1.07	0.81	0.82
Tue	6/17	1.08	1.12	1.16	1.07	0.89	0.72	1.13	1.09	1.16	1.13	1.00	0.77
Wed	6/18	0.90	0.83	0.90	0.88	0.68	0.71	0.99	0.80	0.81	0.80	0.70	0.69
Thu	6/19	0.91	0.80	0.63	0.56	0.56	0.54	0.93	0.76	0.70	0.66	0.63	0.59
Fri	6/20	0.91	0.89	0.69	0.75	0.58	0.73	0.95	0.79	0.76	0.77	0.69	0.73
Sat	6/21	0.76	0.64	0.65	0.63	0.62	0.59	0.78	0.64	0.63	0.63	0.60	0.59
Wed	7/2	0.98	0.88	0.84	0.85	0.73	0.69	1.05	0.99	0.92	0.91	0.74	0.71
Thu	7/3	1.02	0.79	0.70	0.66	0.55	0.58	1.07	0.80	0.73	0.71	0.59	0.59
Fri	7/4	0.99	0.83	0.77	0.72	0.69	0.63	1.03	0.88	0.77	0.75	0.71	0.65
Sat	7/5	0.80	0.71	0.77	0.74	0.70	0.65	0.86	0.73	0.72	0.71	0.68	0.64
Sun	7/6	0.76	0.68	0.72	0.71	0.61	0.66	0.80	0.65	0.66	0.67	0.62	0.65
Mon	7/7	0.85	0.74	0.77	0.81	0.81	0.75	0.95	0.72	0.73	0.72	0.79	0.77
Tue	7/8	0.83	0.84	0.84	0.84	0.72	0.73	0.91	0.89	0.84	0.84	0.72	0.73
2030 (1.0 x ROG, 0.3 x NOx)													
Sun	6/15	0.82	0.82	0.79	0.70	0.65	0.59	0.92	0.81	0.81	0.79	0.74	0.68
Mon	6/16	1.16	1.05	0.88	0.86	0.70	0.72	1.26	1.08	0.98	0.97	0.72	0.74
Tue	6/17	0.99	0.97	1.01	0.93	0.79	0.63	1.03	0.96	1.02	1.01	0.89	0.68
Wed	6/18	0.80	0.71	0.77	0.76	0.59	0.60	0.88	0.70	0.71	0.70	0.61	0.61
Thu	6/19	0.79	0.70	0.56	0.48	0.48	0.46	0.82	0.65	0.61	0.57	0.54	0.51
Fri	6/20	0.80	0.77	0.60	0.64	0.49	0.63	0.86	0.69	0.67	0.68	0.60	0.63
Sat	6/21	0.65	0.54	0.55	0.53	0.52	0.50	0.69	0.56	0.55	0.55	0.52	0.50
Wed	7/2	0.91	0.75	0.72	0.73	0.63	0.60	0.98	0.87	0.81	0.80	0.65	0.63
Thu	7/3	0.91	0.69	0.61	0.58	0.48	0.49	0.98	0.70	0.63	0.62	0.51	0.50
Fri	7/4	0.96	0.73	0.67	0.62	0.60	0.54	0.98	0.78	0.67	0.66	0.61	0.56
Sat	7/5	0.71	0.61	0.67	0.64	0.61	0.56	0.77	0.64	0.63	0.62	0.59	0.56
Sun	7/6	0.67	0.58	0.63	0.62	0.52	0.58	0.72	0.57	0.57	0.59	0.53	0.58
Mon	7/7	0.75	0.64	0.67	0.70	0.70	0.69	0.86	0.63	0.64	0.64	0.71	0.72
Tue	7/8	0.77	0.73	0.73	0.72	0.62	0.63	0.84	0.78	0.73	0.73	0.62	0.63

Table 5-10. Relative response factors (RRF) referenced to 2008 base case with 2.0 times 2008 base ROG emissions.

		1-hour max ozone (ppb)						Max Ozone 8-hour					
DOW	date	LA	Azusa	Pomona	Upland	Rubidoux	Crestline	LA	Azusa	Pomona	Upland	Rubidoux	Crestline
2030 (1.0 x ROG, 1.0 x NOx)													
Sun	6/15	0.72	0.65	0.62	0.60	0.58	0.61	0.76	0.68	0.68	0.68	0.64	0.69
Mon	6/16	0.94	0.79	0.75	0.73	0.69	0.71	0.97	0.90	0.86	0.85	0.74	0.76
Tue	6/17	0.82	0.84	0.84	0.79	0.73	0.67	0.89	0.86	0.88	0.87	0.80	0.72
Wed	6/18	0.72	0.68	0.70	0.71	0.63	0.64	0.82	0.71	0.72	0.71	0.67	0.68
Thu	6/19	0.73	0.75	0.62	0.61	0.62	0.61	0.77	0.71	0.70	0.67	0.67	0.66
Fri	6/20	0.72	0.72	0.64	0.67	0.61	0.66	0.78	0.73	0.72	0.71	0.70	0.67
Sat	6/21	0.63	0.61	0.62	0.62	0.63	0.60	0.71	0.66	0.66	0.65	0.65	0.63
Wed	7/2	0.79	0.73	0.72	0.71	0.67	0.65	0.90	0.81	0.79	0.76	0.68	0.68
Thu	7/3	0.82	0.74	0.67	0.65	0.61	0.60	0.87	0.74	0.70	0.70	0.64	0.64
Fri	7/4	0.86	0.75	0.71	0.68	0.68	0.65	0.94	0.80	0.75	0.72	0.70	0.67
Sat	7/5	0.73	0.69	0.72	0.69	0.68	0.65	0.79	0.72	0.70	0.69	0.69	0.67
Sun	7/6	0.72	0.70	0.71	0.70	0.67	0.68	0.75	0.69	0.69	0.71	0.68	0.71
Mon	7/7	0.77	0.68	0.70	0.72	0.73	0.82	0.83	0.71	0.72	0.74	0.78	0.84
Tue	7/8	0.80	0.77	0.77	0.74	0.69	0.70	0.86	0.81	0.79	0.77	0.71	0.72
2030 (1.0 x ROG, 0.75 x NOx)													
Sun	6/15	0.89	0.83	0.79	0.73	0.69	0.65	0.96	0.84	0.83	0.81	0.78	0.70
Mon	6/16	1.04	0.94	0.83	0.84	0.72	0.74	1.08	0.99	0.92	0.91	0.74	0.77
Tue	6/17	0.89	0.88	0.90	0.82	0.76	0.63	0.93	0.87	0.91	0.89	0.82	0.69
Wed	6/18	0.73	0.67	0.72	0.71	0.61	0.62	0.83	0.69	0.70	0.69	0.65	0.64
Thu	6/19	0.77	0.76	0.60	0.56	0.57	0.56	0.79	0.68	0.67	0.63	0.62	0.61
Fri	6/20	0.77	0.73	0.61	0.64	0.56	0.64	0.80	0.71	0.70	0.69	0.66	0.65
Sat	6/21	0.64	0.59	0.60	0.59	0.61	0.57	0.70	0.62	0.62	0.62	0.61	0.59
Wed	7/2	0.79	0.72	0.70	0.69	0.63	0.61	0.93	0.82	0.77	0.74	0.66	0.65
Thu	7/3	0.87	0.74	0.68	0.64	0.57	0.57	0.90	0.72	0.67	0.66	0.60	0.59
Fri	7/4	0.87	0.74	0.69	0.65	0.66	0.61	0.95	0.78	0.71	0.69	0.67	0.63
Sat	7/5	0.74	0.66	0.71	0.67	0.66	0.63	0.79	0.69	0.67	0.66	0.66	0.63
Sun	7/6	0.71	0.66	0.68	0.67	0.63	0.65	0.75	0.65	0.66	0.67	0.64	0.67
Mon	7/7	0.77	0.66	0.68	0.70	0.71	0.77	0.84	0.68	0.69	0.71	0.76	0.80
Tue	7/8	0.78	0.76	0.75	0.72	0.66	0.66	0.85	0.80	0.76	0.75	0.67	0.68
2030 (1.0 x ROG, 0.5 x NOx)													
Sun	6/15	0.89	0.81	0.78	0.70	0.67	0.59	0.97	0.81	0.81	0.78	0.76	0.65
Mon	6/16	1.08	0.97	0.83	0.81	0.67	0.71	1.12	0.98	0.89	0.89	0.69	0.72
Tue	6/17	0.90	0.82	0.85	0.77	0.71	0.57	0.93	0.82	0.85	0.84	0.78	0.63
Wed	6/18	0.70	0.61	0.67	0.66	0.55	0.56	0.80	0.63	0.64	0.63	0.59	0.59
Thu	6/19	0.72	0.70	0.57	0.50	0.51	0.49	0.75	0.63	0.61	0.57	0.56	0.55
Fri	6/20	0.75	0.68	0.55	0.58	0.50	0.58	0.77	0.65	0.65	0.64	0.61	0.59
Sat	6/21	0.59	0.53	0.54	0.53	0.55	0.51	0.65	0.56	0.56	0.56	0.55	0.52
Wed	7/2	0.84	0.66	0.64	0.63	0.57	0.55	0.92	0.76	0.71	0.69	0.60	0.59
Thu	7/3	0.84	0.68	0.63	0.59	0.51	0.51	0.89	0.66	0.61	0.60	0.54	0.53
Fri	7/4	0.87	0.69	0.63	0.59	0.60	0.55	0.94	0.73	0.65	0.63	0.60	0.57
Sat	7/5	0.71	0.60	0.65	0.61	0.60	0.57	0.76	0.63	0.61	0.61	0.60	0.57
Sun	7/6	0.68	0.60	0.62	0.62	0.56	0.59	0.71	0.59	0.59	0.61	0.57	0.61
Mon	7/7	0.73	0.61	0.62	0.65	0.64	0.71	0.81	0.62	0.63	0.65	0.71	0.74
Tue	7/8	0.75	0.71	0.69	0.66	0.60	0.60	0.82	0.74	0.70	0.68	0.61	0.62
2030 (1.0 x ROG, 0.3 x NOx)													
Sun	6/15	0.77	0.67	0.66	0.59	0.56	0.51	0.85	0.69	0.69	0.67	0.64	0.60
Mon	6/16	1.02	0.87	0.73	0.72	0.58	0.63	1.06	0.89	0.81	0.80	0.62	0.65
Tue	6/17	0.82	0.71	0.74	0.67	0.63	0.50	0.85	0.73	0.75	0.75	0.69	0.56
Wed	6/18	0.62	0.52	0.58	0.57	0.47	0.47	0.71	0.55	0.56	0.55	0.51	0.52
Thu	6/19	0.63	0.61	0.50	0.43	0.43	0.42	0.66	0.54	0.53	0.50	0.48	0.48
Fri	6/20	0.66	0.59	0.48	0.50	0.42	0.50	0.69	0.57	0.56	0.56	0.53	0.52
Sat	6/21	0.50	0.44	0.45	0.44	0.47	0.42	0.58	0.48	0.48	0.48	0.47	0.44
Wed	7/2	0.78	0.57	0.55	0.54	0.49	0.48	0.87	0.68	0.62	0.60	0.52	0.52
Thu	7/3	0.75	0.59	0.55	0.51	0.44	0.44	0.82	0.57	0.53	0.52	0.46	0.45
Fri	7/4	0.85	0.60	0.55	0.51	0.52	0.47	0.89	0.64	0.57	0.55	0.52	0.49
Sat	7/5	0.63	0.52	0.56	0.53	0.52	0.49	0.68	0.55	0.53	0.53	0.52	0.49
Sun	7/6	0.60	0.52	0.54	0.54	0.48	0.52	0.64	0.52	0.52	0.54	0.50	0.54
Mon	7/7	0.65	0.53	0.53	0.56	0.56	0.66	0.73	0.54	0.56	0.58	0.63	0.69
Tue	7/8	0.70	0.61	0.59	0.57	0.52	0.51	0.76	0.65	0.60	0.59	0.52	0.54

Table 5-11. Projected 2030 basin design values using relative response factors (RRF) referenced to 2008 base case without adjustments to base ROG emissions.

		1-hour max ozone (ppb)						Max Ozone 8-hour					
DOW	date	LA	Azusa	Pomona	Upland	Rubidoux	Crestline	LA	Azusa	Pomona	Upland	Rubidoux	Crestline
2030 (1.0 x ROG, 1.0 x NOx)													
Sun	6/15	93	144	145	150	128	157	68	97	106	116	103	119
Mon	6/16	133	172	165	173	142	163	102	129	137	139	116	122
Tue	6/17	132	234	235	246	173	188	99	151	179	185	151	134
Wed	6/18	133	192	197	210	156	182	97	121	133	142	118	124
Thu	6/19	145	147	118	126	116	130	97	108	103	105	97	97
Fri	6/20	121	174	160	168	135	189	93	109	113	123	105	131
Sat	6/21	121	158	139	151	114	159	80	92	95	102	92	105
Wed	7/2	114	179	185	211	158	173	84	130	137	147	115	122
Thu	7/3	133	156	129	132	109	125	93	112	109	113	88	100
Fri	7/4	115	163	156	160	128	147	83	116	113	120	107	110
Sat	7/5	104	151	152	154	135	145	76	100	109	114	103	113
Sun	7/6	104	134	133	146	116	150	73	86	92	99	89	101
Mon	7/7	117	148	149	165	173	151	87	99	105	105	106	109
Tue	7/8	111	164	166	189	148	186	78	117	126	139	116	127
2030 (1.0 x ROG, 0.75 x NOx)													
Sun	6/15	115	185	184	181	153	166	86	120	130	139	127	122
Mon	6/16	147	204	182	199	148	170	114	142	147	149	117	123
Tue	6/17	144	245	251	255	180	178	105	154	183	188	155	129
Wed	6/18	135	189	201	211	150	175	99	118	129	138	113	118
Thu	6/19	151	148	114	116	107	119	98	105	98	99	91	90
Fri	6/20	130	177	152	162	125	182	96	106	109	120	100	126
Sat	6/21	123	151	133	144	110	151	78	87	90	97	86	99
Wed	7/2	115	177	180	205	151	163	86	130	134	143	110	116
Thu	7/3	141	155	130	130	101	118	97	109	105	108	83	93
Fri	7/4	117	161	151	153	125	138	84	114	108	114	103	104
Sat	7/5	106	145	151	149	131	139	76	96	104	109	98	106
Sun	7/6	104	128	128	141	109	142	73	82	87	94	84	95
Mon	7/7	117	144	144	161	167	142	88	95	100	100	104	103
Tue	7/8	108	163	163	184	142	177	77	115	122	134	110	120
2030 (1.0 x ROG, 0.5 x NOx)													
Sun	6/15	115	180	182	175	150	151	87	116	126	133	123	113
Mon	6/16	153	210	182	193	138	163	118	141	143	145	109	115
Tue	6/17	144	229	237	239	169	161	104	145	172	177	146	118
Wed	6/18	130	172	187	195	135	158	94	108	119	127	103	107
Thu	6/19	143	138	108	103	95	105	93	96	89	90	81	80
Fri	6/20	126	164	138	147	111	165	92	98	101	110	91	115
Sat	6/21	114	136	120	129	99	134	73	78	81	87	77	88
Wed	7/2	122	162	164	187	136	147	86	122	123	132	101	105
Thu	7/3	136	143	121	120	90	106	96	100	95	98	74	83
Fri	7/4	118	149	138	139	113	124	83	106	98	105	93	93
Sat	7/5	101	132	138	136	119	126	73	88	95	99	89	96
Sun	7/6	99	116	117	129	98	130	69	74	79	86	75	86
Mon	7/7	110	132	131	148	152	132	85	86	92	92	97	96
Tue	7/8	104	151	150	168	128	160	75	106	111	122	99	109
2030 (1.0 x ROG, 0.3 x NOx)													
Sun	6/15	99	149	154	146	124	130	76	99	107	115	103	104
Mon	6/16	145	188	161	170	119	145	111	129	129	132	97	105
Tue	6/17	132	199	207	208	149	140	95	128	152	159	130	105
Wed	6/18	114	147	162	168	117	135	84	94	104	111	90	95
Thu	6/19	124	120	95	88	81	89	82	83	77	78	70	70
Fri	6/20	110	143	118	126	93	141	83	86	88	97	79	100
Sat	6/21	97	114	101	108	84	113	65	68	70	75	66	75
Wed	7/2	113	139	142	160	117	128	80	108	108	116	88	93
Thu	7/3	121	124	105	105	77	91	88	87	83	85	64	70
Fri	7/4	115	130	120	120	98	106	79	94	86	92	81	81
Sat	7/5	90	113	120	117	103	108	65	77	83	87	77	83
Sun	7/6	87	100	102	112	84	114	62	65	69	76	65	77
Mon	7/7	98	115	114	128	132	121	77	76	81	82	86	90
Tue	7/8	97	130	129	145	110	137	69	93	97	106	86	95
1.0xROG, 1.0 NOx													
Mean		120	165	159	170	138	160	86	112	118	125	108	115
Stdev		14	25	30	34	21	21	11	17	23	23	16	12
1.0xROG, 0.75 NOx													
Mean		125	170	162	171	136	154	90	112	118	124	106	110
Stdev		16	30	36	37	24	22	12	20	26	26	19	13
1.0xROG, 0.5 NOx													
Mean		122	158	151	158	124	140	88	105	109	115	97	100
Stdev		17	31	36	37	24	21	13	21	26	26	20	13
1.0xROG, 0.3 NOx													
Mean		110	136	131	136	106	121	80	92	95	101	84	89
Stdev		17	28	31	32	21	18	13	19	23	24	18	13

Table 5-12. Projected 2030 basin design values using relative response factors (RRF) referenced to 2008 base case with 1.5 x base ROG emissions.

			1-hour max ozone (ppb)						Max Ozone 8-hour				
DOW	date	LA	Azusa	Pomona	Upland	Rubidoux	Crestline	LA	Azusa	Pomona	Upland	Rubidoux	Crestline
2030 (1.0 x ROG, 1.0 x NOx)													
Sun	6/15	83	112	105	108	94	117	60	76	82	88	79	93
Mon	6/16	115	135	127	131	117	132	84	104	107	113	92	104
Tue	6/17	107	161	162	165	128	138	79	108	124	130	110	104
Wed	6/18	100	130	133	143	110	134	74	86	93	99	86	95
Thu	6/19	100	121	98	102	96	109	71	82	83	85	80	85
Fri	6/20	95	132	114	128	99	137	70	84	88	95	85	98
Sat	6/21	88	105	106	110	100	116	62	72	76	81	77	84
Wed	7/2	99	136	134	145	119	133	75	100	105	111	91	99
Thu	7/3	108	123	106	110	94	111	76	86	86	90	76	85
Fri	7/4	104	129	123	125	109	122	75	92	91	94	87	91
Sat	7/5	89	115	120	126	112	123	65	80	85	89	84	90
Sun	7/6	87	110	116	120	101	125	62	73	78	85	79	90
Mon	7/7	97	116	123	135	129	140	71	79	86	91	93	103
Tue	7/8	96	129	132	142	117	140	69	93	99	105	90	101
2030 (1.0 x ROG, 0.75 x NOx)													
Sun	6/15	103	143	133	130	112	124	76	94	100	105	97	95
Mon	6/16	127	161	140	151	122	138	94	115	115	121	93	104
Tue	6/17	116	168	173	171	133	131	83	111	127	132	113	100
Wed	6/18	101	128	136	144	106	128	75	84	91	96	83	91
Thu	6/19	105	122	95	95	89	101	72	79	79	80	75	79
Fri	6/20	102	134	108	124	92	132	72	82	85	92	81	95
Sat	6/21	89	101	102	105	96	109	61	68	72	77	72	78
Wed	7/2	100	135	130	141	113	126	77	101	103	108	87	93
Thu	7/3	114	122	107	107	88	105	79	84	83	86	71	79
Fri	7/4	106	127	119	119	106	115	76	91	87	90	83	86
Sat	7/5	90	111	118	123	108	118	66	77	82	85	80	85
Sun	7/6	87	105	111	116	95	119	62	69	74	81	74	85
Mon	7/7	97	113	119	132	125	133	72	76	82	86	91	98
Tue	7/8	93	129	129	138	112	133	69	92	95	101	85	95
2030 (1.0 x ROG, 0.5 x NOx)													
Sun	6/15	103	139	132	126	109	113	77	91	97	101	94	88
Mon	6/16	132	165	140	146	114	132	97	113	112	118	87	98
Tue	6/17	117	157	164	161	125	118	82	104	120	125	107	91
Wed	6/18	97	117	126	132	96	116	72	77	84	88	75	83
Thu	6/19	99	113	89	84	79	89	68	73	72	72	67	70
Fri	6/20	99	125	98	112	81	120	70	76	79	85	74	86
Sat	6/21	82	91	92	94	86	97	57	62	65	69	64	70
Wed	7/2	106	123	118	128	103	114	76	95	95	100	80	85
Thu	7/3	110	112	99	99	78	94	78	77	75	78	63	70
Fri	7/4	107	117	108	108	97	103	76	85	79	82	76	77
Sat	7/5	87	100	109	112	99	107	63	70	74	78	73	77
Sun	7/6	82	95	102	106	85	108	59	63	68	74	66	77
Mon	7/7	92	104	109	121	114	123	69	69	75	79	85	92
Tue	7/8	90	119	119	126	101	120	66	85	87	92	77	86
2030 (1.0 x ROG, 0.3 x NOx)													
Sun	6/15	89	115	111	105	91	97	67	78	83	87	79	81
Mon	6/16	125	148	124	129	99	118	92	104	101	107	77	89
Tue	6/17	107	136	143	140	111	103	75	92	105	111	95	81
Wed	6/18	86	99	109	114	83	99	64	67	73	77	65	73
Thu	6/19	86	98	79	72	67	75	60	63	63	63	58	61
Fri	6/20	86	109	84	96	68	103	62	67	69	75	64	75
Sat	6/21	70	76	77	79	73	82	50	53	56	60	55	59
Wed	7/2	98	106	102	110	88	99	72	84	83	88	69	75
Thu	7/3	98	97	86	87	67	81	72	67	65	68	55	60
Fri	7/4	104	103	94	94	83	88	72	75	69	72	65	67
Sat	7/5	77	86	94	96	85	92	56	61	65	68	63	66
Sun	7/6	73	82	88	93	73	95	53	55	59	65	57	69
Mon	7/7	81	90	94	105	98	113	63	61	66	71	76	85
Tue	7/8	84	103	103	109	87	103	62	75	75	80	66	76
1.0xROG, 1.0 NOx													
Mean		98	125	121	128	109	127	71	87	92	97	86	94
Stdev		9	14	16	17	12	11	7	11	13	13	9	7
1.0xROG, 0.75 NOx													
Mean		102	129	123	128	107	122	74	87	91	96	85	90
Stdev		11	19	20	20	14	12	8	14	16	16	11	8
1.0xROG, 0.5 NOx													
Mean		100	120	115	118	98	111	72	81	84	89	78	82
Stdev		14	22	21	20	15	12	10	15	16	17	12	9
1.0xROG, 0.3 NOx													
Mean		90	104	99	102	84	96	66	71	74	78	68	73
Stdev		15	20	18	18	13	12	11	14	15	16	11	9

Table 5-13. Projected 2030 basin design values using relative response factors (RRF) referenced to 2008 base case with 2.0 x base ROG emissions.

		1-hour max ozone (ppb)						Max Ozone 8-hour					
DOW	date	LA	Azusa	Pomona	Upland	Rubidoux	Crestline	LA	Azusa	Pomona	Upland	Rubidoux	Crestline
2030 (1.0 x ROG, 1.0 x NOx)													
Sun	6/15	77	92	88	91	81	101	56	65	70	75	68	82
Mon	6/16	101	112	106	109	97	116	71	86	88	93	79	91
Tue	6/17	88	119	119	119	102	109	65	82	91	96	86	86
Wed	6/18	78	96	99	106	88	105	60	68	74	78	72	80
Thu	6/19	79	106	88	91	87	99	56	68	72	74	72	79
Fri	6/20	78	101	91	100	85	108	57	70	74	79	75	80
Sat	6/21	68	86	87	92	89	99	52	63	68	72	70	75
Wed	7/2	86	102	101	107	93	106	66	78	81	84	73	81
Thu	7/3	89	105	95	98	86	99	63	71	72	77	69	76
Fri	7/4	92	106	101	103	96	106	68	76	77	79	74	80
Sat	7/5	79	97	101	104	95	107	58	69	73	76	74	79
Sun	7/6	77	98	100	105	93	111	55	66	71	78	73	84
Mon	7/7	83	96	99	108	102	134	61	68	74	82	83	100
Tue	7/8	86	108	108	111	97	114	63	78	81	85	76	86
2030 (1.0 x ROG, 0.75 x NOx)													
Sun	6/15	96	118	111	109	96	106	70	80	86	89	84	83
Mon	6/16	112	133	117	125	101	121	79	95	95	100	79	91
Tue	6/17	96	124	127	123	106	104	68	84	93	97	88	82
Wed	6/18	79	95	101	107	85	101	61	66	72	76	69	77
Thu	6/19	83	107	85	85	80	92	58	66	69	70	67	73
Fri	6/20	84	103	86	96	79	105	59	68	72	76	71	77
Sat	6/21	69	83	84	88	85	93	51	60	64	68	65	70
Wed	7/2	86	101	99	104	89	100	68	78	79	82	70	77
Thu	7/3	94	104	95	96	80	94	66	69	69	73	64	71
Fri	7/4	94	105	98	98	93	100	69	75	73	76	71	75
Sat	7/5	80	94	100	101	92	103	58	66	69	73	71	75
Sun	7/6	77	94	96	101	88	106	55	63	67	74	68	79
Mon	7/7	83	94	96	106	99	126	61	65	71	78	81	95
Tue	7/8	84	108	106	109	93	108	62	77	79	82	72	81
2030 (1.0 x ROG, 0.5 x NOx)													
Sun	6/15	96	114	110	106	94	97	71	78	83	86	81	77
Mon	6/16	116	136	117	122	94	116	82	94	92	97	74	86
Tue	6/17	97	116	120	116	100	94	68	79	88	92	83	75
Wed	6/18	76	86	94	99	77	91	58	61	66	69	63	70
Thu	6/19	78	99	80	75	71	81	55	60	62	63	60	65
Fri	6/20	81	96	78	88	70	95	56	63	66	70	65	71
Sat	6/21	64	74	76	79	77	83	48	54	58	61	58	62
Wed	7/2	91	93	90	94	80	90	67	73	73	76	64	70
Thu	7/3	91	96	88	89	71	84	65	63	63	66	57	63
Fri	7/4	94	97	89	89	85	90	69	70	67	69	65	68
Sat	7/5	77	85	92	92	84	93	55	60	63	67	64	67
Sun	7/6	73	85	88	93	79	96	52	57	61	67	61	72
Mon	7/7	79	86	87	97	90	117	59	59	65	71	76	89
Tue	7/8	81	99	97	99	84	98	60	71	72	75	65	74
2030 (1.0 x ROG, 0.3 x NOx)													
Sun	6/15	83	94	93	88	78	83	62	66	71	74	68	71
Mon	6/16	110	122	103	107	81	103	77	86	83	89	66	78
Tue	6/17	89	101	105	101	88	82	62	70	77	82	74	67
Wed	6/18	67	73	81	85	66	78	52	53	58	61	55	61
Thu	6/19	68	86	71	64	60	69	48	52	54	55	52	57
Fri	6/20	71	83	67	75	58	81	51	55	58	62	56	61
Sat	6/21	54	62	64	66	65	70	42	46	50	53	50	53
Wed	7/2	85	80	77	81	69	79	63	65	64	66	56	62
Thu	7/3	81	83	77	77	61	72	60	55	55	58	49	54
Fri	7/4	92	85	77	77	73	77	65	62	59	61	56	59
Sat	7/5	68	73	80	79	72	80	50	53	55	58	55	58
Sun	7/6	64	73	77	81	68	85	47	50	54	59	53	64
Mon	7/7	70	74	75	84	78	108	54	52	57	63	68	82
Tue	7/8	75	86	84	85	72	84	56	62	62	65	56	64
1.0xROG, 1.0 NOx													
Mean		83	102	99	103	92	108	61	72	76	80	75	83
Stdev		8	8	9	8	7	9	6	7	7	7	5	6
1.0xROG, 0.75 NOx													
Mean		87	104	100	103	90	104	63	72	76	80	73	79
Stdev		11	13	12	11	8	10	7	10	9	10	7	7
1.0xROG, 0.5 NOx													
Mean		85	97	93	95	82	95	62	67	70	74	67	72
Stdev		13	16	14	13	9	11	9	11	10	11	8	8
1.0xROG, 0.3 NOx													
Mean		77	84	81	82	71	82	56	59	61	65	58	64
Stdev		14	15	12	12	9	11	9	10	10	10	8	9

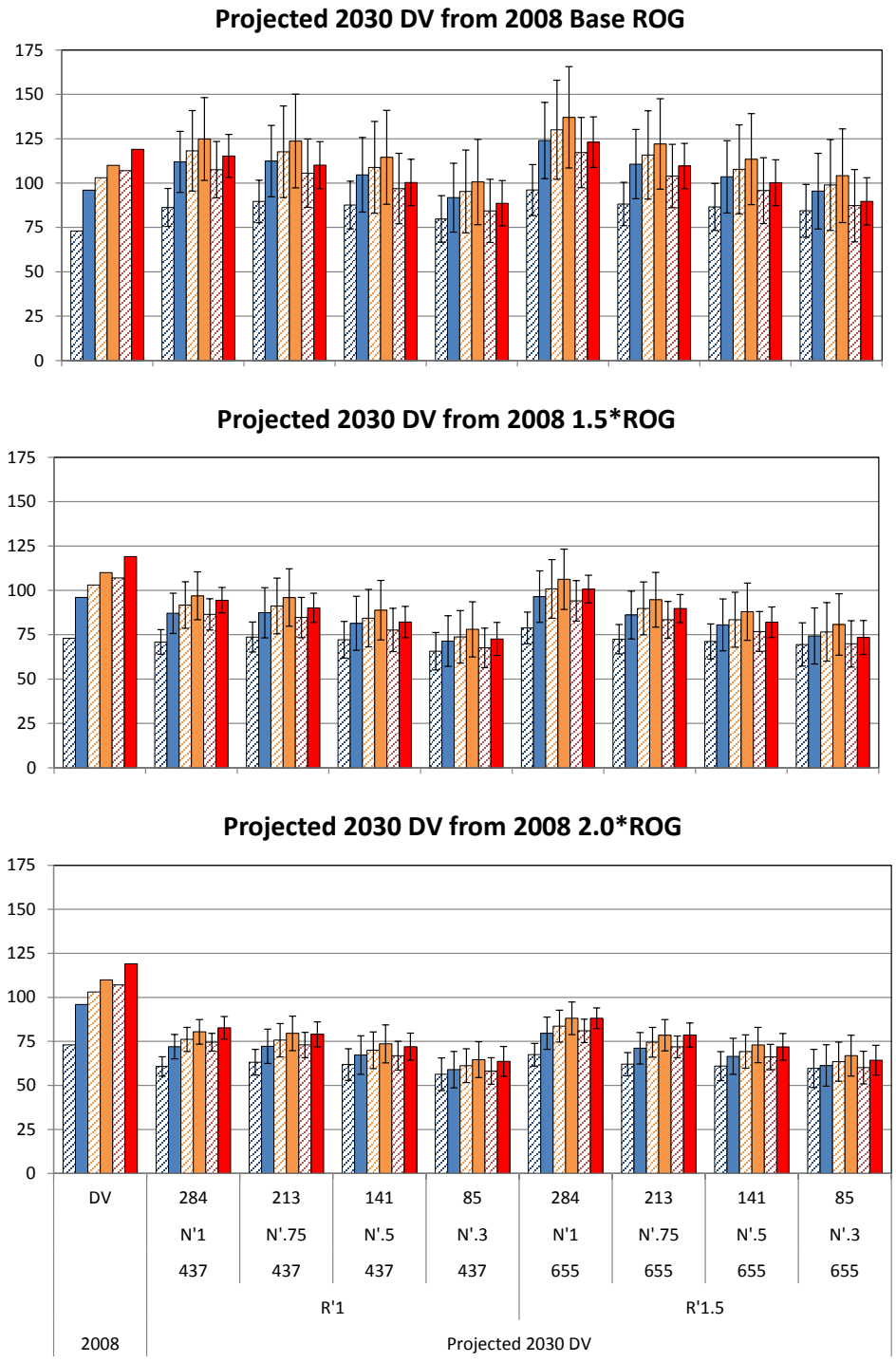

Figure 5-10. 2008 design values and average projected 2030 design values using relative response factors (RRF) referenced to 2008 year with base ROG emissions without adjustments (top), 1.5 x base ROG (center) and 2.0 x base ROG (bottom). R'1 and R'1.5 represent the 2030 baseline ROG emissions without adjustment and increased by a factor of 1.5, respectively. Error bars are standard deviations of the projected design values using the 14 day-specific for the June 15-21 and July 2-8 episodes.

The top graph in Figure 5-10 (no adjustment in 2008 base ROG emissions) shows that the projected all 2030 projected DVs exceed the ozone NAAQS with 2030 baseline ROG emissions (reductions from 2008 of 639 to 477 tpd) and incremental NOx reductions of -61%, -70%, -81% and -88% from 2008 emissions. With the exception of N'1, further ROG reductions have little effect on ozone at lower NOx levels, indicating that ozone formation has become NOx limited. The projected DVs are progressively lower with higher adjustments to the 2008 base ROG emissions. The projected DVs are at or below 75 ppb for NOx reduction of 88% from 2008 with 1.5 x 2008 base ROG and for NOx reductions of -70% from 2008 with 2.0 x 2008 base ROG. As previously noted, the 2008 base year simulations with base ROG emissions increased by a factor of 1.5 produced the best agreement between predicted and observed ozone. While these results are generally consistent with SCAQMD's preliminary assessment that reductions in NOx emissions of about 90% would be necessary for attainment of the 8-hour ozone NAAQS, they show that uncertainties in the base year ROG can greatly affect the projected NOx reductions needed to show attainment.

5.3 References

South Coast Air Quality Management District (2013). Final 2012 Air Quality Management Plan. SCAQMD, Diamond Bar, CA, Feburary 2013.

6. HISTORIC AND FUTURE EVOLUTION OF THE OZONE-PRECURSOR RELATIONSHIP IN THE SOCAB

This section describes the application of the U. S. Environmental Protection Agency's chemical box model OZIPR (Ozone Isopleth Plotting Program, version R, Gery and Crouse, 1990) to simulate the effects of changes in precursor concentrations on the maximum ozone mixing ratios and rates of ozone formation that would be expected given the historic and projected trends in the ambient VOC and NOx mixing ratios in the basin. Unlike the CMAQ model used in the previous chapter, the box model procedure examines changes in ozone photochemistry rather than the combined effects of chemistry and pollutant transport. The modeling results were reconciled with past ambient ozone trends and used to project the effects of future changes in precursor emissions on the ozone-precursor relationship in the SoCAB.

In our prior examinations of the ozone-precursor relationship in the SoCAB (Fujita et al., 2003; Fujita et al, 2013), day-of-week specific initial precursor concentrations were derived from measurements and projected to 2020 based on expected emission reductions from 2005 (-10% VOC and -50% NOx). The results predicted a period of NOx disbenefit for the SoCAB between 2010 and 2020 with planned emission reductions of 50 percent for NOx and 10 percent for VOC. Ozone formation was predicted to become precursor limited by 2020 with greater NOx reductions of 75 percent, but with higher initial ozone formation rates than in 2005 (Figure 2-14). Peak ozone formation rates in 2020 would increase on weekdays by a factor of three relative to 2005 and would be comparable to ozone rates on weekdays in 1995 and Sundays in 2005 (Fujita et al., 2013). While these future changes will likely result in lower ozone levels in downwind areas where transport is more important than local production of ozone, the location of peak ozone levels was predicted to shift westward toward the central basin.

6.1 Approach and Methods

The prior box model simulations were updated in the current study using the latest available Photochemical Assessment Monitoring Station (PAMS) VOC data from the SoCAB to create a representative contemporary mix of VOCs. The PAMS organic compound mixing ratios for the stations: Azusa, Banning-Hathaway, Burbank-West Palm, Los Angeles-West, Pico Rivera and Upland-San Brewer were averaged and assigned to species groupings used in the Regional Atmospheric Chemistry Mechanism, version 2 (RACM2) (Goliff et al., 2013; Sarwar et al., 1993). The organic compounds were allocated according to the assignments for alkanes, alkenes, alkynes and carbonyls in Table 6-1 and for aromatic hydrocarbons in Table 6-2 and used the percentage composition for the RACM2 species from the VOC profile given in Table 6-3. Updated ozone isopleth plots were derived from a matrix of 2000 simulations with varying initial NOx and VOC mixing ratios shown in Table 6-5 for the years 1995-2011. The VOC and NOx mixing ratios for 2008 (or the closest available year) were multiplied by the emission reduction factors given in Table 5-1 to project the VOC and NOx concentrations in 2030. The initial and boundary conditions and other run conditions (e.g., mixing height, temperature, photolysis rate constants) (Table 6-4) were held constant from run to run with the exception of the initial VOC and NOx mixing ratios and the scaled emissions based on these initial conditions.

Table 6-1. Assignments of alkanes, alkenes, alkynes and carbonyls to RACM2 species.

RACM2 Species	Organic Compound	RACM2 Species	Organic Compound
Alkanes		HC8	2,2,4-Trimethylpentane
ETH	Ethane		2,3,4-Trimethylpentane
HC3	Isobutane		N-Octane
	Propane		N-Nonane
	N-Butane		N-Decane
	N-Pentane		N-Undecane
HC5	2-Methylpentane	Alkenes	
	2-Methylhexane	ETE	Ethylene
	2-Methylheptane	OLT	1-Butene
	3-Methylpentane	ISO	Isoprene
	3-Methylhexane	OLI	1-Pentene
	3-Methylheptane		Propylene
	2,2-Dimethylbutane		Cis-2-Butene
	2,3-Dimethylbutane		Cis-2-Pentene
	2,3-Dimethylpentane		Trans-2-Butene
	2,4-Dimethylpentane		Trans-2-Pentene
	Cyclohexane	ACE	Acetylene
	Cyclopentane		
	Isopentane	Carbonyls	
	Methylcyclopentane	HCHO	Formaldehyde
	N-Heptane	ACD	Acetaldehyde
	N-Hexane	ACT	Acetone

Table 6-2. Assignments of aromatics to RACM2 species.

RACM2 Species	Organic Compound	RACM2 Species	Organic Compound
Aromatics		XYM	M/P Xylene 50%
BEN	Benzene		M-Ethyltoluene
TOL	Toluene		M-Diethylbenzene
	Ethylbenzene		1,2,3-Trimethylbenzene 50%
	Isopropylbenzene	XYP	M/P Xylene 50%
	Styrene		P-Ethyltoluene
	N-Propylbenzene		P-Diethylbenzene
XYO	O-Xylene		1,2,4-Trimethylbenzene 50%
	O-Ethyltoluene		
	1,2,4-Trimethylbenzene 50%		
	1,2,3-Trimethylbenzene 50%		
	1,3,5-Trimethylbenzene		

Table 6-3. VOC species profile used for isopleths simulations. The average values were used for the simulations.

RACM2 Species	Average ppbC		Average ppbC
Alkanes		Alkynes	
ETH:	15.0±7.0	ACE:	3.2±1.2
HC3:	36.7±23.6		
HC5:	34.1±14.9	Aromatics	
HC8:	7.6±4.3	BEN:	2.2±1.0
		TOL:	15.7±18.8
Alkenes		XYM:	3.4±2.3
ETE:	4.6±1.6	XYP:	3.5±2.9
OLT:	2.4±1.1	XYO:	3.7±2.9
OLI:	0.7±0.3		
ISO:	0.9±0.7	Aldehydes	
		HCHO:	6.7±4.6
		ACD:	9.5±9.8

Table 6-4. Initial conditions used for a simulation of a polluted urban atmosphere.

Initial Condition	**Value**
Start-Time	6:00
Duration	18 hr
Temperature	298. K
Pressure	1013.25 mbar
Date for photolysis calculation	June 21
Ozone (initial)	30. ppbv
NO / NOx (initial)	0.95
H_2	550.

Table 6-5. Yearly VOC and NOx averages weekday and weekend with projections for VOC and NOx in 2030.

Weekday	Azusa		Ls_Ang-NMain		Pico Rivera		Rvrside-Rubi		Upland-SanBr	
Year	VOC	NOx	VOC	NOx	VOC	NOx	VOC	NOx	VOC	NOx
1995	663.9	67.5	582.7	116.5	N/A	N/A	N/A	N/A	406.1	68.8
1996	511.3	60.7	469.4	137.8	N/A	N/A	N/A	N/A	N/A	N/A
1997	399.8	48.5	416.2	116.8	422.8	97.9	N/A	N/A	298.3	53.9
1998	287.1	53.0	389.5	114.7	316.6	107.5	N/A	N/A	347.2	56.3
1999	393.2	66.2	365.3	125.5	307.1	125.5	N/A	N/A	371.2	64.0
2000	272.7	61.1	450.3	172.3	502.7	105.5	N/A	N/A	257.6	60.9
2001	379.0	55.6	379.2	161.7	364.7	97.6	N/A	N/A	356.4	58.9
2002	419.8	54.1	N/A	N/A	285.5	97.6	N/A	N/A	368.5	55.4
2003	326.8	50.4	N/A	N/A	294.4	92.6	N/A	N/A	346.9	57.5
2004	307.7	36.8	N/A	N/A	249.7	82.6	N/A	N/A	299.8	51.5
2005	327.6	43.5	N/A	N/A	N/A	N/A	N/A	N/A	335.2	49.1
2006	425.5	45.5	N/A	N/A	N/A	N/A	N/A	N/A	285.1	44.6
2007	334.5	38.0	N/A	N/A	N/A	N/A	N/A	N/A	226.3	36.0
2008	147.7	34.8	N/A	N/A	N/A	N/A	N/A	N/A	209.1	34.1
2009	244.3	27.9	271.8	38.6	N/A	N/A	142.9	25.0	200.4	24.3
2010	194.3	28.1	194.6	35.1	N/A	N/A	139.8	23.3	N/A	N/A
2011	171.6	31.8	192.0	33.9	N/A	N/A	130.2	26.2	N/A	N/A
2030_VOC_1NOx_1	67.4	13.7	124.0	15.2	113.9	32.4	65.2	9.8	95.4	13.4
2030_VOC_1.5NOx_1	101.0	13.7	185.8	15.2	170.7	32.4	97.7	9.8	143.0	13.4
2030_VOC_1NOx_0.75	67.4	10.2	124.0	11.4	113.9	24.3	65.2	7.4	95.4	10.1
2030_VOC_1.5NOx_0.75	101.0	10.2	185.8	11.4	170.7	24.3	97.7	7.4	143.0	10.1
2030_VOC_1NOx_0.5	67.4	6.8	124.0	7.5	113.9	16.1	65.2	4.9	95.4	6.7
2030_VOC_1.5NOx_0.5	101.0	6.8	185.8	7.5	170.7	16.1	97.7	4.9	143.0	6.7
2030_VOC_1NOx_0.3	67.4	4.1	124.0	4.5	113.9	9.7	65.2	2.9	95.4	4.0
2030_VOC_1.5NOx_0.3	101.0	4.1	185.8	4.5	170.7	9.7	97.7	2.9	143.0	4.0

Weekend	Azusa		Ls_Ang-NMain		Pico Rivera		Rvrside-Rubi		Upland-SanBr	
Year	VOC	NOx	VOC	NOx	VOC	NOx	VOC	NOx	VOC	NOx
1995	375.5	53.9	543.3	79.7	N/A	N/A	N/A	N/A	354.1	51.4
1996	410.5	47.2	359.2	86.0	N/A	N/A	N/A	N/A	N/A	N/A
1997	219.4	34.0	285.6	76.5	318.0	69.1	N/A	N/A	236.0	40.3
1998	197.1	36.3	313.6	73.2	283.0	76.4	N/A	N/A	268.8	42.0
1999	294.7	48.0	303.5	82.0	224.8	100.3	N/A	N/A	336.9	50.0
2000	209.8	44.7	343.2	133.0	453.3	86.1	N/A	N/A	237.6	45.7
2001	326.2	36.7	344.5	96.0	338.0	73.6	N/A	N/A	297.4	41.2
2002	301.4	35.1	N/A	N/A	269.5	69.6	N/A	N/A	263.4	39.4
2003	304.9	34.9	N/A	N/A	258.9	72.4	N/A	N/A	309.9	41.3
2004	251.5	22.6	N/A	N/A	229.2	56.2	N/A	N/A	269.9	37.3
2005	244.6	25.6	N/A	N/A	N/A	N/A	N/A	N/A	256.7	32.0
2006	411.8	27.0	N/A	N/A	N/A	N/A	N/A	N/A	240.9	30.0
2007	238.3	19.7	N/A	N/A	N/A	N/A	N/A	N/A	195.7	23.6
2008	143.9	21.1	N/A	N/A	N/A	N/A	N/A	N/A	153.9	23.4
2009	196.4	19.5	195.0	26.5	N/A	N/A	136.2	18.6	125.5	23.0
2010	147.8	18.6	119.0	26.7	N/A	N/A	121.6	18.0	N/A	N/A
2011	164.6	17.5	160.1	23.4	N/A	N/A	116.8	18.6	N/A	N/A
2030_VOC_1NOx_1	65.7	8.3	88.9	10.4	104.6	22.1	62.1	7.3	70.2	9.2
2030_VOC_1.5NOx_1	98.4	8.3	133.3	10.4	156.7	22.1	93.1	7.3	105.2	9.2
2030_VOC_1NOx_0.75	65.7	6.2	88.9	7.8	104.6	16.6	62.1	5.5	70.2	6.9
2030_VOC_1.5NOx_0.75	98.4	6.2	133.3	7.8	156.7	16.6	93.1	5.5	105.2	6.9
2030_VOC_1NOx_0.5	65.7	4.1	88.9	5.2	104.6	11.0	62.1	3.6	70.2	4.6
2030_VOC_1.5NOx_0.5	98.4	4.1	133.3	5.2	156.7	11.0	93.1	3.6	105.2	4.6
2030_VOC_1NOx_0.3	65.7	2.5	88.9	3.1	104.6	6.6	62.1	2.2	70.2	2.8
2030_VOC_1.5NOx_0.3	98.4	2.5	133.3	3.1	156.7	6.6	93.1	2.2	105.2	2.8

6.2 Results and Discussion

Isopleths for daily average ozone are given in Figure 6-1 for Azusa and Figure 6-2 for Upland-San Bernardino. The average weekday (black diamonds) and weekend (red diamonds) concentrations of VOC and NOx for the years 1995-2011 are shown on the ozone isopleths in comparison to the ridgeline. Projections for 2030 are also plotted as rectangles on the isopleths where the black rectangle represents weekdays and the red rectangle represents weekends. The black and red lines indicate the trend lines for the weekday and weekend VOC and NOx concentrations, respectively. Isopleths are also shown for HNO_3, PAN and H_2O_2 because they are necessary for estimating the ozone production efficiency. Figure 6-3 and Figure 6-4 show show HNO_3 for Azusa and Upland-San Bernardino, respectively, with the same VOC and NOx data and projections used in the ozone isopleth plots. Observed HNO_3 concentrations would not be as high as those presented on the isopleths due to dry deposition and other losses that are not included in the model so the concentrations on the isopleths represent the total HNO_3 production over one day. Figure 6-5 and Figure 6-6 show simulated daily maximum PAN and Figure 6-7 and Figure 6-8 show the daily H_2O_2 production. Similar to HNO3 the concentrations on the H_2O_2 would not be observed due to H_2O_2 dry deposition and other loss processes. Figure 6-9 and Figure 6-10 show VOC/NOx ratios for Azusa and Upland-San Bernardino, respectively, with the weekend and weekday historical VOC and NOx concentrations and their projections for 2030 on the isopleths. Figure 6-11 and Figure 6-12 show the daily average production rate ((maximum O_3 (ppbv) – 30 ppbv)/(time of peak – start of simulation)). Figure 6-13 and Figure 6-14 show the Maximum Ozone/(HNO_3 + PAN + organic nitrate) which is the ozone production efficiency as discussed below.

Figure 6-1 shows that the VOC and NOx concentrations at Azusa were greater on weekdays than on weekends. The isopleths show that ozone concentrations were greater on weekdays than weekends during 1995. Both weekday and weekend VOC and NOx concentrations followed similar trends resulting in the same or higher ozone concentrations on weekdays and weekends. The 2030 projected VOC and NOx concentrations approach the ridgeline and ridgeline may be crossed at Azusa around that time. The isopleth for Upland-San Bernardino (Figure 6-2) shows different behavior. There was little difference in ozone levels in 1995 between weekday and weekend. In 1995 the concentrations of VOC and NOx were greater on weekdays than on weekends but their downward trends of VOC and NOx have crossed, though within the range of the 2030 projected VOC and NOx. Differences between weekend and weekday emissions show the effects of NOx emission reductions on ozone concentrations. An increase in ozone during weekends indicates that an ozone disbenefit is likely to result from modest NOx reductions. However, sufficiently large NOx reductions may result in an ozone benefit following the disbenefit. Figure 5-1 shows the trajectory of the ozone concentrations at Azusa and in general reductions should occur but ozone at Upland-San Bernardino is little changed until after.

The HNO_3 trends for Azusa (Figure 6-3) and Upland-San Bernardino (Figure 6-4) show a strong decrease in the production of HNO3 from a high of 55 ppbv in 1995 to a low near 5 ppbv in 2030. For both locations the VOC and NOx trend lines are somewhat vertical with respect to the HNO_3 contour lines indicating that there should be a strong difference in HNO_3 production between weekdays and weekends with HNO_3 higher on the weekdays. Changes in PAN concentrations are more similar to the ozone changes.

Figure 6-5 shows that the weekday simulated PAN for Azusa is high at 9 or 10 ppbV during 1995. The simulations indicate that it should drop to near 1 ppbv and that by 2030 it will fall to very low concentrations. For Upland-San Bernardino, Figure 6-6, is similar except that in 1995 the predicted maximum PAN concentration is about half (5 ppbv) the concentration for Azusa.

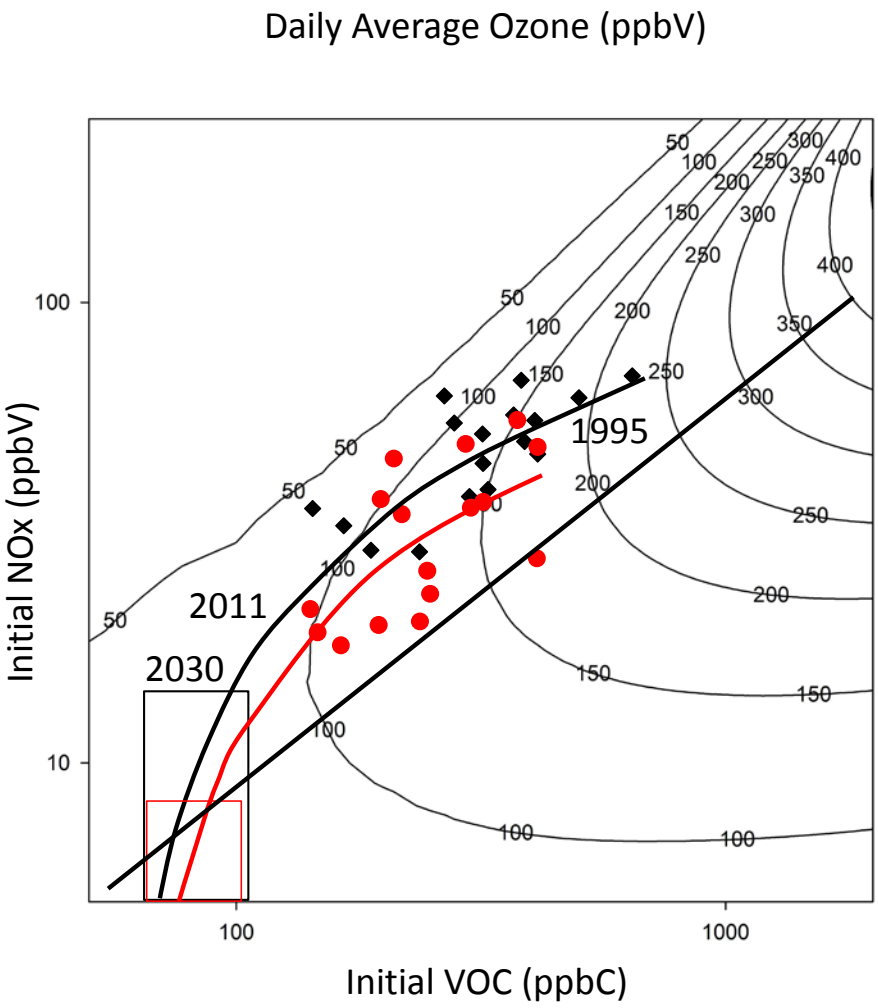

Figure 6-1. Isopleths for daily average ozone for Azusa. Plotted on the ozone isopleths are average values of VOC and NOx for the years 1995-2011. The black diamonds are weekday averages and the red circles are weekends. Projections for 2030 are plotted as rectangles on the isopleths were the black rectangle represents weekdays and the red rectangle represents weekends. The trend lines for the VOC and NOx weekday (black line) and weekend (red line) concentrations are plotted.

H_2O_2 is more of an indicator species than a pollutant of health concern and it is difficult to measure, so there are few long-term measurements. The VOC and NOx trends in H_2O_2 are

somewhat more complex. Figure 6-7 shows that its daily production was 8 ppbv in 1995 for Azusa. The VOC NOx trend lines suggest that the H_2O_2 concentration soon dropped to 2 ppbv on weekdays and 4 on weekends; this is consistent with lower NOx on the weekends. The weekday trend line is roughly parallel to 2 ppbv the H_2O_2 contour line during the years before 2011 and the H_2O_2 production may increase to 4 ppbv by 2030. The weekend trend follows the weekday trend line and the H_2O_2 contour line but the weekend H_2O_2 concentration is about 1 ppbv greater. Figure 6-8 shows that for Upland-San Bernardino the weekend H_2O_2 production was 4 ppbv and the weekday production was 2 ppbv. Both trend lines a roughly parallel to the H_2O_2 contour line so little change in the H_2O_2 concentration is seen until 2030 where it increases for both weekdays and weekends to 4 to 5 ppbv.

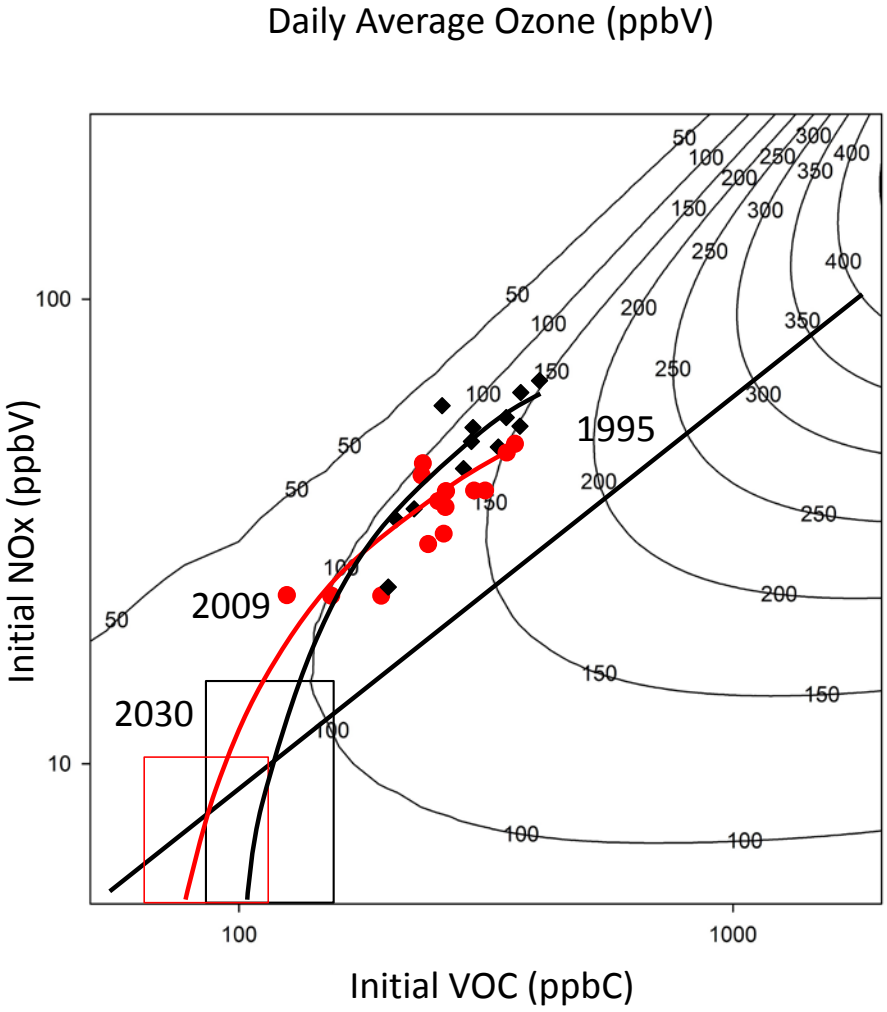

Figure 6-2. Isopleths for daily average ozone for Upland-San Bernardino. Plotted on the ozone isopleths are average values of VOC and NOx for the years 1995-2011. The black diamonds are weekday averages and the red circles are weekends. Projections for 2030 are plotted as rectangles on the isopleths were the black rectangle represents weekdays and the red rectangle represents weekends. The trend lines for the VOC and NOx weekday (black line) and weekend (red line) concentrations are plotted.

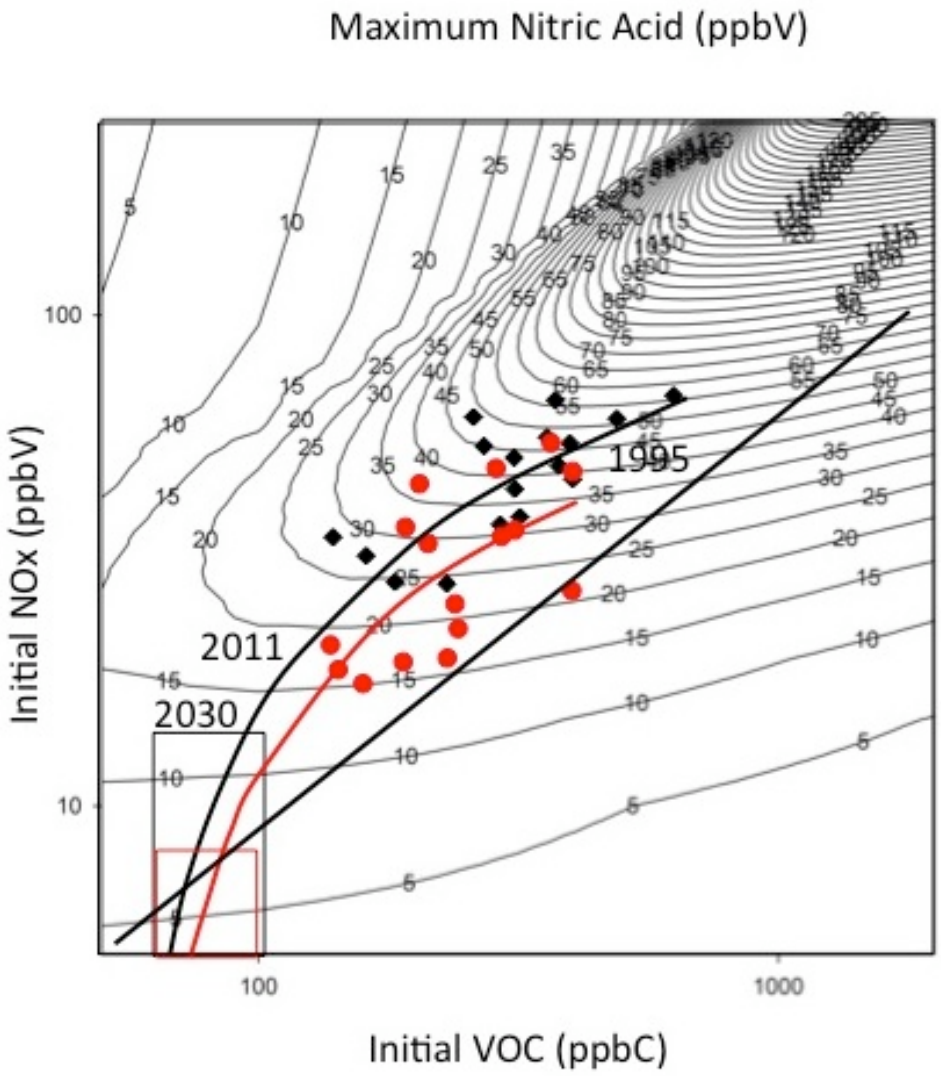

Figure 6-3. Isopleths for daily HNO_3 production for Azusa. Plotted on these isopleths are average values of VOC and NOx for the years 1995-2011. The black diamonds are weekday averages and the red circles are weekends. Projections for 2030 are plotted as rectangles on the isopleths were the black rectangle represents weekdays and the red rectangle represents weekends. The trend lines for the VOC and NOx weekday (black line) and weekend (red line) concentrations are plotted. The ozone ridge-line is plotted for reference to the ozone isopleth.

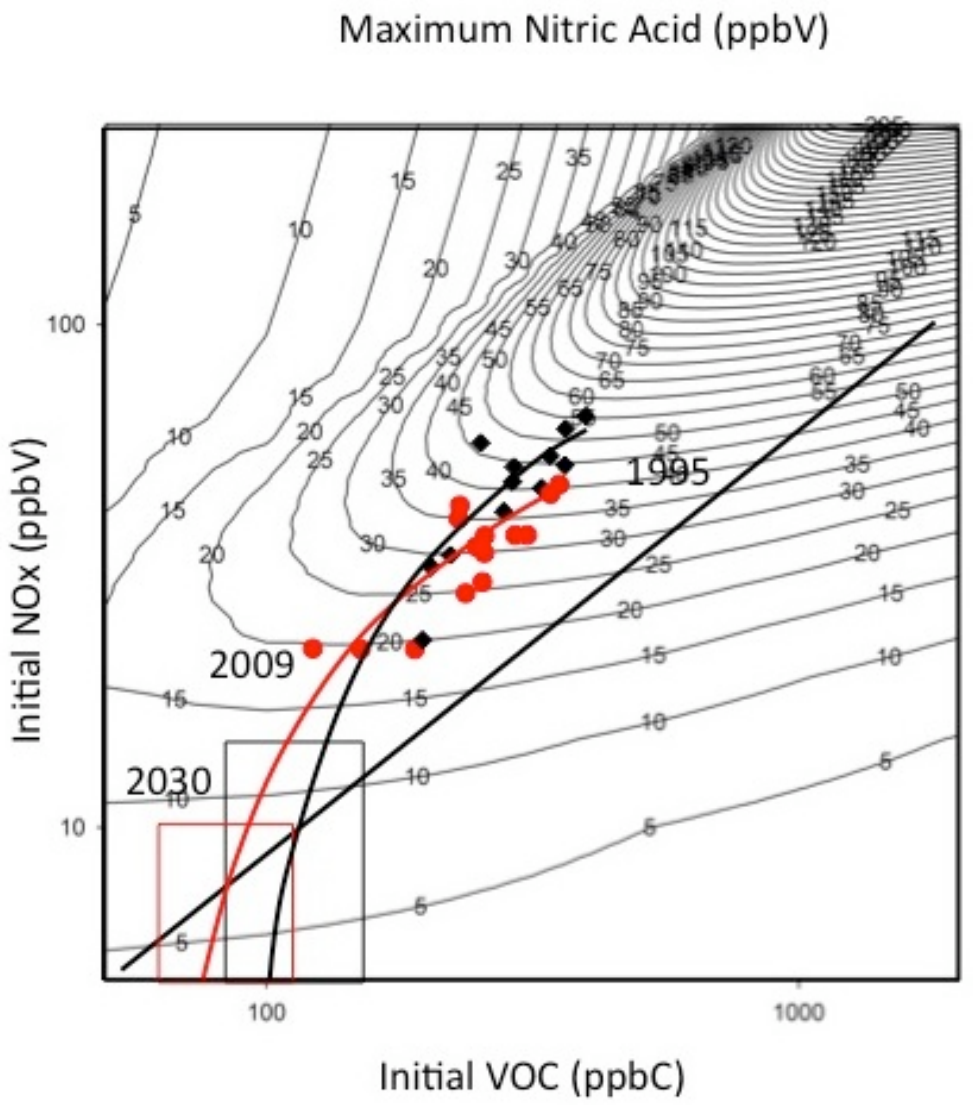

Figure 6-4. Isopleths for daily HNO_3 production for Upland-San Bernardino. Plotted on the ozone isopleths are average values of VOC and NOx for the years 1995-2011. The black diamonds are weekday averages and the red circles are weekends. Projections for 2030 are plotted as rectangles on the isopleths were the black rectangle represents weekdays and the red rectangle represents weekends. The trend lines for the VOC and NOx weekday (black line) and weekend (red line) concentrations are plotted. The ozone ridge line is plotted for reference to the ozone isopleth.

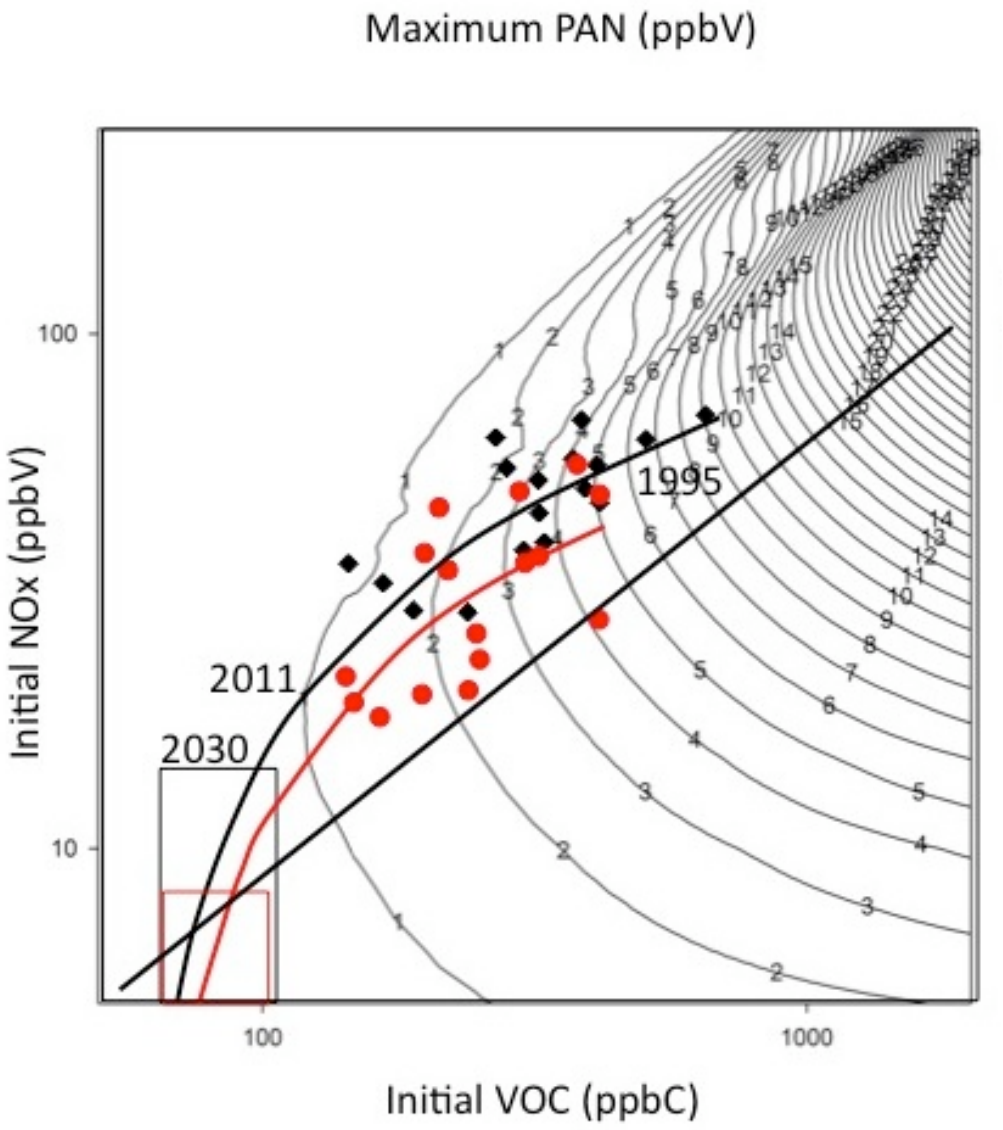

Figure 6-5. Isopleths for daily maximum PAN for Azusa. Plotted on these isopleths are average values of VOC and NOx for the years 1995-2011. The black diamonds are weekday averages and the red circles are weekends. Projections for 2030 are plotted as rectangles on the isopleths were the black rectangle represents weekdays and the red rectangle represents weekends. The trend lines for the VOC and NOx weekday (black line) and weekend (red line) concentrations are plotted. The ozone ridge-line is plotted for reference to the ozone isopleth.

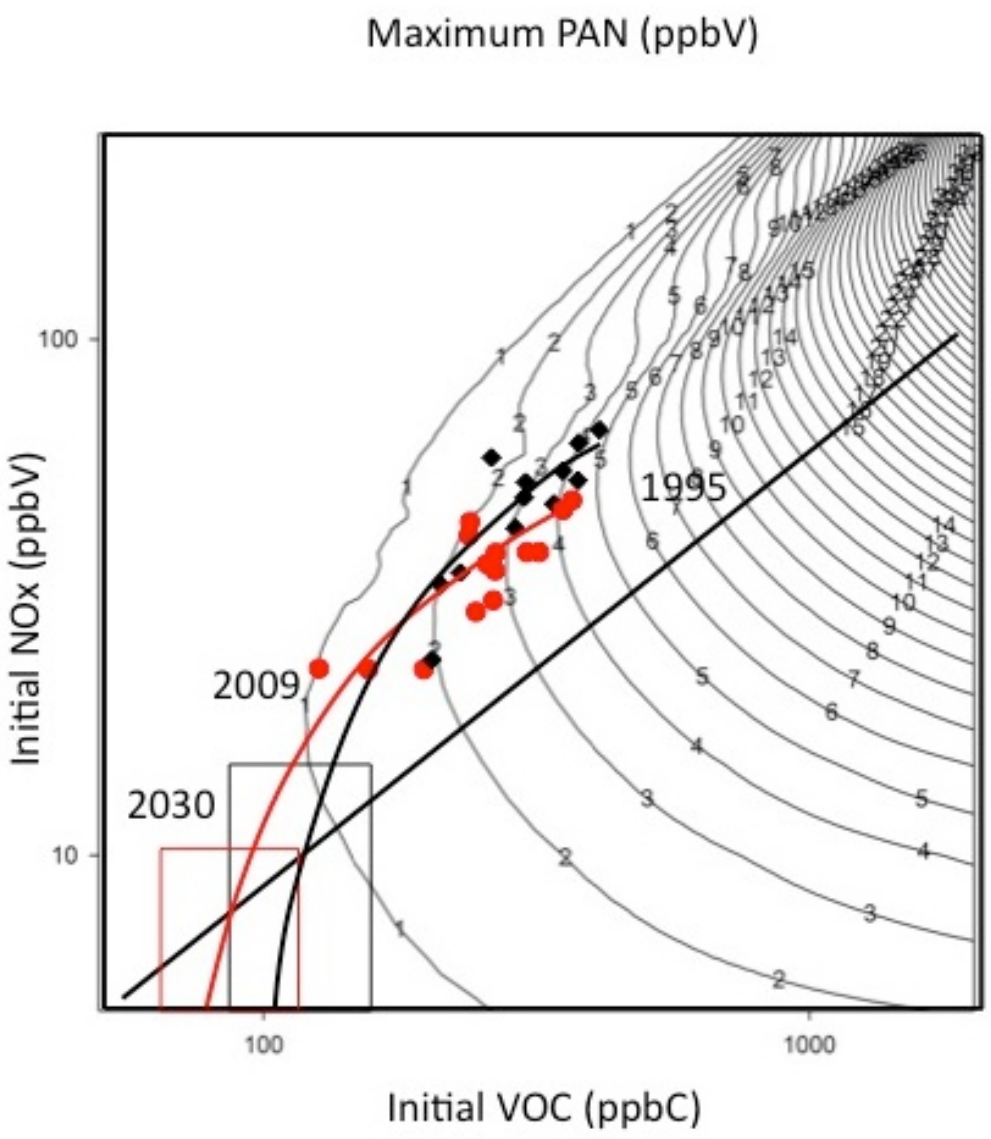

Figure 6-6. Isopleths for daily maximum PAN for Upland-San Bernardino. Plotted on the ozone isopleths are average values of VOC and NOx for the years 1995-2011. The black diamonds are weekday averages and the red circles are weekends. Projections for 2030 are plotted as rectangles on the isopleths were the black rectangle represents weekdays and the red rectangle represents weekends. The trend lines for the VOC and NOx weekday (black line) and weekend (red line) concentrations are plotted. The ozone ridge line is plotted for reference to the ozone isopleth.

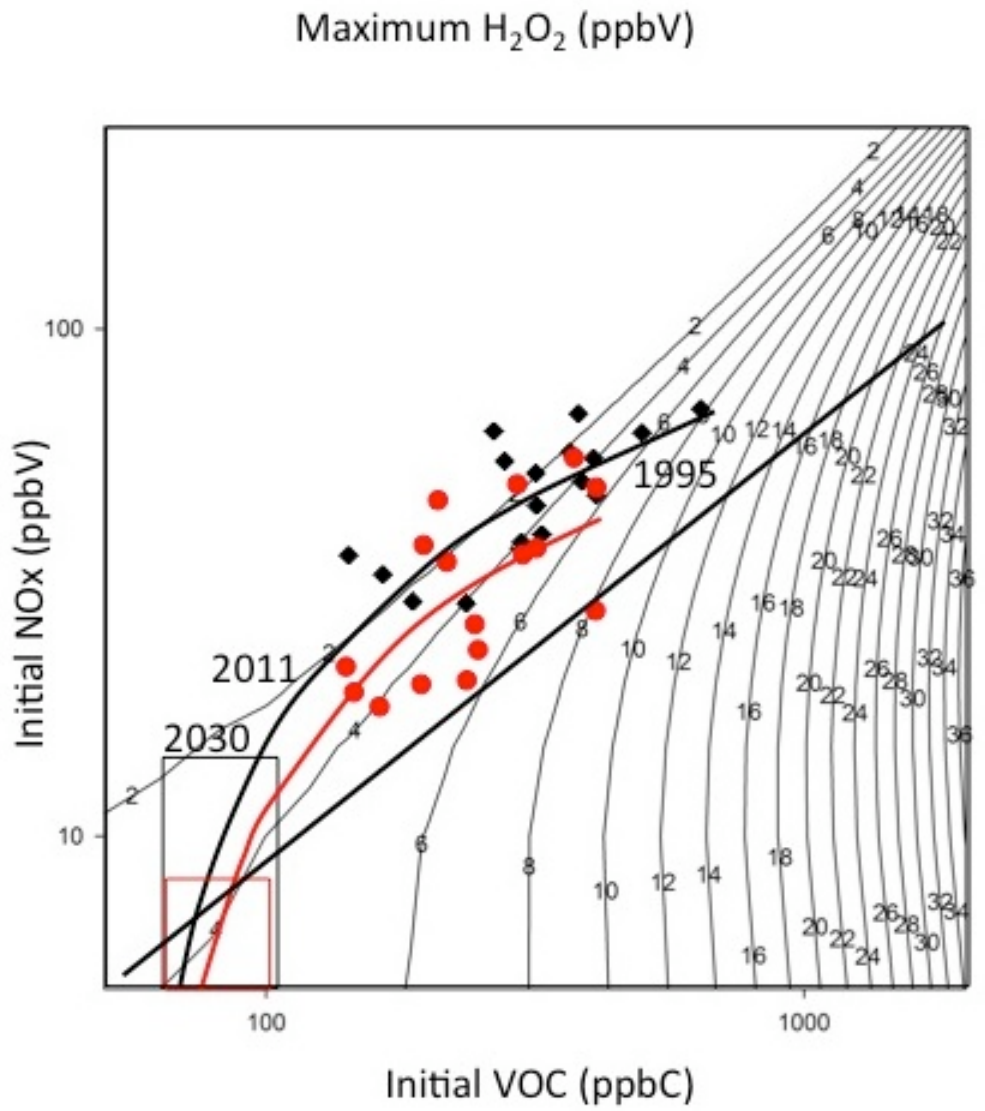

Figure 6-7. Isopleths for daily H_2O_2 production for Azusa. Plotted on these isopleths are average values of VOC and NOx for the years 1995-2011. The black diamonds are weekday averages and the red circles are weekends. Projections for 2030 are plotted as rectangles on the isopleths were the black rectangle represents weekdays and the red rectangle represents weekends. The trend lines for the VOC and NOx weekday (black line) and weekend (red line) concentrations are plotted. The ozone ridge-line is plotted for reference to the ozone isopleth.

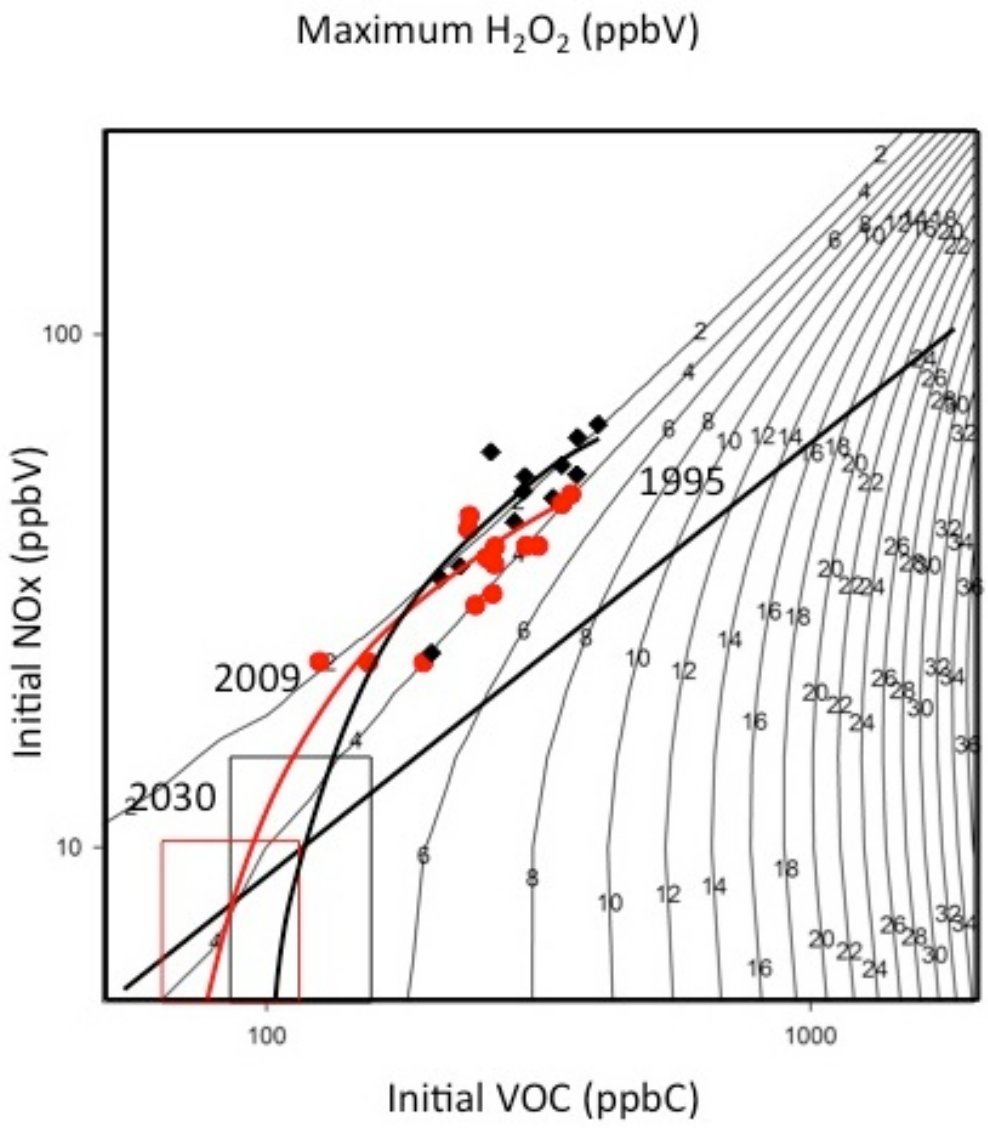

Figure 6-8. Isopleths for daily H_2O_2 production for Upland-San Bernardino. Plotted on the ozone isopleths are average values of VOC and NOx for the years 1995-2011. The black diamonds are weekday averages and the red circles are weekends. Projections for 2030 are plotted as rectangles on the isopleths were the black rectangle represents weekdays and the red rectangle represents weekends. The trend lines for the VOC and NOx weekday (black line) and weekend (red line) concentrations are plotted. The ozone ridge line is plotted for reference to the ozone isopleth.

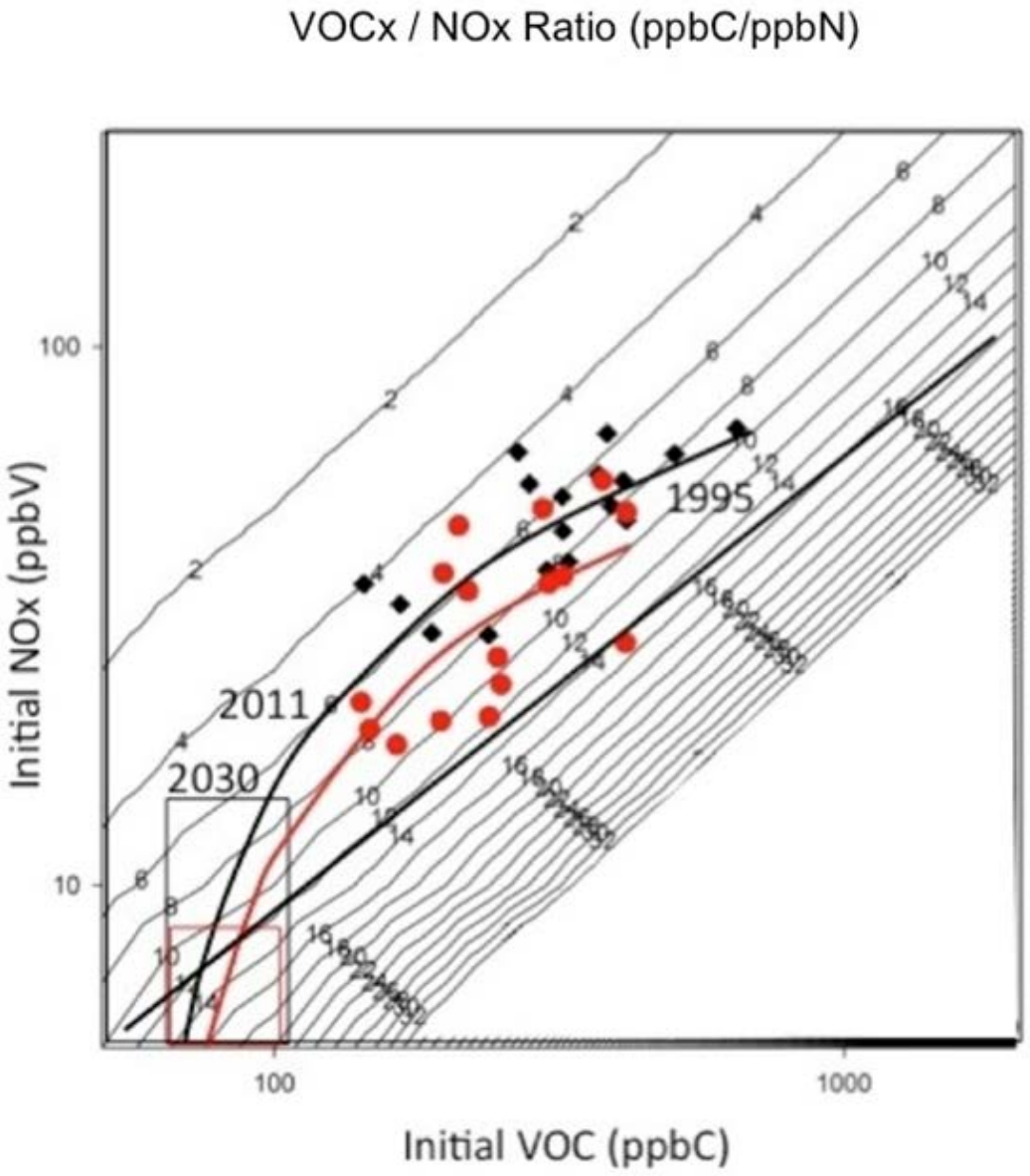

Figure 6-9. Isopleths for VOC/NOx Ratios (ppbC/ppbN) for Azusa. Plotted on these isopleths are average values of VOC and NOx for the years 1995-2011. The black diamonds are weekday averages and the red circles are weekends. Projections for 2030 are plotted as rectangles on the isopleths were the black rectangle represents weekdays and the red rectangle represents weekends. The trend lines for the VOC and NOx weekday (black line) and weekend (red line) concentrations are plotted. The ozone ridge-line is plotted for reference to the ozone isopleth.

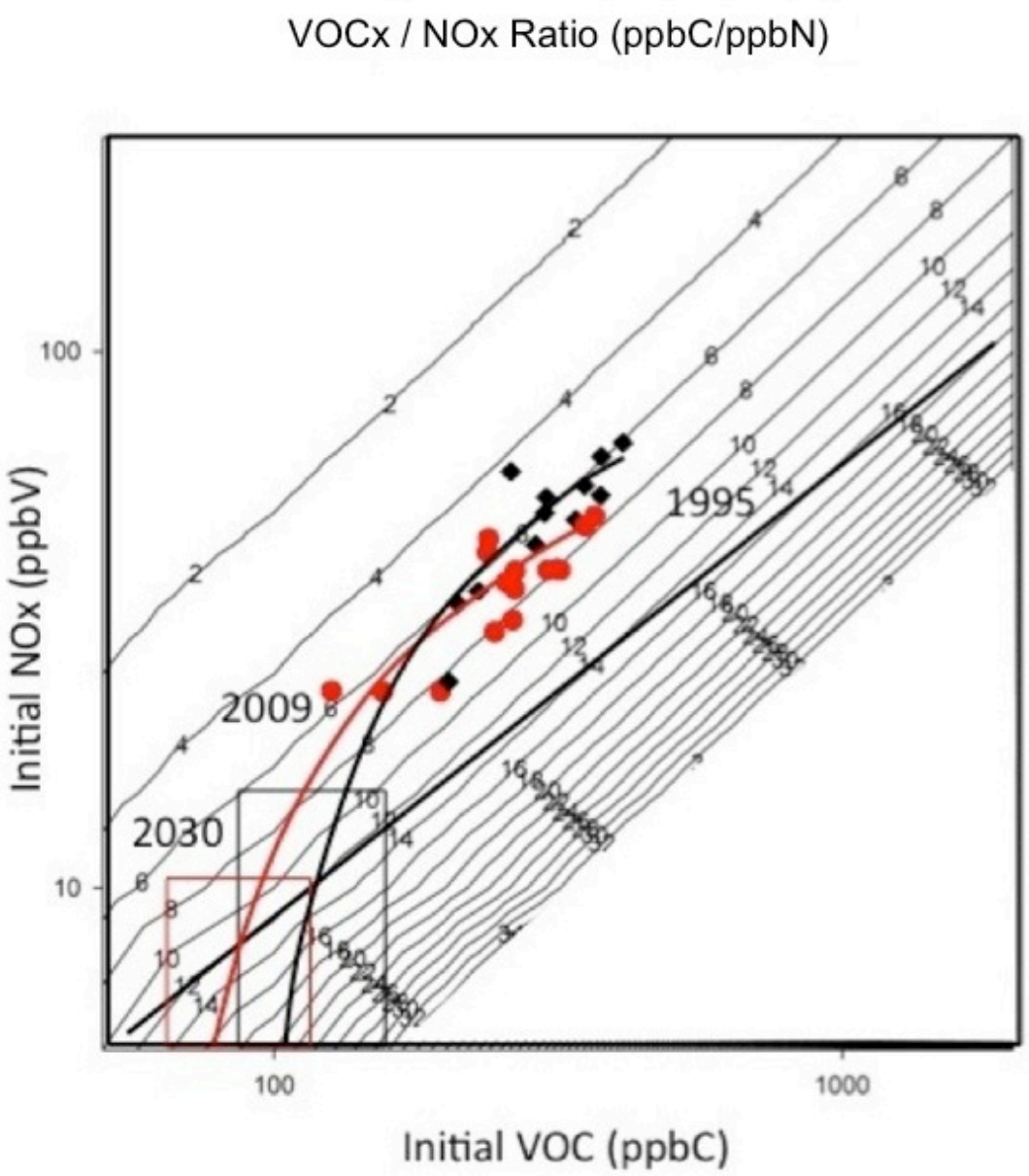

Figure 6-10. Isopleths for VOC/NOx Ratios (ppbC/ppbN) for Upland-San Bernardino. Plotted on the ozone isopleths are average values of VOC and NOx for the years 1995-2011. The black diamonds are weekday averages and the red circles are weekends. Projections for 2030 are plotted as rectangles on the isopleths were the black rectangle represents weekdays and the red rectangle represents weekends. The trend lines for the VOC and NOx weekday (black line) and weekend (red line) concentrations are plotted. The ozone ridge line is plotted for reference to the ozone isopleth.

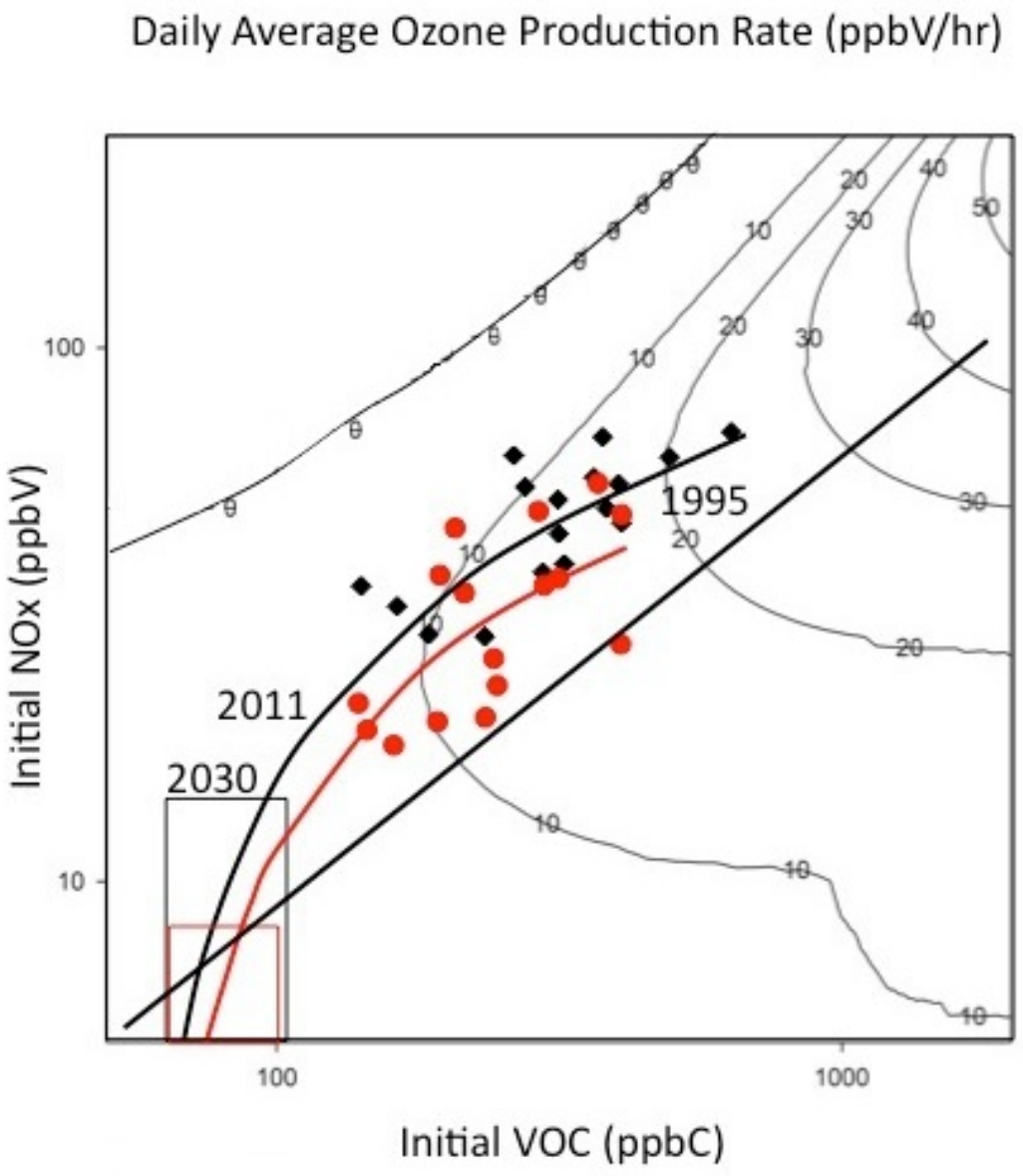

Figure 6-11. Isopleths for ozone production rates (ppbv / hr) for Azusa. Plotted on these isopleths are average values of VOC and NOx for the years 1995-2011. The black diamonds are weekday averages and the red circles are weekends. Projections for 2030 are plotted as rectangles on the isopleths were the black rectangle represents weekdays and the red rectangle represents weekends. The trend lines for the VOC and NOx weekday (black line) and weekend (red line) concentrations are plotted. The ozone ridge-line is plotted for reference to the ozone isopleth.

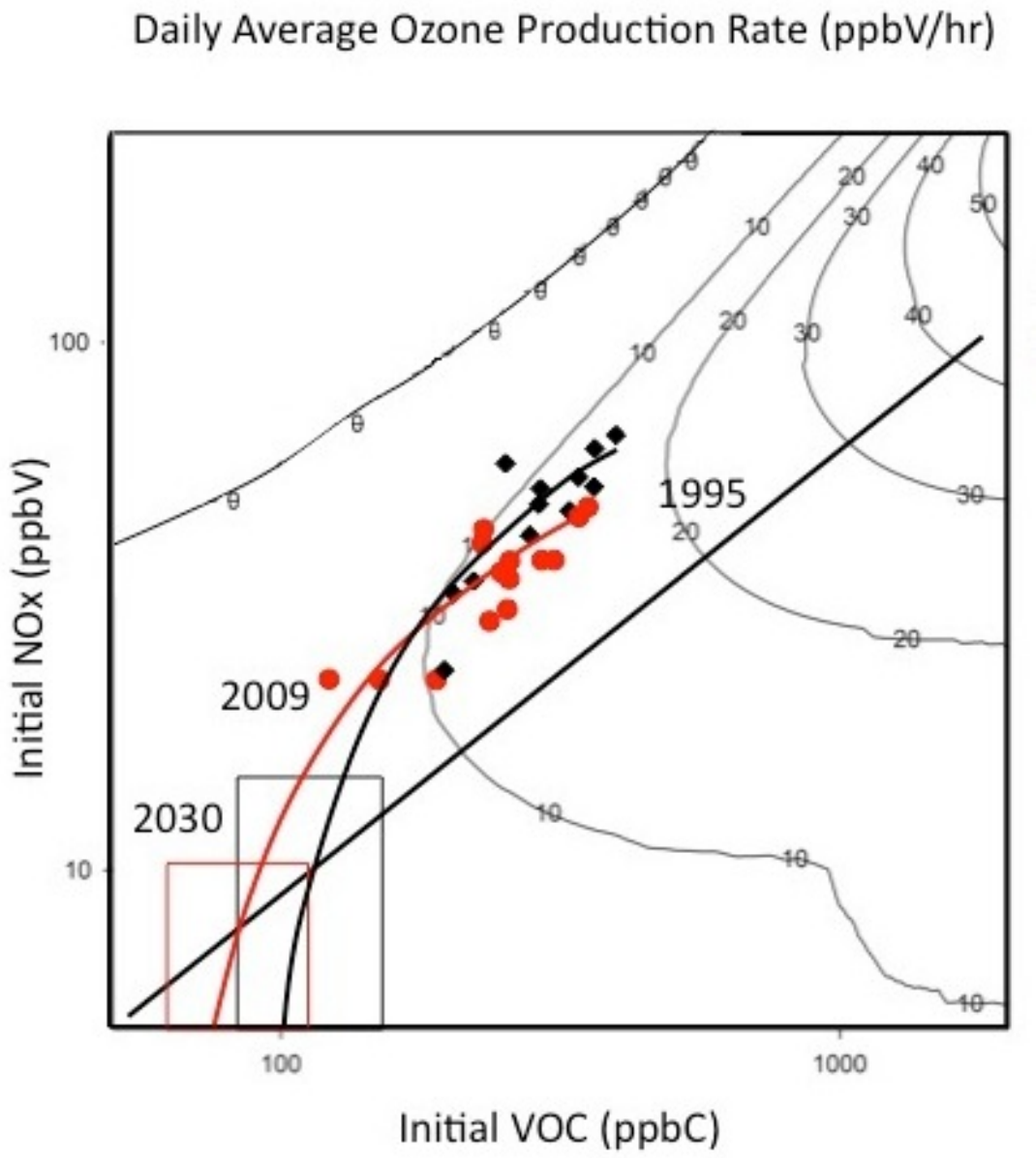

Figure 6-12. Isopleths for ozone production rates (ppbv / hr) for Upland-San Bernardino. Plotted on the ozone isopleths are average values of VOC and NOx for the years 1995-2011. The black diamonds are weekday averages and the red circles are weekends. Projections for 2030 are plotted as rectangles on the isopleths were the black rectangle represents weekdays and the red rectangle represents weekends. The trend lines for the VOC and NOx weekday (black line) and weekend (red line) concentrations are plotted. The ozone ridge line is plotted for reference to the ozone isopleth.

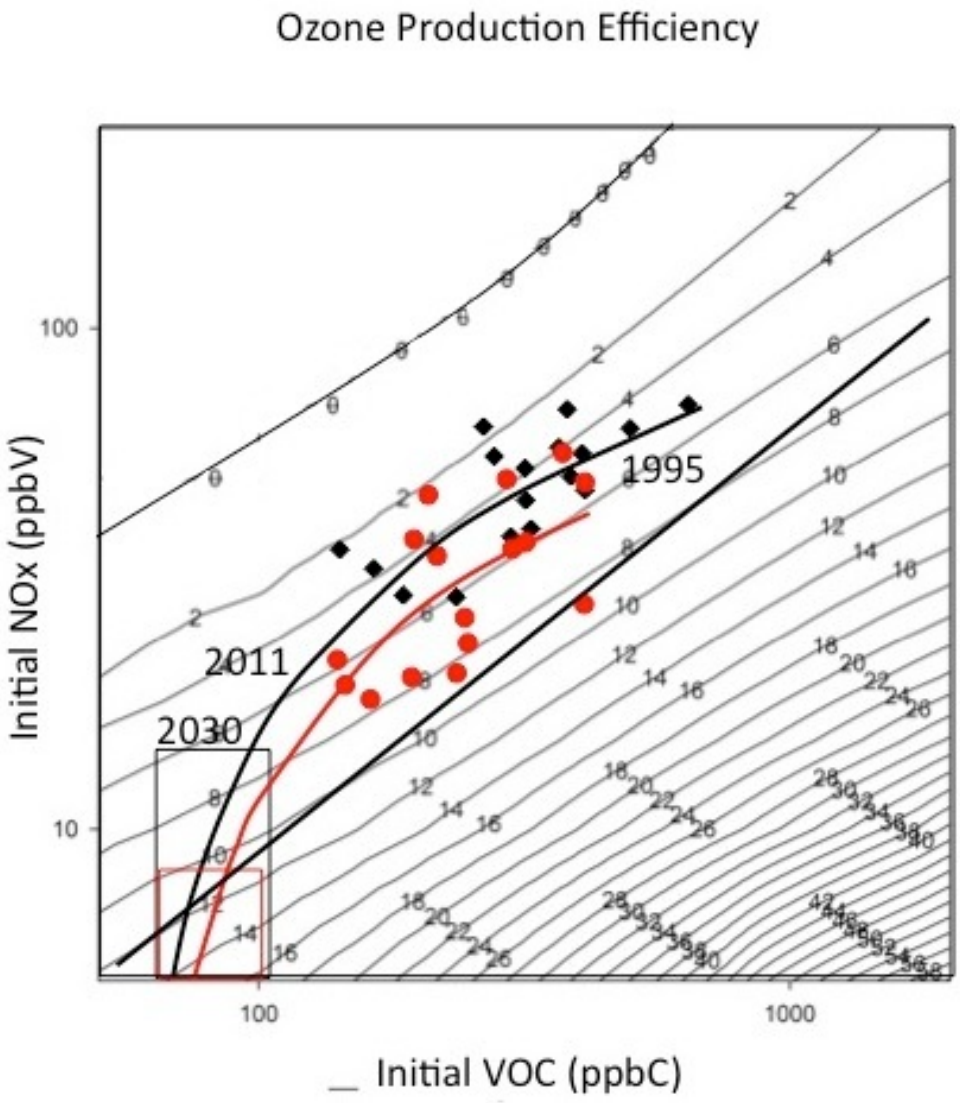

Figure 6-13. Isopleths for the efficiency of ozone production for Azusa. Plotted on these isopleths are average values of VOC and NOx for the years 1995-2011. The black diamonds are weekday averages and the red circles are weekends. Projections for 2030 are plotted as rectangles on the isopleths were the black rectangle represents weekdays and the red rectangle represents weekends. The trend lines for the VOC and NOx weekday (black line) and weekend (red line) concentrations are plotted. The ozone ridge-line is plotted for reference to the ozone isopleth.

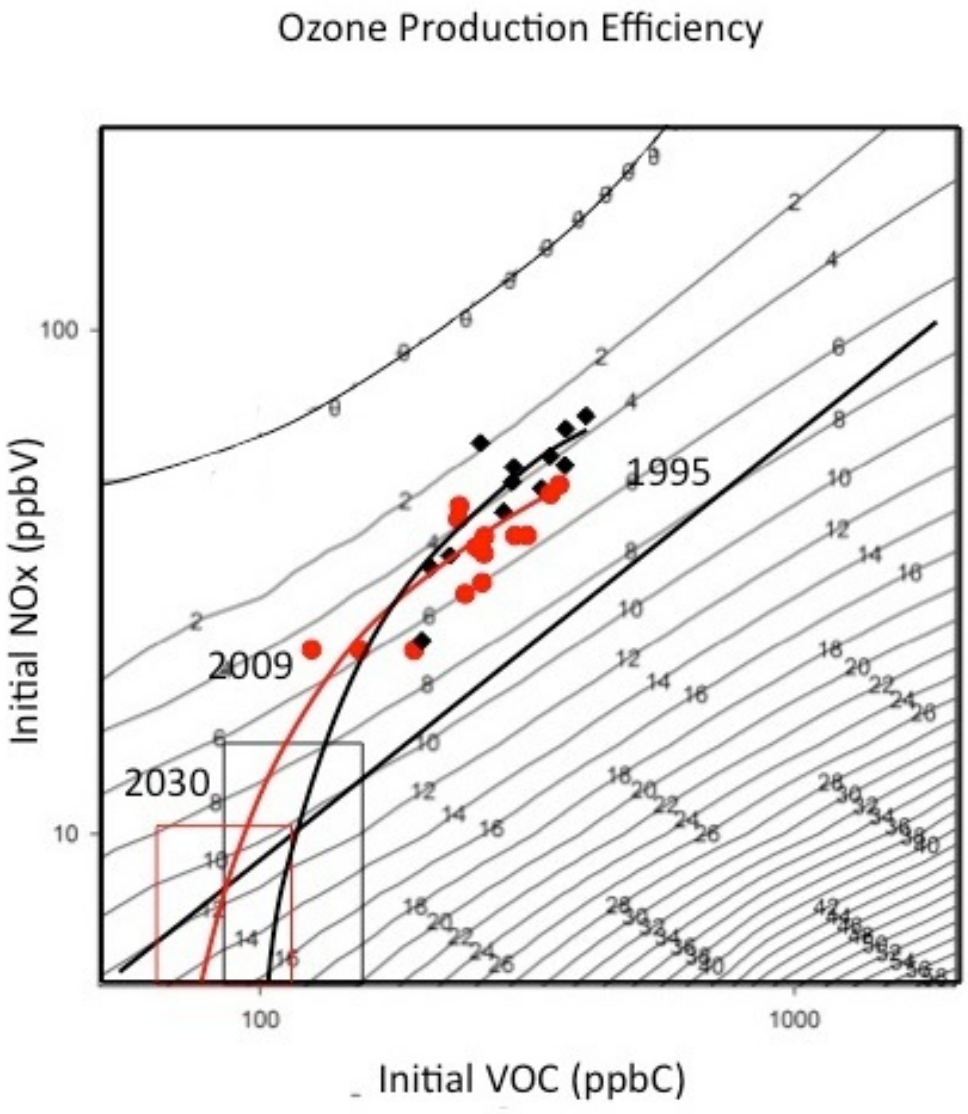

Figure 6-14. Isopleths for the efficiency of ozone production for Upland-San Bernardino. Plotted on the ozone isopleths are average values of VOC and NOx for the years 1995-2011. The black diamonds are weekday averages and the red circles are weekends. Projections for 2030 are plotted as rectangles on the isopleths were the black rectangle represents weekdays and the red rectangle represents weekends. The trend lines for the VOC and NOx weekday (black line) and weekend (red line) concentrations are plotted. The ozone ridge line is plotted for reference to the ozone isopleth.

6.2.1 Ozone Production Efficiency and Production Rates

NOx can be considered as the catalyst for the production of ozone from VOC. The oxidation of VOC produces peroxy radicals (HO_2 and organic peroxy radicals RO_2) that convert NO to NO_2. Ozone is produced by the subsequent photolysis of NO_2 that reproduces NO.

$HO + VOC \rightarrow \ldots HO_2$ and RO_2

$HO_2 + NO \rightarrow NO_2 + HO$ Propagation
$RO_2 + NO \rightarrow NO_2 +$ Organic Products $+ HO_2$ Propagation
$NO_2 + h\nu\ (+ O_2) \rightarrow NO + O_3$

The reactions of HO_2 and RO_2 with NO are chain reactions propagate the chemical reactions. The free radical chains are terminated through a number of reactions. NOx is lost when the radical chains are terminated by the reactions of NOx to form nitric acid, organic nitrates and PAN.

$HO + NO_2 \rightarrow HNO_3$
$RO_2 + NO \rightarrow RNO_3$
$RCO_3 + NO_2 \rightarrow PAN$

At lower NOx concentrations the radical chains may be terminated through the reactions of HO_2 and organic peroxy radicals (RO_2) to form peroxides and other stable compounds.

$HO_2 + HO_2 \rightarrow H_2O_2$
$HO_2 + RO_2 \rightarrow HO_2R$
$RO_2 + RO_2 \rightarrow RO_2R$ + CARB + Alcohols

Note that NOx is both the catalyst for the production of ozone and it is a major source of termination of the peroxy radicals that convert NO to NO_2 that photolyzes to produce more ozone. If the concentration of NOx is too high or too low relative to VOC then ozone formation is inhibited. This relationship between VOC and NOx makes the VOC / NOx ratio an important indicator for the potential to form ozone. Furthermore the interplay between termination of the radical chains by NOx reactions and peroxide forming reactions can be seen in the inverse relationship between the concentrations of the HNO_3 and H_2O_2 isopleths (e.g. compare Figure 6-3 and Figure 6-7).

Figure 6-9 and Figure 6-10 show the VOC/NOx ratios and their trends for Azusa and Upland-San Bernardino, respectively. Initially emission controls for VOC decreased the weekday VOC/NOx ratio from 10 to 6 ppbC/ppbN and during that same time period the weekend VOC/NOx ratio varied from 10 to about 7 ppbC/ppbN. New NOx controls are expected to increase the VOC/NOx ratios for both weekdays and weekends; and by 2030 they could return to the value of 1995, 10 ppbC/ppbN and may even reach 14 ppbC/ppbN or more. The rate of ozone production is affected by the concentrations of VOC and NOx. For Azusa, Figure 6-11, the trend from 1995 to the 2030 projected levels show a steady decrease in the ozone production rate for both weekends and weekdays. For Upland-San Bernardino, Figure 6-12, the relative decrease in the ozone production rate between 1995 and 2009 is much less than for Azusa. The

ozone production rate continues its decrease up through the projected VOC and NOx concentrations for 2030.

NOx chain-length is a measure of ozone production efficiency. Chain-length is the rate of propagation divided by the rate of termination. An approximation to the NOx chain-length is the ozone production divided by the NOx converted to NOy where NOy is the sum of the HNO3, PAN and organic nitrate. As the atmospheric concentration of NOx decreases the ozone production efficiency should increase due to lower rates of termination. Figure 6-13 and Figure 6-14 show the isopleth for the ozone production efficiency / chain-length with the trends for Azusa and Upland-San Bernardino, respectively. Comparison of these figures with the VOC/NOx ratios, Figure 6-9 and Figure 6-10, shows that the chain-length is highly correlated with the VOC/NOx ratio at all concentration levels. For Azusa the weekday chain-length is lower (a value of 4) than on the weekend (a value of 6) with little change between 1995 and 2030. Projected emission reductions may increase the chain-length to 14 or higher at Azusa by 2030. Figure 6-14 shows that for Upland-San Bernardino there was much less difference in the chain-length between weekdays and weekends, both were near 4 in 1995. Here the chain-length increased to 6 by 2009. The projected emissions lead to a widening of the difference in chain-length by 2030. The weekend chain-length may be a bit higher than 14 on weekends and on weekends it may be 16 at Upland-San Bernardino.

6.2.2 An Alternative View of the Ozone Isopleth

The simulations for the ozone isopleths were used to derive Figure 6-15 and Figure 6-16. These figures consist of line plot showing the response of daily average ozone to changes in the initial VOC with the initial NOx constant. In addition, points were plotted showing average ozone concentrations for average initial VOC and NOx concentrations (Table 6-5) at Azusa and Upland-San Bernardino for the years 1995, 2005 and 2008 (base year). The black diamonds represent weekdays and the red circles represent weekends. The points plotted for 2030 are the ozone concentrations paired with the lowest projected NOx paired with the lowest VOC and the highest projected NOx paired with the highest VOC in Table 6-5; pairs of these points for weekdays and weekends are plotted. The points for 2030 represent the range of ozone concentrations based on the four future scenarios. Figure 6-15 and Figure 6-16 shows that reductions in initial VOC leads to reductions in the daily average ozone concentrations although the reductions are lower for the portions of the curves where the VOC/NOx ratio is high. The points show that for both Azusa and Upland-San Bernardino have followed a relatively low NOx pathway. The response of ozone to VOC is relatively low for initial NOx concentrations less than 30 ppb. The points for the future year 2030 are at the lowest VOC and NOx but very low VOC emissions are required to reduce ozone to acceptable levels for these low levels of NOx. Figure 6-17 and Figure 6-18 show that the response of the daily average ozone to changes in initial NOx have a more complicated appearance. Reductions in initial NOx may lead to increases in the daily average ozone. There is a maximum point in the daily average ozone for each level of initial VOC as the initial NOx is varied. The lower the initial VOC the lower the initial NOx required to reach the ozone maximum point. In other words, as the initial VOC is decreased the lower the level of NOx required to reach the point where reductions in NOx lead to lower daily O_3 concentrations. The points on figure show that at both Azusa and Upland-San Bernardino the reductions in VOC and NOx have not followed an optimum path to lower daily average O_3 concentrations. The figure shows that there has been some dis-benefit in the path followed.

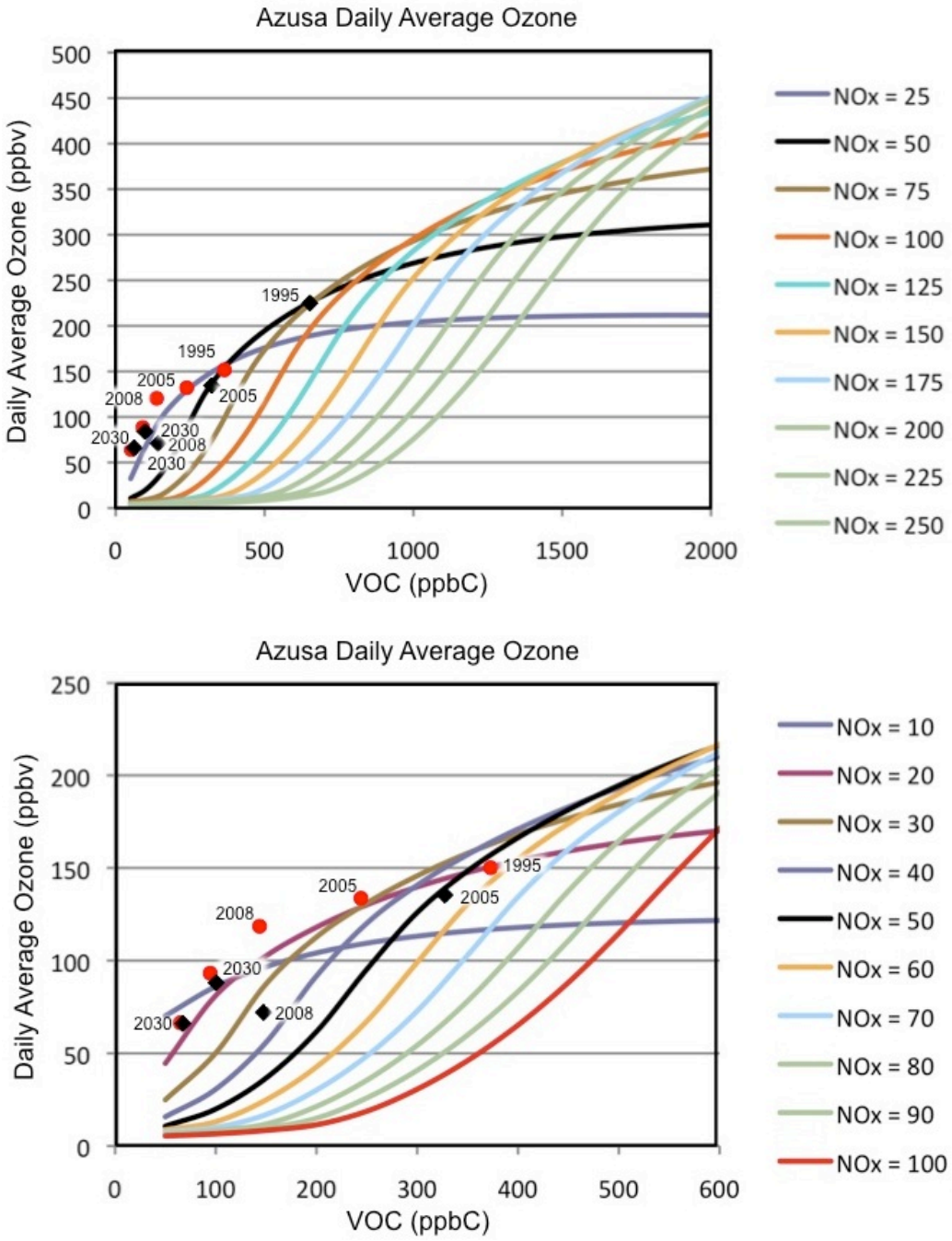

Figure 6-15. The daily average ozone plotted as functions of the initial VOC (ppbC) with the initial NOx constant. The numbers to the right of the plots are the initial NOx concentrations in ppbv. Symbols indicate ozone concentrations for average initial NOx and VOC at Azusa for the years 1995, 2005, 2008 (base year) and 2030 (from Table 6-5). The black diamonds represent weekdays and the red circles represent weekends. The points for 2030 represent the range of the scenarios between the minimum and maximum projected NOx and VOC (minimum NOx paired with minimum VOC and maximum NOx paired with maximum VOC). The lower plot is an expanded view for lower VOC and NOx concentrations.

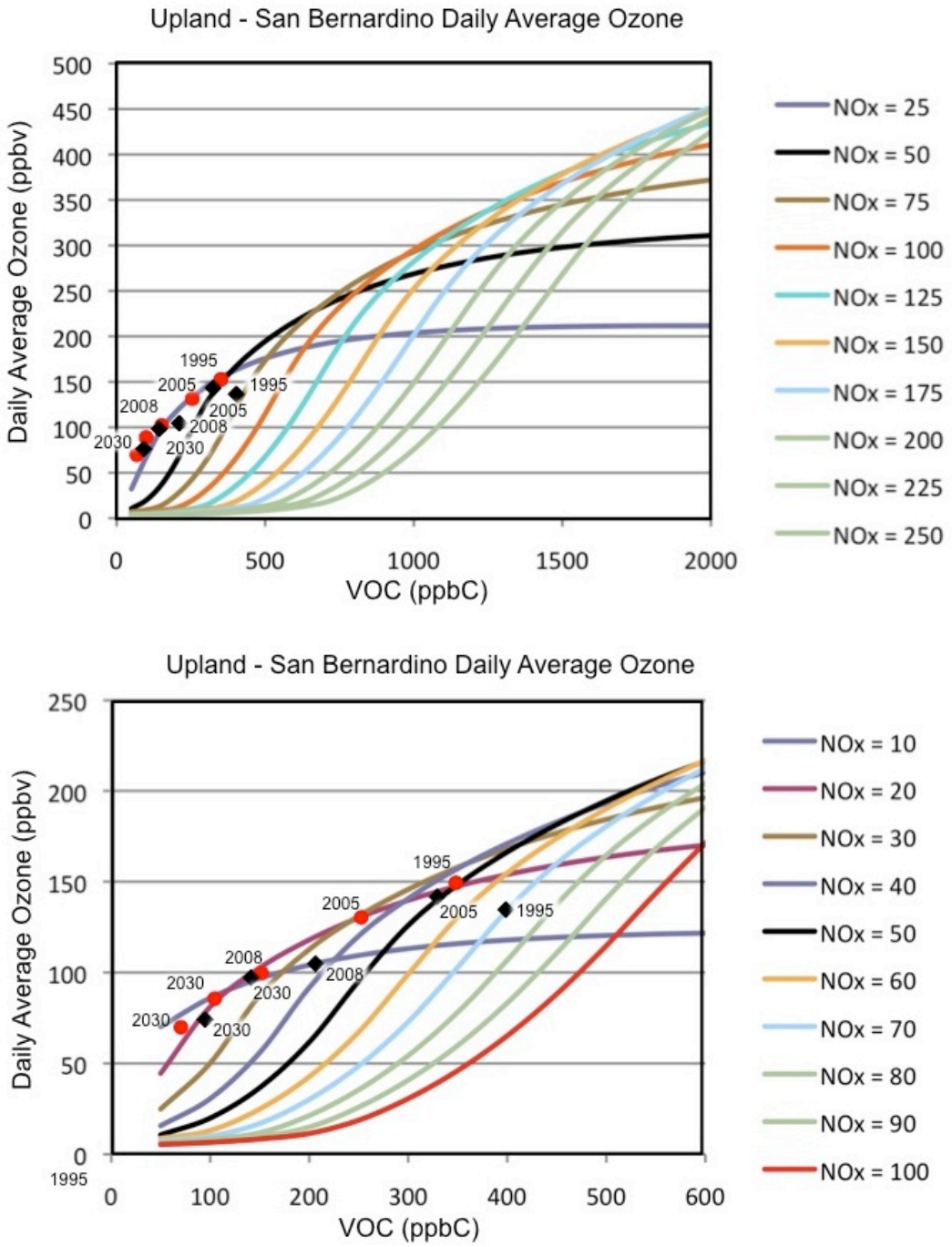

Figure 6-16. The daily average ozone plotted as functions of the initial VOC (ppbC) with the initial NOx constant. The numbers to the right of the plots are the initial NOx concentrations in ppbv. Symbols indicate ozone concentrations for average initial NOx and VOC at Upland-San Bernardino for the years 1995, 2005, 2008 (base year) and 2030 (from Table 6-5). The black diamonds represent weekdays and the red circles represent weekends. The points for 2030 represent the range of the scenarios between the minimum and maximum projected NOx and VOC (minimum NOx paired with minimum VOC and maximum NOx paired with maximum VOC). The lower plot is an expanded view for lower VOC and NOx concentrations.

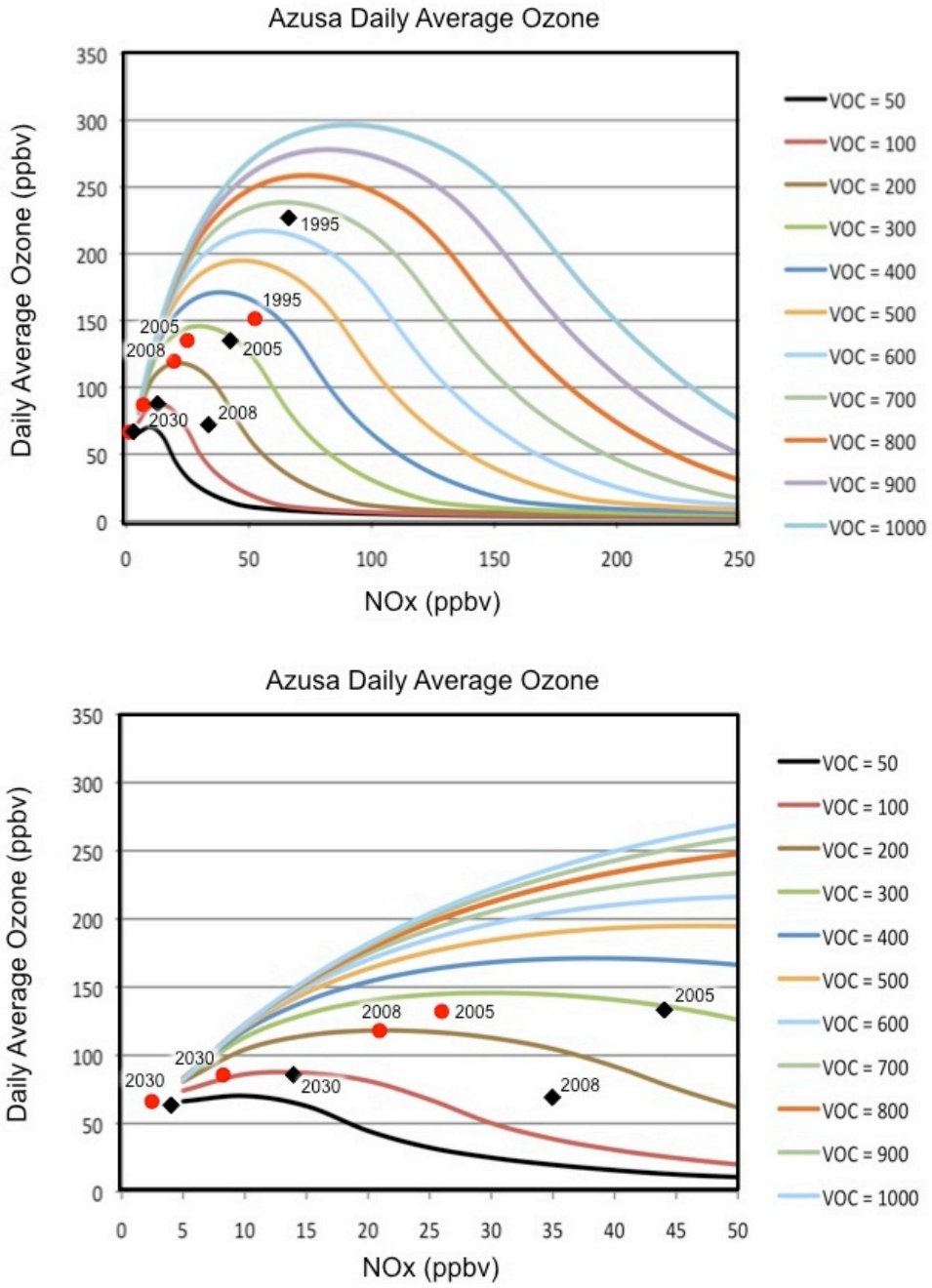

Figure 6-17. Daily average ozone plotted as functions of the initial NOx with the initial VOC (ppbC) constant. The numbers to the right of the plots are the initial VOC concentrations in ppbC. The ozone concentrations for average initial concentrations of NOx and VOC (Table 6-5) at Azusa for the years 1995, 2005, 2008 (base year) and 2030. The black diamonds represent weekdays and the red circles represent weekends. The points for 2030 represent the range of the scenarios between the minimum and maximum projected NOx and VOC (Table 6-5); minimum NOx paired with minimum VOC and maximum NOx paired with maximum VOC). The lower plot is an expanded view for lower VOC and NOx concentrations.

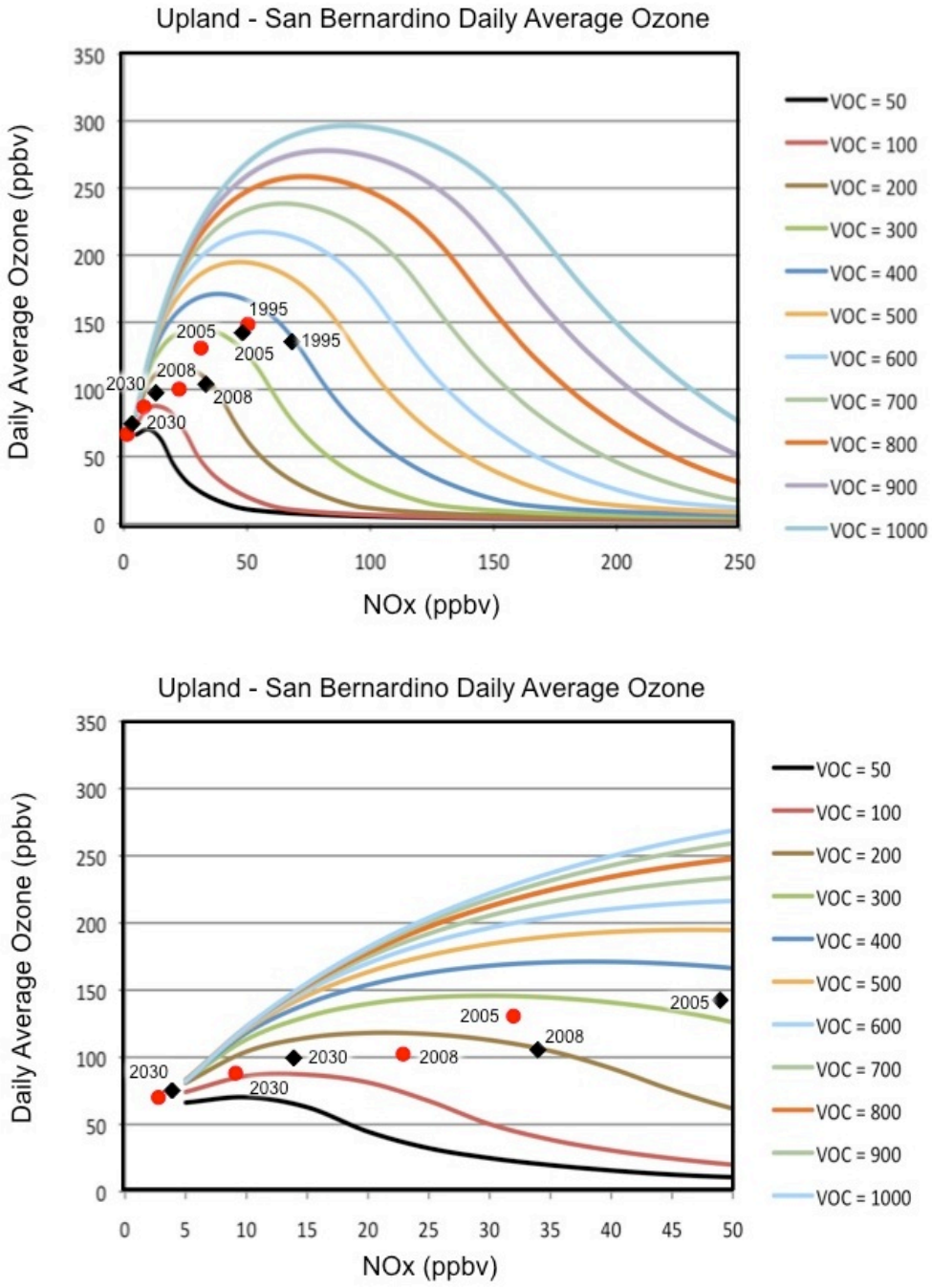

Figure 6-18. Daily average ozone plotted as functions of the initial NOx with the initial VOC (ppbC)constant. The numbers to the right of the plots are the initial VOC concentrations in ppbC. The ozone concentrations for average initial concentrations of NOx and VOC (Table 6-5) at Upland-San Bernardino for the years 1995, 2005, 2008 (base year) and 2030. The black diamonds represent weekdays and the red circles represent weekends. The points for 2030 represent the range of the scenarios between the minimum and maximum projected NOx and VOC (Table 6-5); minimum NOx paired with minimum VOC and maximum NOx paired with maximum VOC). The lower plot is an expanded view for lower VOC and NOx concentrations.

6.2.3 Simulation of the Response of Ozone to Changes in Initial VOC and NOx

The response of ozone concentrations to changes in initial NOx and VOC can be characterized by the following two equations that correspond to VOC and NOx reactivity (Carter, 1994).

$$\text{Ozone response to changes in initial VOC} = \frac{\Delta O_4}{\Delta VOC};$$

$$\text{Ozone response to changes in initial NOx} = \frac{\Delta O_3}{\Delta NOx}.$$

The data used to make the ozone isopleths were used to calculate the two ozone response functions. Figure 6-19 through Figure 6-22 show that these functions are accord with the discussion of the alternative isopleth figures. Figure 6-19 and Figure 6-20 show the ozone response to changes in initial VOC as a function of NOx. The figure shows that reductions in VOC lead to reductions in the daily average ozone concentrations. However there is a maximum point in the response of ozone to reductions in VOC and that point depends on the initial NOx and VOC. As the initial VOC is reduced, the response of ozone to changes in initial VOC becomes greater and lower concentrations of initial NOx. The plots show that the ozone response to reductions in VOC may have peaked at 2005 and the ozone response to reductions in VOC has become less in 2008 and for the 2030 projected year. Figure 5-18 shows the ozone response to initial NOx as a function of VOC. What is striking in this figure is that the ozone response to changes in initial NOx is sometimes positive (reductions in initial NOx lead to less ozone) and it is sometimes negative (reductions in initial NOx lead to more ozone). For the time period between 1995 and 2008 reductions in NOx have been dis-beneficial for these two stations. Only for the high reductions in VOC projected for 2030 do reductions in NOx become beneficial according to Figure 6-21 and Figure 6-22.

6.3 Conclusions

Future ozone reductions in the SoCAB are complicated by the chemical fact that ozone production becomes more efficient as the initial concentrations are reduced. The response of ozone to reductions in VOC are beneficial but become less and less effective as the initial NOx concentrations are reduced to low levels. Reductions in NOx are dis-beneficial at current VOC levels but reductions may become beneficial if VOC and NOx can be reduced to very low levels. The path to these low levels may lead through higher ozone concentrations until NOx is sufficiently reduced. Although the ozone response to changes in initial NOx is sometimes positive (reductions in initial NOx lead to less ozone) and it is sometimes negative (reductions in initial NOx lead to more ozone) for the time period between 1995 and 2008 reductions in NOx have been dis-beneficial for Azusa and Upland-San Bernardino.

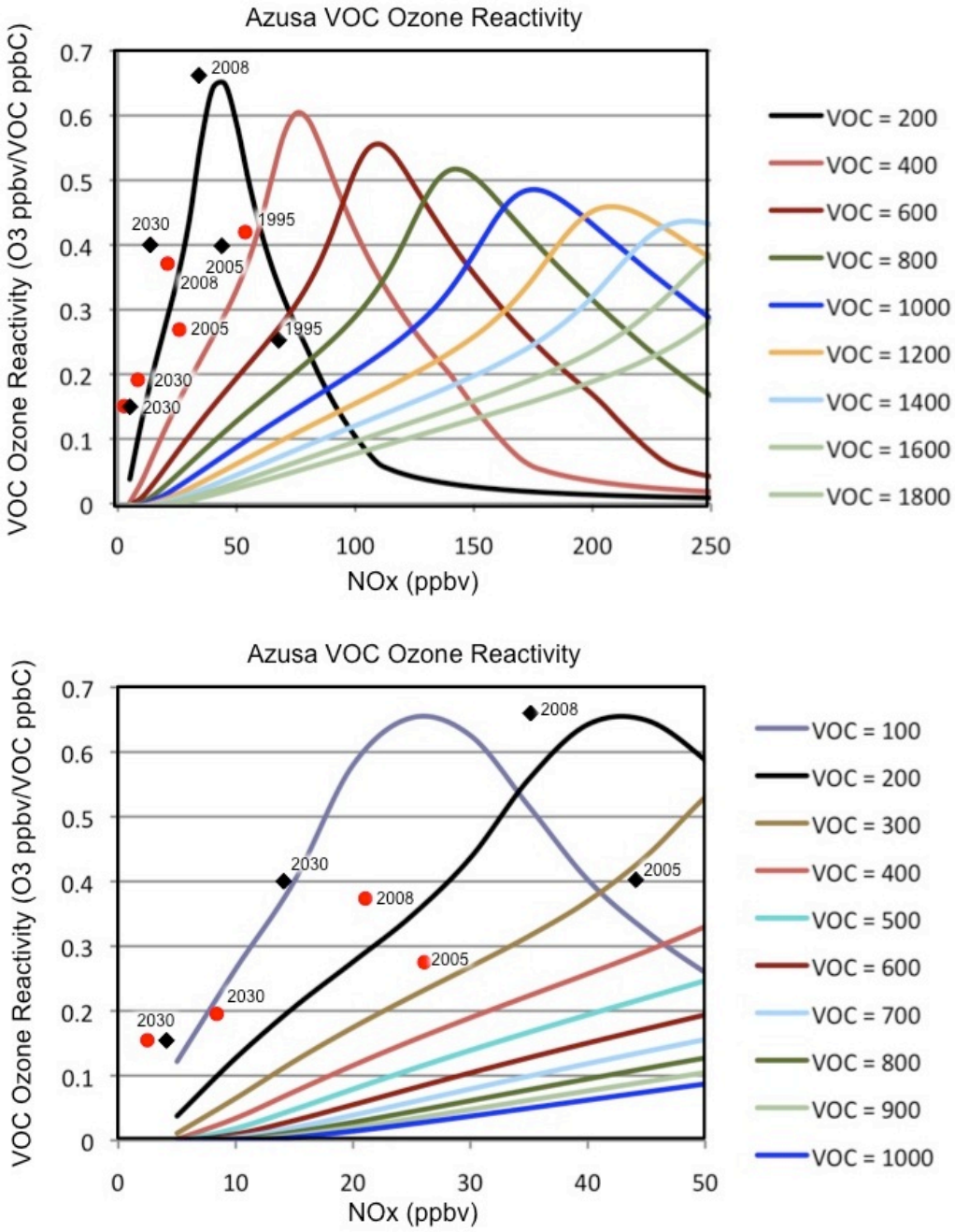

Figure 6-19. The daily average ozone response (VOC reactivity) to changes in initial VOC concentrations. The response of ozone to changes in initial VOC is plotted as a function of the initial NOx with the initial VOC constant. The numbers to the right of the plots are the initial VOC concentrations in ppbC. Symbols represent ozone response at Azusa for the years 1995, 2005, 2008 (base year) and 2030. The black diamonds represent weekdays and the red circles represent weekends. The points for 2030 represent the range of the scenarios between the minimum and maximum projected NOx and VOC (Table 6-5); minimum NOx paired with minimum VOC and maximum NOx paired with maximum VOC). The lower plot is an expanded view for lower VOC and NOx concentrations.

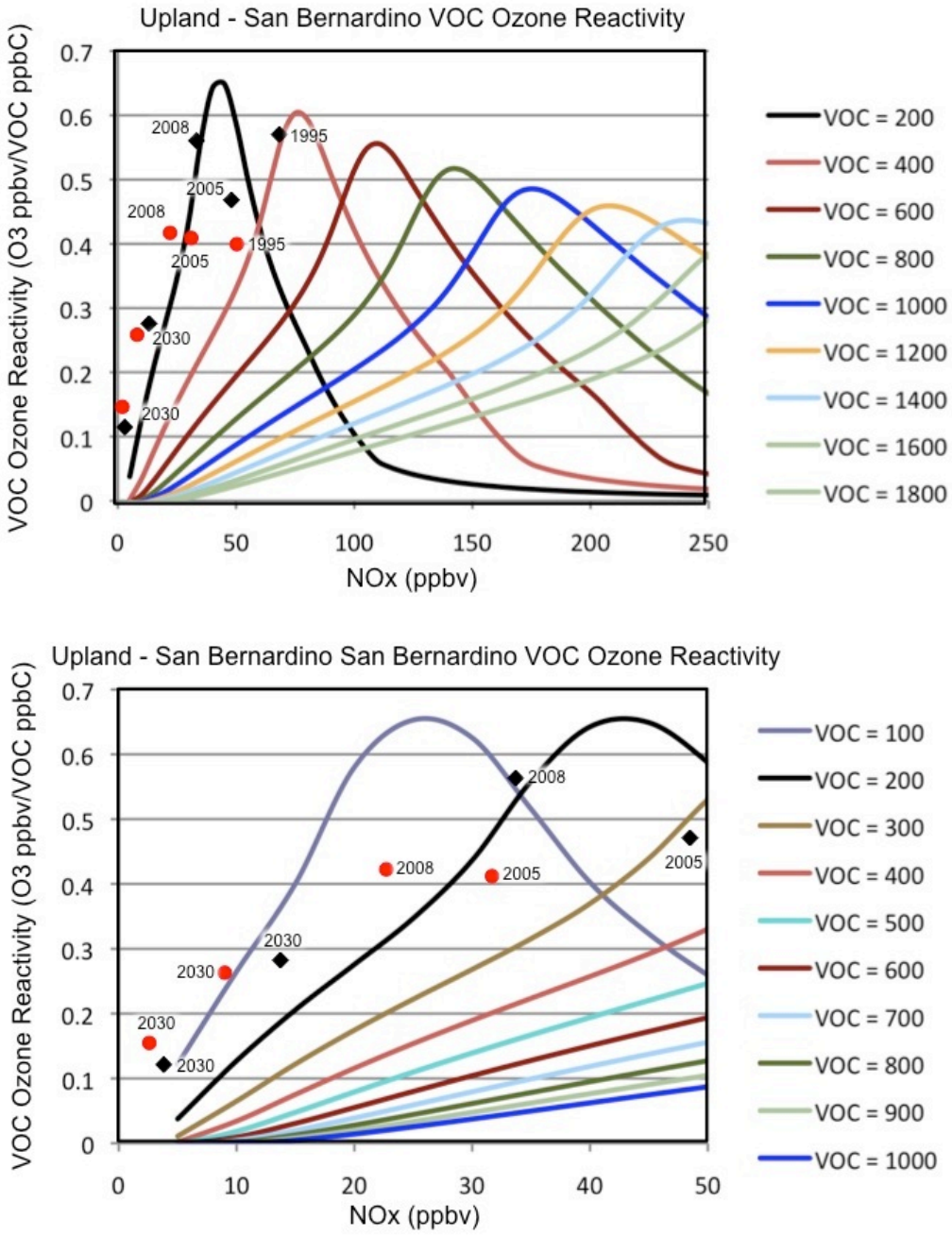

Figure 6-20. The daily average ozone response (VOC reactivity) to changes in initial VOC concentrations is presented. The response of ozone to changes in initial VOC is plotted as a function of the initial NOx with the initial VOC constant. The numbers to the right of the plots are the initial VOC concentrations in ppbC. Symbols represent ozone response at Upland-Ssan Bernardino for the years 1995, 2005, 2008 (base year) and 2030. The black diamonds represent weekdays and the red circles represent weekends. The points for 2030 represent the range of the scenarios between the minimum and maximum projected NOx and VOC (Table 6-5); minimum NOx paired with minimum VOC and maximum NOx paired with maximum VOC). The lower plot is an expanded view for lower VOC and NOx concentrations.

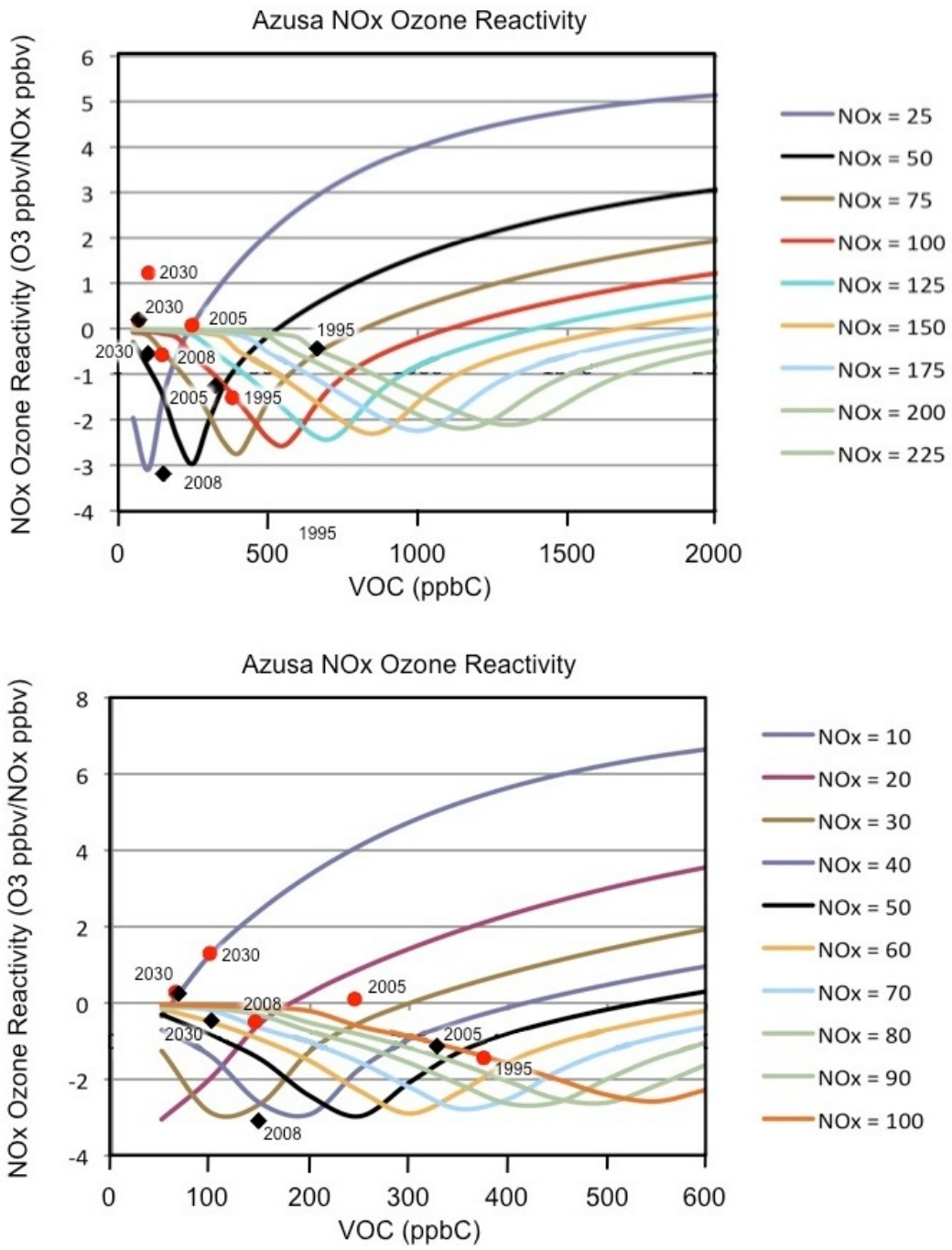

Figure 6-21. Ozone response to changes in initial VOC concentrations. The daily average ozone response (VOC reactivity) to changes in initial NOx concentrations is presented. The response of ozone to changes in initial NOx is plotted as a function of the initial VOC with the initial NOx constant. The numbers to the right of the plots are the initial NOx concentrations. Symbols represent ozone response at Azusa for the years 1995, 2005, 2008 (base year) and 2030. The black diamonds represent weekdays and the red circles represent weekends. The points for 2030 represent the range of the scenarios between the minimum and maximum projected NOx and VOC (Table 6-5); minimum NOx paired with minimum VOC and maximum NOx paired with maximum VOC). The lower plot is an expanded view for lower VOC and NOx concentrations.

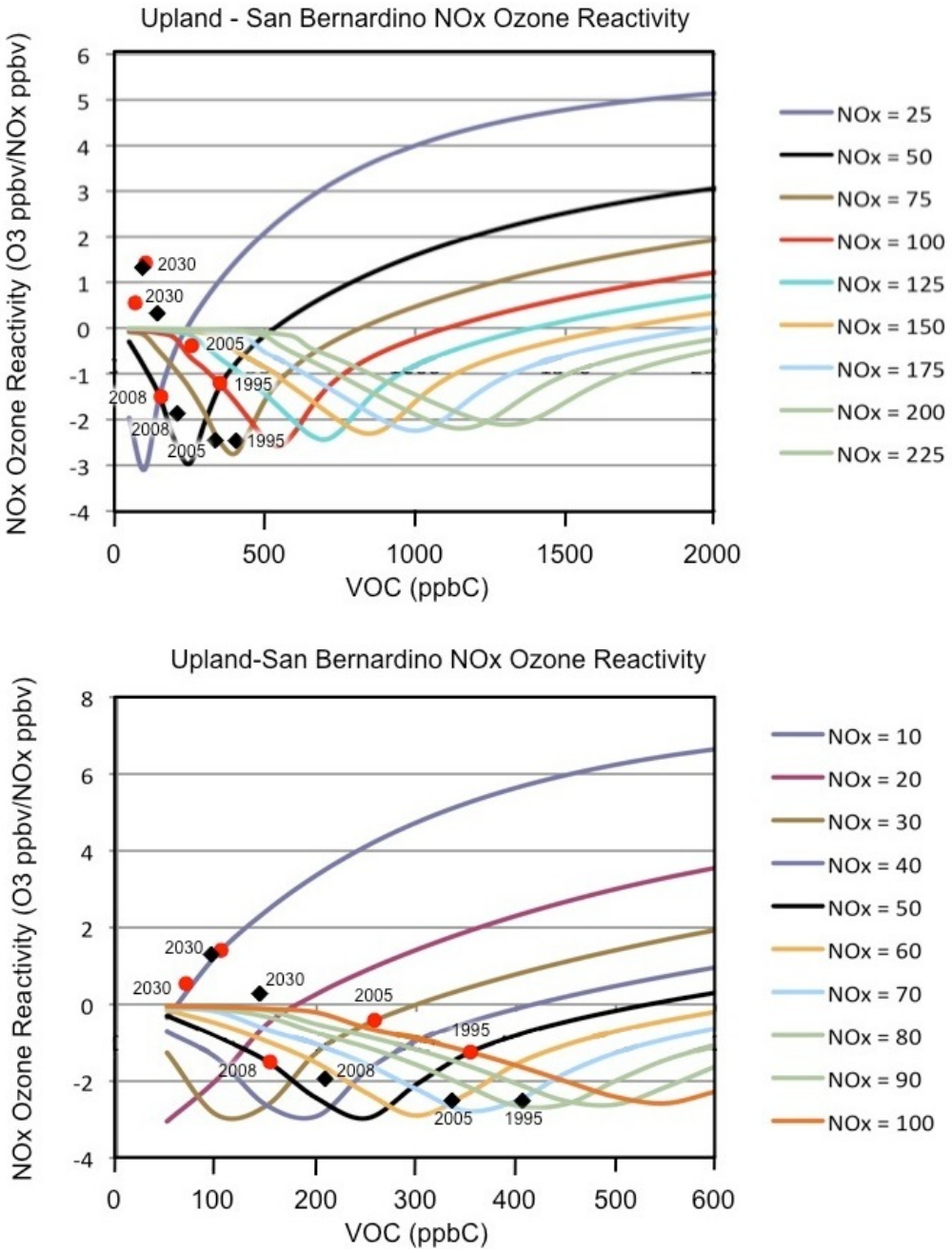

Figure 6-22. Ozone response to changes in initial VOC concentrations. The daily average ozone response (VOC reactivity) to changes in initial NOx concentrations is presented. The response of ozone to changes in initial NOx is plotted as a function of the initial VOC with the initial NOx constant. The numbers to the right of the plots are the initial NOx concentrations. Symbols represent ozone response at Upland-San Bernardino for the years 1995, 2005, 2008 (base year) and 2030. The black diamonds represent weekdays and the red circles represent weekends. The points for 2030 represent the range of the scenarios between the minimum and maximum projected NOx and VOC (Table 6-5); minimum NOx paired with minimum VOC and maximum NOx paired with maximum VOC). The lower plot is an expanded view for lower VOC and NOx concentrations.

6.4 References

1. Carter, WPL. Development of Ozone Reactivity Scales for Volatile Organic Compounds, J. Air and Waste Management Association, 44, 881-899, 1994.
2. Fujita, E.M., D.E. Campbell, W.R. Stockwell and D.R. Lawson, Past and Future Ozone Trends in California's South Coast Air Basin: Reconciliation of Ambient Measurements with Past and Projected Emission Inventories, J. Air and Waste Management Association, 63, 54-69, 2013. (doi: 10.1080/10962247.2012.735211)
3. Fujita, E.M, D.E. Campbell, B. Zielinska, J.C. Sagebiel, J.L. Bowen, W.S. Goliff, W.R. Stockwell and D.R. Lawson, Diurnal and Weekday Variations in the Source Contributions of Ozone Precursors in California's South Coast Air Basin, J. Air and Waste Management Association, 53, 844-863, 2003.
4. Goliff, W.S., W.R. Stockwell and C.V. Lawson, The Regional Atmospheric Chemistry Mechanism, Version 2, Atmos. Environ., 68, 174-185, 2013.
5. Sarwar, G., J. Godowitch, B. Henderson, K. Fahey, G. Pouliot, W. Hutzell, R. Mathur, D. Kang, W.S. Goliff and W.R. Stockwell. A Comparison of Atmospheric Composition using the Carbon Bond and Regional Atmospheric Chemistry Mechanisms, Atmos. Chem. Phys., 13, 1-18, 2013.